Fluorinated Electrolytes for High Performance Rechargeable Lithium-Sulfur Batteries

BY

NASIM AZIMI
B.S., Amirkabir University of Technology, Iran, 2008
M.S., University of Illinois at Chicago, Chicago, 2011

THESIS

Submitted as partial fulfillment of the requirements
for the degree of Doctor of Philosophy in Chemical Engineering
in the Graduate College of the
University of Illinois at Chicago, 2015

Chicago, Illinois

Defense Committee:

Dr.Christos Takoudis, Chair and Advisor
Dr.Zhengcheng Zhang, Argonne National Laboratory
Dr.Alan Zdunek
Dr.Michael McNallan, Department of Civil and Materials Engineering
Dr.Amid Khodadoust, Department of Civil and Materials Engineering

This thesis is dedicated to my parents,
my husband, Hamed, and my brothers, Moein & Amin for their love,
endless support and encouragement.

ACKNOWLEDGEMENTS

I would like to express my sincere appreciation to my supervisors Professor Christos Takoudis and Dr. Zhengcheng Zhang for their excellent guidance and priceless support during the course of my research work. I would like to thank you for encouraging my research and for allowing me to grow as a research scientist.

I would like to express thanks to my thesis committee members Professor Alan Zdunek, Professor Michael McNallan and Professor Amid Khodadoust for their kind support and invaluable guidance.

I would remember with deep sense of appreciation Dr. Zheng Xue and Dr. Libo Hu for their constant support and friendship.

Lastly, I would like to thank my family. Words cannot express how grateful I am to my parents for all of the sacrifices that you've made on my behalf. Your prayer for me was what sustained me thus far. Also, I would like express appreciation to my beloved husband Hamed who was always my support in the moments when there was no one to answer my queries.

Contribution of Authors

Chapter 1 is a literature review and highlights the significance of my research question.

Chapter 2 represents a series of my own experiments and procedures directed for studying the electrochemistry of the lithium sulfur battery with different electrochemical testing and characterization methods.

Chapter 3 represents three accepted published manuscripts, (*Nasim Azimi, Wei Weng, Christos Takoudis, and Zhengcheng Zhang, "Improved Performance of Lithium-Sulfur Battery with Fluorinated Electrolyte", Electrochemistry Communications, Volume 37, Pages 96–99, 2013*), (*Nasim Azimi, Zheng Xue, Ira bloom, Donghai Wang, Tad Daniel, Christos Takoudis, Zhengcheng Zhang"Understanding the Effect of Fluorinated Ether on the Improved Performance of Lithium-Sulfur Batteries" ACS Appl. Mater. Interfaces.2015*) and *(Nasim Azimi, Zheng Xue, Nancy Dietz Rago, Christos Takoudis , Mikhail L. Gordin, Jiangxuan Song, Donghai Wang, Zhengcheng Zhang, "Fluorinated Electrolytes for Li-S Battery: Suppressing the Self-discharge with an Electrolyte Containing Fluoroether Solvent", Journal of The Electrochemical Society, Volume 162 (1), Page A64-A68, 2015.)* for which I was the primary author and major driver of the research. The other authors helped me with the details of some testing, characterization and analysis of the data.

Chapter 4 represents another accepted published manuscript, (*Nasim Azimi , Zheng Xue , Libo Hu , Christos Takoudis, Shengshui Zhang , and Zhengcheng Zhang, "Additive Effect on the Electrochemical Performance of Lithium-Sulfur Battery", Electrochimica Acta ,Volume 154, Pages 205–210, 2015.)* and an unpublished manuscript, *(Nasim Azimi, Zheng Xue , Libo Hu , Christos Takoudis and Zhengcheng Zhang, Fluorinated Additive for Lithium-Sulfur Battery)* which is in submission. I was the primary author of this research and the other authors helped me with the details of data analysis.

Chapter 5 represents an unpublished manuscript, (Nasim Azimi, Zheng Xue , Libo Hu , Christos Takoudis and Zhengcheng Zhang*, "Teflon-Coated Carbon Paper Electrodes for Rechargeable Lithium-Sulfur Batteries"*, in submission) which is in submission.

Chapter 6 represents the overall conclusions of this dissertation and includes the future prospective of this research.

Table of Contents

LIST OF TABLES

LIST OF FIGURES

2. EXPERIMENTAL METHODS

3. FLUORINATED ETHER CONTAINING LITHIUM-SULFUR BATTERY ELECTROLYTE

LIST OF ABBREVIATIONS

DME	1,2-dimethoxyethane
DOL	1,3-dioxolane
CNT	Carbon Nanotube
CE	Coulombic Efficiency
CV	Cyclic Voltammetry
DPE	Dipropyl Ether
EV	Electric Vehicles
EIS	Electrochemical Impedance Spectroscopy
EDS	Energy-dispersive X-ray spectroscopy
GPE	Gel Polymer Electrolyte
HOMO	Highest Occupied Molecular Orbital
HPLC	High Performance Liquid
HEV	Hybrid Electric Vehicles
LIB	Li Ion Battery
LiPS	Lithium Polysulfides
LIBOB	Lithium bis(oxalato) borate
Li-S	Lithium Sulfur
LUMO	Lowest Unoccupied Molecular Orbital
MFCP	Microfiber Carbon Paper
MWNT	Multi-Walled Carbon Nanotubes
PHEV	Plug-In Hybrid Electric Vehicle

PEO	Polyethylene oxide
PTFE	Polytetrafluoroethylene
PVDF	Polyvinylidene fluoride
PS	Polysulfides
RGO	Reduced Graphene Oxide
SEM	Scanning Electron Microscope
SEI	Solid Electrolyte Interphase
SPE	Solid Polymer Electrolyte
S-C	Sulfur Carbon
SPAN	Sulfurized Polyacrylonitrile
S-PPy	Sulfur Polypyrrole
TCCP	Teflon Coated Carbon Paper
TEGDME	Tetra (Ethylene Glycol)Dimethyl Ether
UV-VIS	Ultraviolet Visible Spectroscopy
XRD	X-Ray Diffraction
XPS	X-ray photoelectron spectroscopy

SUMMARY

The high demand for clean, efficient, and renewable energy and, the necessity for solving the CO_2 issue and global warming are only a few of the major motivations for exploring renewable energy technologies. Since the energy must be stored in order for renewable energy to become part of a practical energy solution, there have been many studies of secondary batteries for energy storage applications that benefit from high specific energy, high rate capability, high safety, and low cost.

Lithium-sulfur (Li-S) batteries have received a great amount attention in recent years, as sulfur exhibits an order of magnitude higher theoretical specific capacity than that achievable with intercalation-type cathodes in lithium-ion batteries. In addition, sulfur is abundant in nature and non-toxic, which leads to low cell cost and significant environmental benefits. However, low active material utilization and poor cycle life hinder the commercial application of the Li-S chemistry.

In this thesis, two concepts were studied with the aim of improving the performance of Li-S batteries.

First, the effects of different electrolyte solvents on the Li-S battery were investigated, as electrolyte is one of the key components in determining the performance of this battery. We have reported a novel fluorianted electrolyte, 1,1,2,2-Tetrafluoroethyl-2,2,3,3-tetrafluoropropyl ether (TTE), which suppresses the deleterious shuttling effect and improves capacity retention and coulombic efficiency in cell tests. The cell containing this electrolyte was reported to deliver an initial discharge capacity of 1400 mAh/g while maintaining a capacity of 1100 mAh/g after 50 cycles. The coulombic efficiency was also reported to be more than 96% for the first 50 cycles. Next, as severe self-discharge has become the major issue for high-loading sulfur cathodes (> 5 mg (S)/cm^2), the effect of different electrolyte systems was investigated with regard to the self-discharge behavior of Li-S cells. Our test results suggest that utilizing TTE and $LiNO_3$ additive can effectively suppress this fatal effect and would pave the way for practical applications of a high energy density Li-S battery.

In addition, the effect of two fluorinated electrolyte additives was investigated in Li-S batteries for the first time. The experimental data showed that cell performance was much improved when utilizing fluorinated additives such as lithium difluoro(oxalato) borate (LiDFOB) or Tris(pentafluorophenyl)borane ($B(C_6F_5)_3$); as these additives are effective due to their capability of forming a passivation layer on the surface of the sulfur electrode which prevents the dissolution of the polysulfides and results in higher coulombic efficiency.

In the second part of this study, we report on a modification to the traditional Li-S battery configuration to achieve high capacity and efficiency with a long cycle life. The performance of Li-S batteries using Teflon® coated carbon paper (TCCP) was investigated in this study for the first time. The TCCP is composed of carbon microfibers that act as an excellent substrate while the hydrophobic Teflon (PTFE) coating facilitates the absorption of soluble polysulfides to the cathode. This novel cathode design is not only simpler than methods used in synthesizing sulfur carbon composites, but it also improves the capacity and cycle life of the Li-S battery; where the cell using this novel cell configuration was shown to deliver an initial discharge capacity of 1400 mAh/g while maintaining a capacity of 1000 mAh/g after 50 cycles. The efficiency was also stable at 90% for the first 50 cycles.

In summary even though lithium sulfur batteries are very promising for the next generation of electric vehicles, the current state of the battery is still far away from the requirements for practical applications. Based on our studies, utilizing fluorinated solvents and additive can open a new window for engineering Li-S cells with much improved performance.

1. INTRODUCTION

1.1 Motivation and Overview

The demand for energy, high petroleum consumption and CO_2 emissions, global warming and increasing urban pollution are all global challenges that motivate the exploration for renewable energy technologies to meet these challenges (1-3). Although wind and solar generated electricity are becoming increasingly popular in several industrialized countries, these kinds of energy are intermittent, so the energy must be stored in order for renewable energy to become part of a practical energy solution (4). Rechargeable batteries, which convert chemical energy to electrical energy during discharge and store electrical energy via the reverse process during charging, are the most convenient form to store electrical energy (5). Consequently, there have been many studies aimed at designing rechargeable batteries for transportation to replace or complement internal combustion engines.

There are three types of electrically powered vehicles, including pure electric vehicles (EVs) (such as the *Tesla*); hybrid electric vehicles (HEVs) (such as the *Prius*), and plug-in hybrid electric vehicles (PHEVs) (such as the *Karma*) (6). Pure electric vehicles basically use only the battery to power the engine. Although using EVs significantly reduces CO_2 emissions, the lifetime of the battery can provide a range of only 30-50 miles (7). Hybrid electric vehicles (HEVs) are designed to use both battery power and the combustion engine, so HEVs are able to travel longer distances. Plug-in hybrid electric vehicles (PHEVs) can be charged by plugging them into charging stations and use a combination of electricity and an internal combustion engine. The engine is designed to operate serially, and the battery can store enough electricity to significantly reduce petroleum consumption (6, 7). Electric cars are estimated to have 35% of the car market by 2025, with 10% being pure EVs and 25% HEVs (8).

In order for these vehicles to compete with conventional internal combustion engine cars, they need secondary batteries that benefit from high specific energy, high rate capability, high safety and low cost (2, 4). Some of these batteries are as the following:

1.1.1 Li-Ion Battery Technology

Lithium batteries were first commercialized by Sony in 1990, although pioneering studies had been carried out as early as the 1970s by Whittingham and Goodenough (9). Among all rechargeable batteries, lithium-ion secondary batteries are very promising for powering electric vehicles due to their high energy density and high durability over many charges and discharge cycles. These batteries were born from the determined efforts of many innovators seeking light weight, compact electrical power sources in the last century. Military and space programs were in search for high-performance battery systems that can function in a wide range of circumstances.

The motivation for using a lithium-ion battery (LIB) relied on the fact that lithium is the most electro positive metal (–3.04 V versus standard hydrogen electrode). In addition, it is the lightest metal (equivalent weight 46.94 g mol^{-1}, and specific gravity 40.53 g cm^{-3}); therefore it facilitates the design of storage systems with high energy density (10). A typical LIB consists of a graphite anode, a lithium transition-metal oxide cathode, and a lithium ion-conducting separator with a non-aqueous electrolyte between the two electrodes. The electrolyte is typically a solution of lithium salt in organic solvents (11). During the charge-discharge process, the lithium ions shuttle between cathode and anode through electrolyte and separator. LIBs are the most successful commercialized secondary power sources and are widely used in many fields including consumer electronics, medicine, the military, and research due to their good capacity reversibility, and relatively high energy and power densities. While Li-ion batteries rule the present, a number of emerging chemistries are competing for a leading role in the future. Below are some of the primary candidates.

1.1.2 Magnesium Battery Technology

Rechargeable magnesium batteries were first presented more than a decade ago. Their components included magnesium metal or an Mg alloy anode, and complex electrolyte solutions. Since magnesium compound are highly abundant in the earth and are environmentally friendly, this makes magnesium another potential candidate to be used as anode material.

This type of battery has twice the life capacity of the zinc/manganese dioxide (Zn/MnO_2) battery of same size. It is very durable and storable since it always forms a protective layer on the surface of the magnesium anode. In this regard, the magnesium based battery system has gained considerable attention as an alternative system making it an attractive candidate for electrical storage systems supporting wind and solar energy, energy systems, or grid operations. However, these batteries also suffer from several drawbacks where the battery generally loses its storability once it has been partially discharged and for this reason it is not very suitable for using in long-term intermittent applications (12, 13).

1.1.3 Li-Air Battery Technology

Since the theoretical specific energy densities for metal-air batteries are higher than for ion-based approaches, metal-air batteries have received great attention. Recently, lithium-air batteries have been proposed as the next step in lithium battery industry, due to the viewpoint that an electric car equipped with this type of battery could travel more than 500 miles on a single charge. This will finally put battery-driven vehicles on equivalent ground with conventional models.

The lithium-air battery uses the oxidation of lithium at the anode and reduction of oxygen at the cathode to induce a current flow and have the potential of 5–15 times the specific energy of current lithium-ion batteries (14). However this battery technology has not been commercialized due to several challenges, where the anode which is pure lithium metal and can provide high amounts of energy, ignites when exposed to water, carbon dioxide, or other contaminants. In addition, the lithium-oxygen can be converted to unwanted lithium carbonate. Therefore, the battery would need screening technology to take benefit of this its exceptional properties (14).

1.1.4 Lithium- Sulfur Battery Technology

Even though LIBs rule the present generation of batteries and are recognized to be one of the best candidates for energy storage, at present they cannot offer a suitably long driving range (i.e., >300 km) for plug-in electric vehicles (PEVs) due to their limited theoretical capacity of about 170 mAh g^{-1} (15,16). In addition, the rapid development of emerging applications, including military power supplies, civil transportation, and stationary storage, have placed higher demands on the energy density of the battery. To compete in the market with gasoline-based vehicles and fulfill these needs, new batteries are required for the next-generation EV's to provide much higher energy density, and reduce cost factors. Examples include a new group of batteries with triple the power of LiB's (Figure 1). Lithium–sulfur batteries (Li-S) are considered to be very appropriate power sources due to their high energy density of about 2600 Wh/ kg. Also, sulfur has the highest theoretical capacity value of 1675 mAh/gr of all known solid-state cathode materials which make these batteries appealing for stationary storage of renewable energies, such as solar and wind, if long cycle life and high system efficiency can be achieved. In addition, this battery system has a wide range of applications due to its high theoretical capacity, intrinsic overcharge protection, elemental abundance, low cost and nontoxicity (16-20).

A typical Li-S battery is composed of a lithium anode, a sulfur cathode, and an electrolyte in between. A Li-S battery works on the basis of redox reactions between the lithium anode and the sulfur cathode. The reaction in these batteries is a reversible conversion reaction as shown:

$$16Li^{+} + S_8 + 16e^{-} \rightleftharpoons 8Li_2S \quad (1.1)$$

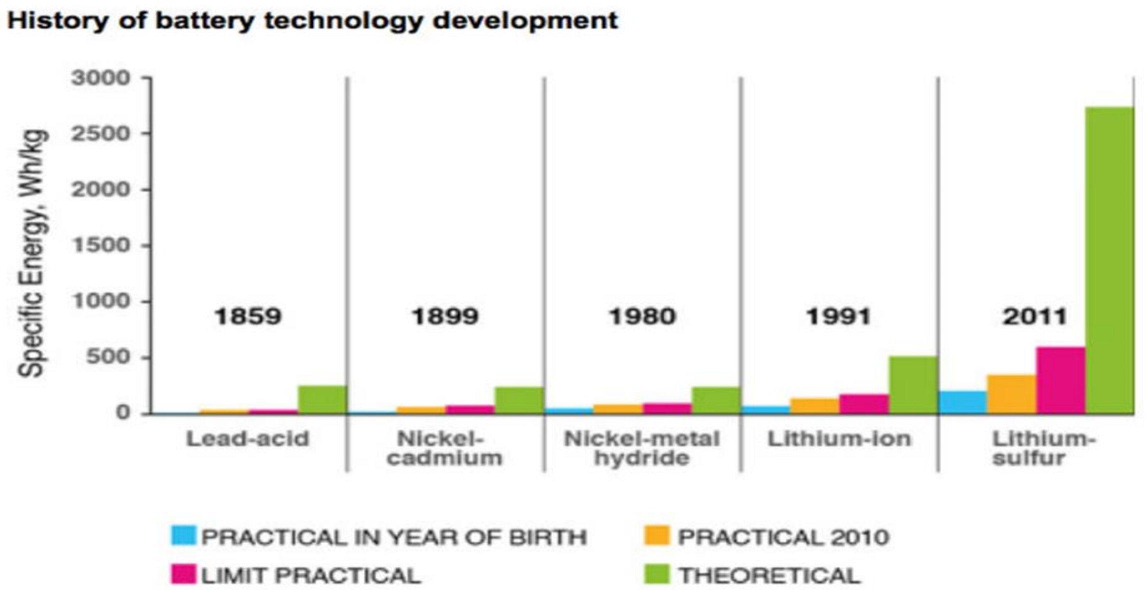

Figure 1. Specific energies of various rechargeable batteries.

Basic Properties of Sulfur Material

Sulfur is the seventeenth richest element in the Earth's crust. In nature, the most common form is cyclic octa-sulfur (S_8), followed by the cyclic S_{12} allotrope. Sulfur has a melting point of 112.8°C (rhombic) or 119.0°C (monoclinic), boiling point of 444.6°C, specific gravity of 2.07 (rhombic) or 1.957 (monoclinic) at 20°C, and sublimes easily. It is a pale yellow, brittle, odorless solid. It is insoluble in water, but soluble in carbon disulfide. In the molten state, the viscosity of sulfur exhibits a unique temperature-dependent behavior. During heating, the viscosity of sulfur gradually decreases, followed by a significant increase around 160°C. This is due to the polymerization of the S_8 rings until near 190°C at which point sulfur starts depolymerizing and the viscosity decreases. As a result of this behavior and the minimum viscosity value around 160°C, sulfur can be impregnated into porous material such as carbon to synthesize sulfur composite materials (18).

Anatomy of a Lithium-Sulfur Battery

A typical Li-S battery is composed of a lithium anode, a sulfur cathode containing elemental sulfur, electronic conductors such as carbon or metal powder and binders, and an electrolyte. The cathode is separated from the metallic lithium negative electrode by an organic electrolyte (Figure 2) (21). The Li-S battery holds a maximum voltage at the open-circuit state, which is in direct proportion to the difference between the electrochemical potentials of the Li anode and the S cathode. During the discharging process, S reacts with Li by a two-electron reduction process to form polysulfide intermediates (Li_2S_x, x=2–8), and to generate Li sulfide (Li_2S) at the end of discharge (22). Despite the considerable advantages of the Li–S cell, this battery technology has not matured to date due to several technological barriers such as rapid capacity fading and low coulombic efficiency, which are believed to be mainly associated with the loss of sulfur active material during a repeated charge and discharge process. This phenomenon happens through the dissolution of lithium polysulfides into the electrolyte and side reactions of dissolved polysulfide species with the electrolyte solvent and the lithium anode (15,16,18-20,23).

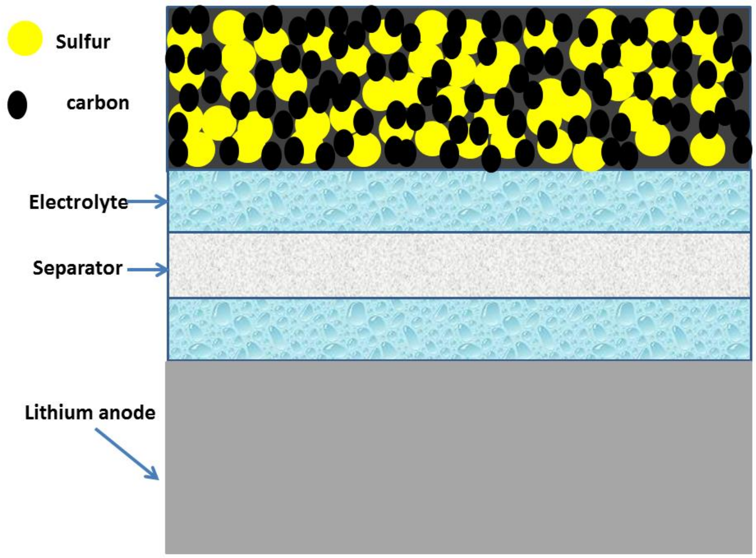

Figure 2. Schematic diagrams of the lithium/sulfur cells.

1.2 General Performance Characteristics

Cell Potential

The cell potential, E_{cell}, is a measure of the potential difference between two half-cells in an electrochemical cell (24). For the Li-S battery, the cell voltage is determined by the following equation:

$$E_{cell} = E_{cathode} - E_{anode} \quad (1.2)$$

where:

E_{Cell} = the standard cell potential

$E_{Cathode}$ = the standard reduction potential for the reduction half-reaction occurring at the cathode.

E_{Anode} = the standard reduction potential for the oxidation half-reaction occurring at the anode.

The units of the potentials are typically measured in volts (V).

The reaction of the sulfur is given by Equation (1.3):

$S + 2e^- \rightleftharpoons S^{2-}$ (1.3)

The standard reduction potential of the sulfur reaction relative to the standard hydrogen electrode (SHE) is -0.48.

Equation 1.4 gives the reaction at the lithium anode.

$Li \rightleftharpoons Li^+ + e^-$ (1.4)

The standard reduction potential of this reaction relative to the standard hydrogen electrode (SHE) is -3.05V, therefore the Li-S cell voltage is given by Eq. 1.2 which is 2.57V.

Coulmbic Efficiency

The coulombic efficiency (CE) is defined as the ratio (expressed as a percentage) between the energy removed from a battery during discharge compared with the energy used during charging to restore the original capacity (25). CE is described by:

$$CE = \frac{\text{Discharge Capacity (Ah)}}{\text{Charge Capacity (Ah)}} \quad (1.5)$$

Coulombic efficiency is usually below 100% in a Li-S battery due to losses in charge and other reactions such as the redox shuttle effect.

Theoretical Capacity

The theoretical capacity of a cell is the ideal amount of charge it can deliver in the case where every single atom of the reactant was completely reduced to its final discharge product which in real batteries this does not occur (26). The actual capacity of a cell is always lower than this number due to internal losses. The theoretical capacity of sulfur is 1672mAh/g as explained below:

The theoretical capacity of a battery is the quantity of electricity involved in the electro-chemical reaction. It is denoted Q and is given by Equation (1.6):

$$Q = x.n.F \tag{1.6}$$

Where:

Q = Theoretical capacity of battery

X = number of moles of reaction

n =number of electrons transferred per mole of reaction

F= Faraday's constant (96485 C/mol)

However, the capacity is usually given in terms of mass, not the number of moles:

$$Q = n.F/M_r \tag{1.7}$$

M_r = Molecular Mass (atomic weight of sulfur g/mol)

The overall reaction that occurs at the cathode can be shown by Eq. (1.3):

$S + 2e^- \rightleftharpoons S^{2-}$

Therefore, since n=2:

$Q = (2)\ (96485\ C/mol)/\ 32.064\ (g/mol) = 6018.28\ C/g$

There is 3600 C in 1 A.h therefore the capacity can be converted to:

Q= 6018.28 (C/g)/ 3.6 C/mAh = 1672 mAh/g

Capacity and Rate Capability (C-rate)

The total capacity of a cell is defined as the amount of electric charge that the cell can deliver at a rated voltage when discharged from 100 % state of charge to 0% state of charge and is measured in units such as amp-hour (A·h) (27). Slow discharge results in minimal losses from resistance and heat dissipation which lead to delivery of the maximum charge from a battery. In addition, more electrode material and loadings result in greater capacity.

It is standard practice to define the current levels of a cell by its capacity. For example for a Li-S cell with a capacity of 1.6 Ah, it would take 1 hour to discharge the cell with current of 1.6 A. This is known as C-rate or discharge/ charge currents which are often given in fractions of this rate. A 2C rate would mean a discharge current of 3.2 A, over one half-hour.

Theoretical Energy Density and Specific Energy

Specific energy describes the amount of energy contained within a battery per unit mass (26). The theoretical specific energy of the Li-S couple is 2600Wh/kg as shown below.

The Gibbs free energy equation relates the equilibrium cell potential to the energy available from that reaction for a spontaneous electrochemical reaction, and is given by Equation 1.8.

$$\Delta G = n.F.E \tag{1.8}$$

where:

ΔG = Gibbs free energy

n =number of electrons per mole of product

F = Faraday's constant (96485 C/mol)

E =Electrode potential of the reaction

The final discharge product is Li_2S which has the atomic weight of:

W_{Li2S} = 2× 6.941 + 32.064= 45.95 g/mol or 0.04595 kg/mol

Using an average cell potential of 2.23 V, Gibbs free energy can be calculated from Eq. 1.8 as:

ΔG= (2) (96485) (2.23) = 430323.1 J/ mol= 430323.1(J/mol)/ 3600 (J/Wh) = 119.5 Wh/mol

As mentioned, the final discharge product is Li_2S which has an atomic weight of 0.04595kg/mol. Thus:

ΔG= 119.5 (Wh/mol) / 0.04595 (kg/ mol) = 2600 Wh/kg

Therefore the theoretical specific energy of a lithium sulfur battery is about 2600 Wh/kg.

Energy density is the amount of energy stored in a battery per unit volume. Similarly, the energy density is calculated using the atomic volume. The theoretical energy density for a Li-S battery is 2862 W h/L, as shown below.

V_{Li2S} = 2× 0.0131 L/mol + 0.0155 L/mol= 0.0417 L/mol

ΔG= 119.5 (Wh/mol)/0.0417 (L/mol) = 2860 Wh/L

Therefore, the theoretical energy density of a Li-S cell is calculated to be 2860 Wh/L when an average cell voltage of 2.23 V is used. These values are significantly higher than other known cell couples.

1.3 Voltage Characteristic of Lithium- Sulfur Battery

Figure 3 shows the discharge and charge profile for the first cycle of a regular Li-S cell. The discharge process can be divided into four parts (22, 28, 29).

Section 1: At the beginning of the discharge process, elemental sulfur is reduced initiating a series of reactions with lithium ions. When the cell begins to discharge by application of an external load, the lithium metal is oxidized, supplying electrons to the load and leaving lithium ions at the anode. This first results in the formation of Li_2S_8 which dissolvesinto the liquid electrolyte and leaves numerous voids in the cathode.

$$S_8 + 2Li^+ \rightarrow Li_2S_8 \qquad (1.9)$$

Section 2: A reduction from the dissolved Li_2S_8 results in the formation of different order of lithium polysulfides with the general formula of Li_2S_n, where the initially formed polysulfides have longer chains (4<n<8) and are more soluble in the electrolyte. During this part, the cell's voltage is gradually decreasing and the solution's viscosity is increasing with the decrease in the length of the S-S chains.

$$Li_2S_8 + 2Li^+ \rightarrow Li_2S_{8-n} + Li_2S_n \qquad (1.10)$$

Section 3: In the later stages of the discharging process, the long chains polysulfides are reduced to the lower-order polysulfides ($1<n<3$). The dissolved polysulfides deposit back on to the cathode in the form of insoluble Li_2S_2 and Li_2S and are distributed evenly throughout the carbon matrix of the cathode. This forms an insulating passivation layer and increases the internal resistance of the Li-S cell. This region forms the second plateau that contributes to the major capacity of the Li-S cell.

$$2Li_2S_n + (2n-4)Li^+ \rightarrow nLi_2S_2 \quad (1.11)$$

$$Li_2S_n + (2n-2)\,Li^+ \rightarrow nLi_2S \quad (1.12)$$

Section 4: In the final discharging step, a solid-solid reduction takes place from insoluble Li_2S_2 to Li_2S. At this point no further reduction of sulfide ions is possible, which it is reflected in the steep voltage drop in the discharging profile. The loss of sulfur-active material through this process could be the main factor contributing to the capacity fading of the cell during extended cycling.

$$Li_2S_2 + 2Li^+ \rightarrow 2Li_2S \quad (1.13)$$

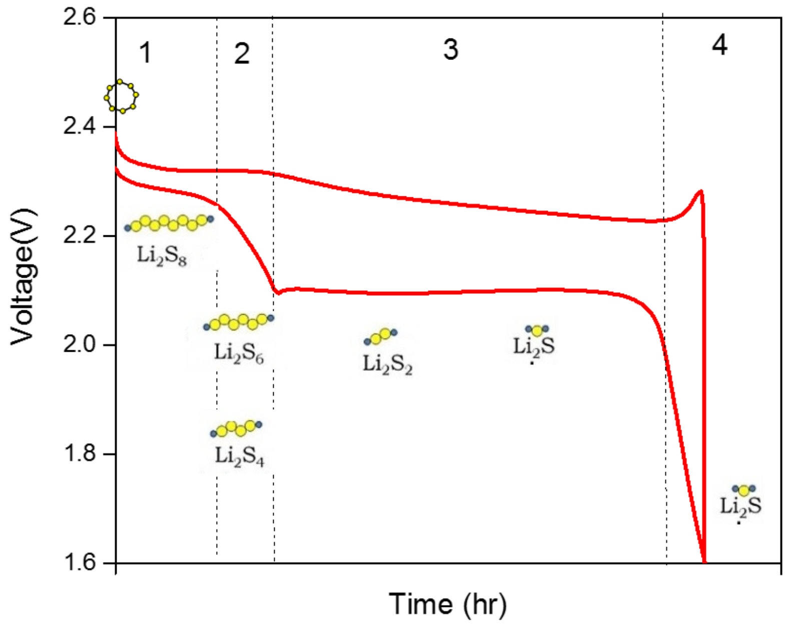

Figure 3. A typical discharge and charge voltage profile of the first cycle of a Li-S cell.

Studies in the detailed mechanism of charging have not been as extensive as for the discharge. As shown in Figure 3, there is a sharp rise in voltage at the very beginning of charging followed by two shallow plateau regions and finally another sharp voltage rise at the end of charging. The initial steep rise is due to the resistance of Li_2S passivating layer on the cathode surface. The subsequent shallow dip may be due to the reduced impedance as the layer has begun to be removed. The two plateaus during charging are due to the oxidation of polysulfides. The first plateau can be attributed to the oxidation of solid Li_2S to longer chain polysulfides and the second to the oxidation of polysulfides to sulfur and highest order polysulfides (19, 22, 30).

Redox Shuttle Phenomena of Lithium Poly-Sulfides

Although the dissolution of lithium polysulfides facilitates the cell's performance, it can cause severe redox shuttle between the sulfur cathode and the Li anode (31, 32). This results in low coulombic efficiency during the charging process and a fast self-discharge rate for storage.

As mentioned above, during discharge elemental sulfur goes through a reduction reaction with lithium ions. This results in the formation of different order of lithium polysulfides which are soluble in the electrolyte. In the later stages of the discharging process, the long-chain polysulfides are reduced to the lower-order polysulfides ($1<n<3$), which are less soluble. In the charging step, the shorter polysulfides are then oxidized and transformed to longer forms. However, these higher-order Li_2S_n are soluble and, due to the concentration gradient, can diffuse into the electrolyte and get reduced by accepting electrons from the cathode side and react with lithium ion to regenerate lower order polysulfides. Again, low-order polysulfides diffuse back to the sulfur cathode surface and get oxidized to higher order polysulfides (Figure 4). The process then repeats itself causing a shuttle effect between the two electrodes (19, 30). These parasitic reactions cause significant problems such as (1) consuming the sulfur active material (2) decomposing Li anode, and (3) polarizing the Li anode since insoluble Li_2S and Li_2S_2 are formed and deposited on the Li surface (18).

The rate of the shuttle effect depends on the (1) the rate of reaction of polysulfides on the anode surface, (2) the solubility of the lithium polysulfides in the electrolyte, (3) the mobility of the polysulfides through the electrolyte and the dissolution rates on the electrodes (33). In addition, the shuttle effect is very strong at high states of charging where the solubility and activity of the polysulfides is at its highest. Accordingly, Sion Power has reported earlier that this shuttle effect depends significantly on electrolyte composition and also the charging current, where the cells showed high shuttling when the viscosity of the electrolyte was lower, as there was less force to oppose the mobility and diffusion of the polysulfides in the organic electrolyte (34). In addition, when the charging current is low, the cell takes longer to charge therefore there is more time for the diffusion of the polysulfides thus increasing the shuttle effect.

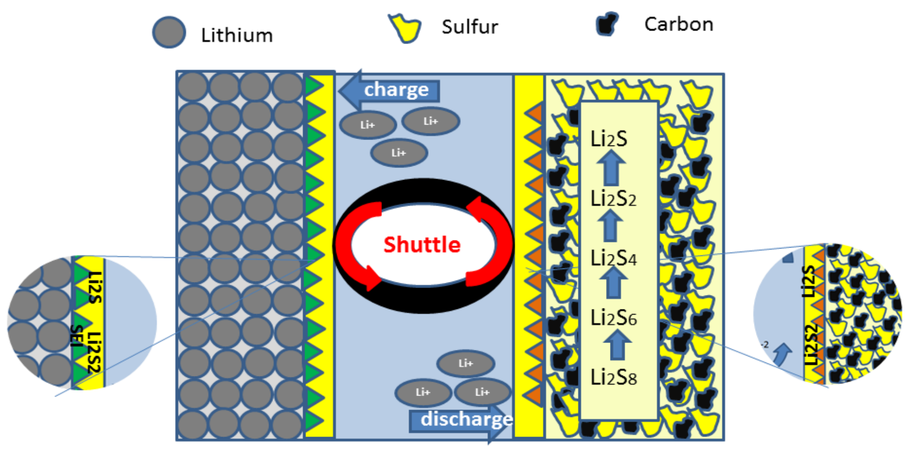

Figure 4. A typical Li-S cell with redox shuttle behavior

1.4 Great Challenges Of Lithium Sulfur Battery

There are several challenges involved with the lithium sulfur battery which prevent them from competing in the market (35-37). For example, since sulfur is an insulator, high amounts of conductive additives are needed to achieve reasonable utilization of the active material. However, sulfur content of at least 70% is required to retain the advantage of sulfur's high energy density.

In addition, the insoluble products at the end of discharge such as Li_2S_2 and Li_2S will accumulate on the cathode after the battery is fully discharged. Since these species are also insulating, this can result in the formation of a passivation layer on the electrode and the loss of active material. This Li_2S does not contribute to any future electrochemical reactions causing irreversible capacity loss. It is also possible that the formation of these species and their build up can cause the carbon matrix to break away from the active material. This decreases the active area of the cathode material. In addition, when the Li-S cell is cycled at higher currents, there is more Li_2S build up, and it is not uniformly distributed on the cathode which results in more destruction of the cathode structure.

The most common solution to this problem is to synthesize an appropriate carbon-sulfur composite cathode, in which the carbon matrix can offer both an electron transport network and reaction sites for lithium-sulfur redox reactions. Therefore, many chemical-free processes such as ball-milling techniques are used to prepare composite sulfur cathode materials. During the milling process, the stainless balls rotate around a horizontal axis in a tumbler, partially filled with the sulfur/carbon slurry. The continuous rotation can reduce the size of particles within the sulfur mixture. The sulfur cathode material prepared with ball-milling method can achieve a relatively good distribution of sulfur particles.

Another challenge is the significant volumetric increase of about 79% due to the conversion process between sulfur and lithium during charge and discharge (18). This is due to the dissolution and precipitation of the sulfur active material and final products on the cathode which can result in aging of the electrodes and quick fading of the battery's charge. By trapping sulfur into porous carbon, the free volume of thte carbon matrix can provide a buffer for the expansion and contraction of sulfur content, which can contribute to the improvement of cycle stability.

The next major problem is the formation of voids at the end of discharge due to the dissolution of the sulfur into the organic electrolyte. In addition, Li_2S and Li_2S_2 deposit back on to the cathode. Conventional binders such as PVDF are known to swell and cannot retain the porous structure of the cathode in the cycling process. Even though some reported sulfur cathodes have achieved high specific capacity over 1000 mAh/g at high rates, it is still difficult to retain the high and stable capacity of sulfur over 100 cycles (36-38).

The situation at the lithium anode in Li-S batteries is very different from other lithium electrodes studied before (39-41).The presence of an unstable interface between the lithium anode and the electrolyte solution is reported earlier. The main problem with the lithium anode in this system is the low coulombic efficiency and rough morphology of the Li plating, which are both related to the polysulfide redox shuttle. The lithium is highly reactive with the organic electrolyte. These reactions lead to formation of side products which can also cause the capacity fading of Li-

S cells. In addition, the reaction between dissolved polysulfides and the lithium anode is recognized as the most important factor in initializing thermal runaway of the cell at high temperatures.

In addition, the high solubility of sulfur active material and the formation of polysulfides dictate that electrolytes used for LIBs can no longer be used for Li-S batteries. Generally, the requirements for the electrolyte used in an Li-S battery include high ionic conductivity, moderate polysulfide solubility, low viscosity, electrochemical stability, chemical stability against lithium, and safety (18). Many studies have been reported earlier on the effect of electrolyte component, including 1,2-dimethoxyethane (DME), 1,3-dioxolane (DOL), and tetra(ethylene glycol)dimethyl ether (TEGDME), on the electrochemical performance of Li-S batteries. (41-46) It has been reported that ether-type solvents such as 1,2-dimethoxyethane (DME) have good solubility of elemental sulfur and good stability of polysulfide in electrolyte solution. It also appears that these solvents offer faster polysulfide reaction kinetics while being more reactive with the lithium anode. Alternatively, cyclic solvents such as DOL are superior for stabilizing the surface of Li metal by forming a protective layer over the lithium surface through the ring-opening reaction; while providing lower polysulfide solubility. However, it appears relatively difficult for any single organic solvent to satisfy all of those conditions of the Li-S battery electrolyte. A practical solution is to use an electrolyte with an optimized formula based on a mixture of solvents and additives. Therefore, the combination of these two solvents leads to improved electrochemical performance as compared to each solvent alone and is used as the conventional electrolyte for Li-S batteries (47,48). As for the salt, chemical compatibility with polysulfides is the highest priority. Conventional salts such as $LiPF_6$, LiBOB and $LiBF_4$ cannot be used for the electrolyte in Li-S batteries due to side reactions with lithium polysulfides. $LiN(SO_2CF_3)_2$ and LiTFSI are found to play important roles in reactions that lead to the formation of a protective film comprising Li_xNO_y and/or Li_xSO_y on the lithium anode surface (9,49).

The cell's self-discharge property is one of the other key factors for commercialization of the battery. These batteries suffer from severe self-discharge which is caused by the corrosion of the lithium metal anode due to the dissolution of sulfur active materials in the electrolyte. In general, a secondary battery will naturally lose its charge capacity when kept for a period of time at a certain temperature. This occurrence is referred as battery self-discharge and it basically depends on battery chemistry, electrode composition, electrolyte formulation, and the storage temperature. There have been only a few studies on the self-discharge behavior of Li/S batteries. Mikhaylik and Akridge reported that preventing the redox shuttle effect results in less self-discharge of the cell (50). Ryu *et al*. have reported that cells stored at the full charge state show severe self-discharge which is shown to be due to the conversion of elemental sulfur to Li_2S and intermediate lithium polysulfides resulting in a decrease in discharge capacity. They have also reported that stainless steel is not a very appropriate current collector for Li-S cells. By analyzing the samples after self-discharge, the researchers found that this behavior is related to the corrosion of the stainless current collectors and the formation of lithium polysulfides such as Li_2S_n from the reaction of lithium and sulfur (51).

1.5 Recent Progress of Li-S Battery

1.5.1 Sulfur Active Materials

To overcome the challenges stated above, many efforts have been dedicated to improving the performance of the Li-S battery by enhancing the cathode properties. The development of the sulfur cathode materials can be divided into several categories: sulfur-carbon composite, sulfur-graphene composite, and sulfur-polymer composite. During the past decades, various kinds of sulfur-carbon (S-C) composites have been developed with the aim to reduce the polysulfide diffusion out of the cathode and to increase the conductivity of the electrode. Early work on this subject was performed by Shim et al., (43) who reported that more than 10% carbon black is necessary to meet cathode conductivity. The capacity fading was influenced by the carbon content of the electrode. An increase in the carbon content of the cathode generally resulted in higher initial capacity but faster capacity fading. Another example is the composite based on a highly porous carbon (HPC) material with good conductivity and high specific surface area (1500 m^2/g). After using HPC as the conductive matrix and adsorbent agent for polysulfides, the Li-S cell presented a capacity of 770 mAh g^{-1} at 110 cycles (52). A novel concept regarding the S-C composite is the nanostructured polymer-modified (polyethylene glycol) mesoporous carbon sulfur composites (CMK-3/S nano-composite) as reported by Ji et al. (23, 35). In this composite, the close contact between carbon frameworks and sulfur increases the utilization of sulfur active material, and the nano-pores accommodate volume changes of the sulfur species during cycling. Furthermore, the polymer coating on the surface of the composite prevents the PS from diffusing out of the composite particles. This approach proves to be very effective for improving the performance of the Li-S battery with low sulfur-loading cathode. However, this strategy is still not satisfactory for those with high sulfur-loading cathode.

Carbon nanotubes offer a great opportunity for the design of S-C composites, in which the carbon nanotubes not only trap PS but also serve as a reservoir for the redox reaction of PS. An example is given by Ji et al and Zheng et al. who encapsulated sulfur within the porous carbon nanofibers (CNFs) (53) and reported about a novel conductive sulfur-containing nanocomposite cathode material, which was prepared by heating a mixture of sublimed sulfur and multi-walled carbon nanotubes (MWNTs) in certain conditions (54). The Li-S cell containing this type of cathode shows considerable improvement in the capacity retention and prevents redox shuttle behavior, which is attributed to the fact that the MWNTs not only strongly adsorb the sulfur and resulting PS within the nanotubes but also are an excellent electronic conductor (55).

Graphene is a 2-dimensional crystalline allotrope of carbon; it consists of planar sheets of carbon atoms and has high electrical conductivity. Due to the superior electrical conductivity, high specific surface area of over 2600 m^2/g, and excellent chemical tolerance, graphene has attracted considerable attention in the research of electrochemical energy storage (56-58).

In addition, Li et al. (59) obtained excellent cycling performance by coating a reduced graphene oxide (RGO) onto the S-C nanocomposite. The Li-S cell with this cathode material showed a specific capacity of 667 mAh g^{-1} and a coulombic efficiency of 96% at 0.95C even after 200 cycles. This excellent performance is partially attributed to the strong adsorption of PS on the RGO coating layer in addition to the highly conductive carbon framework that efficiently prevents the diffusion of PS out of the cathode structure.

In order to further enhance the electrical conductivity of sulfur active materials, more intimate connection between the sulfur active material and the supporting conductive network can be established by attaching sulfur active species onto conductive polymer backbones or encapsulating sulfur active species within conductive polymer shells. For example, Polyacrylonitrile (PAN) is an excellent precursor for the conductive polymer of sulfur-polymer composites (60, 61). The rate capability of sulfurized polyacrylonitrile (SPAN) can be further improved by the incorporation of MWCNTs, in which the MWCNTs enhance the structural stability and electronic conductivity of SPANs (62,63). In the same line of work, a pyrolyzed PAN-sulfur-graphene nanosheet (pPAN-S-GNS) composite was prepared by impregnating sulfur into a PAN-GNS composite synthesized by in-situ polymerization of acrylonitrile and chemical reduction of graphene oxide (Figure 5) (64). With 4 wt% GNS added, the composite showed a specific capacity of 800 mAh/g at relatively high C-rates (up to 6C) and a 99.9% of coulombic efficiency. The excellent performance is attributed to the three-dimensional GNS networks that enhance electronic conductivity and facilitate distribution of the active material in the composite.

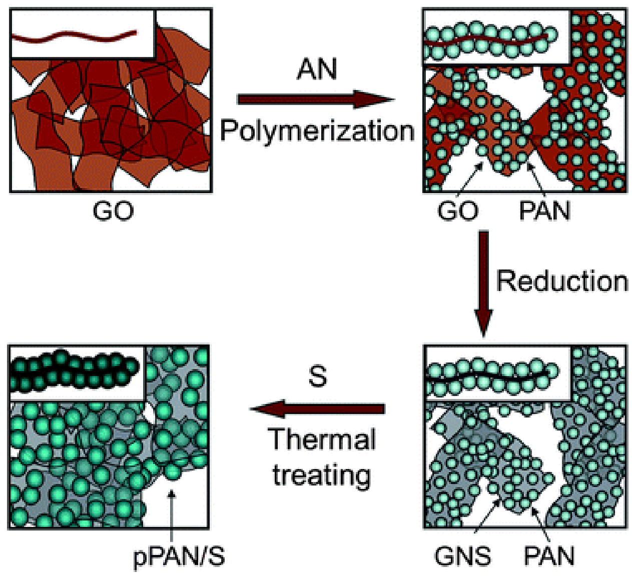

Figure 5**.** Schematic diagram of the in situ polymerization and synthesis of the pPAN-S/GNS composite, in which the insets are cross sectional views of the samples. (64)

It is evident that the conductive polymer coating on the surface of sulfur active cathode material, either being bare elemental sulfur or S-C composite, is beneficial in several ways to the successful development of composite sulfur cathodes (65-80). The proven benefits include increasing the electronic conductivity, facilitating sulfur distribution, alleviating PS dissolution and the loss of sulfur active material during charge/discharge cycling.

1.5.2 <u>Binder</u>

The discharge procedure results in significant volume changes. The polymer binder that ensures the physical integrity of the cathode thus is needed to be capable of retaining the highly porous structure during the cycling process. Conventional binders such as polyvinylidene fluoride (PVDF) fail to retain structural integrity because they become swollen or gelled by the electrolyte solvents. On the other hand, due to the high reactivity of PS, polymers that contain functional groups susceptible to nucleophilic attack may not be appropriate for the binder of the sulfur cathode. Polymer binder in the Li-S battery is more than an "adhesive" to ensure the mechanical integrity of the sulfur cathode. An ideal binder for the Li-S battery should be able to not only endure the structural changes of the electrode, but facilitate ion transport in the charge-discharge processes.

Polymers such as Nafion, (81) blend of polyvinyl pyrrolidone (PVP) and polyethyleneimine (PEI), (82) and cross-linked vinyl ethers (83) are shown to lead to good cycling performance of the Li-S battery. In several accounts PEO was studied as the binder (84,85) and found to function similarly to the PEO coating on the sulfur cathode and PEGDME solvent in the electrolyte, which trap PS and suppress the passivation of the cathode surface (84).

A class of water-based binders shows promising results in the Li-S battery systems. Wang et al. (86) chemically oxidized β-cyclodextrin (β-CD) into water soluble carbonyl-β-cyclodextrin (C-β-CD), and used C-β-CD as the binder for a SPAN-based cathode. As shown in Figure 6, compared with the PVDF and polytetrafluoroethylene (PTFE) binders, C-β-CD was shown to assist the distribution of sulfur active material and improve the mechanical stability of the electrode upon cycling, leading to the improved cycling performance. Other water-soluble or water-dispersible binders include Na-alginate, (87) polyacrylic acid (PAA), (88) poly (acrylamide-co-diallyldimethylammonium chloride) (AMAC) (89), styrene-butadiene rubber (SBR)-carboxymethyl cellulose (CMC), (90,91) and PTFE/CMC. (92) As demonstrated by AMAC binder, (89) the waster-based binders feature low swellability in the organic liquid electrolytes. As a result, during cycling these binders are able to remain the highly porous structure of the sulfur cathode, which leads to better capacity retention. Another well-studied water-soluble binder is gelatin-based natural polymer. (93-98)

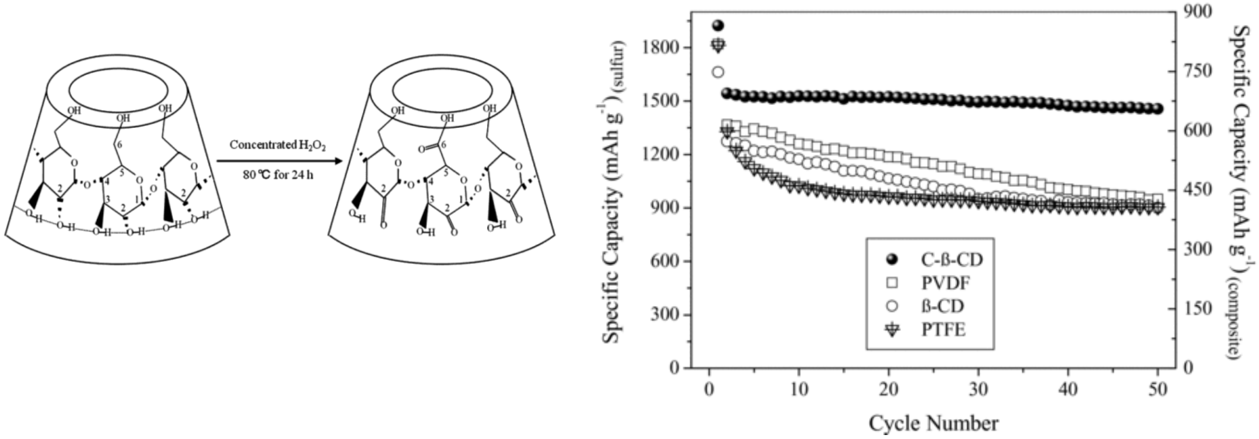

Figure 6. Schematic reaction of β-CD with H2O2 (left); cycle performance of cathodes with β-CD, C-β-CD, PVDF, and PTFE binders at 0.2 C (right). (86)

1.5.3 <u>Electrolyte</u>

Due to the high solubility of PS in the organic electrolytes and the high reactivity of PS with the electrolyte components, common electrolytes used in Li-ion batteries are not suitable for the Li-S battery. For example, Barchasz et al, (99) reported that carbonate solvents severely react with PS, and therefore cannot be used in the electrolyte of the Li-S batteries. It is also reported (100) that in discharge, PS may precipitate out of the electrolyte in the forms of elemental sulfur and Li_2S_2 or Li_2S due to the disproportionation, which not only clogs the pores of separator but also makes these sulfur species electrochemically inactive. This results in the loss of sulfur active materials and the capacity fading of the Li-S battery. In view of the battery performance, an ideal electrolyte for the Li-S battery should be able to solvate and stabilize PS, and capable of forming SEI on the Li surface to protect the Li anode from reaction with PS. Recent efforts regarding the Li-S battery electrolytes are summarized in the following sections:

Solvent

Since carbonate solvents are chemically incompatible with the Li-S chemistry and the voltages for charging Li-S batteries are not more than 3 V, the linear and cyclic ethers seem to be the best choice for the solvent of Li-S battery electrolytes. Therefore, most of studies have been focused on the ether solvents, including 1,2-dimethoxyethane (DME), 1,3-dioxolane (DOL), tetra(ethylene glycol)dimethyl ether (TEGDME), and their mixture. It is unlikely that a single solvent will satisfy all requirements for Li-S battery electrolytes. A practical solution is to use a mixture of solvents and additives. Among common ethers, DME has a good ability to dissolve elemental sulfur and PS, and to stabilize PS, whereas DOL is superior for forming a stable SEI to protect metallic Li from corrosion (101). Therefore, the combination of DME and DOL has become the most popular solvent system for Li-S battery electrolytes, and the electrolytes based on their mixture have been often employed as the baseline for the evaluation of new electrolytes.

As reported by Céline Barchasz, (99) ether solvents offer interesting features, making it possible to improve the electrochemical performance by combining different ether solvents. This is because ether chain length affects the solvation ability. The solvents DME, diethylene glycol dibutyl ether (DEGDBE) and DOL can dissolve PS to some extent, which induces the redox shuttle and leads to low coulombic efficiency. Since the electrolytes with these solvents often lead to fast active material precipitation and positive electrode passivation, polyethylene glycol dimethyl ether (PEGDME) has been used to mitigate these problems. The incorporation of PEGDME is shown to alleviate the buildup of the electrode passivation layer and increase the length (capacity) of the second discharge voltage plateau. By using PEGDME as the co-solvent, a discharge capacity of about 1100 mAh g^{-1} was reached for the first discharge of a Li-S cell, which remained at 550 mAh/g after 10 cycles.

In this regard, Wang et al. (102) observed that sulfur has appropriate solubilities and undergoes a three-step reduction in the PEGDME-based electrolyte in comparison with the DOL/DME electrolyte in which sulfur shows a typical two-step reduction process. These results indicate that the discharge mechanism of the Li-S battery is quite complicated and involves many intermediate compounds. Shim et al. (43) studied PEGDME 250 and 500 solvents, and found that these solvents redcued the redox shuttle of PS and accordingly increased the coulombic efficiency of the Li-S battery. In particular, the Li-S cell containing the PEGDME 500 electrolyte showed the best cycling behavior, yielding a specific capacity of more than 100 mAh/g after 600 cycles. This is attributed to the higher viscosity and better ability in stabilizing PS of these solvents. The viscocity generally influences the penetration of the liquid electrolyte into the sulfur cathode and the diffusion of the dissolved PS. Meanwhile, the electrolyte affects the disproportation of PS, the utilization of sulfur active material and the capacity retention of the Li-S battery.

Regarding the effect of solvent composition on the performance of the Li-S cell, Kim et al. (103) reported that the specifc capacity and capacity retention depend on the nature of the solvents as well as the composition of mixed solvents. Because DOL solvent forms a better SEI with the Li anode, the specific capacity of the Li-S battery for a DOL solvent system is shown to increase with the content of DOL within a limited content range.

Ruy et al. (104) investigated the effect of temepature on the discharge behavior of the Li-S cell with TEGDME-based electrolytes. The specific capacity of the Li-S cell fell greatly as the temperature decreased to −10°C due to a dramatic increase in the viscosity of electrolyte, especially in the presence of PS. In addition, TEGDME freezes at −27 ◦C, which also limits the operation temperature range of TEGDME-based electrolytes. In order to reduce the electrolyte viscosity and enable the Li-S battery to operate at low temperature, the TEGDME is often combined with the solvents having low viscosity and low melting point, such as DME and DOL.

In the cycling of the Li-S battery, PS undergoes a series of reduction and oxidation reactions, and the chemical equilibriums in the electrolyte solution vary with the PS concentration (33). Since the PS concentration is determined by the amount of liquid electrolyte in the battery, there is an optimized electrolyte/sulfur (E/S) ratio for the cyclability of Li-S cell system. The E/S ratio affects the cell's performance through the viscosity of PS solution and the chemical stability of PS in the solution. It is shown that high PS concentration favors suppressing the disproportionation of PS but increases the viscosity of the solution, which oppositely affects the cycling performance of the Li-S battery. That is, the reduced disproportionation increases the utilization of sulfur active material, whereas the increased viscosity reduces the ionic conductivity of the electrolyte. Interaction of these two opposite effects leads to an optimized E/S ratio for each Li-S cell system. From Li-S coin cells, Zhang obtained an optimized E/S ratio of 10 mL/g for a 0.25 m $LiSO_3CF_3$-0.25 m $LiNO_3$ DME: DOL (1:1 wt.) electrolyte. By using the optimized E/S ratio (10 mL/g), the Li-S cell with a cathode containing 77% sulfur and 2 mg/cm^2 sulfur-loading is shown to retain a specific capacity of 780 mAh/g after 100 cycles at 0.5 mA/cm^2 between 1.7 V and 2.8 V.

Similar results were demonstrated by Choi et al. (105), who reported that a large amount of electrolyte (i.e., high E/S ratio) led to higher initial capacity but faster capacity fading. They explained that the high amount of electrolyte increased the utlization of sulfur active material through the dissolution of PS, and meanwhile resulted in more loss of sulfur active material in the form of insoluble Li_2S and Li_2S_2 through the disproportionation of PS. They also showed that the Li-S cell had good capacity retention when small amount of electrolyte was used as long as the bettery components (sulfur cathode, separator and Li anode) could be properly wetted by the liquid electrolyte.

The effect of electrolyte composition on cell performance for a TEGDME/DOL binary solvent system was investigated by Barchasz et al. (106) It was shown that the best TEGDME/DOL ratio was about 15/85 by volume, which formed a high conductive electrolyte with good solvation ability for the PS and lithium bis(trifluoromethanesulfonyl) imide (LiTFSI). The presence of DOL was shown to improve the ionic conductivity and discharge capacity by reducing the electrolyte viscosity. However, a high amount of DOL negatively affected the performance of the Li-S battery since the conductivity severly decreased. This result suggests that the viscosity may not be the only factor determining the ionic conductivity of the electrolyte. The dielectric constant and the donor number of the solvents seem not to be sufficient to explain the ionic conductivity and lithium salt's dissociation. A more reasonable explaination could be that the high amount of DOL promotes the disproportanation of PS, which produces neither soluble nor conductive elemental sulfur, Li_2S and Li_2S_2. Due to precipatation, these sulfur species (disproportionation products) become electrochemically inactive and meanwhile clog the pores of the separator, resulting in low sulfur utilization and high polarization.

Lithium salt has been shown to affect the electrochemical performance of Li/S cells. In comparison with $LiCF_3SO_3$, LiTFSI provides higher ionic conductivity (106). The concentration of lithium salts affects the ionic conductivity of the electrolyte through the salt dissociation, charge carrier number, and ionic mobility, which generally results in a maxinum conductivity in a certain salt concentration region. A more recent work by Suo et al. showed that when the salt concentration in a LiTFSI-TEGDME electrolyte is increased until reversed to a "solvent-in-salt" system, the Li^+ ion transfer number is dramatically increased to 0.73, and the redox shuttle of PS is greatly reduced (107). Using such an electrolyte, the Li-S cell was able to retain over 800 mAh/g at 0.2C for 100 cycles with nearly 100% coulbomic efficiency. The similar approach was pursued by Dokko et al., (108) who first made a glyme–Li salt molten complexe and then mixed it with a nonflammable hydrofluoroether solvent (1,1,2,2–tetrafluoroethyl 2,2,3,3–tetrafluoropropyl ether (HFE)) to form a [Li(glyme)1][TFSA]/HFE electrolyte, which resulted in improved performancers, including higher coulombic efficiency, better cycle stability, and higher rate capability.

Ionic Liquid

An ionic liquid typically consist of a weakly Lewis acidic cation and a weakly Lewis basic anions, and features the non-flammability and involatility. Special significance of the ionic liquids in the Li-S battery is their weakly Lewis acidic cations, which are capable of stabilizing polysulfide anions. Based on the "hard and soft (Lewis) acids and bases" (HSAB) theory, the cation of ionic liquid is a soft acid, and the polysulfide anion is a soft base, and their combination leads to a stable compound (salt). In addition to stabilizing the PS anion, the ionic liquid also affects the mobility of PS anion (and redox shuttle issue) through the interaction between the ionic liquid cation and

PS anion. Ionic liquids have been used in Li-S batteries in two forms: (1) employ as an "ionic" solvent to dissolve a lithium salt, and (2) add as an additive into the conventional liquid electrolyte.

Yuan et al. (109) reported a binary salt electrolyte based on a N-methyl-N-butyl-piperidinium bis(trifluoromethanesulfonyl) imide room temperature ionic liquid (PP14-RTIL) and a LiTFSI lithium salt. Cyclic voltammetry (CV) results showed that the RTIL electrolyte has a wide potential window of 5.2-0.15 V (vs. Li) and is chemically stable with metallic lithium and sulfur active materials. The Li-S cells using the ionic liquid electrolyte showed an initial capacity of 1055 mAh g^{-1} and retained a reversible capacity of 750 mAh g^{-1} after a few of cycles.

In order to reduce the viscosity and increase the ionic conductivity of the ionic liquid electrolyte, Wang et al. (102) added a small amount of DME as the co-solvent into a N-methyl-N-propylpiperidinium bis(trifluoromethanesulfonyl)imide-LiTFSI (PP13-TFSI) ionic liquid electrolyte. It was observed that the PP13-TFSI/DME electrolyte afforded outstanding capacity retention and high coulombic efficiency for the Li-S cell. In the similar approach, Park et al. made an ionic liquid electrolyte by mixing a N,N-diethyl-N-methyl-N-(2-methoxyethyl)ammonium bis(trifluoromethanesulfonyl)amide (DEME-TFSI) with a LiTFSI salt (110) , and compared it with a 0.98 M LiTFSI/ TEGDME liquid electrolyte. The results indicated that the ionic liquid electrolyte cell outperformed the liquid electrolyte cell. The performance improvement by the ionic liquid electrolyte was attributed to the fact that the ionic liquid suppresses the redox shuttle of PS, which results in a higher coulombic efficiency for the Li-S cell.

Polymer electrolyte

Leakage and flammability are the intrinsic problems for all liquid electrolytes, and the severe redox shuttle of PS originates from the high solubility and fast diffusion of PS in the liquid electrolyte. For these reasons, polymer electrolytes have been proposed to overcome the problems of liquid electrolytes. Based on the composition and ionic conduction mechanism, the polymer electrolytes can be classified as the solvent-free solid polymer electrolyte (SPE) and gel polymer electrolyte (GPE).

Solid polymer electrolyte

Polyethylene oxide (PEO) is the most intensively studied polymer for solvent-free SPE, in which the Li^+ ions are solvated by the ether oxygen atoms in PEO chains and conducted through the segmental motion of the PEO chains (111). The ionic conduction in such SPEs mainly occurs in the amorphous phase, therefore, an elevated temperatures (>60 ^oC) is needed to retain sufficient conductivity. In this effort, Carins (112) and Kim (113) independently studied PEO-based electrolytes for the Li-S cells, and showed that Li-S cells had a high initial capacity of 1600 mAh/g, followed by fast fading with further cycling. This unsatisfactory performance can be attributed to the low ionic conductivity of the SPE and the insulating nature of elemental sulfur and its reduction products. Unlike in the liquid electrolytes, in the SPE the sulfur reduction products are unable to diffuse off the carbon surface, but instead accumulate on the carbon surface as an insulating passivation layer to block the outer sulfur from electrical contact with the carbon. As a result, the SPE Li-S battery suffers from low utilization of sulfur active material and fast capacity fading. Shin et al. (114) found that ball-milling could effectively reduce the crystallinity of PEO, and therefore improved the ionic conductivity of SPE. This led to a significant improvement in the specific capacity and capacity retention of the Li-S battery.

Gel polymer electrolyte

In order to overcome the low ionic conductivity of solvent-free SPEs, PEO-miscible electrolyte solvent has been used as the plasticizer to promote the segmental motion of PEO chains. When the amount of the liquid plasticizer reaches such a level that the ionic conduction is dominated by the liquid-in-polymer, instead of the segmental motion of polymer chains, the SPE becomes a GPE. The GPE combines the advantages of the polymer electrolyte (high viscoelasticity) and liquid electrolyte (high ionic conductivity), and is of great significance in the Li-S batteries. The earliest practice for this concept was to plasticize the PEO-based SPE with a TEGDME solvent, (115) however, latter the fluorinated polymer based GPEs, such as those based on PVDF (116) and poly (vinylidenefluoride)-hexafluoropropylene (PVDF-HFP) copolymer (117), have been more intensively studied due to the easiness of *in-situ* formation of these GPEs by activating a porous polymer membrane with a liquid electrolyte. The GPEs typically have an ionic conductivity ranging from 10^{-4} to 10^{-3} S/cm at room temperature, depending on the type and amount of liquid electrolyte. Interestingly, ionic liquid is found to be miscible with PVDF-HFP polymer and has been successfully prepared into a GPE, showing good thermal property and stability towards oxidation (118). The Li-S cell with this GPE exhibited comparable capacities as the liquid electrolyte-based cells and had high coulombic efficiencies of over 95%, indicating that the GPE effectively suppresses the redox shuttle of PS.

Composite polymer electrolyte

PEO-based composite electrolyte with inorganic fillers, such as Al_2O_3, (113) γ-$LiAlO_2$, (119) and SiO_2 (120), have been developed for the Li-S batteries. In this practice, Scrosati (121) used a nano-ZrO_2-PEO-$LiCF_3SO_3$ membrane as the separator and Li_2S as the sulfur active material to assemble an all-solid-state Li-S cell, in which the Li_2S is in the discharged state and can be coupled with the carbon or silicon anode material to build a metallic lithium- free lithium-ion battery. The cell delivered a specific capacity of 900 mAh/g at 90 °C and decreased to less than 400 mAh/g at 70 °C, clearly indicating the effect of ionic conductivity of the solid-state electrolyte. On the other hand, the cell had a coulombic efficiency of over 99% even at high temperatures, which validates the effectiveness of this solid-state electrolyte in preventing polysulfide shuttling redox. Other composite gel polymer electrolytes (CGPEs) are based on a fluorinated polymer and an inorganic filler, such as one consisting of a PVDF-HFP and a nano-sized silicate (122) or mesoporous silica (123). The CGPEs are typically made by first preparing a porous composite membrane and then gelling it with a liquid electrolyte. The incorporated inorganic filler is found to be capable of adsorbing PS, being favorable for increasing coulombic efficiency and capacity retention over prolonged cycles. The CGPE can also be prepared with high filler content in favor of high conductivity and wettability. A composite membrane containing at least 50% SiO_2 in high-molecular weight PEO has been made in the form of an electrode-supporting electrode-membrane-assemble (EMA), (124) a freestanding membrane, (125) or a coating on a conventional separator. The high filler content enables high uptake of liquid electrolyte or ionic liquid without dimensional shrinkage. However, the high amount of SiO_2 adsorbs PS and makes these PS electrochemically inactive by trapping PS in the membrane, resulting in lower specific capacity.

Ceramic solid state electrolyte

The ceramic solid-state electrolyte is the most effective approach to avoid the PS dissolution and the resulting redox shuttle. In this approach, nearly all efforts have been centered on the Li_2S-P_2S_5 (LPS) family of solid electrolyte glasses mainly because of their chemical compatibility with the sulfur cathode and metallic Li. Liang et al assembled an all-solid-state Li-S cell by using a Li_3PS_4 (namely a form of the $3Li_2S$-P_2S_5 glass) as the solid electrolyte and a Li_3PS_{4+n} (n = 2~8) as the cathode (125). In their cells, nano-structured electrolyte and cathode materials allowed for intimate contact to reduce the particle boundary resistance; the similar chemistry of the electrolyte and cathode materials allowed to form a favorable electrolyte-electrode interface. As a result, the all-solid-state Li-S cell showed a capacity of 1200 mAh/g after 300 cycles at 60 °C. Thio-LISICON ($Li_{3.25}Ge_{0.25}P_{0.75}S_4$), a version of the Ge-doped LPS glasses, has an ionic conductivity of 2.2×10^{-3} S cm^{-1} at 25 °C, (126,127) and is demonstrated to be suitable for the solid-state electrolyte used in the Li-S battery. Hayashi et al systematically studied the Li_2S-P_2S_5 glass electrolytes by coupling it with sulfur/copper (128,129) or sulfur/carbon (130) composite cathodes. In particular, an all-solid-state cell with sulfur/carbon composite cathode and Li_2S-P_2S_5 electrolyte could be cycled over a wide temperature range from −20 °C to 80 °C. The cell performance remained above 800 mAh/g at ambient temperature for 200 cycles with coulombic efficiency of about 100%. By ball-milling to reduce the crystallinity and particle size of the electrode and electrolyte materials, an all-solid-state Li_2S/carbon cell was shown to have a specific capacity of 700 mAh/g when cycled between 3.6 V and 0.6 V at 25 °C (131).

Electrolyte additives

With the aim of eliminating or reducing the mentioned obstacles of Li–S batteries, many electrolyte additives have been studied to improving the Li/S battery electrolytes. The functions of these additives include: (1) protecting the Li anode, (2) enhancing the solubility and stability of PS, and (3) reducing the viscosity of the liquid electrolyte.

The most important finding is (132) that $LiNO_3$ can remarkably inhibit the redox shuttle of PS. Using the $LiNO_3$ additive, Liang et al showed that the Li-S cell had a high coulombic efficiency of 95% and a discharge capacity of ca. 527 mAh/g after 50 cycles. It is believed that on Li anode, the $LiNO_3$ encourages the formation of a passivation film composed of Li_xNO_y and Li_xSO_y, which prevents the electrochemical reduction of PS at the anode and the chemical reduction of PS by metallic Li. Since stripping of Li in the following discharging destroys the already–formed passivation film, new passivation film must be re-formed in the next charging step. Thus, $LiNO_3$ will be slowly consumed with the repeated cycling of the Li-S battery (133) Beside the above, Zhang observed that $LiNO_3$ might be reduced on the cathode at below 1.6 V, which adversely affected the cycling performance of the Li-S batteries (31), and concluded that the $LiNO_3$ additive is helpful for the Li-S battery only when the irreversible reduction on the sulfur cathode is avoided. This can be done easily by raising the discharge cutoff voltage of the Li-S batteries above 1.7 V.

Lithium bis(oxalato) borate (LiBOB) has been studied as the electrolyte additive in a concentration range of 1-10 wt.% by Xiong et al. (134) The Li-S batteries containing the LiBOB additive demonstrate improvement in both the discharge capacity and cycle performance, with a maximum discharge capacity of 1,191 mAh g^{-1} when a 4 wt.% LiBOB was added. Based on the electrochemical impedance spectroscopy (EIS) and SEM analysis, this improvement was found to be due to the formation of a passivating surface film on the Li anode, which reduces the parasitic reaction between PS and the Li anode.

In another study by Lin et al., P_2S_5 was shown to enhance the dissolution of PS and protect the Li anode (135). In the electrolyte, P_2S_5 combines insoluble Li_2S and Li_2S_2 to form soluble LPS complexes, which suppresses the precipitation out of sulfur species out of the electrolyte. On the Li anode, P_2S_5 combines with pre-deposited Li_2S to form a highly conductive Li_3PS_4 passivation layer, which protects the Li anode from reactions with PS and meanwhile reduces the cell's polarization. As a result, both the specific capacity and capacity retention of the Li-S cell are significantly improved, which leads to a specific capacity of 800 mAh/g after 40 cycles.

1.5.4 New Concepts

In recent years, many new concepts have been proposed to improve the performance of Li-S batteries, which include the use of novel materials and innovative cell designs, as discussed below.

Binder-Free Cathode

Zu et al. (136) introduced a binder-free, interwoven S-C cathode, in which a binder-free carbon nanofiber (CNF) paper was used as the current collector and elemental sulfur was directly impregnated into the pores of CNFs. This cathode has the advantages of low manufacturing cost and high sulfur-loading in comparison to the conventional sulfur cathodes. The outstanding improvement of this cathode is because (1) the 3D interwoven structure of the CNF paper allows sulfur reactions within a confined environment and (2) CNFs offer long and continuous electron conduction pathway. SEM and x-ray diffraction (XRD) analyses reveal that crystalline Li_2S species are found within the large interspaces of the 3D electrode after the first discharge, which avoids the formation of a dense passivation layer on the surface of the cathode. A Li-S battery with such a cathode exhibited an initial capacity of 1094 mAh g^{-1} after 80 cycles at a C/5 rate and coulombic efficiencies of more than 98% with a sulfur-loading of 1.7 mg/cm^2. After increasing the sulfur loading to 5.1 mg/cm^2, a stable reversible capacity of 900 mAh/g was obtained, making this battery configuration very promising for practical applications. In another study, Hassoun et al. (137) assembled a new type of Li-S cells by starting with a carbon–lithium sulfide (C-Li_2S) composite cathode. Cycling tests demonstrate that this cell has a good performance, high reversibility, and high coulombic efficiency. It was verified by *in-situ* XRD that the Li_2S formed after each discharging step can be converted into sulfur in following charge and re-converted back to Li_2S again in the next discharge process. In the same principle, Fu et al. (138) reported a novel cathode configuration which was composed of pristine Li_2S powder sandwiched between two layers of self-weaving, binder-free carbon nanotube (CNT) papers. The excellent performances of these cells are attributed to: (1) efficient electron conduction within the sandwiched electrode; (2) fast ion transport through the nano-space within the carbon nanotube electrode; and (3) trapping of dissolved PS within the sandwiched electrode.

Carbon Paper Interlayer

As shown in Figure 7, Su et al (139) designed a new cell configuration by placing a bifunctional microporous carbon paper between the cathode and separator, which resulted in significant improvement in the capacity retention of the cell. This interlayer improves the cycling performances of the Li-S cells by on one hand absorbing the PS diffused out of the cathode and on the other hand providing additional reaction sites to accommodate the formed Li_2S_2 or Li_2S. It is shown that the pore size of carbon in the carbon interlayer strongly affects the effectiveness of the improvement. For example, the improvement by a mesoporous carbon paper (micropores ~ 5 nm; mesopores ~6 nm) is not as effective as that by the microporous carbon paper under the same conditions. In a similar work, Zu et al (37) employed a treated carbon paper, prepared by an alcohol-alkaline/thermal treatment of a commercial Toray carbon paper, as the interlayer, and showed that the Li–S cells had an initial capacity of 1651 mAh/g at 1.5–2.8 V at a rate of C/5. This excellent capacity is attributed to the fact that the treatment introduced hydroxyl functional groups and micro-cracks into the carbon surfaces, which enhances the PS's chemo-adsorption and the carbon paper's surface areas. The insertion of the carbon interlayer generally reduces the interfacial resistance of sulfur cathode and delocalizes the PS in the electrolyte. The interlayer configuration offers a possible approach for making Li-S batteries more viable for practical applications.

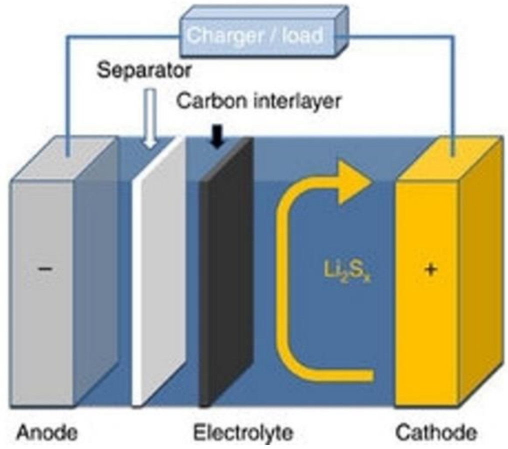

Figure 7**.** Schematic configuration of a Li–S cell with a carbon interlayer inserted between the sulfur cathode and the separator. (139)

Alternative Anode

Use of lithium metal is one of the main causes for the safety issues of the Li-S batteries. Therefore, much effort has been devoted to the development of the lithium metal-free anodes. For example, Yang et al. (140) proposed a Li_2S-mesoporous carbon composite as the starting cathode and silicon nanowires as the anode. Thus, the Li-S cell is assembled in the discharged state, and Li_2S is the only source for Li^+ ions. By overcoming the poor electrical conductivity and volume expansion of the sulfur cathode and silicon anode, the resulting Li-S Li-ion battery is shown to have four times theoretical capacity of the current Li-ion battery technology. Following the above concept, Hassoun et al. (141) assembled a lithium metal-free silicon–sulfur cell using a high-rate S-C composite cathode, a prelithiated Si-C nano-composite anode, and a glycol-based electrolyte. Results showed that such a cell could deliver a specific capacity of about 500 mAh/g, which declined to 300 mAh/g after 100 cycles. Based on the same cell chemistry, Liu et al. (142) used elemental sulfur as the cathode material and prelithiated silicon nanowires as the anode material.

They stated that by a 20 min prelithiation process, the amount of lithium equivalent to a capacity of ~2000 mAh g^{-1} Si could be lithiated into the SiNWs, and that the amount of prelithiation can be controlled by changing the prelithiation time. Using this anode material, the Li-free Li-S cell can maintain ~80% of its initial capacity after 10 cycles, however, the capacity fades with a constant slope throughout cycling.

Catholyte

Based on the fact that long-chain PS are highly soluble in the organic electrolytes, Zhang et al. (143) used a 0.25 m Li_2S_9 solution as the catholyte and a porous carbon electrode as the current collector to build a "liquid" Li-S cell. In order to protect the Li anode from corrosion and increase the cell's coulombic efficiency, $LiNO_3$ is used as a co-salt in the Li_2S_9 catholyte. Results indicate that Li/Li_2S_9 "liquid" cells are superior to the conventional Li/S cells in specific capacity and capacity retention. The capacity of such cells is affected by two factors: (1) the porosity of the carbon electrode, and (2) the PS concentration in the catholyte and the amount of catholyte in the cell. Specifically, the former determines how much Li_2S can be accommodated by the porous carbon electrode, and the latter determines how much sulfur active materials can be contained in the battery.

In order to avoid the difficulty of filling highly viscous PS catholyte in the battery assembly and increase the PS concentration of the catholyte, Zhang (101) further suggested that the "liquid" Li-S cell could be built by using a highly porous carbon cloth and a porous sulfur paper. This innovative technique led to a Li/S cell having an initial capacity of 778 mAh/g, equaling to an area specific capacity of 10.1 mAh/cm^2. The other significance of this work is to reveal that the initial mixing state of the sulfur and carbon is not important for the performance of the Li-S batteries as elemental sulfur will eventually converted to highly soluble Li_2S_8 and dissolve into the electrolyte in the first discharge.

Fu et al. (144) demonstrated the similar approach by using a PS catholyte and a self-weaving and free-standing MWCNT paper as the carbon electrode. Due to the high porosity and high conductivity of the MWCNT paper, the catholyte-based Li/S cell showed high specific capacity of 1411 mAh/g after 50 cycles at C/10 rate and much improved rate capability, as indicated by a very similar capacity at C/10, C/5, and C/2.

Beside the sealed cell design, the PS catholyte also has been proposed to build an opened semi-flow battery (145). In this design, the PS catholyte solution is stored in a separate tank, and is pumped into the cell as needed, however, the anode still uses metallic Li and is sealed in the cell. To maintain the flow of the PS cathode solution, the PS species are controlled to cycle only in the solution range (i.e., $n \geq 4$ in Li_2S_n). A proof-of-concept cell has shown a constant capacity of 200 mAh/g over 2000 cycles. This excellent cyclability is attributed to the fact that the operation of the PS catholyte is only limited within the solution region without the formation of solid state Li_2S_2 and Li_2S.

Alternatively, the low concentration PS catholyte can be used as the normal electrolyte to provide extra capacity for the conventional Li-S battery. To demonstrate this, Chen et al. (146) used a PS-containing electrolyte to activate the conventional Li-S cell with a C-S composite as the cathode active material. The amount and concentration of PS was shown to affect the capacity as well as sulfur utilization. An optimal concentration of PS was found to be 2 M based on sulfur, which maximized the utilization of sulfur active materials as compared with the PS catholyte of higher concentration. A specific capacity of 1250 mAh/g was obtained after 40 cycles under optimized conditions

CITED LITERATURE

1. Thackeray MM, Wolverton C, Isaacs ED. Electrical energy storage for transportation-approaching the limits of, and going beyond, lithium-ion batteries. Energy & Environmental Science. 2012;5(7):7854-63.

2. Scrosati B, Garche J. Lithium batteries: Status, prospects and future. Journal of Power Sources. 2010;195(9):2419-30.

3. Cuisinier M, Cabelguen PE, Adams BD, Garsuch A, Balasubramanian M, Nazar LF. Unique behaviour of nonsolvents for polysulphides in lithium-sulphur batteries. Energy & Environmental Science. 2014;7(8):2697-705.

4. Scrosati B, Hassoun J, Sun Y-K. Lithium-ion batteries. A look into the future. Energy & Environmental Science. 2011;4(9):3287-95.

5. Armand M, Tarascon JM. Building better batteries. Nature. 2008;451(7179):652-7.

6. Knowles M. Through-life Management of Electric Vehicles. Procedia CIRP. 2013;11(0):260-5.
7. Hickman J. Clean Vehicles. Renewable Energy Focus. 2009(March/April):33-4.

8. Harrop P, Das, R. Hybrid and pure electric cars 2009-2019. 2009.

9. WHITTINGHAM MS. Electrical Energy Storage and Intercalation Chemistry. Science. 1976;192(4244):1126-7.

10. Tarascon JM, Armand M. Issues and challenges facing rechargeable lithium batteries. Nature. 2001;414(6861):359-67.

11. Nishi Y. 2 - Past, Present and Future of Lithium-Ion Batteries: Can New Technologies Open up New Horizons? In: Pistoia G, editor. Lithium-Ion Batteries. Amsterdam: Elsevier; 2014. p. 21-39.

12. Saha P, Datta MK, Velikokhatnyi OI, Manivannan A, Alman D, Kumta PN. Rechargeable magnesium battery: Current status and key challenges for the future. Progress in Materials Science. 2014;66(0):1-86.

13. Aurbach D, Suresh GS, Levi E, Mitelman A, Mizrahi O, Chusid O, et al. Progress in Rechargeable Magnesium Battery Technology. Advanced Materials. 2007;19(23):4260-7.

14. Girishkumar G, McCloskey B, Luntz AC, Swanson S, Wilcke W. Lithium−Air Battery: Promise and Challenges. The Journal of Physical Chemistry Letters. 2010;1(14):2193-203.

15. Bruce PG, Freunberger SA, Hardwick LJ, Tarascon J-M. Li-O2 and Li-S batteries with high energy storage. Nat Mater. 2012;11(1):19-29.

16. Bruce PG, Hardwick LJ, Abraham KM. Lithium-air and lithium-sulfur batteries. MRS Bulletin. 2011;36(07):506-12.

17. Weng W, Pol VG, Amine K. Ultrasound Assisted Design of Sulfur/Carbon Cathodes with Partially Fluorinated Ether Electrolytes for Highly Efficient Li/S Batteries. Advanced Materials. 2013;25(11):1608-15.

18. Zhang SS. Liquid electrolyte lithium/sulfur battery: Fundamental chemistry, problems, and solutions. Journal of Power Sources. 2013;231(0):153-62.

19. Nelson J, Misra S, Yang Y, Jackson A, Liu Y, Wang H, et al. In Operando X-ray Diffraction and Transmission X-ray Microscopy of Lithium Sulfur Batteries. Journal of the American Chemical Society. 2012;134(14):6337-43.

20. Yang Y, Zheng G, Misra S, Nelson J, Toney MF, Cui Y. High-Capacity Micrometer-Sized Li2S Particles as Cathode Materials for Advanced Rechargeable Lithium-Ion Batteries. Journal of the American Chemical Society. 2012;134(37):15387-94.

21. Chen L, Shaw LL. Recent advances in lithium–sulfur batteries. Journal of Power Sources. 2014;267(0):770-83.

22. Barchasz C, Molton F, Duboc C, Leprêtre J-C, Patoux S, Alloin F. Lithium/Sulfur Cell Discharge Mechanism: An Original Approach for Intermediate Species Identification. Analytical Chemistry. 2012;84(9):3973-80.

23. Zhang B, Qin X, Li GR, Gao XP. Enhancement of long stability of sulfur cathode by encapsulating sulfur into micropores of carbon spheres. Energy & Environmental Science. 2010;3(10):1531-7.

24. Petrucci H, Herring, and Madura. General Chemistry: Principles and Modern Applications. . 9th ed: Prentice Hall; 9 edition; 2007.

25. Ltd WC. Electropaedia Battery Technology Glossary 2005. Available from: http://www.mpoweruk.com/glossary.htm.

26. Battery University 2014. Available from http://batteryuniversity.com/learn/article/battery_definitions.

27. Battery Glossary 2014. Available from http://www.enviroharvest.ca/battery_glossary.htm.

28. Natalia A. Cañasa NWaKAF. Importance of in-situ techniques in the investigation

of rechargeable lithium-sulfur batteries. Batteries 2nd Workshop on Lithium sulfur batteries. 2013.

29. Shizhao X, Xie K, Xiaobin H, Yan D. Effect of LiBOB as additive on electrochemical properties of lithium-sulfur batteries. Ionics. 2012;18(3):249-254254.

30. Cañas NA, Wolf S, Wagner N, Friedrich KA. In-situ X-ray diffraction studies of lithium–sulfur batteries. Journal of Power Sources. 2013;226(0):313-9.

31. Zhang SS. Role of LiNO3 in rechargeable lithium/sulfur battery. Electrochimica Acta. 2012;70(0):344-8.

32. Zhang SS, Tran DT. A proof-of-concept lithium/sulfur liquid battery with exceptionally high capacity density. Journal of Power Sources. 2012;211(0):169-72.

33. Zhang S. Improved Cyclability of Liquid Electrolyte Lithium/Sulfur Batteries by Optimizing Electrolyte/Sulfur Ratio. Energies. 2012;5(12):5190-7.

34. Akridge JR. Lithium Sulfur Rechargeable Battery Safety. Moltech Corporation dba Sion Power Corporation, 2001.

35. Ji X, Lee KT, Nazar LF. A highly ordered nanostructured carbon-sulphur cathode for lithium-sulphur batteries. Nat Mater. 2009;8(6):500-6.

36. Jeong S, Bresser D, Buchholz D, Winter M, Passerini S. Carbon coated lithium sulfide particles for lithium battery cathodes. Journal of Power Sources. 2013;235(0):220-5.

37. Zu C, Su Y-S, Fu Y, Manthiram A. Improved lithium-sulfur cells with a treated carbon paper interlayer. Physical Chemistry Chemical Physics. 2013;15(7):2291-7.

38. Ji X, Nazar LF. Advances in Li-S batteries. Journal of Materials Chemistry. 2010;20(44):9821-6.

39. Chung K-i, Kim W-S, Choi Y-K. Lithium phosphorous oxynitride as a passive layer for anodes in lithium secondary batteries. Journal of Electroanalytical Chemistry. 2004;566(2):263-7.

40. Lee YM, Choi N-S, Park JH, Park J-K. Electrochemical performance of lithium/sulfur batteries with protected Li anodes. Journal of Power Sources. 2003;119–121(0):964-72.

41. Mikhaylik YV, Kovalev I, Schock R, Kumaresan K, Xu J, Affinito J. High Energy Rechargeable Li-S Cells for EV Application: Status, Remaining Problems and Solutions. ECS Transactions. 2010;25(35):23-34.

42. Chu MY, De Jonghe LC, Visco SJ, Katz BD. Liquid electrolyte lithium-sulfur batteries. Google Patents; 2000.

43. Shim J, Striebel KA, Cairns EJ. The Lithium/Sulfur Rechargeable Cell: Effects of Electrode Composition and Solvent on Cell Performance. Journal of The Electrochemical Society. 2002;149(10):A1321-A5.

44. Peled E, Sternberg Y, Gorenshtein A, Lavi Y. Lithium-Sulfur Battery: Evaluation of Dioxolane-Based Electrolytes. Journal of The Electrochemical Society. 1989;136(6):1621-5.

45. Kolosnitsyn VS, Karaseva EV, Seung DY, Cho MD. Cycling a Sulfur Electrode in Mixed Electrolytes Based on Sulfolane: Effect of Ethers. Russian Journal of Electrochemistry. 2002;38(12):1314-8.

46. Wang W, Wang Y, Huang Y, Huang C, Yu Z, Zhang H, et al. The electrochemical performance of lithium–sulfur batteries with LiClO4 DOL/DME electrolyte. J Appl Electrochem. 2010;40(2):321-5.

47. Wu F, Wu SX, Chen RJ, Chen S, Wang GQ. Electrochemical performance of sulfur composite cathode materials for rechargeable lithium batteries. Chinese Chemical Letters. 2009;20(10):1255-8.

48. Yuan L, Yuan H, Qiu X, Chen L, Zhu W. Improvement of cycle property of sulfur-coated multi-walled carbon nanotubes composite cathode for lithium/sulfur batteries. Journal of Power Sources. 2009;189(2):1141-6.

49. Aihara Y, Bando T, Nakagawa H, Yoshida H, Hayamizu K, Akiba E, et al. Ion Transport Properties of Six Lithium Salts Dissolved in γ-Butyrolactone Studied by Self-Diffusion and Ionic Conductivity Measurements. Journal of The Electrochemical Society. 2004;151(1):A119-A22.

50. Mikhaylik YV, Akridge JR. Polysulfide Shuttle Study in the Li/S Battery System. Journal of The Electrochemical Society. 2004;151(11):A1969-A76.

51. Ryu HS, Ahn HJ, Kim KW, Ahn JH, Lee JY, Cairns EJ. Self-discharge of lithium–sulfur cells using stainless-steel current-collectors. Journal of Power Sources. 2005;140(2):365-9.

52. Lai C, Gao XP, Zhang B, Yan TY, Zhou Z. Synthesis and Electrochemical Performance of Sulfur/Highly Porous Carbon Composites. The Journal of Physical Chemistry C. 2009;113(11):4712-6.

53. Ji L, Rao M, Aloni S, Wang L, Cairns EJ, Zhang Y. Porous carbon nanofiber-sulfur composite electrodes for lithium/sulfur cells. Energy & Environmental Science. 2011;4(12):5053-9.

54. Zheng W, Liu YW, Hu XG, Zhang CF. Novel nanosized adsorbing sulfur composite cathode materials for the advanced secondary lithium batteries. Electrochimica Acta. 2006;51(7):1330-5.

55. Ahn W, Kim K-B, Jung K-N, Shin K-H, Jin C-S. Synthesis and electrochemical properties of a sulfur-multi walled carbon nanotubes composite as a cathode material for lithium sulfur batteries. Journal of Power Sources. 2012;202(0):394-9.

56. Wang J-Z, Lu L, Choucair M, Stride JA, Xu X, Liu H-K. Sulfur-graphene composite for rechargeable lithium batteries. Journal of Power Sources. 2011;196(16):7030-4.

57. Cao Y, Li X, Aksay IA, Lemmon J, Nie Z, Yang Z, et al. Sandwich-type functionalized graphene sheet-sulfur nanocomposite for rechargeable lithium batteries. Physical Chemistry Chemical Physics. 2011;13(17):7660-5.

58. Wang H, Yang Y, Liang Y, Robinson JT, Li Y, Jackson A, et al. Graphene-Wrapped Sulfur Particles as a Rechargeable Lithium–Sulfur Battery Cathode Material with High Capacity and Cycling Stability. Nano Letters. 2011;11(7):2644-7.

59. Li N, Zheng M, Lu H, Hu Z, Shen C, Chang X, et al. High-rate lithium-sulfur batteries promoted by reduced graphene oxide coating. Chemical Communications. 2012;48(34):4106-8.

60. Wang J, Yang J, Wan C, Du K, Xie J, Xu N. Sulfur Composite Cathode Materials for Rechargeable Lithium Batteries. Advanced Functional Materials. 2003;13(6):487-92.

61. Wang J, Yang J, Xie J, Xu N. A Novel Conductive Polymer–Sulfur Composite Cathode Material for Rechargeable Lithium Batteries. Advanced Materials. 2002;14(13-14):963-5.

62. Yin L, Wang J, Yang J, Nuli Y. A novel pyrolyzed polyacrylonitrile-sulfur@MWCNT composite cathode material for high-rate rechargeable lithium/sulfur batteries. Journal of Materials Chemistry. 2011;21(19):6807-10.

63. Wei W, Wang J, Zhou L, Yang J, Schumann B, NuLi Y. CNT enhanced sulfur composite cathode material for high rate lithium battery. Electrochemistry Communications. 2011;13(5):399-402.

64. Yin L, Wang J, Lin F, Yang J, Nuli Y. Polyacrylonitrile/graphene composite as a precursor to a sulfur-based cathode material for high-rate rechargeable Li-S batteries. Energy & Environmental Science. 2012;5(5):6966-72.

65. Sun M, Zhang S, Jiang T, Zhang L, Yu J. Nano-wire networks of sulfur–polypyrrole composite cathode materials for rechargeable lithium batteries. Electrochemistry Communications. 2008;10(12):1819-22.

66. Fu Y, Su Y-S, Manthiram A. Sulfur-Polypyrrole Composite Cathodes for Lithium-Sulfur Batteries. Journal of The Electrochemical Society. 2012;159(9):A1420-A4.

67. Fu Y, Manthiram A. Enhanced Cyclability of Lithium–Sulfur Batteries by a Polymer Acid-Doped Polypyrrole Mixed Ionic–Electronic Conductor. Chemistry of Materials. 2012;24(15):3081-7.

68. Liang X, Liu Y, Wen Z, Huang L, Wang X, Zhang H. A nano-structured and highly ordered polypyrrole-sulfur cathode for lithium–sulfur batteries. Journal of Power Sources. 2011;196(16):6951-5.

69. Fu Y, Manthiram A. Orthorhombic Bipyramidal Sulfur Coated with Polypyrrole Nanolayers As a Cathode Material for Lithium–Sulfur Batteries. The Journal of Physical Chemistry C. 2012;116(16):8910-5.

70. Fu Y, Manthiram A. Core-shell structured sulfur-polypyrrole composite cathodes for lithium-sulfur batteries. RSC Advances. 2012;2(14):5927-9.

71. Wang J, Chen J, Konstantinov K, Zhao L, Ng SH, Wang GX, et al. Sulphur-polypyrrole composite positive electrode materials for rechargeable lithium batteries. Electrochimica Acta. 2006;51(22):4634-8.

72. Wu F, Chen J, Li L, Zhao T, Chen R. Improvement of Rate and Cycle Performence by Rapid Polyaniline Coating of a MWCNT/Sulfur Cathode. The Journal of Physical Chemistry C. 2011;115(49):24411-7.

73. Li G-C, Li G-R, Ye S-H, Gao X-P. A Polyaniline-Coated Sulfur/Carbon Composite with an Enhanced High-Rate Capability as a Cathode Material for Lithium/Sulfur Batteries. Advanced Energy Materials. 2012;2(10):1238-45.

74. Zhang S-c, Zhang L, Wang W-k, Xue W-j. A Novel cathode material based on polyaniline used for lithium/sulfur secondary battery. Synthetic Metals. 2010;160(17–18):2041-4.

75. Xiao L, Cao Y, Xiao J, Schwenzer B, Engelhard MH, Saraf LV, et al. A Soft Approach to Encapsulate Sulfur: Polyaniline Nanotubes for Lithium-Sulfur Batteries with Long Cycle Life. Advanced Materials. 2012;24(9):1176-81.

76. Zhao X, Kim J-K, Ahn H-J, Cho K-K, Ahn J-H. A ternary sulfur/polyaniline/carbon composite as cathode material for lithium sulfur batteries. Electrochimica Acta. 2013;109(0):145-52.

77. Wu F, Wu S, Chen R, Chen J, Chen S. Sulfur–Polythiophene Composite Cathode Materials for Rechargeable Lithium Batteries. Electrochemical and Solid-State Letters. 2010;13(4):A29-A31.

78. Wu F, Chen J, Chen R, Wu S, Li L, Chen S, et al. Sulfur/Polythiophene with a Core/Shell Structure: Synthesis and Electrochemical Properties of the Cathode for Rechargeable Lithium Batteries. The Journal of Physical Chemistry C. 2011;115(13):6057-63.

79. Chen H, Dong W, Ge J, Wang C, Wu X, Lu W, et al. Ultrafine Sulfur Nanoparticles in Conducting Polymer Shell as Cathode Materials for High Performance Lithium/Sulfur Batteries. Sci Rep. 2013;3.

80. Yang Y, Yu G, Cha JJ, Wu H, Vosgueritchian M, Yao Y, et al. Improving the Performance of Lithium–Sulfur Batteries by Conductive Polymer Coating. ACS Nano. 2011;5(11):9187-93.

81. Schneider H, Garsuch A, Panchenko A, Gronwald O, Janssen N, Novák P. Influence of different electrode compositions and binder materials on the performance of lithium–sulfur batteries. Journal of Power Sources. 2012;205(0):420-5.

82. Jung Y, Kim S. New approaches to improve cycle life characteristics of lithium–sulfur cells. Electrochemistry Communications. 2007;9(2):249-54.

83. Trofimov BA, Morozova LV, Markova MV, Mikhaleva AI, Myachina GF, Tatarinova IV, et al. Vinyl ethers with polysulfide and hydroxyl functions and polymers therefrom as binders for lithium–sulfur batteries. Journal of Applied Polymer Science. 2006;101(6):4051-5.

84. Lacey MJ, Jeschull F, Edstrom K, Brandell D. Why PEO as a binder or polymer coating increases capacity in the Li-S system. Chemical Communications. 2013;49(76):8531-3.

85. Cheon S-E, Cho J-H, Ko K-S, Kwon C-W, Chang D-R, Kim H-T, et al. Structural Factors of Sulfur Cathodes with Poly(ethylene oxide) Binder for Performance of Rechargeable Lithium Sulfur Batteries. Journal of The Electrochemical Society. 2002;149(11):A1437-A41.

86. Wang J, Yao Z, Monroe CW, Yang J, Nuli Y. Carbonyl-β-Cyclodextrin as a Novel Binder for Sulfur Composite Cathodes in Rechargeable Lithium Batteries. Advanced Functional Materials. 2013;23(9):1194-201.

87. Bao W, Zhang Z, Gan Y, Wang X, Lia J. Enhanced cyclability of sulfur cathodes in lithium-sulfur batteries with Na-alginate as a binder. Journal of Energy Chemistry. 2013;22(5):790-4.

88. Zhang Z, Bao W, Lu H, Jia M, Xie K, Lai Y, et al. Water-Soluble Polyacrylic Acid as a Binder for Sulfur Cathode in Lithium-Sulfur Battery. ECS Electrochemistry Letters. 2012;1(2):A34-A7.

89. Zhang SS. Binder Based on Polyelectrolyte for High Capacity Density Lithium/Sulfur Battery. Journal of The Electrochemical Society. 2012;159(8):A1226-A9.

90. Rao M, Song X, Liao H, Cairns EJ. Carbon nanofiber–sulfur composite cathode materials with different binders for secondary Li/S cells. Electrochimica Acta. 2012;65(0):228-33.

91. He M, Yuan L-X, Zhang W-X, Hu X-L, Huang Y-H. Enhanced Cyclability for Sulfur Cathode Achieved by a Water-Soluble Binder. The Journal of Physical Chemistry C. 2011;115(31):15703-9.

92. Kim N-I, Lee C-B, Seo J-M, Lee W-J, Roh Y-B. Correlation between positive-electrode morphology and sulfur utilization in lithium–sulfur battery. Journal of Power Sources. 2004;132(1–2):209-12.

93. Wang Q, Wang W, Huang Y, Wang F, Zhang H, Yu Z, et al. Improve Rate Capability of the Sulfur Cathode Using a Gelatin Binder. Journal of The Electrochemical Society. 2011;158(6):A775-A9.

94. Zhang W, Huang Y, Wang W, Huang C, Wang Y, Yu Z, et al. Influence of pH of Gelatin Solution on Cycle Performance of the Sulfur Cathode. Journal of The Electrochemical Society. 2010;157(4):A443-A6.

95. Wang Y, Huang Y, Wang W, Huang C, Yu Z, Zhang H, et al. Structural change of the porous sulfur cathode using gelatin as a binder during discharge and charge. Electrochimica Acta. 2009;54(16):4062-6.

96. Sun J, Huang Y, Wang W, Yu Z, Wang A, Yuan K. Application of gelatin as a binder for the sulfur cathode in lithium–sulfur batteries. Electrochimica Acta. 2008;53(24):7084-8.

97. Sun J, Huang Y, Wang W, Yu Z, Wang A, Yuan K. Preparation and electrochemical characterization of the porous sulfur cathode using a gelatin binder. Electrochemistry Communications. 2008;10(6):930-3.

98. Huang Y, Sun J, Wang W, Wang Y, Yu Z, Zhang H, et al. Discharge Process of the Sulfur Cathode with a Gelatin Binder. Journal of The Electrochemical Society. 2008;155(10):A764-A7.

99. Barchasz C, Leprêtre J-C, Patoux S, Alloin F. Electrochemical properties of ether-based electrolytes for lithium/sulfur rechargeable batteries. Electrochimica Acta. 2013;89(0):737-43.

100. Zhang SS. New insight into liquid electrolyte of rechargeable lithium/sulfur battery. Electrochimica Acta. 2013;97(0):226-30.

101. Aurbach D, Pollak E, Elazari R, Salitra G, Kelley CS, Affinito J. On the Surface Chemical Aspects of Very High Energy Density, Rechargeable Li–Sulfur Batteries. Journal of The Electrochemical Society. 2009;156(8):A694-A702.

102. Wang Y-X, Chou S-L, Liu H-K, Dou S-X. The electrochemical properties of high-capacity sulfur/reduced graphene oxide with different electrolyte systems. Journal of Power Sources. 2013;244(0):240-5.

103. Kim S, Jung Y, Lim HS. The effect of solvent component on the discharge performance of Lithium–sulfur cell containing various organic electrolytes. Electrochimica Acta. 2004;50(2–3):889-92.

104. Ryu H-S, Ahn H-J, Kim K-W, Ahn J-H, Cho K-K, Nam T-H, et al. Discharge behavior of lithium/sulfur cell with TEGDME based electrolyte at low temperature. Journal of Power Sources. 2006;163(1):201-6.

105. Choi J-W, Kim J-K, Cheruvally G, Ahn J-H, Ahn H-J, Kim K-W. Rechargeable lithium/sulfur battery with suitable mixed liquid electrolytes. Electrochimica Acta. 2007;52(5):2075-82.

106. Barchasz C, Leprêtre J-C, Patoux S, Alloin F. Revisiting TEGDME/DIOX Binary Electrolytes for Lithium/Sulfur Batteries: Importance of Solvation Ability and Additives. Journal of The Electrochemical Society. 2013;160(3):A430-A6.

107. Suo L, Hu Y-S, Li H, Armand M, Chen L. A new class of Solvent-in-Salt electrolyte for high-energy rechargeable metallic lithium batteries. Nat Commun. 2013;4:1481.

108. Dokko K, Tachikawa N, Yamauchi K, Tsuchiya M, Yamazaki A, Takashima E, et al. Solvate Ionic Liquid Electrolyte for Li–S Batteries. Journal of The Electrochemical Society. 2013;160(8):A1304-A10.

109. Yuan LX, Feng JK, Ai XP, Cao YL, Chen SL, Yang HX. Improved dischargeability and reversibility of sulfur cathode in a novel ionic liquid electrolyte. Electrochemistry Communications. 2006;8(4):610-4.

110. Park J-W, Yamauchi K, Takashima E, Tachikawa N, Ueno K, Dokko K, et al. Solvent Effect of Room Temperature Ionic Liquids on Electrochemical Reactions in Lithium–Sulfur Batteries. The Journal of Physical Chemistry C. 2013;117(9):4431-40.

111. Croce F, Appetecchi GB, Persi L, Scrosati B. Nanocomposite polymer electrolytes for lithium batteries. Nature. 1998;394(6692):456-8.

112. Marmorstein D, Yu TH, Striebel KA, McLarnon FR, Hou J, Cairns EJ. Electrochemical performance of lithium/sulfur cells with three different polymer electrolytes. Journal of Power Sources. 2000;89(2):219-26.

113. Jeong SS, Lim YT, Choi YJ, Cho GB, Kim KW, Ahn HJ, et al. Electrochemical properties of lithium sulfur cells using PEO polymer electrolytes prepared under three different mixing conditions. Journal of Power Sources. 2007;174(2):745-50.

114. Shin JH, Lim YT, Kim KW, Ahn HJ, Ahn JH. Effect of ball milling on structural and electrochemical properties of (PEO)nLiX (LiX = LiCF3SO3 and LiBF4) polymer electrolytes. Journal of Power Sources. 2002;107(1):103-9.

115. Jeon BH, Yeon JH, Kim KM, Chung IJ. Preparation and electrochemical properties of lithium–sulfur polymer batteries. Journal of Power Sources. 2002;109(1):89-97.

116. Ryu H-S, Ahn H-J, Kim K-W, Ahn J-H, Lee J-Y. Discharge process of Li/PVdF/S cells at room temperature. Journal of Power Sources. 2006;153(2):360-4.

117. Shin JH, Jung SS, Kim KW, Ahn HJ, Ahn JH. Preparation and characterization of plasticized polymer electrolytes based on the PVdF-HFP copolymer for lithium/sulfur battery. Journal of Materials Science: Materials in Electronics. 2002;13(12):727-33.

118. Jin J, Wen Z, Liang X, Cui Y, Wu X. Gel polymer electrolyte with ionic liquid for high performance lithium sulfur battery. Solid State Ionics. 2012;225(0):604-7.

119. Zhu X, Wen Z, Gu Z, Lin Z. Electrochemical characterization and performance improvement of lithium/sulfur polymer batteries. Journal of Power Sources. 2005;139(1–2):269-73.

120. Liang X, Wen Z, Liu Y, Zhang H, Huang L, Jin J. Highly dispersed sulfur in ordered mesoporous carbon sphere as a composite cathode for rechargeable polymer Li/S battery. Journal of Power Sources. 2011;196(7):3655-8.

121. Hassoun J, Scrosati B. Moving to a Solid-State Configuration: A Valid Approach to Making Lithium-Sulfur Batteries Viable for Practical Applications. Advanced Materials. 2010;22(45):5198-201.

122. Jeddi K, Zhao Y, Zhang Y, Konarov A, Chen P. Fabrication and Characterization of an Effective Polymer Nanocomposite Electrolyte Membrane for High Performance Lithium/Sulfur Batteries. Journal of The Electrochemical Society. 2013;160(8):A1052-A60.

123. Jeddi K, Sarikhani K, Qazvini NT, Chen P. Stabilizing lithium/sulfur batteries by a composite polymer electrolyte containing mesoporous silica particles. Journal of Power Sources. 2014;245(0):656-62.

124. Zhang SS. A Concept for Making Poly(ethylene oxide) Based Composite Gel Polymer Electrolyte Lithium/Sulfur Battery. Journal of The Electrochemical Society. 2013;160(9):A1421-A4.

125. Lin Z, Liu Z, Fu W, Dudney NJ, Liang C. Lithium Polysulfidophosphates: A Family of Lithium-Conducting Sulfur-Rich Compounds for Lithium–Sulfur Batteries. Angewandte Chemie International Edition. 2013;52(29):7460-3.

126. Kanno R, Murayama M. Lithium Ionic Conductor Thio-LISICON: The Li2 S - GeS2 - P 2 S 5 System. Journal of The Electrochemical Society. 2001;148(7):A742-A6.

127. Kobayashi T, Imade Y, Shishihara D, Homma K, Nagao M, Watanabe R, et al. All solid-state battery with sulfur electrode and thio-LISICON electrolyte. Journal of Power Sources. 2008;182(2):621-5.

128. Hayashi A, Ohtomo T, Mizuno F, Tadanaga K, Tatsumisago M. Rechargeable lithium batteries, using sulfur-based cathode materials and Li2S–P2S5 glass-ceramic electrolytes. Electrochimica Acta. 2004;50(2–3):893-7.

129. Hayashi A, Ohtomo T, Mizuno F, Tadanaga K, Tatsumisago M. All-solid-state Li/S batteries with highly conductive glass–ceramic electrolytes. Electrochemistry Communications. 2003;5(8):701-5.

130. Nagao M, Hayashi A, Tatsumisago M. Sulfur–carbon composite electrode for all-solid-state Li/S battery with Li2S–P2S5 solid electrolyte. Electrochimica Acta. 2011;56(17):6055-9.

131. Nagao M, Hayashi A, Tatsumisago M. High-capacity Li2S-nanocarbon composite electrode for all-solid-state rechargeable lithium batteries. Journal of Materials Chemistry. 2012;22(19):10015-20.

132. Mikhaylik YV. US Patent, 7,352,680 (2008).

133. Liang X, Wen Z, Liu Y, Wu M, Jin J, Zhang H, et al. Improved cycling performances of lithium sulfur batteries with LiNO3-modified electrolyte. Journal of Power Sources. 2011;196(22):9839-43.

134. Xiong S, Kai X, Hong X, Diao Y. Effect of LiBOB as additive on electrochemical properties of lithium–sulfur batteries. Ionics. 2012;18(3):249-54.

135. Lin Z, Liu Z, Fu W, Dudney NJ, Liang C. Phosphorous Pentasulfide as a Novel Additive for High-Performance Lithium-Sulfur Batteries. Advanced Functional Materials. 2013;23(8):1064-9.

136. Zu C, Fu Y, Manthiram A. Highly reversible Li/dissolved polysulfide batteries with binder-free carbon nanofiber electrodes. Journal of Materials Chemistry A. 2013;1(35):10362-7.

137. Hassoun J, Sun Y-K, Scrosati B. Rechargeable lithium sulfide electrode for a polymer tin/sulfur lithium-ion battery. Journal of Power Sources. 2011;196(1):343-8.

138. Fu Y, Su Y-S, Manthiram A. Li2S-Carbon Sandwiched Electrodes with Superior Performance for Lithium-Sulfur Batteries. Advanced Energy Materials. 2014;4(1):n/a-n/a.

139. Su Y-S, Manthiram A. Lithium–sulphur batteries with a microporous carbon paper as a bifunctional interlayer. Nat Commun. 2012;3:1166.

140. Yang Y, McDowell MT, Jackson A, Cha JJ, Hong SS, Cui Y. New Nanostructured Li2S/Silicon Rechargeable Battery with High Specific Energy. Nano Letters. 2010;10(4):1486-91.

141. Hassoun J, Kim J, Lee D-J, Jung H-G, Lee S-M, Sun Y-K, et al. A contribution to the progress of high energy batteries: A metal-free, lithium-ion, silicon–sulfur battery. Journal of Power Sources. 2012;202(0):308-13.

142. Liu N, Hu L, McDowell MT, Jackson A, Cui Y. Prelithiated Silicon Nanowires as an Anode for Lithium Ion Batteries. ACS Nano. 2011;5(8):6487-93.

143. Zhang SS, Read JA. A new direction for the performance improvement of rechargeable lithium/sulfur batteries. Journal of Power Sources. 2012;200(0):77-82.

144. Fu Y, Su Y-S, Manthiram A. Highly Reversible Lithium/Dissolved Polysulfide Batteries with Carbon Nanotube Electrodes. Angewandte Chemie International Edition. 2013;52(27):6930-5.

145. Yang Y, Zheng G, Cui Y. A membrane-free lithium/polysulfide semi-liquid battery for large-scale energy storage. Energy & Environmental Science. 2013;6(5):1552-8.

146. Chen S, Dai F, Gordin ML, Wang D. Exceptional electrochemical performance of rechargeable Li-S batteries with a polysulfide-containing electrolyte. RSC Advances. 2013;3(11):3540-3.

2. EXPERIMENTAL METHODS

2.1 Electrode Fabrication and Battery Assembly

2.1.1 Sulfur Electrode Fabrication

The sulfur-carbon nanocomposite was prepared by impregnating sulfur into a micro-sized spherical nanoporous carbon (1). The cathodes for Li/S batteries were prepared by mixing 80 wt% of carbon/sulfur composite (75% sulfur), 10 wt% carbon black (Super-P), and 10 wt% polyvinylidenedifluoride (PVDF) dissolved in 1-methyl-2-pyrrolidinone (NMP, Aldrich) to form a homogeneous slurry. The slurry was then coated onto aluminum foil. The method used in the laboratory for electrode fabrications uses the doctor-blade technique. The doctor-blade coating technique is prepared by using a vertical spatula in order to control the thickness of the electrode film on the aluminum substrate with the distance between the blade tip and the substrate. The electrode paste can form a coating on the substrate through the movement of the blade on the substrate surface. The coated aluminum foils were then transferred into a vacuum oven and dried at 80 °C for 12 hours. After the drying procedure, the coated aluminum foils were cut into round disks with a diameter of 14 mm. The electrodes had 56% sulfur with loadings of 1-5 mg /cm^2.

2.1.2 Chemicals Used For Preparing the Li-S Battery Electrolyte

The chemicals used in this research project are listed in Table 1. Table 1 lists the major solvents and additives that were used for the preparation of different electrolytes. All solvents were dried over 4Å molecular sieves for 24 hours and distilled prior to use. In addition, all additives were dried in a vacuum oven overnight prior to use.

TABLE I.

LIST OF CHEMICALS USED FOR ELECTROLYTE PREPARATION

Chemical Name	Formula	Supplier
Sulfur	S	Sigma- Aldrich
Lithium Sulfide	Li_2S	Sigma- Aldrich
1,3 dioxolane (DOL)	$C_3H_6O_2$	Sigma- Aldrich
1,2-dimethoxyethane (DME)	$C_4H_{10}O_2$	Sigma- Aldrich
lithium bis(trifluoromethanesulfonyl)-imide (LiTFSI)	$LiN(CF_3SO_2)_2$	Sigma- Aldrich
1,1,2,2-tetrafluoroethyl-2,2,3,3-tetrafluoropropyl ether (TTE)	$C_5H_4F_8O$	SynQuest Laboratories
Lithium hexafluorophosphate	$LiPF_6$	Sigma- Aldrich
Lithium Nitrate	$LiNO_3$	Sigma- Aldrich

2.1.3 Battery Assembly

In assembling the battery, lithium foils were used as the negative electrode and were punched to be the same diameter as the cathode. A Celgard separator was used as separator. Test batteries were assembled as type CR2032 coin cells (Figure 1). The solvents mentioned above and 1.0M lithium bis(trifluoromethanesulfonyl)-imide (LiTFSI) salt; were used to prepare the electrolyte.

The preparation of the electrolyte and battery assembly were conducted in argon filled glove-boxes with both moisture and oxygen levels below 0.1 ppm.

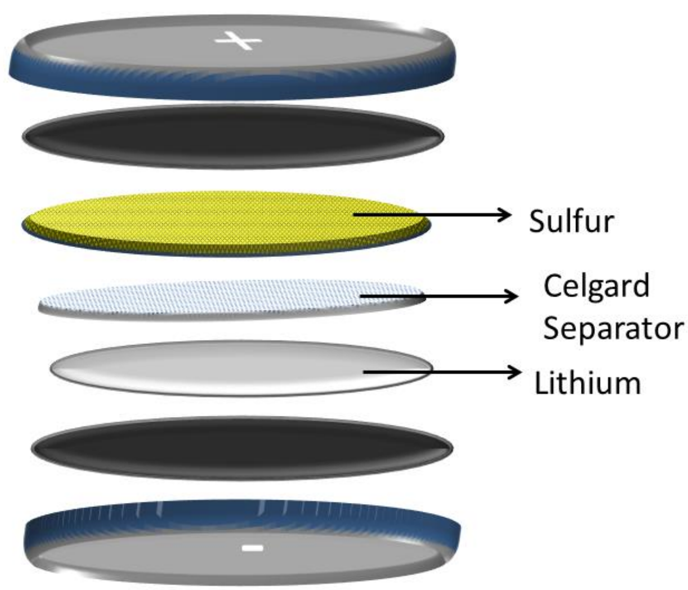

Figure 1. From top to bottom: cathode cap, spacer, sulfur electrode, Celgard separator, lithium anode, spacer, anode cap.

2.2 Material Characterization

The material characterization techniques used in this research are explained below:

2.2.1 Scanning Electron Microscopy

The scanning electron microscope (SEM) is used to explore the structural properties of materials by using a focused beam of high energy electrons. The electrons interact with atoms in the sample, producing various signals that can be detected. This reveals information about the sample's surface topography, chemical composition, and crystalline structure. The SEM is also capable of performing analyses of particular points on the sample; where this approach is especially beneficial in qualitatively or semi-quantitatively determining chemical compositions by means of energy-dispersive X-ray spectroscopy (EDS) (2-4).

For this research study, cycled sulfur electrodes were harvested inside the glove box and were thoroughly rinsed with DOL solvent. The samples were then dried inside a vacuum oven at 70°C and then loaded to the SEM sample holders. In addition, cycled lithium anode samples were also rinsed with DOL solvent and dried in the glove box. The samples were then loaded onto an air-tight SEM sample holder. The morphology of the electrodes was examined by a high resolution JEOL JSM6610 scanning electron microscopy (SEM) operated at 5–10 kV for imaging and 10–20 keV for EDS data.

2.2.2 High-Performance Liquid Chromatography

High-performance liquid chromatography (HPLC) is a technique which has the ability to separate, categorize and quantify each component that is in any sample that can be dissolved in a liquid. HPLC is basically a form of column chromatography which relies on pumps to pass a sample mixture in a solvent (known as the mobile phase) at high pressure through a column filled with a solid adsorbent material (stationary phase). Each component of the sample will interact differently and retention times will vary based on the interaction between the stationary phase, the sample, and the solvents used. This will cause different flow rates for each component of the sample and consequently the separation of these components as they flow out the column (5-7).

2.2.3 Ultraviolet–Visible Spectroscopy

Ultraviolet visible spectroscopy (UV-Vis) spectroscopy is another method used in analytical chemistry for the qualitative and quantitative determination of different species and is used to obtain the absorbance spectra of a compound in the sample. UV-Vis refers to the absorbance of electromagnetic radiation, which excites electrons of the material from the ground state to the first singlet excited state (8-10). The wavelength of the light that the molecule can absorb depends on how easily electrons are excited and the easier the longer the wavelength of light it can absorb (11).

In this study, coin cells were disassembled inside a glove-box and the electrolyte was collected by thoroughly rinsing the cathode and separator with dry, deoxygenated 1,3-dioxolane (DOL). The solution was passed through a 2 µm polytetrafluoroethylene filter to remove residual solids. High-performance liquid chromatography was used to separate the components in a cycled electrolyte. The HPLC apparatus (Agilent 1260 Infinity) consisted of an autosampler, a degasser, a quaternary pump, and a diode array detector (190-950 nm, in steps of 1 nm). The diode array detector (DAD) was used for the qualitative and quantitative determination of the different species. In addition, the DAD also yielded ultraviolet–visible **(**UV/VIS) spectra of the various species. An Ar-purged and filled glove bag was placed over the solvent reservoir tray. The glove bag was purged at least three times with ultra-high purity (UHP) Ar before introducing the solvent reservoir bottle. Dry, deoxygenated 1,3-dioxolane (DOL) was used as the mobile phase. In a typical experiment, the solvent reservoir was filled in an Ar-filled glove box and capped with two layers of parafilm. It was then quickly transferred to the glove bag and placed in the bag under a positive flow of Ar. Positive Ar pressure was maintained throughout the HPLC experiment. A Zorbax® ODS column (250 x 4.6 mm) was used to separate the electrolyte solution, which was thermostated at 25°C. The flow of the mobile phase was 0.5 mL/min. Between 1 and 50 µL of electrolyte solution was injected using the autosampler.

2.2.4 X-Ray Photoelectron Spectroscopy

X-ray photoelectron spectroscopy (XPS) is a widely used surface-sensitive quantitative technique that can analyze the surface chemistry and composition of a material in its as-received state, or after treatment at the parts-per-thousand level. XPS spectras are obtained by irradiation of the sample with a beam x-rays rays, causing photoelectrons to be emitted from the sample surface, yielding a measurement of the binding energies of the photoelectrons. The elemental characteristics, chemical state, and quantity of an element are determined from the binding energy measurement (12, 13). In this study, analyses were performed on a monochromatic Al Kα source instrument (Kratos, Axis 165, England) operating at 12 kV and 10 mA for an x-ray power of 120

W. Spectra were collected with a photoelectron takeoff angle of 90° from the sample surface plane, energy steps of 0.1 eV, and a pass energy of 20 eV for all elements. All spectra were referenced to the C 1s binding energy at 284.8 eV.

2.3 Electrochemical Investigation

The electrochemical testing techniques that are most common for battery research are electrochemical analysis measurements such as cyclic voltammetry, electrochemical impedance spectroscopy and galvanostatic charge-discharge tests; where most of these tests were conducted with in the voltage window between 1.6 V and 2.6 V.

2.3.1 Ionic Conductivity

The electrolyte used in Li-S batteries should have a high ionic conductivity. This property of the electrolyte is measured by determining the resistance of the solution between the two electrodes which are separated by a fixed distance. The conductivity of the electrolytes was calculated from the ohmic resistance of coin cells assembled by sandwiching a rubber ring filled with electrolyte between two stainless-steel electrodes (Figure 2). The resistance was measured using a Solartron Multistat1480 coupled with a 1260 Frequency Response Analyzer System over a frequency range of 1 Hz to 10^6 Hz at different temperature then the conductivity was calculated using the following equation: (14)

$$\sigma = L/RA \qquad (2.1)$$

where σ is the Li^+ conductivity in mS/cm , L is the distance between the two electrodes (thickness of the rubber ring), R is resistance of the coin cell and A is the area of the rubber ring (inner circle).

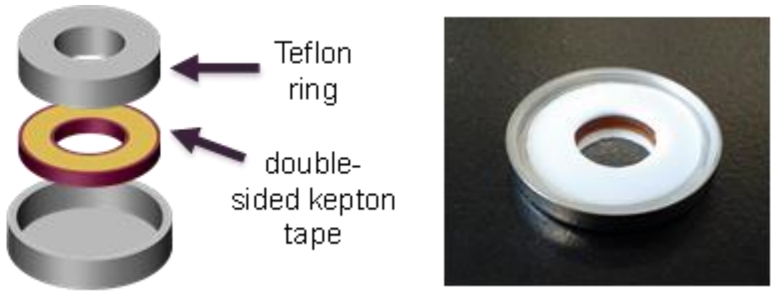

Figure 2. Coin cell assembled by sandwiching a rubber ring filled with electrolyte between two stainless-steel electrodes for conductivity measurements.

Thickness of the rubber ring with kepton tape: 0.18 cm

Area of the rubber ring (inner circle): 0.49 cm^2

Ionic movement, and therefore the conductivity measurement, is directly proportional to temperature, T.

The effect is repeatable for most chemicals, and is very significant. The temperature dependence of the ionic conductivity is by the traditional Arrhenius equation.

$$\sigma = \frac{\sigma 0}{T} \, exp\,(\frac{-E}{kT}) \quad (2.2)$$

where:

E= activation energy for ionic conduction

$\sigma 0$= material constant

k =Boltzmann constant

T= temperature

A linear relationship between log σT and $1/T$, can be predicted by this equation which will be presented in the next sections.

2.3.2 Galvanostatic Charge-Discharge Cycling

In order to evaluate the performance of a Li-S cell, capacity retention, coulombic efficiency and many other properties of the battery, galvanostatic cycling tests are conducted. The voltage-capacity (dV/dQ) curves can also be generated from charge-discharge cycle tests which can be used for understanding the electrochemical reduction/oxidation mechanisms of the sulfur electrode.

In this study, 2032 Li-S coin cells were assembled in a glove box and cycled at the C/10 rate with a Maccor series 4000 cycler (Figure 3) over a voltage range of 1.6-2.6 V at room temperature, or higher temperatures for temperature studies. Different current rates were also applied in order to investigate the effect of rate on the performance of the Li-S cells. The specific capacity of all the tested electrodes is based on the sulfur weight in the electrode according to the following equations:

$$C_{sc} = C / W_s \quad (2.3)$$

$$W_s = (W_e - W_a) \bullet (R_s) \quad (2.4)$$

Where

C_{sc} = specific capacity of sulfur within the cathode

C =discharge (or charge) capacity attained from the software for cycle tests

W_s = sulfur mass of particular tested cathode

W_e = weight of the electrode which is the total weight of aluminum foil with cathode paste

W_a =weight of aluminum foil which is used as electrode substrate

R_s = ratio of sulfur in the electrode (in this study 60%)

Figure 3. Picture of a Maccor series 4000 cycler with 96 test channels

2.3.3 Cyclic Voltammetry

Cyclic voltammetry (CV) is a widely used method in electrochemical experimenting for obtaining qualitative information about electrochemical reactions of batteries, which can be used to get valuable kinetic information of the electrode reaction. Cyclic voltammetry is often the first experiment performed in an electro-analytical study. During the cyclic voltammetry test, an electrode's potential is controlled while the resultant current is measured. The voltage is swept back and forth between the upper and lower limits (1.6- 2.6V) and the corresponding currents are monitored. At that point, the received current is plotted as a function of voltage. A CV scan starts with zero current flow where no electrode reaction occurs and moves to potentials where an oxidation or reduction reaction occurs and a current flow begins to form and eventually reaches a peak and then starts to fall. Using this principle, we can determine the potentials of electrochemical reactions within a test cell. The CV results depend on the voltage, scan rate, the reactivity of the electrode/electrolyte species, and the rate of the electron transfer reactions (15-17).

In general, cyclic voltammetry has many applications such as determining (1) the stability of reaction products, (2) the reversibility of a reaction, (3) the existence of intermediates in oxidation-reduction reactions, (4) the reaction and electron transfer kinetics, and (5) the diffusion coefficient.

2.3.4 Electrochemical Impedance Spectroscopy

The concept of resistance is explained first to help understand the definition of impedance. The ability of a circuit element to resist the flow of electrical current is known as resistance; where Ohm's law (Equation 2.5) defines this term as follows:

$$R = \frac{E}{I} \tag{2.5}$$

where:

R= Resistance

E =Voltage

I = current

Even though this relationship is well known, its use is limited to only one circuit and an ideal resistor. Since in reality circuit elements reveal much more complex behavior, a more general circuit parameter called impedance is used.

Like resistance, impedance is the response of an electrochemical system to an applied potential and a measure of the ability of a circuit to resist the flow of electrical current, but unlike resistance, it is not limited to the simplifying properties listed above.

In an electrochemical impedance spectroscopy (EIS) measurement, a battery is considered as a parallel circuit that consists of a capacitance (C_p) and an ohmic resistance (R_p). These values can also be represented as complex numbers; therefore, the impedance response is described by a real part-imaginary couple. The data from an impedance measurement is plotted in a complex plane with the frequency as a parameter. Impedance measurements are usually applied over a very wide frequency range (e.g. from 100 kHz to 0.001 Hz). The impedance changes between its high-frequency limit and low-frequency limit. (18, 19).

The electrochemical impedance measurements in this study were carried out with a Solartron analytical 1400 cell test impedance system by applying a 10 mV voltage over a frequency range from 0.01 Hz to 1.0 MHz and the resulting spectrum was fit using ZView softwar

CITED LITERATURE

1. Sohn H, Gordin ML, Xu T, Chen S, Lv D, Song J, et al. Porous Spherical Carbon/Sulfur Nanocomposites by Aerosol-Assisted Synthesis: The Effect of Pore Structure and Morphology on Their Electrochemical Performance As Lithium/Sulfur Battery Cathodes. ACS Applied Materials & Interfaces. 2014;6(10):7596-606.

2. Susan Swapp UoW. Scanning Electron Microscopy (SEM).

3. University P. Scanning Electron Microscope 2014. Available from: http://www.purdue.edu/ehps/rem/rs/sem.htm.

4. Weilie Zhou RA, Zhong Lin Wang, David Joy. Fundamentals of Scanning Electron Microscopy (SEM): Springer New York; 2007.

5. Clark J. HIGH PERFORMANCE LIQUID CHROMATOGRAPHY - HPLC 2007. Available from: http://www.chemguide.co.uk/analysis/chromatography/hplc.html.

6. Waters. How Does High Performance Liquid Chromatography Work? 2014. Available from: http://www.waters.com/waters/en_US/How-Does-High-Performance-Liquid-Chromatography-Work%3F/nav.htm?cid=10049055&locale=en_US.

7. Agilent Technologies I. Fundamentals of Liquid Chromatography (HPLC) Available from: http://polymer.ustc.edu.cn/xwxx_20/xw/201109/P020110906263097048536.pdf.

8. Andrew R. Barron BLO-C. Basics of UV-Visible Spectroscopy 2014. Available from: http://cnx.org/contents/02e7b3d6-cf47-4c92-a380-d011ce5658b1@1/Basics_of_UV-Visible_Spectrosc.

9. Reusch W. Visible and Ultraviolet Spectroscopy 2013. Available from: https://www2.chemistry.msu.edu/faculty/reusch/virttxtjml/Spectrpy/UV-Vis/spectrum.htm.

10. D. A. Skoog FJH, S. R. Crouch. Principles of Instrumental Analysis, 6th Ed: Thomson Brooks/Cole 2007.

11. Liebhafsky HA, Pfeiffer HG. Beer's law in analytical chemistry. Journal of Chemical Education. 1953;30(9):450.

12. Hollander JM, Jolly WL. X-ray photoelectron spectroscopy. Accounts of Chemical Research. 1970;3(6):193-200.

13. Paterson E, Swaffield R. X-ray photoelectron spectroscopy. In: Wilson MJ, editor. Clay Mineralogy: Spectroscopic and Chemical Determinative Methods: Springer Netherlands; 1994. p. 226-59.

14. Conductivity of electrolyte solutions 2009. Available from: https://www.csun.edu/~jeloranta/CHEM355L/experiment4.pdf.

15. Kissinger PT, Heineman WR. Cyclic voltammetry. Journal of Chemical Education. 1983;60(9):702.

16. Vielstich W. Cyclic voltammetry. Handbook of Fuel Cells: John Wiley & Sons, Ltd; 2010.

17. Nicholson RS. Theory and Application of Cyclic Voltammetry for Measurement of Electrode Reaction Kinetics. Analytical Chemistry. 1965;37(11):1351-5.

18. Instruments G. Basics of Electrochemical Impedance Spectroscopy 2014. Available from: http://www.gamry.com/application-notes/basics-of-electrochemical-impedance-spectroscopy/.

19. Macdonald EBaJR. Impedance Spectroscopy: Theory, Experiment, and Applications: Wiley-Interscience; 2005.

3. FLUORINATED ETHER CONTAINING LITHIUM-SULFUR BATTERY ELECTROLYTE

3.1 Introduction

There are numerous problems involved with Li–S batteries that arise from a difficult multistep discharge process (1-4). The redox shuttling effect of polysulfides originates from its high solubility and fast diffusion in an organic electrolyte. Even though the protection of the lithium anode has shown to assist in reducing the shuttling effect (5-7), there are still many issues regarding the positive electrode and the electrolyte. Therefore, many researchers have focused their efforts on developing new electrolytes which play a pivotal role in Li-S cell performance.

To mitigate the severe shuttling effect of polysulfides in the conventional electrolyte, new electrolytes were investigated by incorporating a fluorinated solvent in the electrolyte formulation (8, 9). Due to the lower solubility of the lithium polysulfides in this electrolyte system, the idea is to reduce the dissolution of the PS and therefore improve the efficiency of the cell. As shown in Figure 1, based on this idea the polysulfides are prevented from diffusing into the fluorinated electrolyte (DOL/TTE) and reacting with the lithium anode, whereas the polysulfides have high solubility in the conventional DOL/DME-1.0M LiTFSI electrolyte.

The fluorinated 1,1,2,2-Tetrafluoroethyl-2,2,3,3-tetrafluoropropyl ether (TTE) solvent has also been reported to enhance the performance of the Li-ion due to the formation of an electrochemically stable SEI, which protects the cathode against further decomposition of the electrolyte at the electrode surface (10-13). For comparison reasons, a non-fluorinated solvent was used as co-solvent, and the results are shown in figure 2. It is noticed that when a mixture of dipropyl ether (DPE) and DOL with 1.0M LiTFSI is used as electrolyte, the charging step is not possible for the Li-S battery due to the very low solubility of the polysulfides in this solvent.

1,1,2,2-tetrafluoroethyl-2,2,3,3-tetrafluoropropyl ether (TTE), as shown in Figure 2, was one of the solvents with the highest efficiency and capacity retention that was studied in great detail in this project. Based on the density functional theory data shown in Table 1, the fluorine substitution in ethyl propyl ether lowers both the lowest unoccupied molecular orbital (LUMO) and the highest occupied molecular orbital (HOMO) energy levels, resulting in simultaneously high reduction potential and oxidation stability of the fluorinated ether. The theoretical calculation indicates that the fluorinated electrolyte solvents are thermodynamically more likely to form a passivation layer on both electrodes by means of an electrochemical reduction reaction than their non-fluorinated counterparts under certain voltage conditions. Our experimental results demonstrated that a binary solvent electrolyte comprising of TTE and 1, 3-dioxolane (DOL) displayed superior cycling performance in a Li-S cell employing a carbon/sulfur nanocomposite electrode with 75% of sulfur content.

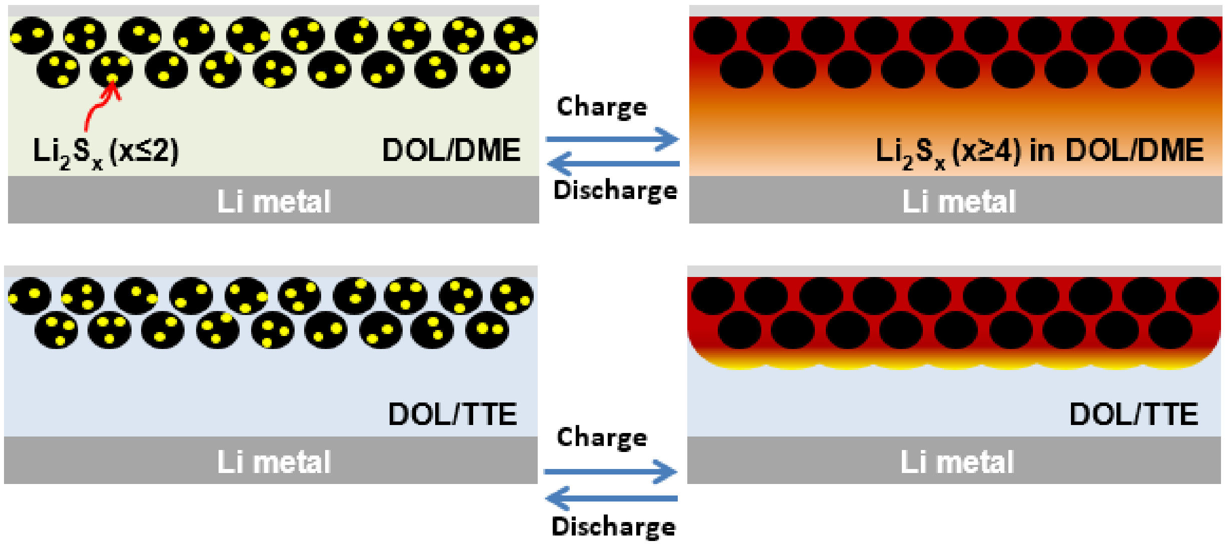

Figure 1. Schematic showing the diffusion of lithium polysulfides during charge and discharge in (top) conventional DOL/DME-1.0M LiTFSI electrolyte and (bottom) a fluorinated DOL/TTE-1.0M LiTFSI electrolyte.

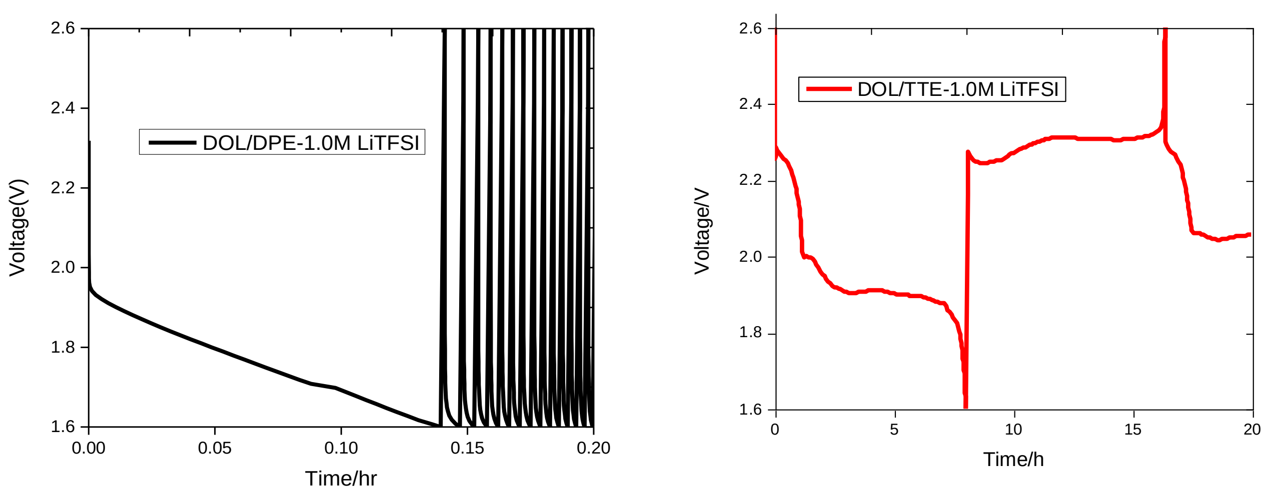

Figure 2. Voltage profile for cells cycled with different solvents.

TABLE I

THE STRUCTURE, THEORETICAL OXIDATION POTENTIAL (VS. LI+/LI) AND HOMO AND LUMO ENERGY

Ether	Structure	Pox (V, Theory)	HOMO (au)	LUMO (au)
EPE	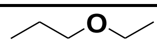	5.511	-0.26153	0.00596
TTE	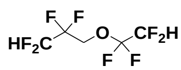	7.24	-0.35426	-0.00356

3.2 Charge and Discharge Characteristics

The electrochemical performance of a Li-S cell containing a conventional and fluorinated electrolyte is presented in Figure 3 (8). Figure 3a shows the initial charge and discharge voltage profiles of Li-S cells with 1.0M LiTFSI DOL/DME (5/5) and 1.0M LiTFSI DOL/TTE (5/5) as the electrolyte, which consist of two plateaus in the discharge process, in agreement with following results. The first plateau at higher voltage (from 2.4 V~2.2 V) is due to the reduction of elemental sulfur to high order lithium polysulfides (Li_2S_x, where x=4-8) and further reduction of these polysulfides to low order species (Li_2S_2 and/or Li_2S) occurs at the lower voltage plateau observed at 2.1 V~2.0 V (14, 15). Compared with the Li-S cell using baseline electrolyte 1.0M LiTFSI DOL/dimethoxy ethane (DME) (5/5), the fluorinated electrolyte cell showed slightly lower voltage and much higher capacity during the first discharge. Nevertheless, a significant difference was observed for both cells during the charge process. The TTE-based electrolyte cell displayed a long and flat plateau and a drastic voltage rise at the end of the charging step without any shuttling behavior. In contrast, two plateaus were observed for the baseline cell with the lower voltage plateau associated with the oxidation of the longer polysulfides and the second plateau at 2.35 V reflecting the shuttle effect of the dissolved polysulfides in the electrolyte, which prevents the cell from reaching the charge voltage limit of 2.6 V. The voltage profiles remain unchanged even at deep cycles (Fig.3b). The low polarity of the TTE helps reduce the dissolution of polysulfides into the electrolyte as confirmed by the fact that the synthesized Li_2S_9 does not dissolve in the TTE solvent. The capacity retention profile of Li-S cells with both electrolytes is presented in Figure 3c. A stable discharge capacity of 1100 mAh/g (based on the sulfur content in the cathode) was maintained for the first 50 cycles after several charge discharge formation cycles for cell containing the fluorinated electrolyte. Moreover, the cell containing the TTE electrolyte showed a coulombic efficiency of 97.5% during the whole range of the 50 cycles as evidenced in Figure 3d, indicating the successful inhibition of the polysulfide shuttling effect in the fluorinated electrolyte. In contrast, the baseline cell showed a much lower initial capacity (Figure 3a) and rapid fading of the capacity retention (Figure 3c). Actually, in order to enable the normal operation of the baseline cell, an arbitrary limit was set to terminate the shuttling of polysulfides during the charging process, i.e. the charging of the baseline cell would be complete when the capacity reaches 120% of the preceded discharge capacity, accounting for the constant of the coulombic efficiency of 88.33% (Figure 3d). Such capacity fade and low coulombic efficiency are common features for Li-S cells using conventional electrolytes due to the dissolution of lithium polysulfide intermediates into the electrolyte, which leads to active sulfur loss and shuttle reactions.

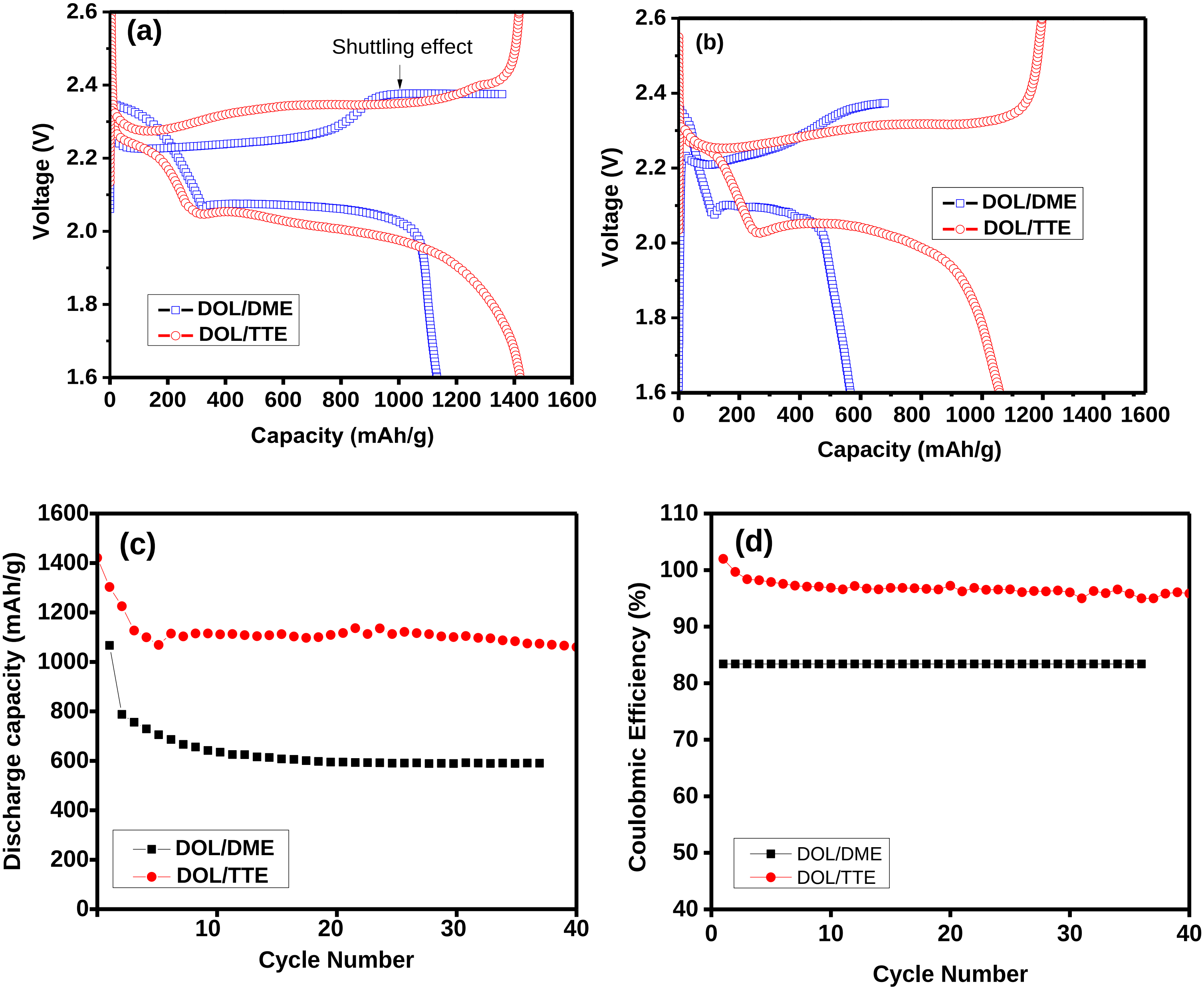

Figure 3. Galvanostatic potential profile of the (a) 1st charge and discharge and (b) 30th charge and discharge, (c) capacity retention, and (d) coulombic efficiency of Li-S cells with 1.0M LiTFSI DOL/DME (5/5) and 1.0M LiTFSI DOL/TTE (5/5) electrolyte with a 0.1 C rate.

3.3 Effect of Fluoroether Solvent Ratio

To further prove the effectiveness of this electrolyte solvent, a solubility test was conducted by testing different ratios of the fluorinated electrolyte vs. the conventional electrolyte. Li_2S_8 was synthesized by adding stoichiometric amount of Li_2S and S in the 1.0 M LiTFSI with each electrolyte solvent solution (16). The dark-red catholyte (4.0 M normalized to S) showed much higher solubility in the conventional electrolyte, DOL/DME solvent solution as shown in figure 4a on left. By using the TTE solution, ratios increasing from DOL: TTE (2:1) to (1:1) to (1:2), the solubility is significantly reduced due to using the fluorinated solvent. Based on this test result, it is manifest that TTE solvent has a significant effect on the performance of the Li-S cell due to suppressing the redox shuttling of lithium polysulfides by preventing their diffusion into the electrolyte.

The performance of the first 50 cycles of the cells containing different ratios is also shown in figure 4b. The cell containing the electrolyte with a DOL/TTE ratio of 1:2 shows the best capacity retention after 50 cycles, whereas the cell containing nonfluorinated electrolyte DOL/DME=1:1 results in the lowest capacity within the same cycles. Surprisingly, even without the use of the widely adopted LiNO3 additive, the cells containing fluorinated electrolytes showed very high coulombic efficiency, as shown in Figure 4c. However, when the ratio is increased to DOL/ TTE (1:3) the capacity has dropped due to the very low solubility of the lithium salt and sulfur in this electrolyte. The efficiency of the cell containing the (1/3) ratio has the highest value among the other solvent ratios due to the higher concentration of the fluorinated electrolyte and concentrated effect of the SEI formation and low PS solubility (figure 4c) (17).

The 1st discharge and 1st charge voltage profiles for Li-S cells with different ratios of fluorinated electrolyte are shown in Figure 4d. As expected, higher TTE ratio electrolyte are low in conductivity (data shown later in Figure 7), which results in high over potential and caused huge voltage drop for both the high order and the low order polysulfide discharge plateau. Interestingly, for the TTE electrolyte cells, the contribution to the overall capacity from the high order polysulfide reduction (the first plateau on discharge profile) becomes smaller with an increasing amount of TTE in the DOL/TTE electrolyte. For the baseline cell, the high order polysulfide contribution is 37.5% (600 out of 1600mAh/g), and this value becomes 33.0% for DOL/TTE 2/1 (500 out of 1500 mAh/g), 16.5% for DOL/TTE 1/1 (260 out of 1620 mAh/g) and 14.2% for DOL/TTE 1/2 (200 out of 1400 mAh/g). This results implies that the reduction reaction from S to high order PS is transient and the kinetics of the high order PS further reaction to low order ones is more favorable when the fluorinated electrolytes are used. It is worth to be noted that this phenomena is always associated with the appearance of a lower discharge voltage around 1.8 V, corresponding to the gradual slope at the end of the first discharge process as indicated in Fig.4d, and was confirmed by the 1st cycle dQ/dV profile as shown in Fig.5. This behavior is associated with the reductive decomposition of the fluorinated TTE solvent on the surface of the sulfur/carbon particles during the discharge, forming a passivation layer as the so-called solid-electrolyte interphase (SEI) (8).

(a)

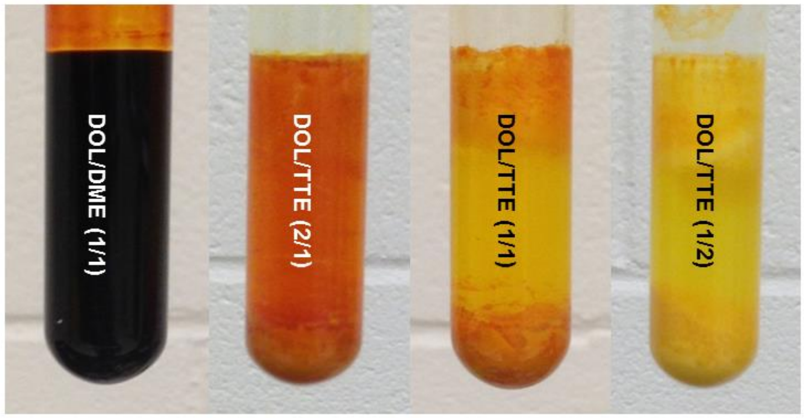

DOL/DME (1/1)
DOL/TTE (2/1)
DOL/TTE (1/1)
DOL/TTE (1/2)

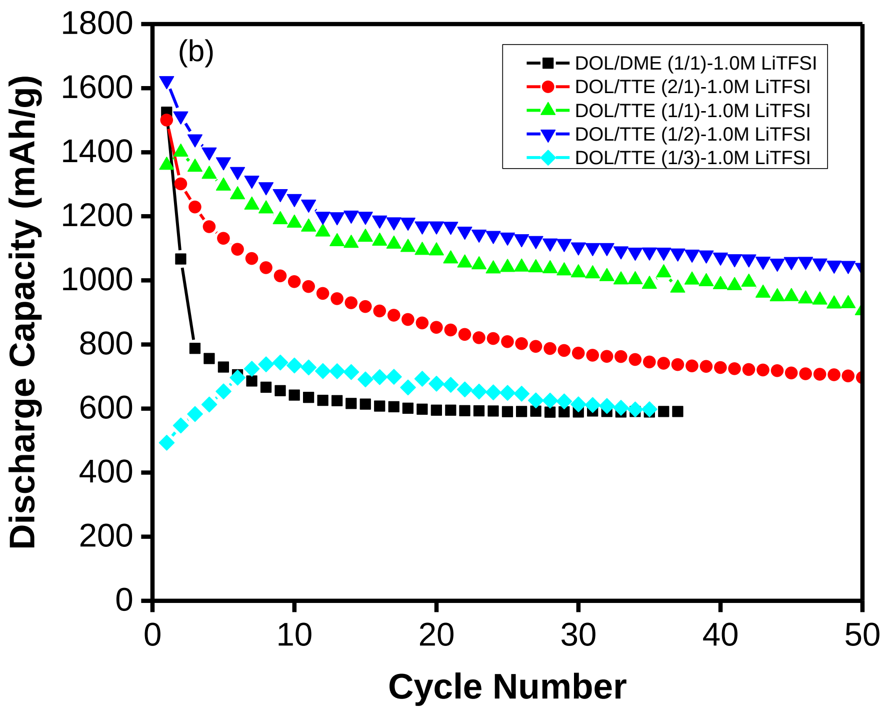

(b)
DOL/DME (1/1)-1.0M LiTFSI
DOL/TTE (2/1)-1.0M LiTFSI
DOL/TTE (1/1)-1.0M LiTFSI
DOL/TTE (1/2)-1.0M LiTFSI
DOL/TTE (1/3)-1.0M LiTFSI
Discharge Capacity (mAh/g)
Cycle Number
0
200
400
600
800
1000
1200
1400
1600
1800
0
10
20
30
40
50

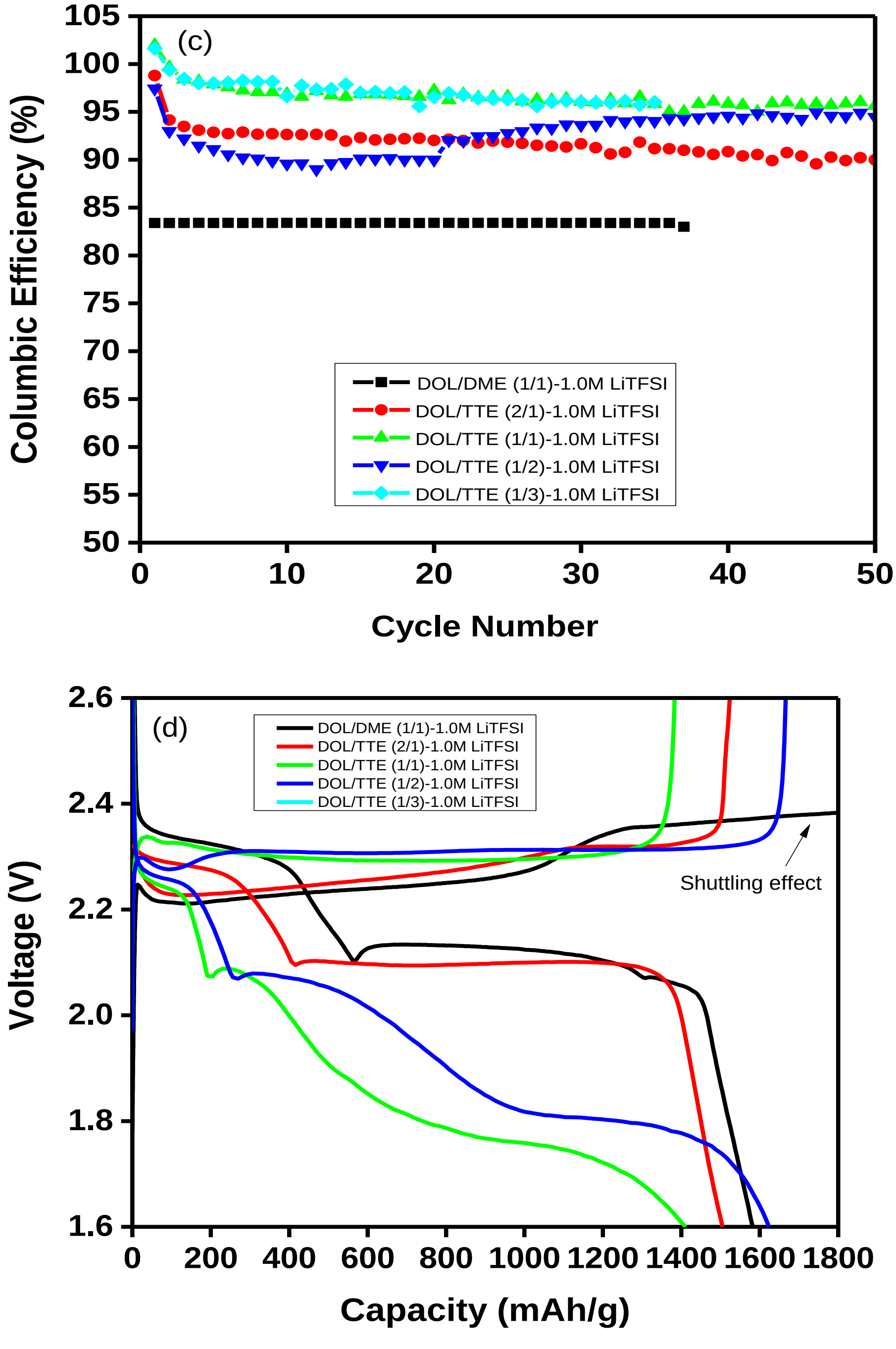

Figure 4. (a) Solubility test with 4.0M Li_2S_8 in (left to right) DOL/DME (1/1), DOL/TTE (2/1), DOL/TTE (1/1), DOL/DME (1/2) and performance of Li-S cells with different solvent ratios of DOL/TTE for 50 cycles (b) capacity retention (c) coulombic efficiency profile and (d) first cycle voltage profile.

3.4 SEI Formation

To further investigate the mechanism of the shuttle inhibition due to the fluorinated electrolyte, cyclic voltammetry measurement was carried out (8). For the baseline cell, two distinguished cathodic peaks are observed at 2.35 and 2.0 V in the first discharge corresponding to the reduction of elemental sulfur and the intermediate polysulfides (Figure 5a). For the fluorinated electrolyte, in addition to the 2.24 V and 1.9 V cathodic peaks (Figure 5b), a third reduction peak appeared at 1.8 V, corresponding to the gradual slope at the end of the first discharge process, and was confirmed by the 1st cycle dQ/dV profile as shown in Figure 5c. The intensity of this peak gradually decreased and eventually disappeared with cycling as evidenced by Figure.5d. This phenomenon is associated with the reductive decomposition of the fluorinated TTE solvent on the surface of the sulfur/carbon particles during the discharge process forming a passivation layer called SEI. Another noticeable difference for the TTE electrolyte cell is the significant decrease in redox current of the 2nd reduction peak, indicating slow reaction kinetics to the discharge product Li_2S and/or Li_2S_2, therefore preventing the loss of active material. Interestingly, in the 1st charging process, only one major anodic peak was observed at 2.45 V for the TTE electrolyte cell with relatively high intensity accounting for the oxidation reaction of high order polysulfides and the small shoulder peak (2.35V) being associated with the transition of low concentration Li_2S_2 and/or Li_2S to higher order ones, suggesting that the oxidation reaction of high order polysulfides dominates the charging process when fluorinated electrolyte was used. As discussed above, the higher order polysulfides are not fully reduced to insoluble low order polysulfides during the discharge process, thus can be converted to sulfur with fast kinetics during charging. Theoretically, a specific capacity of 1675 mAh/g can be achieved from S to Li_2S and

837.5 mAh/g from S to Li_2S_2., therefore a stable capacity of 1100 mAh/g for the fluorinated electrolyte Li-S cell indicates the discharged product in this cell could be a mixture of Li_2S and Li_2S_2.

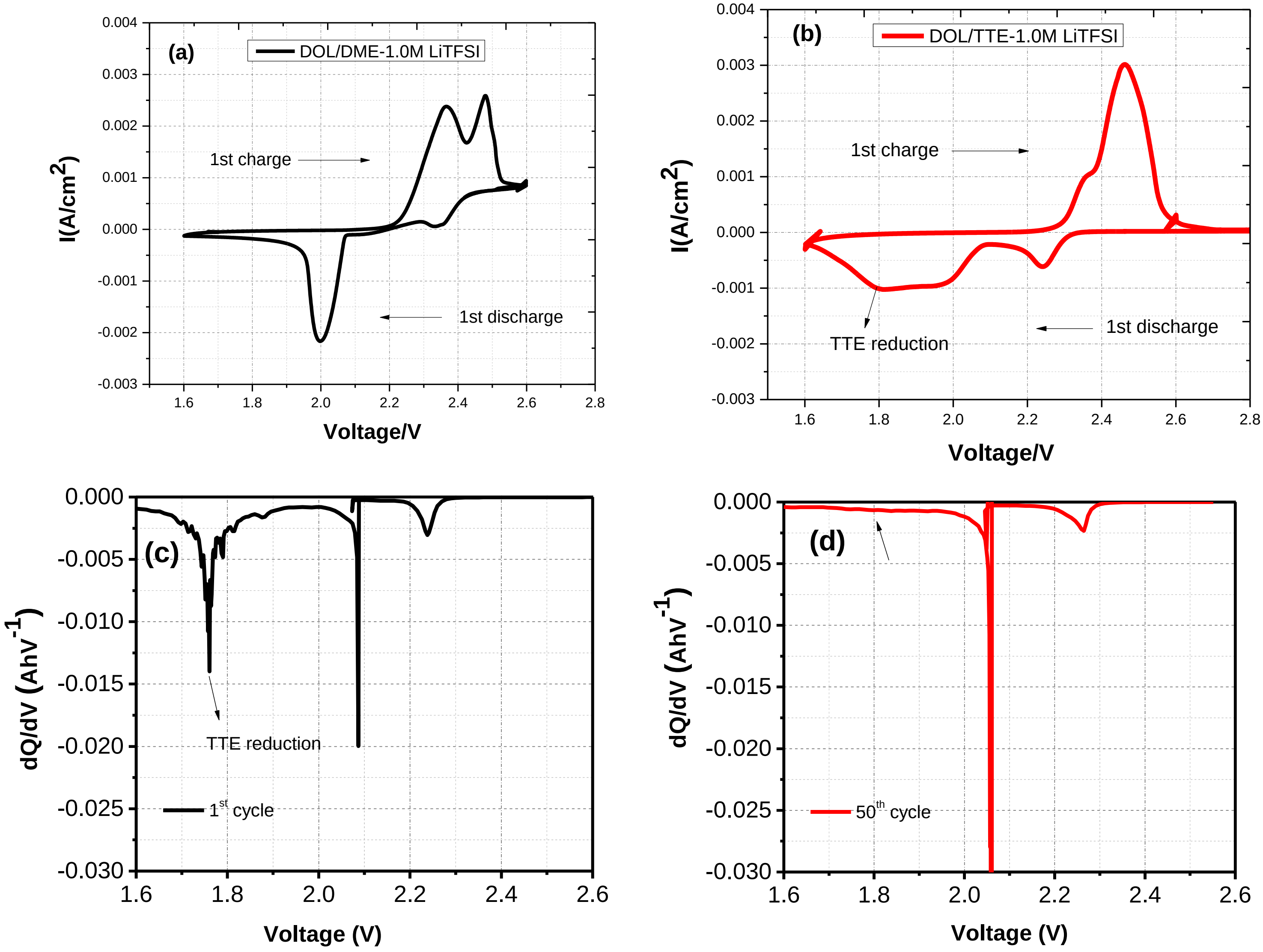

Figure 5**.** Cyclic voltammograms of the 1st cycle for Li-S cell with (a) 1.0 M LiTFSI DOL/DME and (b) 1.0 M LiTFSI- DOL/TTE electrolyte (scanning rate of 27 μV s-1); Differential capacity dQ/dV profiles of (c) the 1st discharge and (d) the 50th discharge for Li-S cell with 1.0 M LiTFSI-DOL/TTE electrolyte.

3.5 Electrochemical Impedance Spectroscopy

The formation of this passivation layer on the surface of the sulfur cathode helped retain the polysulfides inside the structure of the S/carbon composite thus preventing the shuttle effect. It has been reported by Liang et al. (5) that the shuttle reaction can be suppressed by addition of $LiNO_3$ to the electrolyte, which could significantly improve the coulombic efficiency. $LiNO_3$ participates in the formation of a stable passivation film on the surface of Li anode protecting Li anode from chemically reacting with the dissolved polysulfides and the electrochemical reduction of polysulfides on the Li anode surface. However, the drastic capacity fade was observed indicating the $LiNO_3$ could not eliminate the active material loss (6) therefore using the fluorinated electrolyte has much more significant effect than to using this additive. It is well known that fluorinated compounds are thermodynamically unstable when in contact with lithium metal and tend to chemically react with it forming organolithium compounds/inorganic LiF composite deposited on the surface of the Li. The formation of this composite layer is speculated to act as a physical barrier and an electronic isolating layer inhibiting the chemical and electrochemical reactivity of polysulfides with lithium anode.

The essential role of the fluorinated ether in the formation of the passivation film on both electrodes is examined by electrochemical impedance spectroscopy and the data are illustrated in Figure 6. At 1st and 10th discharge state (Figure 6a and c), the ohmic and interfacial resistance of the TTE electrolyte cell is smaller than that of the baseline cell. At charged state, the impedance profile of TTE electrolyte cell is composed of two flatted semicircles (Figure 6b and d). In general, the semicircles in the high frequency range correspond to the passivation films on the electrode surface and the one in lower frequency range corresponds to the charge-transfer process occurring on the electrolyte-electrode interfaces. Compared with baseline cell, the TTE electrolyte cell has higher passivation resistance, which is a good indication that the passivation formed in the TTE electrolyte is denser and hence more protective.

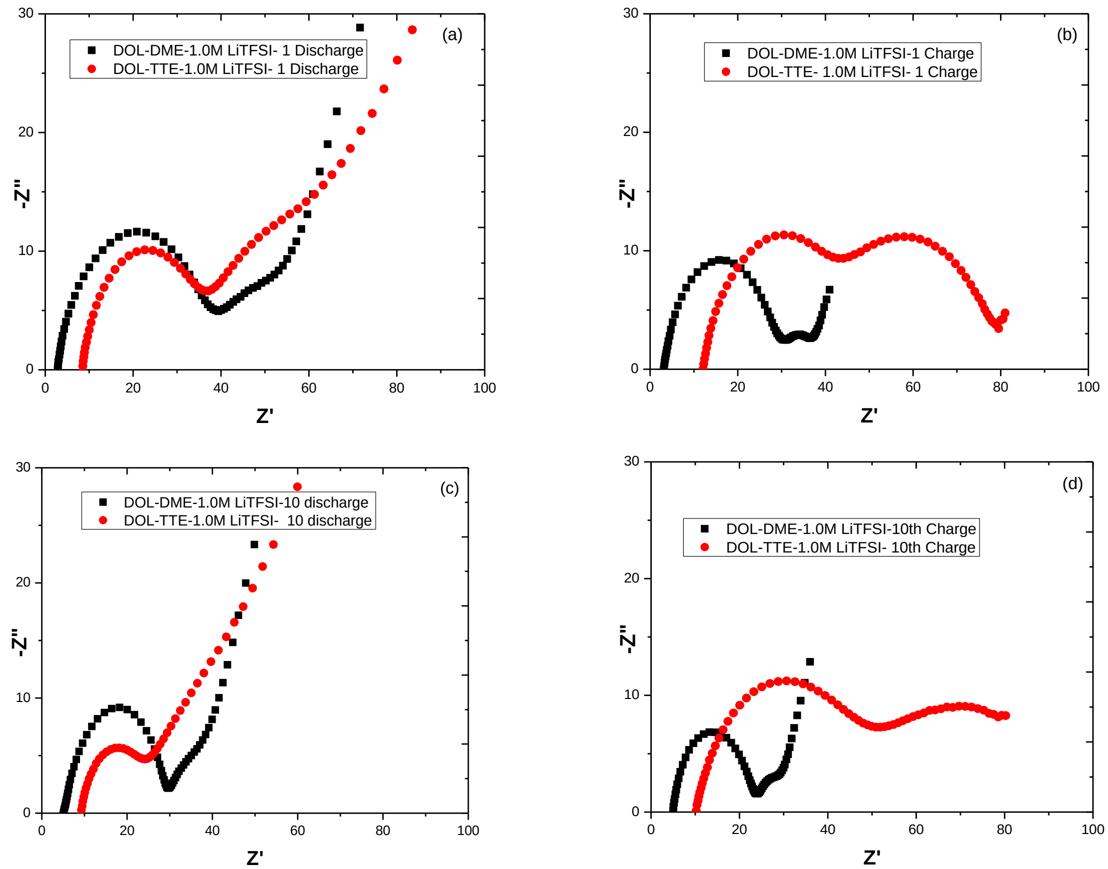

Figure 6. AC impedance spectra of Li-S cells measured at stage of (a) 1st discharge, (b) 1st charge, (c) 10th discharge, and (d) 10th charge.

3.6 Ionic Conductivity of the Fluorinated Electrolyte

The ionic conductivity of the two electrolytes was also measured at different temperatures using the method described earlier and the results are shown in figure 7. As observed, the conventional DOL/DME-1.0M LiTFSI electrolyte shows higher conductivity, and its conductivity increases from 9 mS/cm to 10.5 mS/cm when the temperature is raised from 10 °C to 60 °C; while for the cell containing the DOL/TTE-1.0M LiTFSI the conductivity is much lower and increases from 2 mS/cm to 3 mS/cm in the same temperature range. The result obtained in this study are consistent with the EIS study in which the cell containing the fluorinated electrolyte has higher passivation resistance, which is a good indication that the passivation formed in the TTE electrolyte is denser and hence more protective.

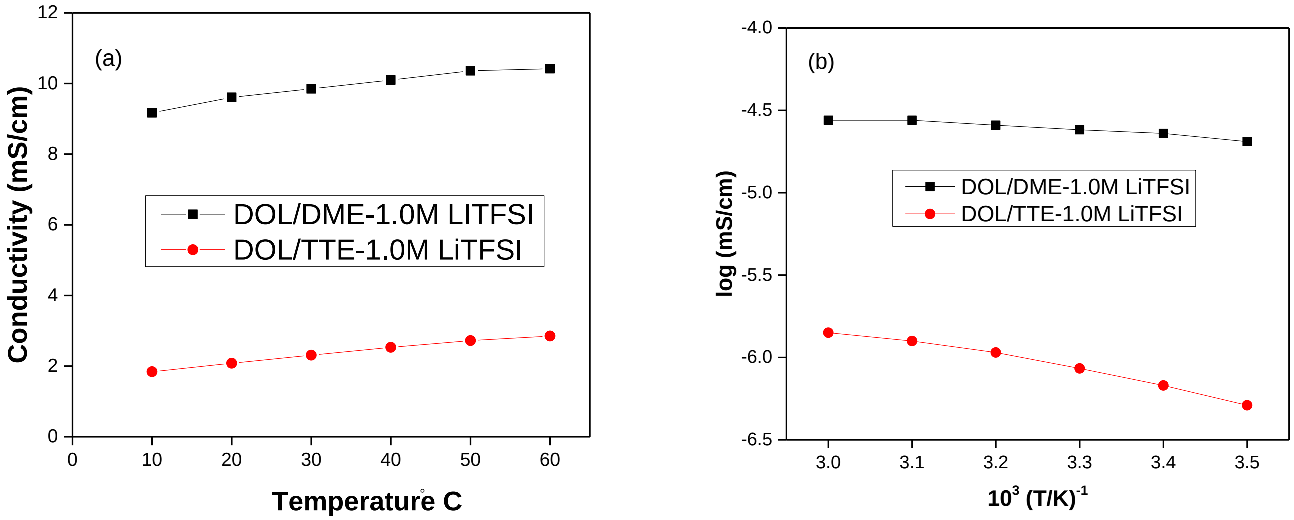

Figure 7. The effect of temperature on the ionic conductivity of (a) DOL/DME-1.0M LiTFSI and DOL/TTE-1.0MLiTFSI and (b) Arrhenius relation of σT and 1000/T for DOL/DME-1.0M LiTFSI and DOL/TTE-1.0MLiTFSI .

3.7 Characterization Study

Different characterization techniques were used in order to gain more knowledge about the electrode and electrolyte in the Li-S cell containing different electrolyte solvents.

Scanning Electron Microscopy

<u>Sulfur cathode</u>

We also determined the morphological changes of the sulfur electrode being discharged in both electrolytes. Figure 8a is the typical SEM image of the pristine sulfur/carbon electrode. After the first discharge in baseline electrolyte, the surface of sulfur cathode was deposited with large quantities of crystal-like discharged products (Figure 8b) of insoluble lithium sulfides (Li_2S and/or Li_2S_2) species during the discharge process (8). Further analysis of the deposit using energy-dispersive x-ray (EDS) spectroscopy revealed the dominate sulfur-rich agglomeration as shown in Figure 8d. However, the discharged electrode showed morphology similar to the pristine cathode filled with fine discharged product particles/flakes hidden in the porous structure of the S/carbon composite when using the TTE fluorinated electrolyte as illustrated in Figure 8c. Much less polysulfide deposition was observed from the EDS spectrum for the discharged cathode surface when 1.0 M LiTFSI DOL/TTE electrolyte was used (Figure 8e). This is evident that the SEI formation on the surface of cathode suppresses the dissolution and the agglomeration of the discharged species when using the fluorinated electrolytes, an observation which is supported by the improved specific capacity with superior coulombic efficiency when the fluorinated electrolyte was used.

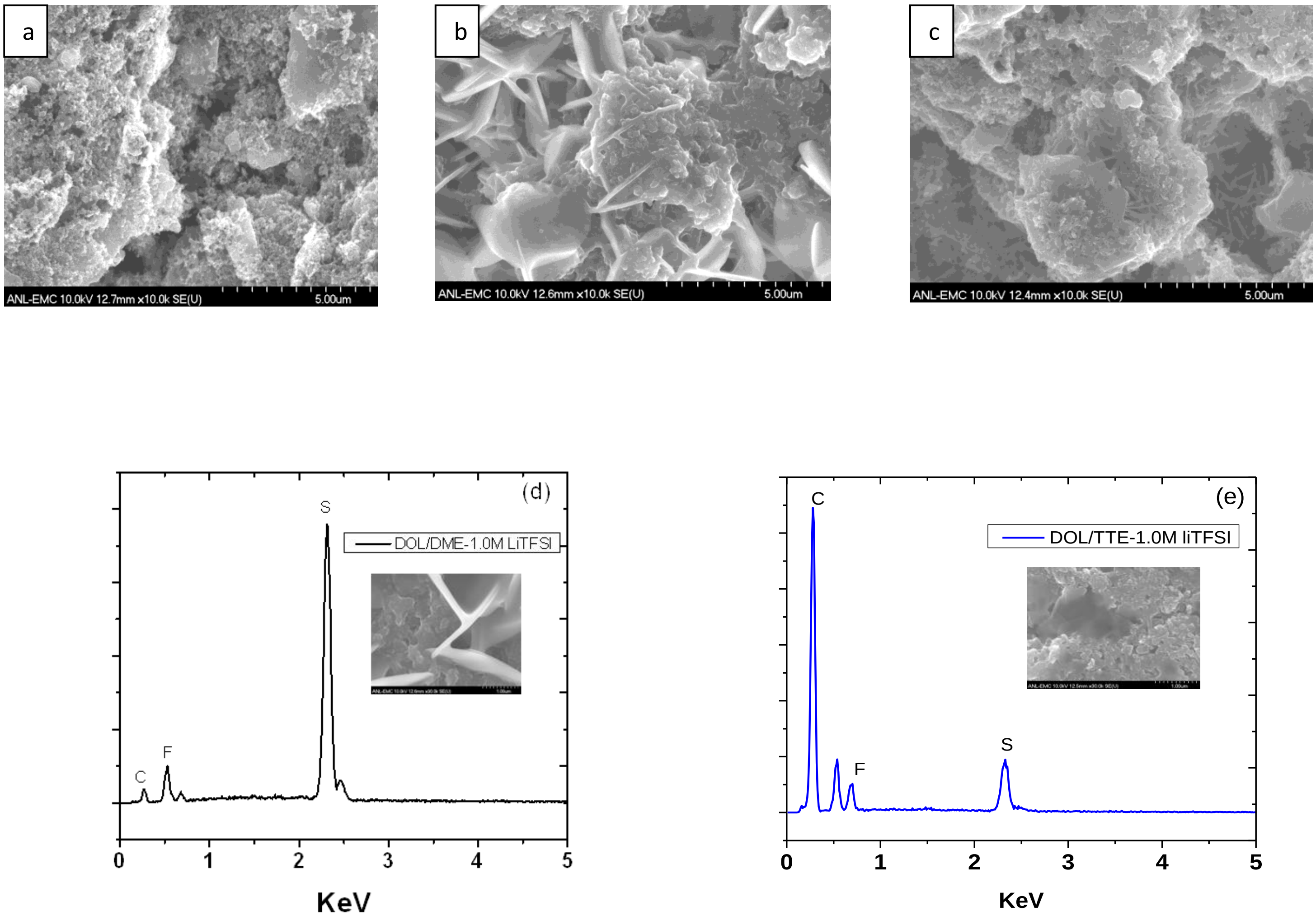

Figure 8. SEM images of (a) pristine electrode, (b) discharged electrode using 1.0M LiTFSI DOL/DME, (c) discharged electrode using 1.0M LiTFSI DOL/TTE, and EDS spectra of sulfur electrode at the 1st discharged state using (d) 1.0 M LiTFSI DOL/DME and (e)1.0 M LiTFSI DOL/TTE.

Lithium anode

Figure 9 shows the morphologies of the lithium anode after being cycled for 1st cycle in the baseline electrolyte and the fluorinated electrolyte (18). As observed in figure 9, the pristine lithium has a smooth surface; while for the cycled lithium pronounced morphological changes of the electrode are observed. The Li anode cycled in DOL/DME electrolyte surface has structures which appear to be voids on the surface of the lithium. There is also another layer of material on top of the anode which is beam sensitive. This layer of material, which is formed by the deposition of insoluble PS, disappears with prolonged exposure to the electron beam. EDS spectrum in Figure 9c clearly indicates that sulfur has the highest concentration inside these pits on the surface of the anode. In comparison, a more dense layer of passivation was observed on the cycled Li anode with fluorinated electrolyte (Figure 9d, 9e) and EDS spectrum of this layer showed less sulfur deposition (Figure 9f), which is in agreement with the observations reported in our previous study (8). The lower diffusion of LiPS and mitigated parasitic reaction of these species with the lithium anode results in higher coulombic efficiency and less self-discharge of the Li-S cell.

.

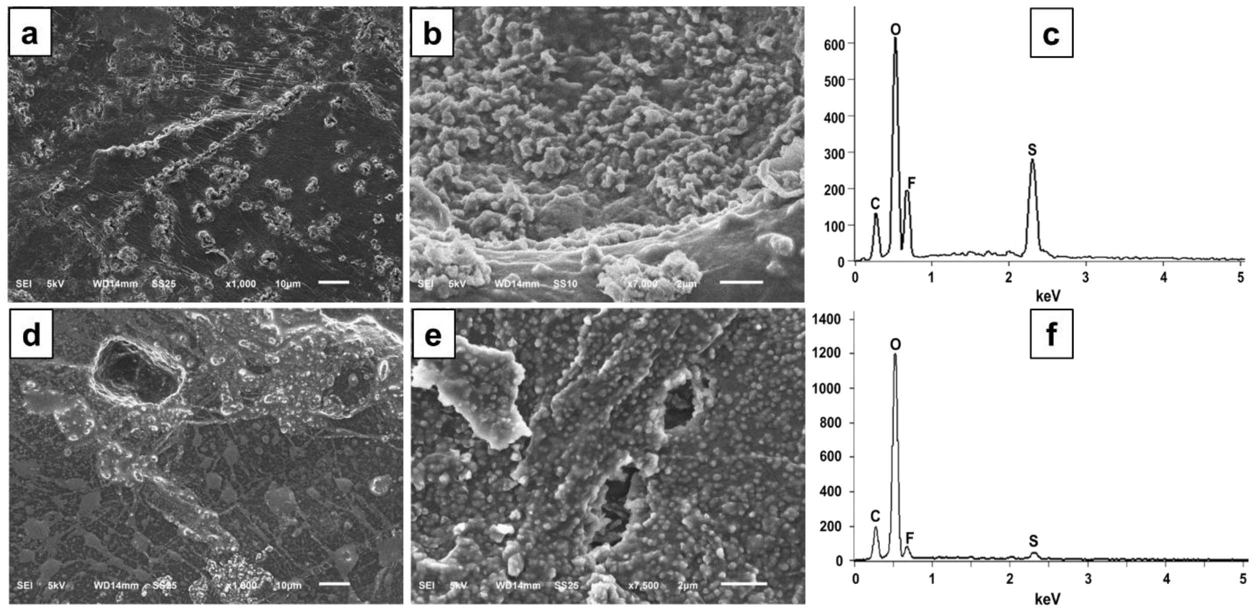

Figure 9. SEM images and EDS data of lithium anodes cycled after 1st discharge: (a), (b) and (c) with DOL/DME-1.0 M LiTFSI; (d), (e), and (f) with DOL/TTE-1.0 M LiTFSI.

HPLC/UV-VIS study

In a Li-S cell, sulfur is electrochemically reduced to polysulfide intermediates through a multistep process, in which the long polysulfide chains are soluble in the electrolyte. [3, 4] At the final step, insoluble discharge products such as Li_2S_2 and Li_2S are generated through the reactions shown below:

$$S_8 + 2Li^+ \rightarrow Li_2S_8 \quad (3.1)$$

$$Li_2S_8 + 2Li^+ \rightarrow Li_2S_{8-n} + Li_2S_n \quad (3.2)$$

$$2Li_2S_n + (2n-4)Li^+ \rightarrow nLi_2S_2 \quad (3.3)$$

$$Li_2S_n + (2n-2)\,Li^+ \rightarrow nLi_2S \quad (3.4)$$

$Li_2S_2 + 2Li^+ \rightarrow 2Li_2S$ (3.5)

The dissolution of these species causes severe capacity fading and redox shuttling effect which are of the main obstacles for commercialization of these batteries (19, 20). Better understanding of the discharge process in Li-S batteries can assist in solving this problem. Recently our group reported about a new electrolyte based on an organo-fluorine solvent that prevents the shuttling effect and improves the performance of the Li–S battery (8).

Since *in situ* measurements of reactions inside the Li-S cell are associated with many difficulties, ex situ analysis methods such as HPLC and UV-VIS were employed to characterize the active species in the electrolyte after cycling. HPLC was first employed for characterizing reference samples of Li_2S_6 and Li_2S_4 and also diffused lithium polysulfides after cycling in the cell. The HPLC chromatograms associated with five different concentrations of 50.0, 25.0, 12.5, 6.0, and 3.0 mM M for Li_2S_6 and Li_2S_4 reference data are shown in figure 10a-c respectively. As shown there are 3 peaks at different retention times (4.8-5 min, 5.8 min and 6.1 min) which are associated with the elution of polysulfides with different chain length and size [3] for Li_2S_6 reference sample, where the major peaks is observed at 6.1min (Fig. 10b). As expected higher concentrations of the polysulfides show higher absorption at 254nm wavelength. The HPLC data for reference Li_2S_4 solution is also shown in figure 10c. As observed there are 6 different peaks were two peaks at 5.8 and 6.1 min are similar to Li_2S_6. Since the major peak at 6.1 min is symmetrical and well-resolved as well as the baseline around this area, its peak position and integrated intensity at different concentrations were used to generate the calibration plot (21). Based on this plot we can approximately calculate the concentration of dissolved sulfur in the cycled electrolyte.

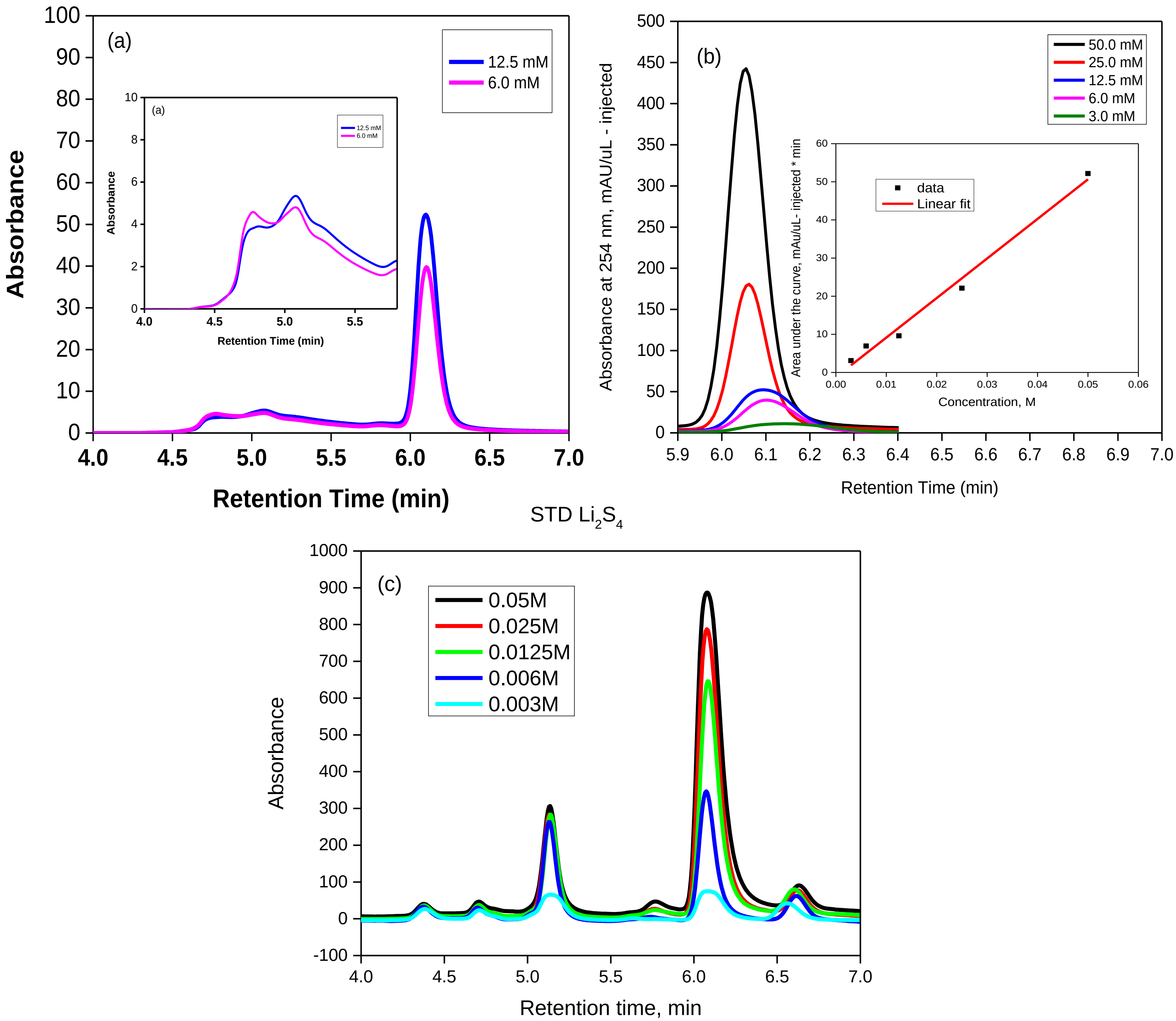

Figure 10. HPLC chromatograms of (a) Li_2S_6 reference sample (b) Li_2S_6 major peak at 6.1min and calibration plot (inset) and (c) Li_2S_4 reference sample in DOL/DME.

In order to characterize the lithium polysulfides in the harvested electrolyte solution, HPLC was used to separate the different lithium polysulfide chain length. In this respect, harvested electrolyte from cells with the baseline electrolyte, 1M LiTFSI in DME/DOL, and fluorinated electrolyte, 1M LiTFSI in DOL/TTE, after 10^{th} discharge was also investigated by using the HPLC method. As shown in figure 11, three main peaks are observed for the polysulfides in the harvested electrolytes at 4.8, 5.2 and 6.1 min in which the major peak is very similar to the Li_2S_6 and Li_2S_4 reference solution retention time. It is evident from this data that the DOL/DME electrolyte has higher solubility for higher order polysulfides where the peak at largest retention time of 6.1 is associated with the elution of longer chain polysulfides. Due to this higher solubility severe shuttling is observed when using this baseline electrolyte in the Li-S cell. The absorbance intensity for this cell is almost 2 times of the intensity for the cell containing the fluorinated electrolyte. By comparing the retention times for the cycled cell and reference catholyte samples, assumptions are made about the composition of the polysulfides. Even though the mechanism of the reduction to the LiPS is still very controversial, qualitative observations are made from this study where the peak at 6.1 min can be associated with the Li_2S_6 and Li_2S_4 PS. In this case we can assume that due to the following series of disproportionation reactions there is also less deposition of the lower insoluble polysulfides such as Li_2S_2 and Li_2S on the electrode surface (3, 4). This is confirmed by scanning electron microscopy (SEM) studies in our previous report (8) and XPS results in the following section.

$$S_6^{-2} \rightarrow 2S_3^{-} \quad (3.6)$$

$$3Li_2S_4 + 2Li^+ \rightarrow 4\,Li_2S_3 \quad (3.7)$$

$$2Li_2S_3 + 2Li^+ \rightarrow 3Li_2S_2 \quad (3.8)$$

$$Li_2S_2 + 2Li^+ \rightarrow 2Li_2S \quad (3.9)$$

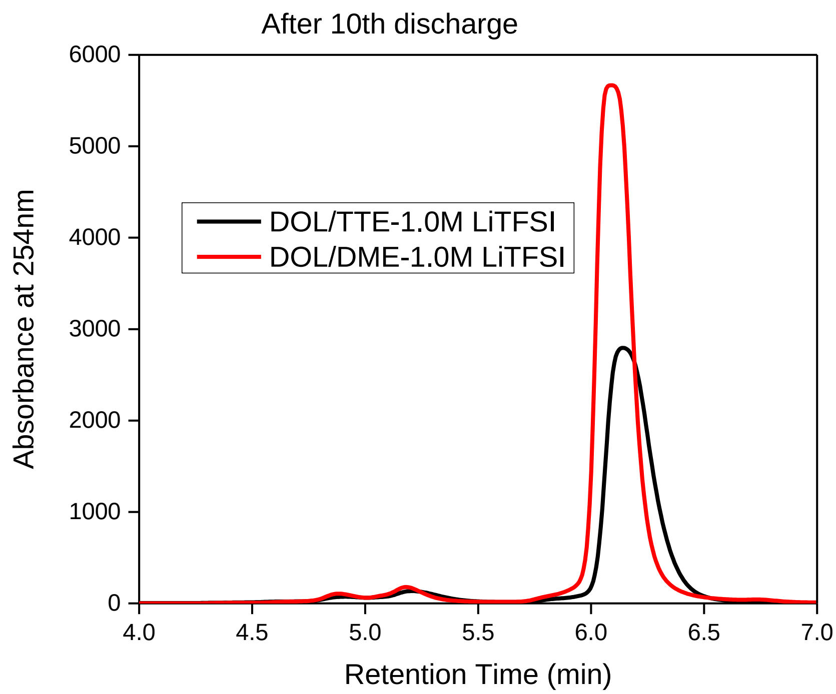

Figure 11. HPLC chromatograms of cells after 10th discharge containing DOL/DME-1.0M LiTFSI and DOL/TTE-1.0M LiTFSI.

Next, in order to study the ratio effect of the fluorinated electrolyte and to calculate the amount of soluble sulfur in these solvents, HPLC measurements were employed for cells containing two other ratio solvents of DOL/TTE (1/2) and (1/3) with 1.0M LiTFSI salt after 10th discharge and the results are shown in figure 12. Based on the intensity and area under each curve, the amount of soluble sulfur and its concentration can be calculated based on the calibration plot (Fig.10b). As shown in figure 12, by increasing the amount of fluorinated solvent in the electrolyte, there is much lower sulfur concentration calculated for the cycled electrolyte. For example the sulfur concentration is about 12.5 mM when the Li-S cell is cycled with the conventional electrolyte, where only 2.9 mM of sulfur concentration is calculated for the cell where a DOL/TTE (1/3) solvent ratio is used as electrolyte. This results in shuttle prevention and less deposition of the insoluble discharge product and clearly shows the reason for improved performance of the DOL/TTE electrolyte in comparison to the conventional electrolyte.

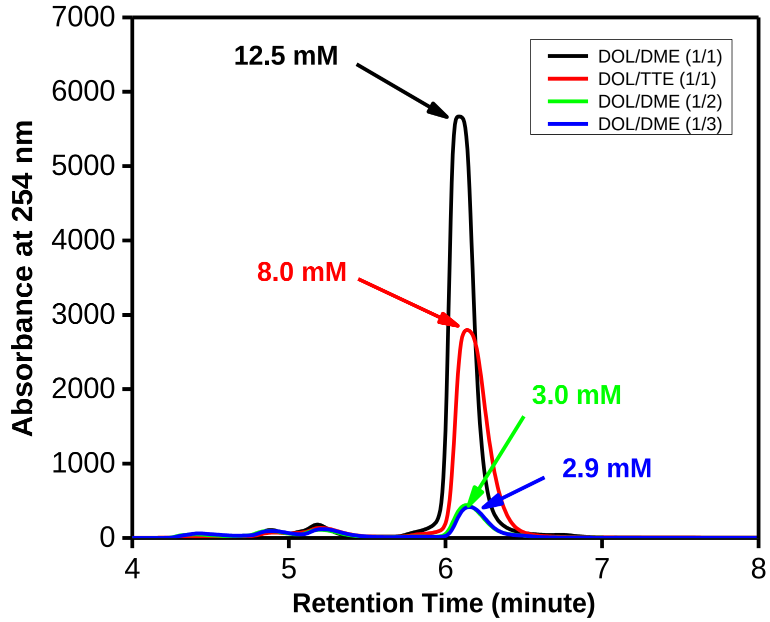

Figure 12. HPLC chromatograms of cells after 10th discharge containing DOL/DME-1.0M LiTFSI and different ratios of DOL/TTE-1.0M LiTFSI.

UV-VIS spectra were also obtained to confirm the consistency of our previous studies. Figure 13a and b show the UV-VIS spectra for five different concentrations of 50.0, 25.0, 12.5, 6.0, and 3.0 mM for Li_2S_6 and Li_2S_4 reference data respectively, where in figure 13c the UV absorption is observed for cells after 10 discharging cycles with different ratios of fluorinated solvent. As expected, the cell containing the conventional DOL/DME-1.0M LiTFSI electrolyte has much higher absorption due to the higher concentration of diffused polysulfides. As the ratio of the fluorinated solvents increases in the cell, lower solubility of the polysulfides is observed after cycling. This data is in agreement with the HPLC data.

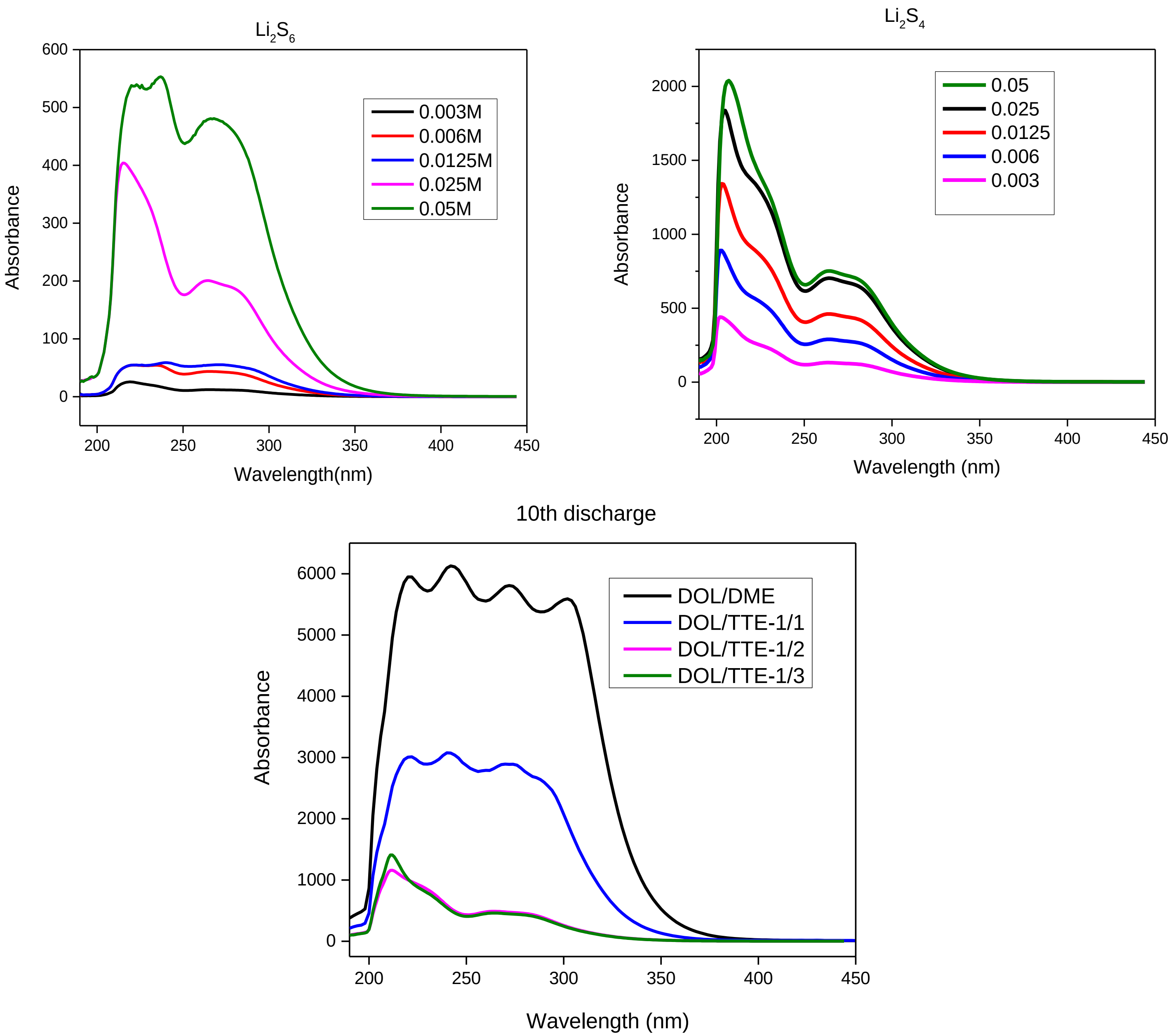

Figure 13. UV-Vis absorption spectra of reference samples in different concentrations (a) Li_2S_6 (b) Li_2S_4 and (c) cells after 10th discharge containing different ratios of DOL/DME-1.0M LiTFSI and DOL/TTE-1.0M LiTFSI.

XPS Analysis

To further understand the effect of different solvents on the Li-S battery performance, ex situ XPS analysis of the cathode surface retrieved from cycled cells was carried out and the result are shown in figure 14 and 15. Figure 14a shows C_{1S} spectra of the sulfur electrodes in DOL-DME-1.0M LiTFSI electrolyte at different charging and discharging states. In the pristine cathode, the C_{1S} peak at 284.8eV is assigned to C-C and peaks at 286.4eV and 290.98eV are assigned to C-H and C-F from PVDF binder (22-24). At the 1st discharge state, the C_{1s} peaks were covered by new species (C=O at 290.2 eV, CF2 at 293.4 eV) due to the SEI formation and the deposition of the discharge product on the electrode surface Also, peak at 293.4 eV is assigned to CF_2 or CF_3 bonds. At the end of discharge cycles, the C_{1S} signals from PVDF were weaker due to the deposition of the discharge products on the surface of the cathode (22, 25, 26). Also, peak at 290.2eV is assigned to C=O. This is in agreement from previous reports where the formation of ROLi and HCO_2Li is confirmed (26). Figure 14b also shows the C_{1S} spectra of the sulfur electrodes after cycling in DOL-TTE-1.0M LiTFSI electrolyte. By comparing the XPS spectra for both electrolytes, it is observed that, the intensity for peak at 290.2eV after first discharge and peak at 293.1 eV after first charge is increased after using fluorinated electrolyte which is due to the higher ratio of fluorinated solvent and the formation of a SEI on the electrode surface after using the fluorinated electrolyte.

Figure 14c and d show S_{2P} spectra of the sulfur electrodes after the 1^{st} cycle in DOL-DME-1.0M LiTFSI and DOL-TTE-1.0M LiTFSI electrolyte respectively. Peaks at 164.4 eV and 165.7 eV are the characteristic peaks of S-S bonds of elemental S_8 in pristine cathode (25, 26). Also the peaks with binding energy over 168 eV are assigned to LiTFSI (S-O from SO_2 or SO_3) and can be found in all samples (Figure 14 e and f) (25, 26). After the first discharge, the S-S peak disappeared and two other peaks at 162.6 and 163.8 eV showed up in the lower energy area at 162.6 and 163.8 eV,confirming the conversion of elemental S to S^{2-} through electrochemical reduction with generation of discharge product Li_2S or Li_2S_2 (22, 25-27) and these peaks remain unchanged even at fully charged state, indicating the loss of the active material due to this irreversible reaction. After comparing XPS S_{2p} spectra when using the fluorinated electrolyte, two observations are made:

-It is observed that peaks at 162.6ev and 163.8 eV which are assigned to Li_2S and Li_2S_2 still appear after first discharge when using any of the two electrolytes. However they have completely vanished after the first charge when only using the fluorinated electrolyte (Fig. 14). This is due to the lower solubility of the poly-sulfides in the fluorinated electrolyte which indicates the good reversibility of the PS and also the formation of the SEI layer on the cathode. This highly reversible process explains the high specific capacity and coulombic efficiency of the DOL/TTE cell. The lower oxidation S_{2p} peaks exist throughout the cycling and accumulate with cycling for the DOL/DME cycled electrode; however, the reversibility maintains with the extent of cycling for the DOL/TTE electrode. No recognizable peaks showed up until the 20th cycle and the intensity of these S_{2p} peaks is still small when DOL/TTE is used as electrolyte.

-It is reported earlier that the formation of Li_xSO_y species from the reaction of the salt with the active material increases with cycling and has been negatively effective in increasing the cell's capacity fading due to the active mass irreversible oxidation (26). When comparing both XPS spectra from both solvents (Figure 14 e and f), it is clear that when using the fluorinated electrolyte the intensity of the peaks are much lower after discharge cycles due to the formation of the SEI and less formation of Li_xSO_y species results in better capacity retention when using the DOL-TTE-1.0M LiTFSI electrolyte. In addition after 20 cycles, the oxidation state of the sulfur products had higher intensity than LiTFSI.

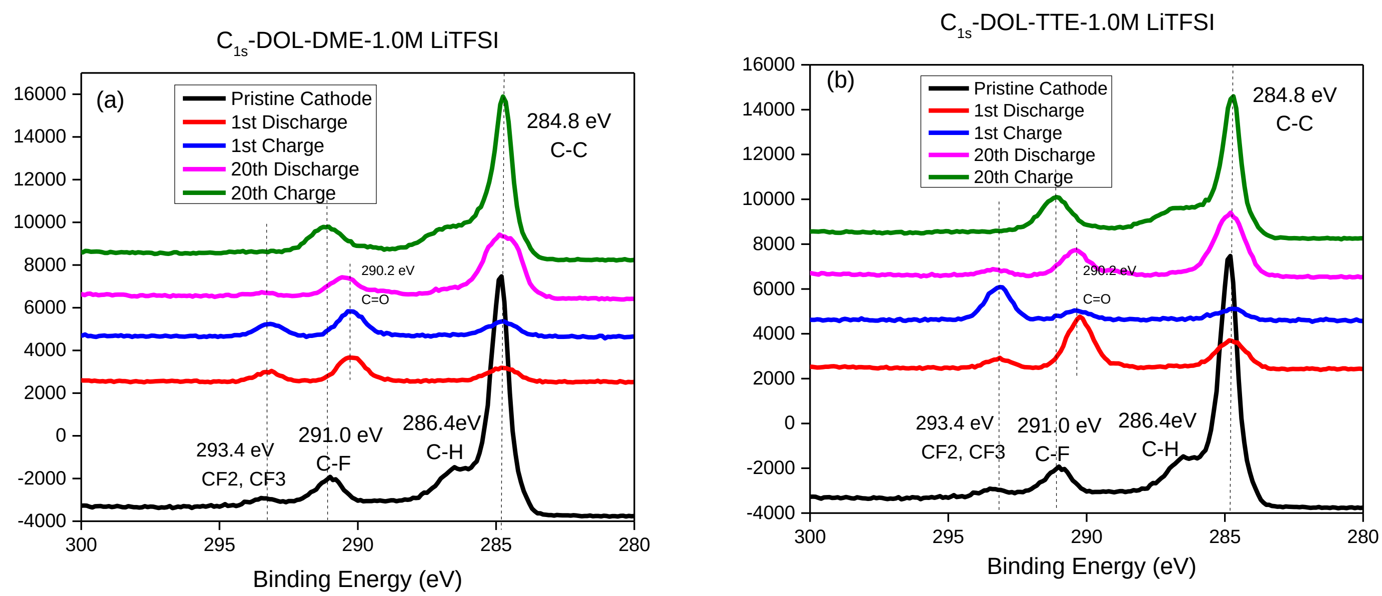

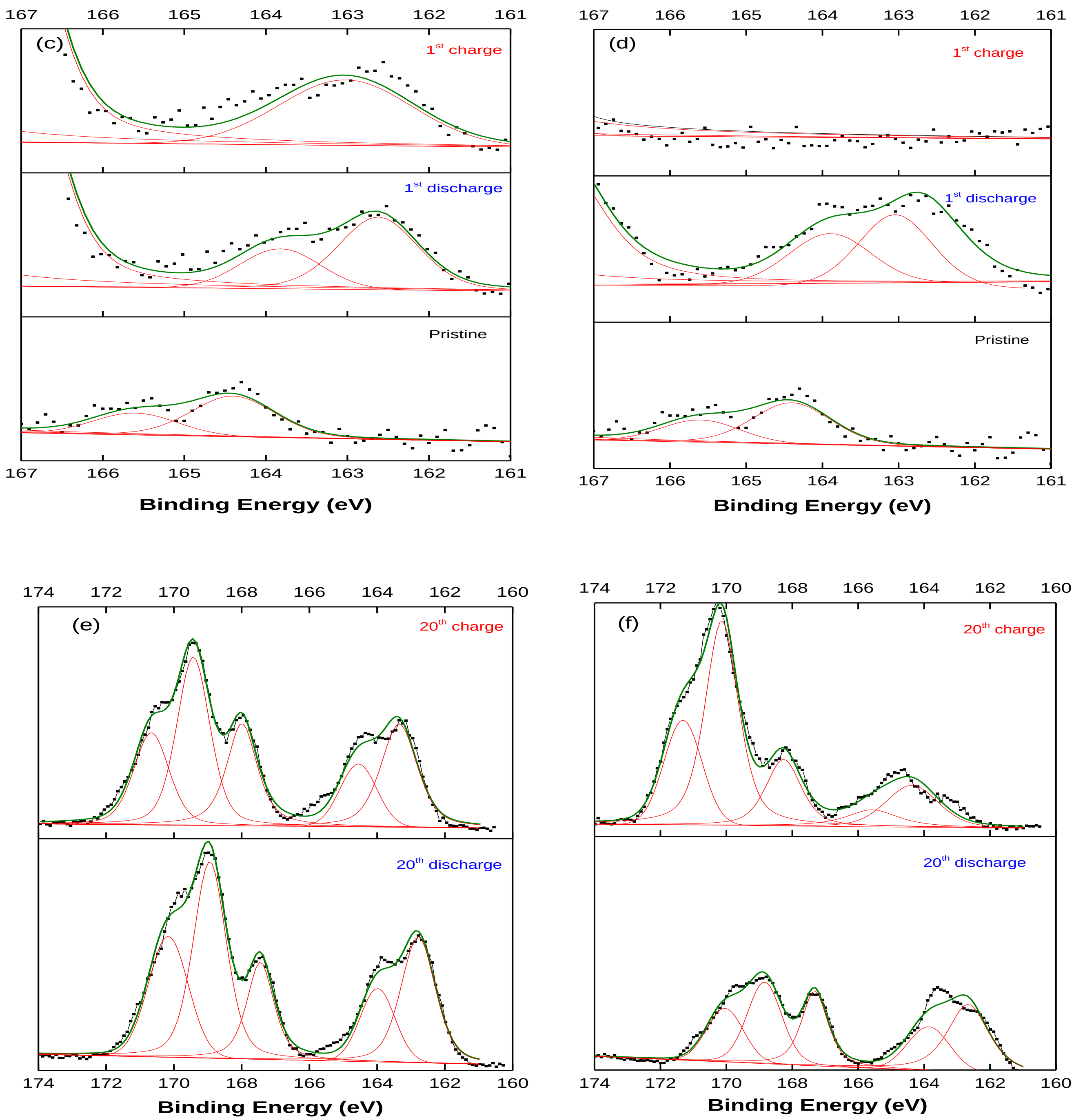

Figure 14. C_{1S} XPS spectra of sulfur cathodes for pristine cathode, cathode of the 1st discharge, cathode of the 1st charge, cathode of the 20th discharge, and cathode of the 20th charge in (a) DOL-DME-1.0M LiTFSI and (b) DOL-TTE-1.0M LiTFSI; and S_{2P} XPS spectra of sulfur cathodes after 1 cycle in (c) DOL-DME-1.0 LiTFSI and (d) DOL-TTE-1.0 M LiTFSI and after 20 cycles in in (e) DOL-DME-1.0 M LiTFSI and (f) DOL-TTE-1.0 M LiTFSI.

Figure 15 also shows the Li_{1S} and F_{1S} spectra for cathodes at different charge and discharging cycles. The peak at 55.5 eV was assigned to Li-S bond from Li_2S/Li_2S_2 at the discharge state for the DOL/DME cell (Figure 15a) and DOL/TTE cell (Figure 15b). However, in the charged state, this peak disappeared and a new peak showed up at a shifted position at 56.2 eV, corresponding to the formation of Li-F bond for the DOL/TTE cell, whereas the peak remains unchanged in terms of position and intensity for the DOL/DME cell. The LiF-rich solid electrolyte interphase formed on the sulfur surface further improves the coulombic efficiency and capacity retention. Figure 15 c and d are F1s XPS profiles. Decomposition products comprising C-F bond dominate the spectra for electrodes cycled with both electrolyte cells. For the pristine sulfur electrode, the peak centered at 688 eV is attributed to the PVDF binder and the peak shifted when LiTFSI was involved in the electrochemical reaction on the electrode surface. However, a larger contribution of C-F showed up for the TTE cell due to the reduction of TTE on cathode surface.

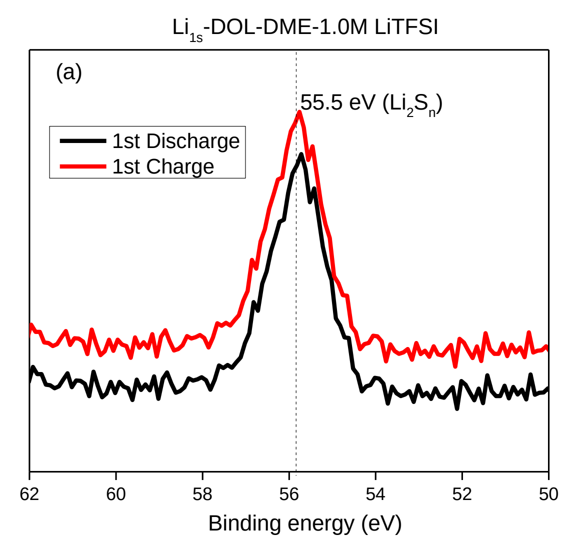

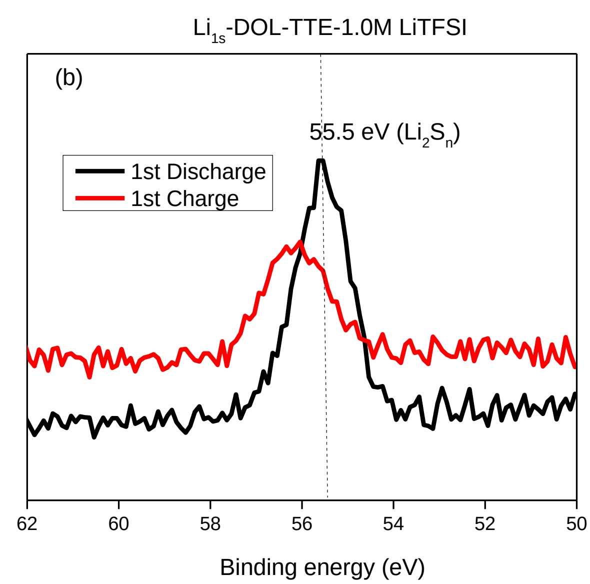

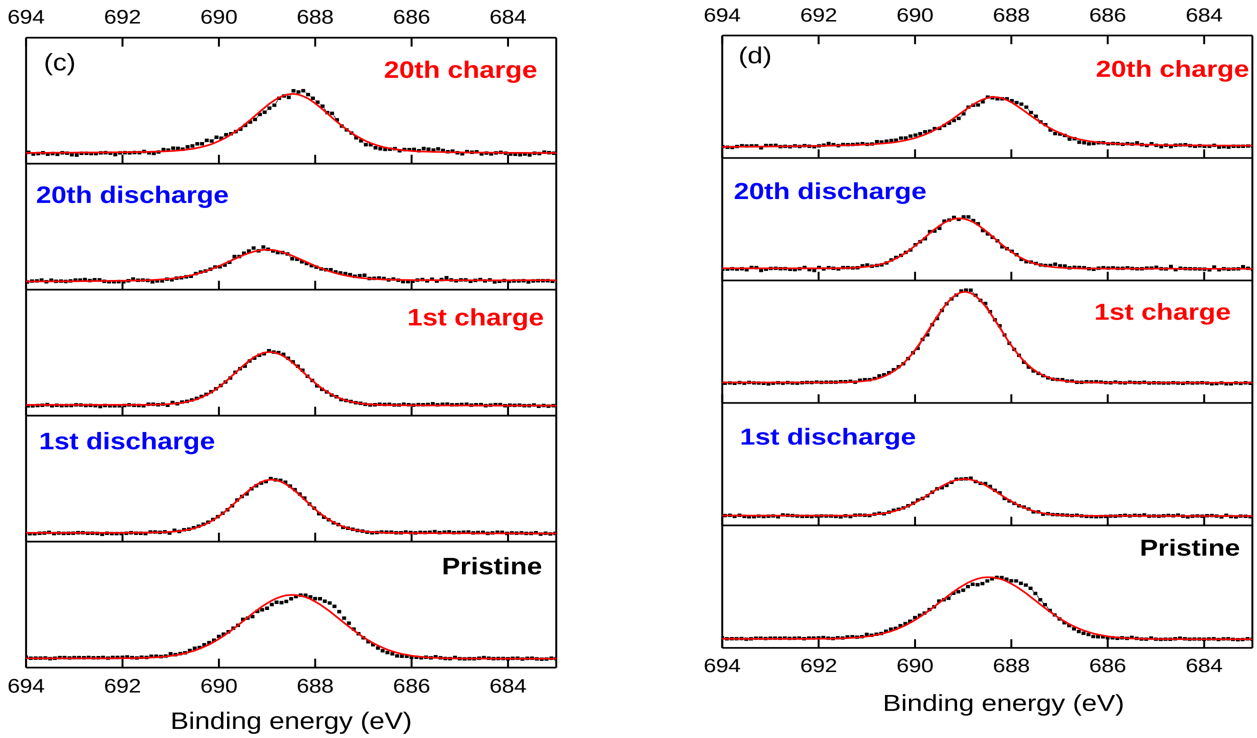

Figure 15. Li_{1S} XPS spectra of sulfur cathodes for pristine cathode, cathode of the 1st discharge, cathode of the 1st charge, cathode of the 20th discharge, and cathode of the 20th charge in (a) DOL-DME-1.0M LiTFSI (b) DOL-TTE-1.0M LiTFSI; and F_{1S} XPS spectra of sulfur cathodes in (c) DOL-DME-1.0 M LiTFSI and (d) DOL-TTE-1.0 M LiTFSI.

3.8 Suppressing the Self-Discharge With Fluoroether Containing Electrolyte

In addition to the many issues involved with Li-S batteries, they also suffer from severe self-discharge, which is one of the biggest hurdles for the commercialization of this battery (28). A secondary battery will lose its charge capacity when kept for a period of time at a certain temperature. This occurrence is referred as battery self-discharge and it basically depends on the battery chemistry, electrode composition, choice of current collector, electrolyte formulation, and the storage temperature (28). For Li-S batteries, the self-discharge is a well-known issue due to the severe corrosion of lithium metal anode in the presence of the LiPS in the electrolyte (28-30).

Many attempts have been taken in order to overcome the poor cycle life and low sulfur utilization of Li-S battery (8,28,31-37). However, there are only a few research focused on solving the self-discharge issue of the Li-S battery. Kazazi *et al*. have reported that the corrosion of the aluminum current collector and the shuttle mechanism play a significant role in the self-discharge of Li/S cells; therefore, $LiNO_3$ is a suitable candidate for an electrolyte additive candidate to prevent self-discharge due to its effect on shuttle prevention (28). Mikhaylik and Akridge reported that self-discharge mainly attributed from the high plateau polysulfide. Electrolytes with higher salt concentration showed lower rates of Li corrosion with LiPS and a lower shuttle constant (38) Ryu *et al*. reported that self-discharge of Li-S battery is dependent on the current collectors. The stainless steel current collector showed the highest self-discharge rate of 59% per month caused by the corrosion of the stainless steel current collectors by LiPS. In comparison, average self-discharge rate for aluminum current collector is 3% per month (39-41).

In this study, the effect of different electrolyte systems was investigated on the self-discharge behavior of Li-S batteries. As severe self-discharge has become the major issue for high-loading sulfur cathodes (> 5 mg (S)/cm^2), our test results suggest that utilizing fluorinated electrolyte to effectively suppress this fatal effect shall pave the way for practical applications of a high energy density Li-S battery (8, 42). Fluoroether-containing electrolytes have been reported by other groups to enhance the performance of the Li-ion battery due to their unique physical and chemical properties; (10-13) however, it is our idea to use it as an electrolyte co-solvent/additive for the Li-S battery.The electrolytes used in these self-discharge studies were (1) 1M LiTFSI in DME/DOL (v:v=1:1); (2) 1M LiTFSI and 0.2M LiNO3 in DME/DOL (v:v=1:1); (3) 1M LiTFSI in DOL/TTE (v:v=1:1); (4) 1M LiTFSI and 0.2M LiNO3 in DOL/TTE (v:v=1:1) and (5) 1M LiTFSI and 1.0 M LiNO3 in DME/DOL (v:v=1:1). For electrolyte (5), LiTFSI salt dissolves easily in DOL/DME (v/v, 1/1) to 1.0 M. This solution can further dissolve $LiNO_3$ to the maximum 1.0 M. The electrolyte (5) is oversaturated and the solution is not completely transparent. Self-discharge was tested by charging and discharging the cells with a C/10 rate for five cycles and then resting them for 10 hours between the fifth charge and sixth discharge step and was then calculated by comparing the discharge capacity of the 6^{th} cycle to the 5th cycle.

Low Loading Cathodes-

To investigate the self-discharge in both electrolytes with low loading sulfur electrodes (2-3 mg/cm^2) the cells were put to rest for 10 hours after 5^{th} charge. As shown in Figure 16, Li-S battery suffers from a loss of 8% in discharge capacity after 10 hours resting when using the baseline electrolyte with 0.1M $LiNO_3$ at room temperature and increases significantly at elevated temperature. Surprisingly, the discharge capacity didn’t decrease but increased after 10h storage for the Li-S cell using the fluorinated TTE electrolyte at charged state at room temperature, as shown in Figure 16b. This phenomenon became significant when 0.1M $LiNO_3$ was added to the TTE electrolyte and a 20% capacity increase was obtained.

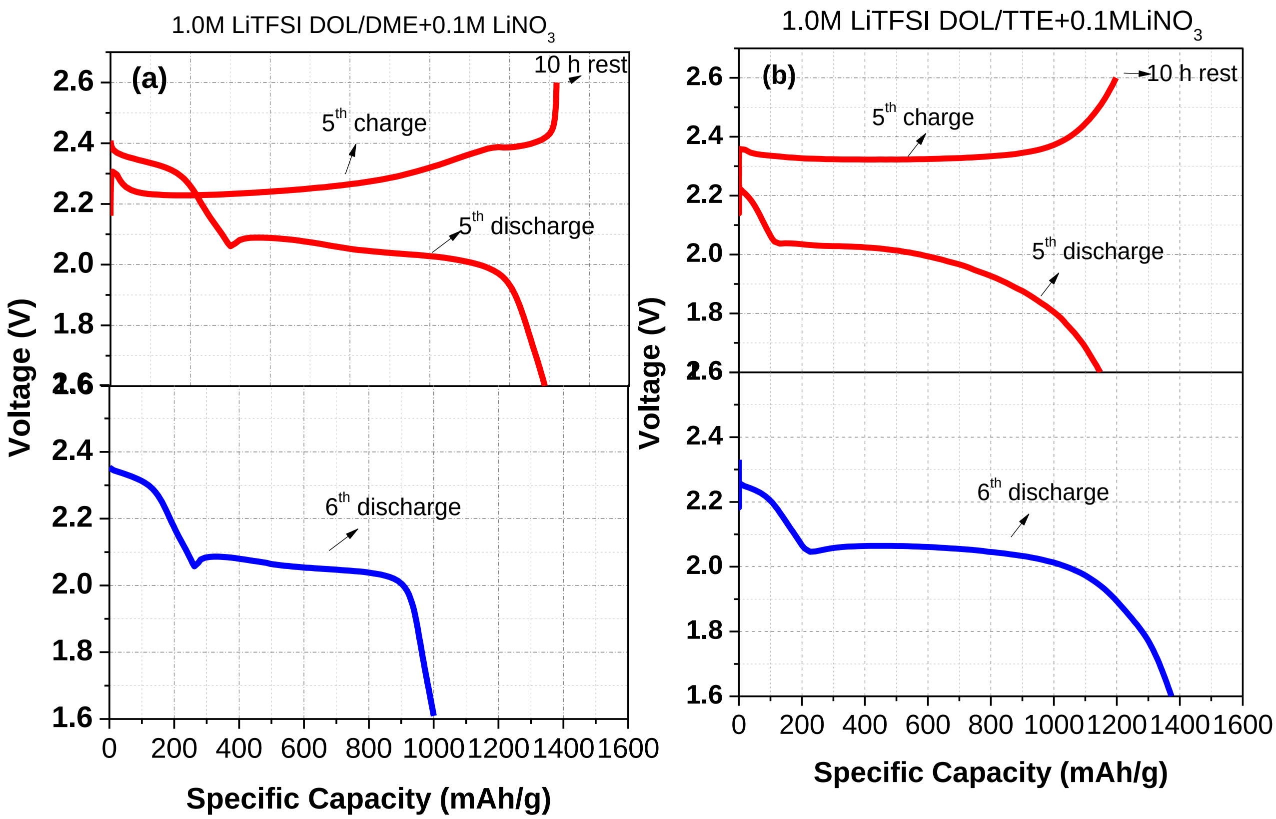

Figure 16. Self-discharge voltage profiles for Li-S cells with low loading cathode at room temperature. (a) Conventional DOL/DME-1.0M LiTFSI-0.1M $LiNO_3$, (b) DOL/TTE-1.0M LiTFSI- 0.1M $LiNO_3$

High Loading Cathodes

To determine the effect of loading, self-discharge behavior of Li-S cells with high loading sulfur electrodes (5 mg/cm^2)containing the conventional DOL/DME-1.0M LiTFSI and fluorinated electrolyte DOL/TTE-1.0M LiTFSI, has been investigated by the same procedure and the results are shown in Figure 17. As expected, by using the baseline DOL/DME-1.0M LiTFSI electrolyte after the 10-hour rest, discharge capacity of 790 mAh/g for the 5th cycle dropped below 650 mAh/g for the 6th cycle. The shuttle phenomenon of the cell was obvious due to lithium polysulfide dissolution during the charge and discharge process, which led to an extremely low coulombic efficiency (Figure 17a). Figure 17a demonstrates that the self-discharge in a Li-S cell using the conventional electrolyte was severe and more than 17%. However, as shown in figure 17b, when the partially fluorinated electrolyte was used as co-solvent and much lower self-discharge of 4% is observed using TTE. Even though using the fluorinated solvent has significantly improved the self-discharge, the same behavior is observed which indicates that self-discharge in both cells is due to both irreversible loss of sulfur active material, and polysulfide shuttling.

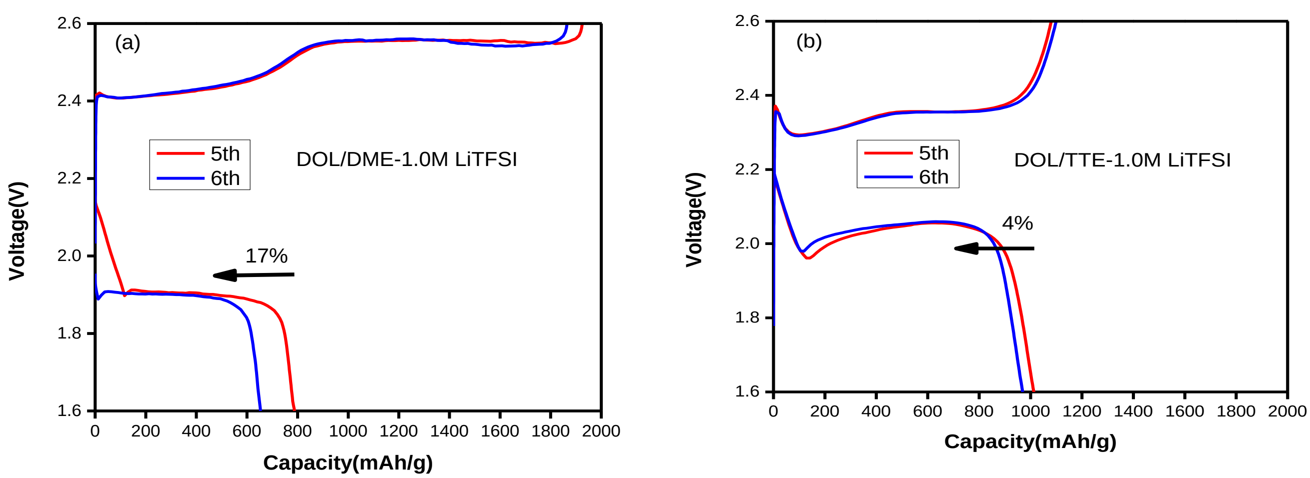

Figure 17- 5th and 6th cycle voltage profile for Li-S cells with high-sulfur-loading cathodes; a) DOL/DME-1.0M LiTFSI electrolyte and b) DOL/TTE-1.0M LiTFSI electrolyte.

3.8.1 $LiNO_3$ Additive Effect

In the next step, $LiNO_3$ additive was used with high loading sulfur electrodes and the self-discharge was investigated at two different temperatures for cells containing this additive. As shown in figure 18a, when 0.2 M $LiNO_3$ is added to the conventional DOL/DME-1.0M LiTFSI, electrolytea loss of 3.8% in discharge capacity is observed after 10 hours resting at room temperature, indicating much less self-discharge that occurs during the storage of the battery. These observations indicate that $LiNO_3$ efficiently prevented self-discharge in a Li-S cell. In addition, the rate of undesirable chemical reactions which cause internal current leakage between the sulfur cathode and lithium anode increases with temperature thus increasing the battery self-discharge rate, and as expected the self-discharge has increased to 8.6% when the temperature was increase to 55°C (Figure 18b). However, by studying this behavior for cells containing DOL/TTE-1.0M LiTFSI-0.2M $LiNO_3$ electrolyte, a decrease of only 0.7% is observed for cells resting at room temperature (Figure 18c). Surprisingly, by even increasing the temperature to 55°C as shown in figure 18d, almost no change is observed for the discharge capacity. We should note that all self-discharge experiments were conducted with cells which have loadings of more than 5 mg/cm^2 and these cells with high-loading electrodes were fabricated with high amount of electrolyte. It is well known that the increased amount of electrolyte can aggravate the polysulfide shuttle effect and therefore degrade the performance of the cell. However, no major self-discharge was observed regardless of the use of thick cathodes.

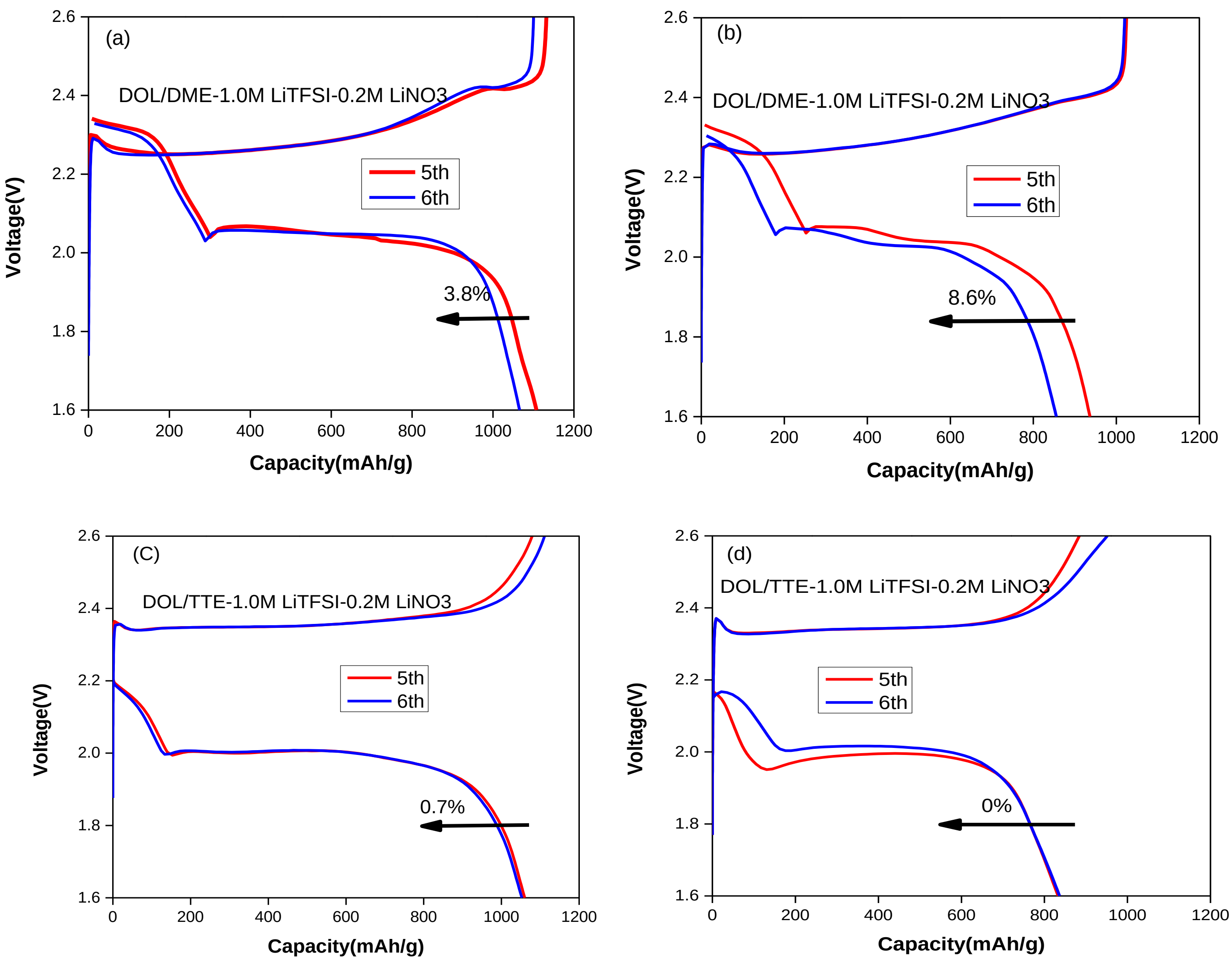

Figure 18- 5th and 6th cycle voltage profile for Li-S cells with high-sulfur-loading cathodes and DOL/DME-1.0M LiTFSI--0.2M LiNO3 electrolyte; a) at room temperature and b) 55°C and DOL/TTE-1.0M LiTFSI- 0.2M LiNO3 electrolyte c) at room temperature and d) 55°C.

To study the effect of $LiNO_3$ in particular on the self-discharge performance, experiments have been conducted with high concentrations of about 1.0M $LiNO_3$ in the electrolyte solvent. As reported earlier in literature, $LiNO_3$ is one of the most important additives reported to enhance the performance of Li-S batteries and is highly effective in inhibiting the PS redox shuttle. Surface analysis shows that $LiNO_3$ generates a protective film composed of Li_xNO_y and Li_xSO_y onto the surface of the lithium anode. However, it has been stated that $LiNO_3$ could not eliminate the active material loss and the repetition of cycling destroys the protective film. The self-discharge procedure has been investigated with cells containing 1.0M $LiNO_3$ as additive and the results are reported in Figure 19. It is observed that for cell containing DOL/DME-1.0MLiTFSI-1.0M $LiNO_3$ at room temperature, a capacity drop of about 2.7% is observed at room temperature, while at 55°C the drop is about 5% . Even though using this additive results in lower rate of self-discharge than for the Li-S cell containing the conventional electrolyte, using this high concentration of $LiNO_3$ additive has a negative effect on the cell performance. This is due to the fact that the irreversible reduction of $LiNO_3$ reduces reversibility of Li_2S and results in permanent loss in the reversibility of the Li-S cell. It is concluded that this additive does not completely prevent the self-discharge even at high concentration, while the fluorinated solvent is not present in the electrolyte. TTE must be combined with $LiNO_3$ for the avoidance of the self-discharge. This could indicate that the major part of self-discharge is due to irreversible loss of active material rather than polysulfide shuttling and that both lower solubility of lithium polysulfides in the fluorinated electrolyte and also the formation of the protective layer as a result of the TTE and $LiNO_3$ reduction (combined) on the lithium anode is the most effective in preventing the self-discharge behavior of the cell. This is due to much less contact between soluble lithium polysulfides and the lithium anode.

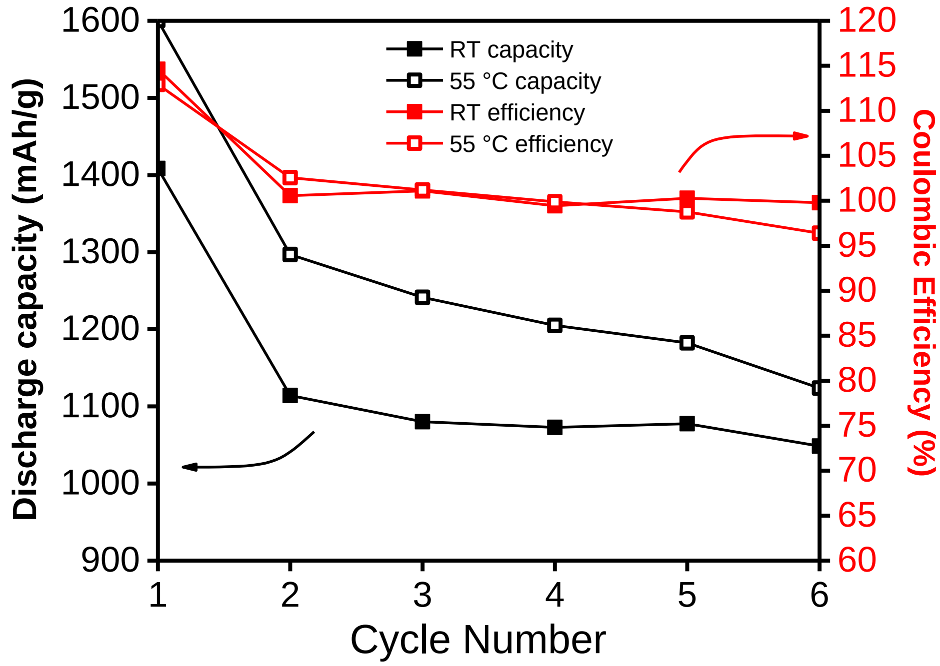

Figure 19- Discharge capacity and coulombic efficiency for Li-S cells with high-sulfur-loading cathodes and DOL/DME-1.0M LiTFSI-1.0M LiNO3 electrolyte; at room temperature and 55°C.

3.8.2 Long Term Self Discharge

Long-term self-discharge behavior of the cells with different electrolyte composition was then evaluated by monitoring the voltage decay during resting. As shown in Figure 20a, the cell containing DOL/DME-1.0 M LiTFSI electrolyte without $LiNO_3$ additive showed severe shuttling during the 1st and 2nd charge. In addition, after the 5th charge, the cell voltage dropped from 2.39 V to 2.11 V within 7 hours and stabilized at this voltage for the rest of testing period. The voltage drop was likely caused by the continuous depletion of the soluble, higher-order LiPS in the cathode. The LiPS could diffuse out of the cathode and migrate to the anode until concentration equilibrium of the polysulfide species in the electrolyte can be reached. In the meanwhile, the polysulfides may undergo reduction reactions with Li metal and deposit on the anode surface, further driving migration of LiPS and resulting in lower capacity in the subsequent discharge step (43).In comparison, the cell containing the fluorinated electrolyte exhibited much slower voltage drop during resting. The cell voltage maintained at a short plateau above 2.25 V for a period of 14 hours before slowly decreasing to a stable plateau of 2.13 V in another 34 hours. This result suggests that the diffusion of LiPS from the cathode was retarded significantly, although prolonged resting still resulted in consumption of the soluble LiPS by Li anode. In the presence of $LiNO_3$ additive, the self-discharging suppression was found to be much improved for both cells with the baseline and fluorinated electrolyte. Figure 20b shows that the baseline cell containing DOL/DME-1.0 M LiTFSI and 0.2 M $LiNO_3$ promptly underwent complete self-discharge from 2.42 V to 2.14 V . A short voltage plateau above 2.35 V was observed for the baseline cell, however the cell was only able to hold this voltage for 25 hours. The cell containing DOL/TTE-1.0 M LiTFSI with 0.2 M $LiNO_3$ showed much better performance in suppressing self-discharge. The cell voltage remained at the 2.27 V plateau for over 1 week (170 hours) and gradually dropped to 2.16 V after another 70 hours. These results indicate that the presence of $LiNO_3$ and thus the protecting layer on Li surface effectively inhibited the reaction of polysulfides with Li, and LiPS diffusion was only suppressed when the fluorinated ether was present. For the fluorinated electrolyte, the rapid voltage drop at the end of resting may be a result of depletion of the protecting layer on Li surface. In this regard, more detailed study is required to investigate the stability of this protecting layer formed by decomposition of $LiNO_3$ in different types of electrolytes.

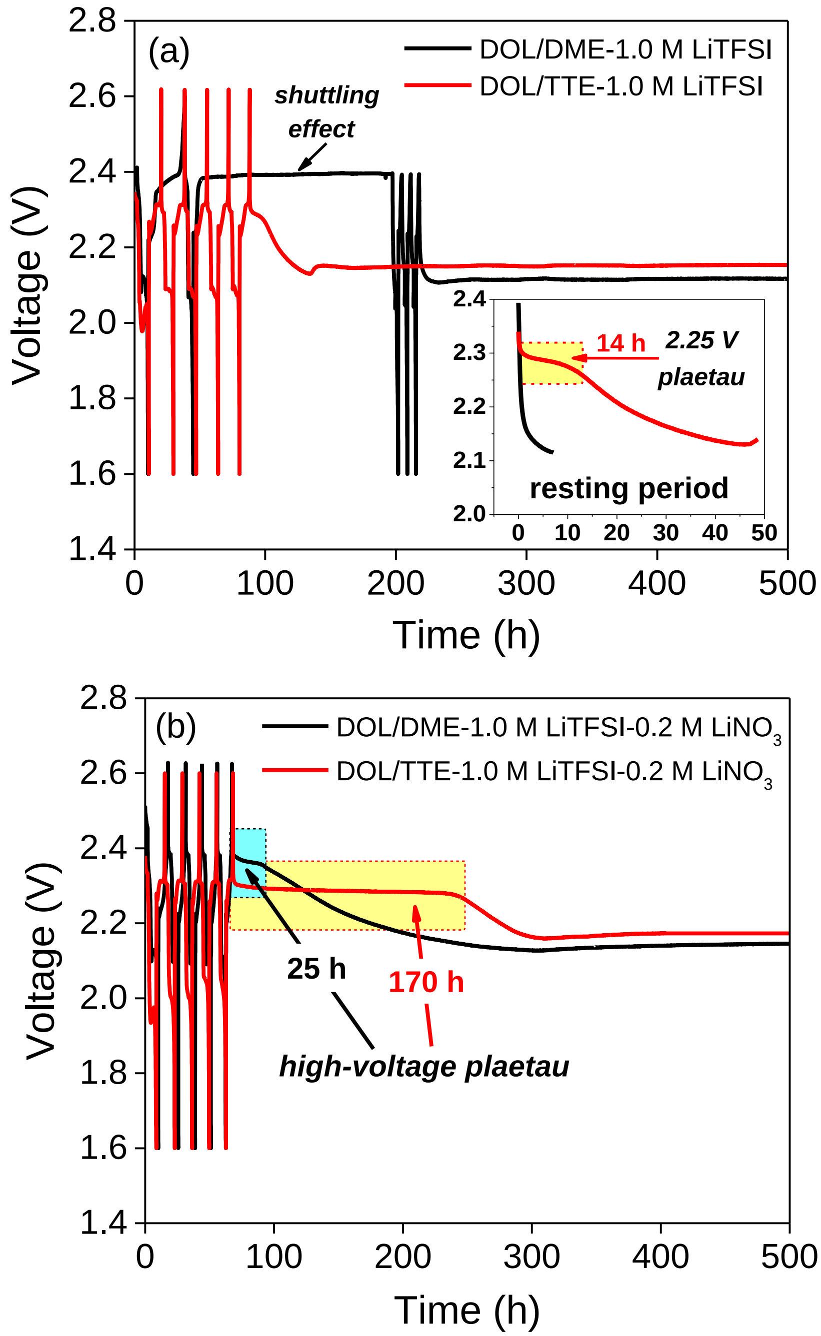

Figure 20. Voltage profile for Li-S cells with long resting hours with DOL/DME-1.0 M LiTFSI and DOL/TTE-1.0 M LiTFSI (a) without $LiNO_3$ and (b) with 0.2 M LiNO3. Inset shows the voltage profile for the resting period after the 5th charge.

3.9 Conclusion

A deep understanding of high performance Li-S battery with fluorinated electrolyte was obtained using electrochemical methods and analytical techniques including HPLC, XPS and SEM. The lithium polysulfide species generated in a Li-S cell were quantitatively analyzed. The results suggested that the improved performance of a Li-S cell with 1,1,2,2-tetrafluoroethyl-2,2,3,3-tetrafluoropropyl ether (TTE) as co-solvent is due to multiple reasons: (1) less solubility of high-order polysulfides as confirmed with solubility test and HPLC experiment mitigates the shuttle effect of polysulfide and promotes the reversible electrochemistry of insoluble Li_2S/Li_2S_2; (2) the SEI formation on the sulfur cathode by reductive decomposition of fluoroether further prevents the dissolution of the polysulfide and improves the sulfur utilization; (3) the electrochemical/chemical reaction of fluoroether with lithium anode forms a protective layer acting as a physical barrier eliminating the parasitic reactions of dissolved polysulfides with lithium.

In addition, the self-discharge behavior of lithium sulfur cells was investigated with high- loading sulfur electrodes. It is shown that using partially fluorinated electrolyte, DOL-TTE-1.0 M LiTFSI with the addition of $LiNO_3$ has an outstanding effect in reducing self-discharge and almost no self-discharge is reported after 10 hours resting at room temperature and storage temperatures of 55 °C. It was shown that combining TTE and $LiNO_3$ can protect both the sulfur cathode due to the formation of a stable SEI layer and also the lithium, due to the $LiNO_3$ reduction on the anode. SEM and EDX results confirm the low concentration of sulfur on the surface of the lithium anode while using the TTE electrolyte which results in lower self-discharge of the cell. It is also shown that using $LiNO_3$ with the conventional electrolyte even at high concentrations had trivial effect on self-discharge.

For future studies different fluorinated electrolytes should be the main focus for the Li-S battery, where in our preliminary experiments it was noticed that solvents having one or two non-fluorinated alkyl chains (such as DPE) show low or no capacity (figure 21). Finding a correlation between the solvent molecular structure and the performance of the lithium sulfur batteries can indeed assist in designing cells with much improved features.

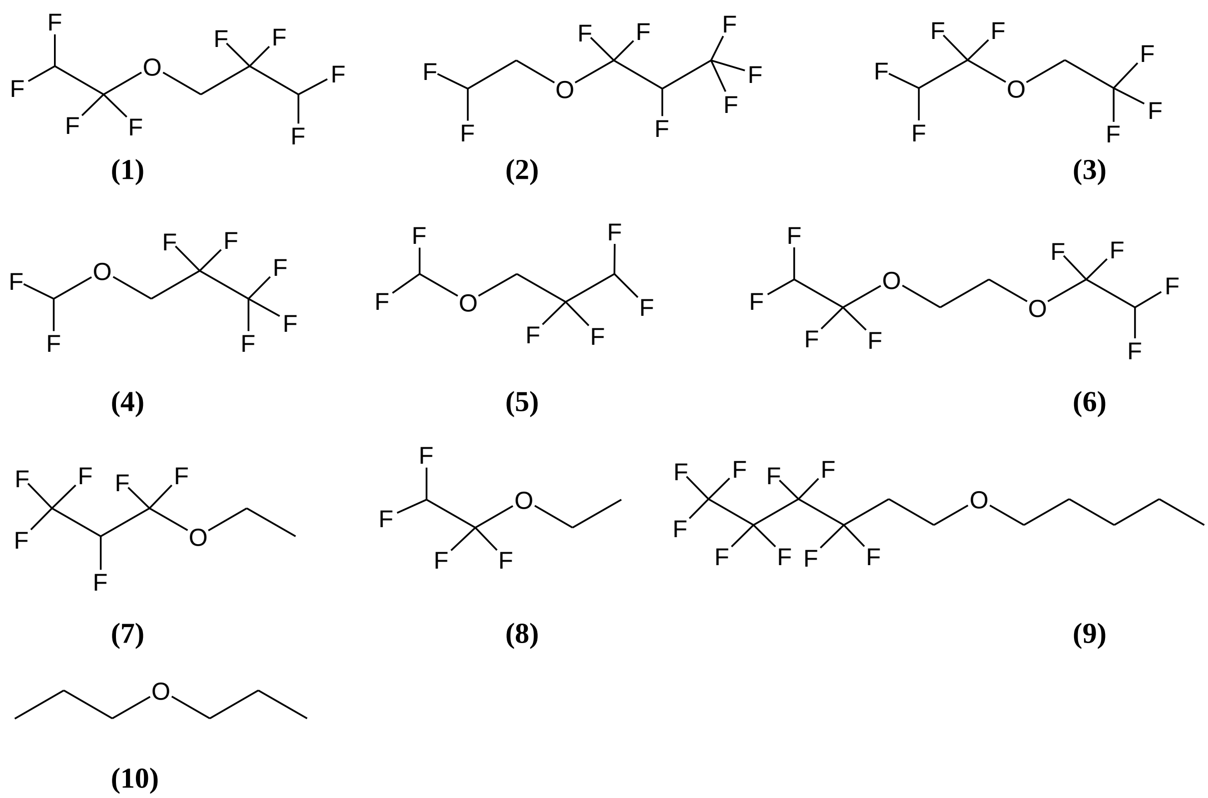

Figure 21. Molecular structure of different fluorinated solvent used as co-solvent in conventional lithium sulfur batter

CITED LITERATURE

1. Zhang SS. Liquid electrolyte lithium/sulfur battery: Fundamental chemistry, problems, and solutions. Journal of Power Sources. 2013;231(0):153-62.

2. Cañas NA, Wolf S, Wagner N, Friedrich KA. In-situ X-ray diffraction studies of lithium–sulfur batteries. Journal of Power Sources. 2013;226(0):313-9.

3. Barchasz C, Molton F, Duboc C, Leprêtre J-C, Patoux S, Alloin F. Lithium/Sulfur Cell Discharge Mechanism: An Original Approach for Intermediate Species Identification. Analytical Chemistry. 2012;84(9):3973-80.

4. Kawase A, Shirai S, Yamoto Y, Arakawa R, Takata T. Electrochemical reactions of lithium-sulfur batteries: an analytical study using the organic conversion technique. Physical Chemistry Chemical Physics. 2014;16(20):9344-50.

5. Liang X, Wen Z, Liu Y, Wu M, Jin J, Zhang H, et al. Improved cycling performances of lithium sulfur batteries with LiNO3-modified electrolyte. Journal of Power Sources. 2011;196(22):9839-43.

6. Zhang SS. Role of LiNO3 in rechargeable lithium/sulfur battery. Electrochimica Acta. 2012;70(0):344-8.

7. Zhang SS, Tran DT. A proof-of-concept lithium/sulfur liquid battery with exceptionally high capacity density. Journal of Power Sources. 2012;211(0):169-72.

8. Azimi N, Weng W, Takoudis C, Zhang Z. Improved performance of lithium–sulfur battery with fluorinated electrolyte. Electrochemistry Communications. 2013;37(0):96-9.

9. Cuisinier M, Cabelguen PE, Adams BD, Garsuch A, Balasubramanian M, Nazar LF. Unique behaviour of nonsolvents for polysulphides in lithium-sulphur batteries. Energy & Environmental Science. 2014;7(8):2697-705.

10. Kitagawa T, Azuma K, Koh M, Yamauchi A, Kagawa M, Sakata H, et al. Application of Fluorine-containing Solvents to LiCoO₂ Cathode in High Voltage Operation. Electrochemistry. 2010;78(5):345-8.

11. Ohmi N, Nakajima T, Ohzawa Y, Koh M, Yamauchi A, Kagawa M, et al. Effect of organo-fluorine compounds on the thermal stability and electrochemical properties of electrolyte solutions for lithium ion batteries. Journal of Power Sources. 2013;221(0):6-13.

12. Achiha T, Nakajima T, Ohzawa Y, Koh M, Yamauchi A, Kagawa M, et al. Thermal Stability and Electrochemical Properties of Fluorine Compounds as Nonflammable Solvents for Lithium-Ion Batteries. Journal of The Electrochemical Society. 2010;157(6):A707-A12.

13. Ishikawa M, Yamagata M, Sugimoto T, Atsumi Y, Kitagawa T, Azuma K. Li-Ion Battery Performance with FSI-Based Ionic Liquid Electrolyte and Fluorinated Solvent-Based Electrolyte. ECS Transactions. 2011;33(28):29-36.

14. Xiong S, Xie K, Diao Y, Hong X. Oxidation process of polysulfides in charge process for lithium–sulfur batteries. Ionics. 2012;18(9):867-72.

15. Zheng S, Han P, Han Z, Zhang H, Tang Z, Yang J. High Performance C/S Composite Cathodes with Conventional Carbonate-Based Electrolytes in Li-S Battery. Sci Rep. 2014;4.

16. Rauh RD, Shuker FS, Marston JM, Brummer SB. Formation of lithium polysulfides in aprotic media. Journal of Inorganic and Nuclear Chemistry. 1977;39(10):1761-6.

17. Nasim Azimi ZX, Ira bloom, Donghai Wang, Tad Daniel, Christos Takoudis , Zhengcheng Zhang. Fluoroether-Based Electrolytes for Lithium-Sulfur Batteries. 2014.

18. Nasim Azimi ZX, Nancy Dietz Rago, Christos Takoudis , Mikhail L. Gordin, Jiangxuan Song, Donghai Wang, Zhengcheng Zhang Fluorinated Electrolytes for Li-S Battery: Suppressing the Self-discharge with an Electrolyte Containing Fluoroether Solvent. 2014.

19. Chen L, Shaw LL. Recent advances in lithium–sulfur batteries. Journal of Power Sources. 2014;267(0):770-83.

20. Su Y-S, Fu Y, Cochell T, Manthiram A. A strategic approach to recharging lithium-sulphur batteries for long cycle life. Nat Commun. 2013;4.

21. Liebhafsky HA, Pfeiffer HG. Beer's law in analytical chemistry. Journal of Chemical Education. 1953;30(9):450.

22. Zu C, Su Y-S, Fu Y, Manthiram A. Improved lithium-sulfur cells with a treated carbon paper interlayer. Physical Chemistry Chemical Physics. 2013;15(7):2291-7.

23. Zhao X, Kim D-S, Manuel J, Cho K-K, Kim K-W, Ahn H-J, et al. Recovery from self-assembly: a composite material for lithium-sulfur batteries. Journal of Materials Chemistry A. 2014;2(20):7265-71.

24. Yu M, Yuan W, Li C, Hong J-D, Shi G. Performance enhancement of a graphene-sulfur composite as a lithium-sulfur battery electrode by coating with an ultrathin Al2O3 film via atomic layer deposition. Journal of Materials Chemistry A. 2014;2(20):7360-6.

25. Fu Y, Su Y-S, Manthiram A. Highly Reversible Lithium/Dissolved Polysulfide Batteries with Carbon Nanotube Electrodes. Angewandte Chemie International Edition. 2013;52(27):6930-5.

26. Yan Diao zKX, Shizhao Xiong,* and Xiaobin Hong. Insights into Li-S Battery Cathode Capacity Fading Mechanisms:
Irreversible Oxidation of Active Mass during Cycling. Journal of The Electrochemical Society. 2012;159(11):A1816-A21.

27. Kim HS, Arthur TS, Allred GD, Zajicek J, Newman JG, Rodnyansky AE, et al. Structure and compatibility of a magnesium electrolyte with a sulphur cathode. Nat Commun. 2011;2:427.

28. Kazazi M, Vaezi MR, Kazemzadeh A. Improving the self-discharge behavior of sulfur-polypyrrole cathode material by LiNO3 electrolyte additive. Ionics. 2014;20(9):1291-300.

29. Yazami R, Reynier YF. Mechanism of self-discharge in graphite–lithium anode. Electrochimica Acta. 2002;47(8):1217-23.

30. Ryu H-S, Ahn H-J, Kim K-W, Ahn J-H, Cho K-K, Nam T-H, et al. Discharge behavior of lithium/sulfur cell with TEGDME based electrolyte at low temperature. Journal of Power Sources. 2006;163(1):201-6.

31. Evers S, Nazar LF. New Approaches for High Energy Density Lithium–Sulfur Battery Cathodes. Accounts of Chemical Research. 2012;46(5):1135-43.

32. Wei Seh Z, Li W, Cha JJ, Zheng G, Yang Y, McDowell MT, et al. Sulphur–TiO2 yolk–shell nanoarchitecture with internal void space for long-cycle lithium–sulphur batteries. Nature Communications. 2013;4:1331.

33. Cao Y, Li X, Aksay IA, Lemmon J, Nie Z, Yang Z, et al. Sandwich-type functionalized graphene sheet-sulfur nanocomposite for rechargeable lithium batteries. Physical Chemistry Chemical Physics. 2011;13(17):7660-5.

34. Gao J, Lowe MA, Kiya Y, Abruña HD. Effects of Liquid Electrolytes on the Charge–Discharge Performance of Rechargeable Lithium/Sulfur Batteries: Electrochemical and in-Situ X-ray Absorption Spectroscopic Studies. The Journal of Physical Chemistry C. 2011;115(50):25132-7.

35. Jeddi K, Ghaznavi M, Chen P. A novel polymer electrolyte to improve the cycle life of high performance lithium-sulfur batteries. Journal of Materials Chemistry A. 2013;1(8):2769-72.

36. Wang H, Yang Y, Liang Y, Robinson JT, Li Y, Jackson A, et al. Graphene-Wrapped Sulfur Particles as a Rechargeable Lithium–Sulfur Battery Cathode Material with High Capacity and Cycling Stability. Nano Letters. 2011;11(7):2644-7.

37. Jeddi K, Zhao Y, Zhang Y, Konarov A, Chen P. Fabrication and Characterization of an Effective Polymer Nanocomposite Electrolyte Membrane for High Performance

Lithium/Sulfur Batteries. Journal of The Electrochemical Society. 2013;160(8):A1052-A60.

38. Mikhaylik YV, Akridge JR. Polysulfide Shuttle Study in the Li/S Battery System. Journal of The Electrochemical Society. 2004;151(11):A1969-A76.

39. Choi J-W, Kim J-K, Cheruvally G, Ahn J-H, Ahn H-J, Kim K-W. Rechargeable lithium/sulfur battery with suitable mixed liquid electrolytes. Electrochimica Acta. 2007;52(5):2075-82.

40. Ryu HS, Ahn HJ, Kim KW, Ahn JH, Lee JY, Cairns EJ. Self-discharge of lithium–sulfur cells using stainless-steel current-collectors. Journal of Power Sources. 2005;140(2):365-9.

41. Ryu HS, Ahn HJ, Kim KW, Ahn JH, Cho KK, Nam TH. Self-discharge characteristics of lithium/sulfur batteries using TEGDME liquid electrolyte. Electrochimica Acta. 2006;52(4):1563-6.

42. Gordin ML, Dai F, Chen S, Xu T, Song J, Tang D, et al. Bis(2,2,2-trifluoroethyl) Ether As an Electrolyte Co-solvent for Mitigating Self-Discharge in Lithium–Sulfur Batteries. ACS Applied Materials & Interfaces. 2014;6(11):8006-10.

43. Hofmann AF, Fronczek DN, Bessler WG. Mechanistic modeling of polysulfide shuttle and capacity loss in lithium–sulfur batteries. Journal of Power Sources. 2014;259(0):300-10.

4. FLUORINATED MATERIALS AS ELECTROLYTE ADDITIVE FOR LITHIUM-SULFUR BATTERY

Various approaches have been investigated to further extend the cycle life and sulfur utilization of the Li-S battery. Just as is the case for Li-ion battery electrolytes, functional additives play an important role in the Li-S battery. In Li-S batteries, an additive is introduced to the liquid electrolyte mainly to passivate the surface of the Li anode and protect Li from chemical and electrochemical reaction with the lithium polysulfides. To date, many researchers have focused their efforts on developing new sulfur materials with unique structures (1-3), yet the electrolyte plays a pivotal role in the Li-S cell performance. Although $LiNO_3$ is widely adopted as an electrolyte additive for Li-S batteries (4,5), recent reports about new electrolytes and new additives suggest that they can make a major contribution to improving the performance (6-11).

We have reported a new electrolyte based on a fluorinated ether solvent, 1,1,2,2-tetrafluoroethyl-2,2,3,3-tetrafluoropropyl ether (TTE) (12). This solvent can be reduced on the cathode side during discharge, forming a solid-electrolyte interphase (SEI) that prevents the dissolution of polysulfides and enables the highly reversible Li-S redox reaction in the cathode. Building upon this result, we have studied two different fluorinated compounds, lithium difluoro(oxalato) borate (LiDFOB) and Tris(pentafluorophenyl)borane ($B(C_6F_5)_3$, as additives for the Li-S battery.

4.1 Lithium Difluoro(Oxalato) Borate (LiDFOB) Additive

In the first study, the effect of lithium difluoro(oxalato) borate (LiDFOB) additive was investigated. Zhang *et al*. (13) first reported LiDFOB as an effective electrolyte salt for lithium-ion batteries. Later, Hu *et al*. (14) found that LiDFOB participates in the formation of an SEI layer on graphite anodes and greatly improves the cycling performance and thermal stability of the Li-ion battery. Very recently, Wu et al. reported that LiDFOB (15) functioned as an efficient additive to improve the capacity retention of the Li-S battery when added to the DOL/DME electrolyte due to the formation of an LiF-rich passivation layer on the lithium anode surface. In fact, we were evaluating LiDFOB as a potential additive for the Li-S battery independently at the same time Wu did his study. However, our initial idea is quite different from Wu's as we conceived of using LiDFOB as an electrolyte additive due to the fact that fluorinated ether solvent is capable of forming a SEI on the sulfur cathode (12). The two fluorine-boron bonds in the structure of LiDFOB might provide the same functionality as fluorinated ether does on the sulfur cathode side.

4.1.1 1.0 M LiPF6 in 1NM3 Electrolyte

Since the redox shuttle effect of polysulfide originates from its high solubility and fast diffusion in the organic electrolyte, polymer-based electrolytes with high molecular weight could be a potential candidate for restraining the dissolution of the polysulfide and its fast diffusion to the anode. It is assumed that the polymer shell acts as a physical barrier and prevents the contact of the polysulfides produced at the cathode with the liquid electrolyte (16). The widely studied polymer electrolytes for the Li-S battery are based on the high molecular weight of poly(ethylene oxide) (PEO). However, high molecular weight PEO has a relatively high glass transition temperature (T_g) and tends to crystallize at temperatures below 60°C, both of which significantly reduce the conductivity of the electrolyte (17). This issue can be mitigated by attaching the PEO groups onto a flexible siloxane (Si-O-Si) backbone (T_g = -123°C) due to their extremely low energy barrier for Si-O bond rotation (18).

In this study, $(CH_3)_3Si(OCH_2CH_2)_3OCH_3$ (1NM3) was evaluated as a new solvent for Li-S batteries. The sulfur cathodes were fabricated by mixing sulfur, Super P carbon, and PVDF (45%:45%:10% by weight). The electrodes had loadings of ~1-2 mg /cm^2. Tri(ethylene glycol)-substituted trimethylsilane (1NM3) and lithium difluoro(oxalato) borate (LiDFOB) were prepared in our laboratory following the literature procedures reported by Dong *et al.* (18) and Zhang *et al.* (13). The following electrolytes were tested: 1.0 M $LiPF_6$ in 1NM3 with and without LiDFOB additive in various concentrations (2%, 5%, and 10%); 1.0 M $LiPF_6$ in 1NM3 with and without 2% $LiNO_3$ additive, and 1.0M LiTFSI in 1NM3 with and without 2% LiDFOB additive.

1NM3 is a colorless liquid at ambient temperature. Since 1NM3 has a Li^+ chelating group in the oligo(ethylene glycol) chain, it dissolves most of the lithium salts used in a lithium-ion battery electrolyte, including $LiPF_6$, LiTFSI, $LiBF_4$, and LiBOB. The electrolyte solution of 1.0M $LiPF_6$ in 1NM3 affords an ambient conductivity of 1.2×10^{-3} S/cm, which is comparable with traditional DOL/DME based electrolyte. The electrochemical performance of a Li-S cell using 1.0 M $LiPF_6$-1NM3 electrolyte is presented in Figure 1. As can be deduced from the voltage profiles of the 1st and 10th cycle in Fig. 1a, the first plateau at 2.4-2.3 V is the sulfur reduction reaction to high-order lithium polysulfides (Li_2S_x, where x=4-8), and further reduction of these polysulfides to lower order species (Li_2S_2 and/or Li_2S) occurs at the lower voltage plateau observed at 2.0-1.9

V. The formation of these lower-order polysulfides contributes to the major capacity of the Li-S cell. The initial discharge capacity was 1200 mAh/g, with 70% of sulfur utilization based on the theoretical capacity of sulfur of 1675 mAh/g. It is very surprising that no shuttling effect of lithium polysulfide was apparent during the 1st charge, as indicated in Figure 1a, probably due to the low solubility of the Li_2S_x and the low kinetics of the Li_2S_x diffusion in this electrolyte. Although no redox shuttling was observed in the subsequent cycles, cell performance faded rapidly with cycling. The discharge capacity rapidly declined to 400mAh/g at the 50th cycle, indicating the side reaction of $LiPF_6$ with Li_2S_x as evidenced by the fluctuations on the voltage profile during charge and the decreasing coulombic efficiency with cycling as shown in Figure 1b.

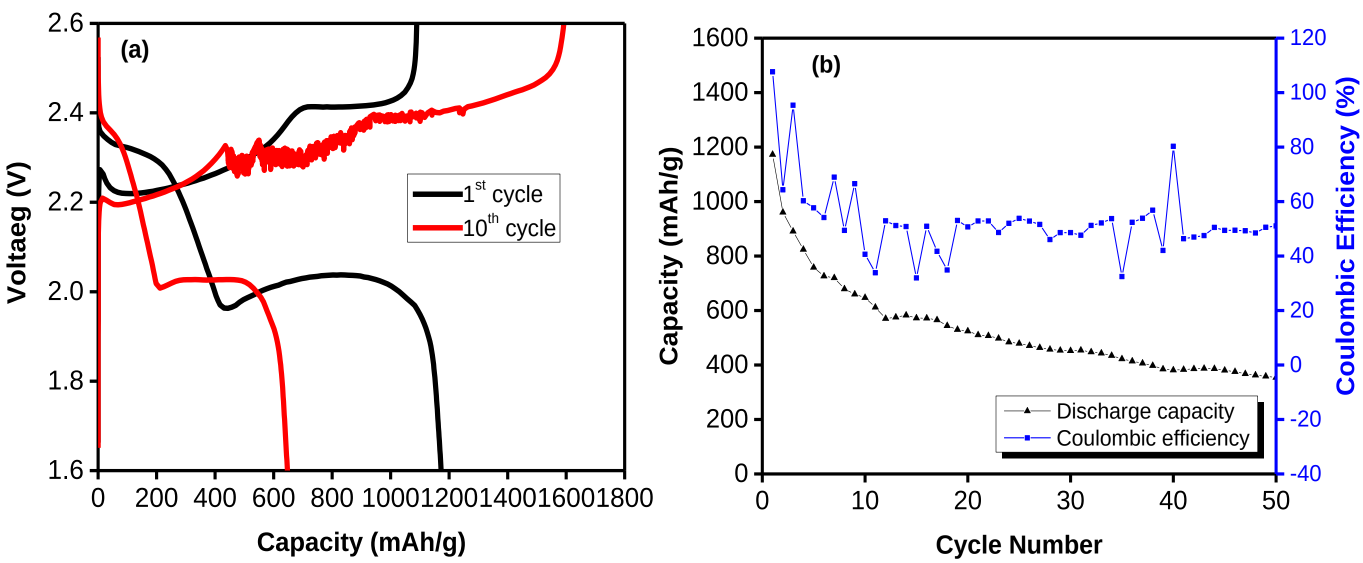

Figure 1. (a) Galvanostatic voltage profiles of Li-S cell with 1.0M LiPF6-1NM3 electrolyte at 1st and 10th charge and discharge. (b) Capacity retention and coulombic efficiency of Li-S cell with 1.0M LiPF6-1NM3 electrolyte at 0.1C rate.

4.1.2 LiDFOB Electrolyte Additive Effect

When 2% LiDFOB was added to the 1.0M $LiPF_6$-1NM3 electrolyte, Li-S cell performance improved significantly. The charge-discharge voltage profile of this Li-S cell is shown in Figure 2a. Apparently, the performance of the additive cell is improved compared with that of the cell without additive (Figure1a) in terms of the specific capacity and the stability of charging. The initial coulombic efficiency is 76% and it increased quickly in a couple of cycles and stabilized to 97%. LiDFOB participates in the reduction reaction during the discharge, as evidenced by the presence of the short plateau on the discharge voltage profiles (Figure 2a). This plateau is buried by the polysulfide reduction peak and showed up clearly in the voltage profiles from the subsequent cycles indicating a gradual reduction of the LiDFOB additive, which forms a protective layer over the cathode surface and thus improves the coulombic efficiency. However, when the concentration of LiDFOB additive is increased from 2% to 5% and 10%, as illustrated in Figures 2c and 2d, respectively, the capacity dropped dramatically. This decrease was attributed to the formation of a thick and resistive decomposition layer on the electrode surface causing the low discharge capacity due to the high interfacial impedance.

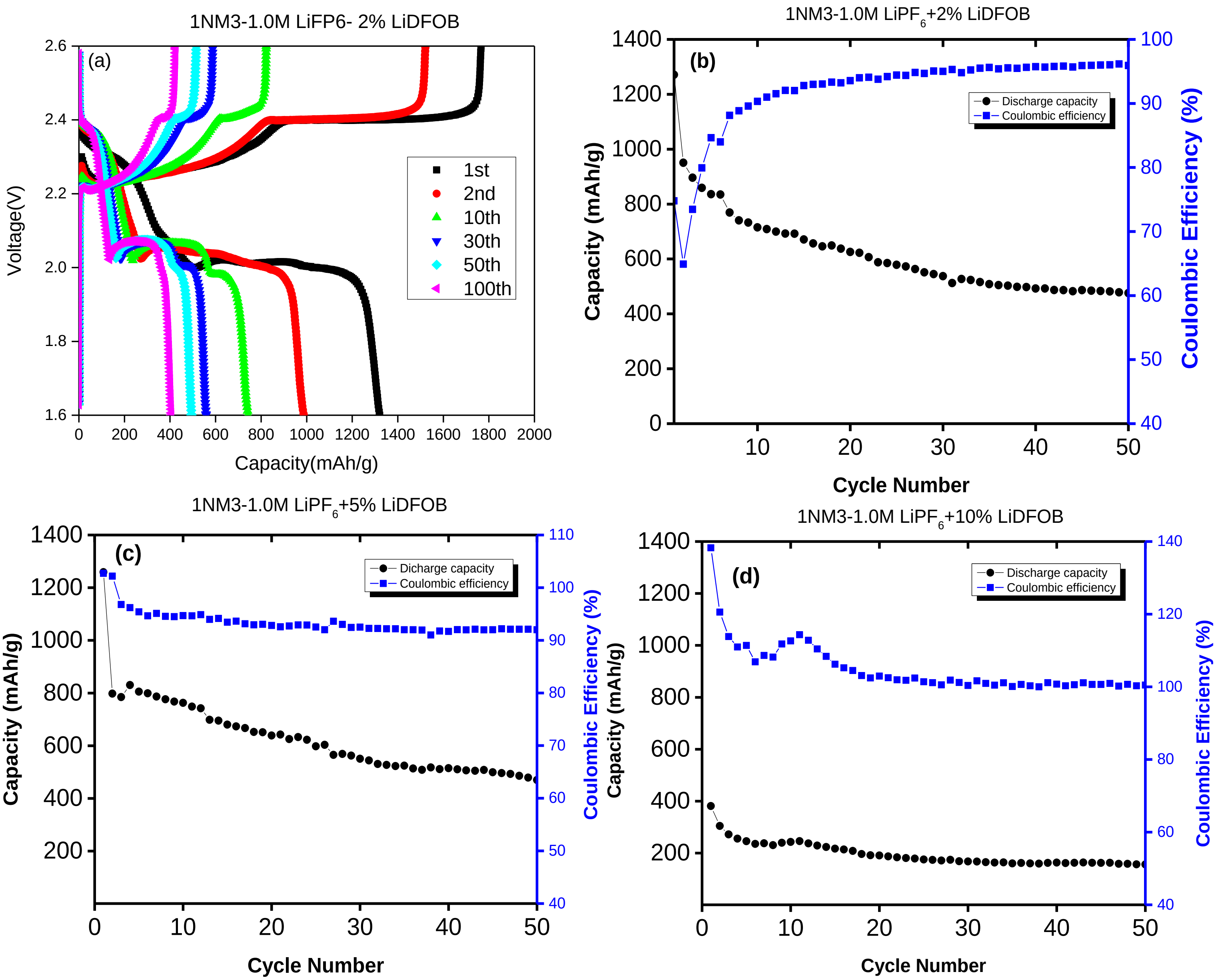

Figure 2. (a) Galvanostatic potential profile of Li-S cell with 1.0 M LiPF6-1NM3 + 2% LiDFOB from 1st to 100th charge and discharge cycle. Capacity retention and coulombic efficiency of Li-S cells with (b) 1.0 M LiPF6-1NM3 + 2% LiDFOB, (c) 1.0 M LiPF6-1 NM3 + 5% LiDFOB, and (d) 1.0 M LiPF6-1NM3 + 10% LiDFOB at a 0.1C rate.

To confirm the presence of a protective layer on the surface of the cathode due to the reduction of LiDFOB, dQ/dV profiles for the 1st, 10th, 30th, 50th, and 100th cycle are presented in Figure 3. In addition to the two peaks which are always observed for Li-S batteries due to the reduction of the PS at 2.4 and 2.1 V, there is an additional 3rd peak observed at 1.95V when using the LiDFOB additive where the intensity of this peak gradually decreased and eventually disappeared after about 100 cycles. This is in agreement with our previous findings about the fluorinated electrolyte for which the same behavior was noticed (12). This is associated with the reductive decomposition of the fluorinated additive on the surface of the sulfur/carbon particles during the discharge and confirms that LiDFOB not only protected the Li anode (15) but also sulfur cathode.

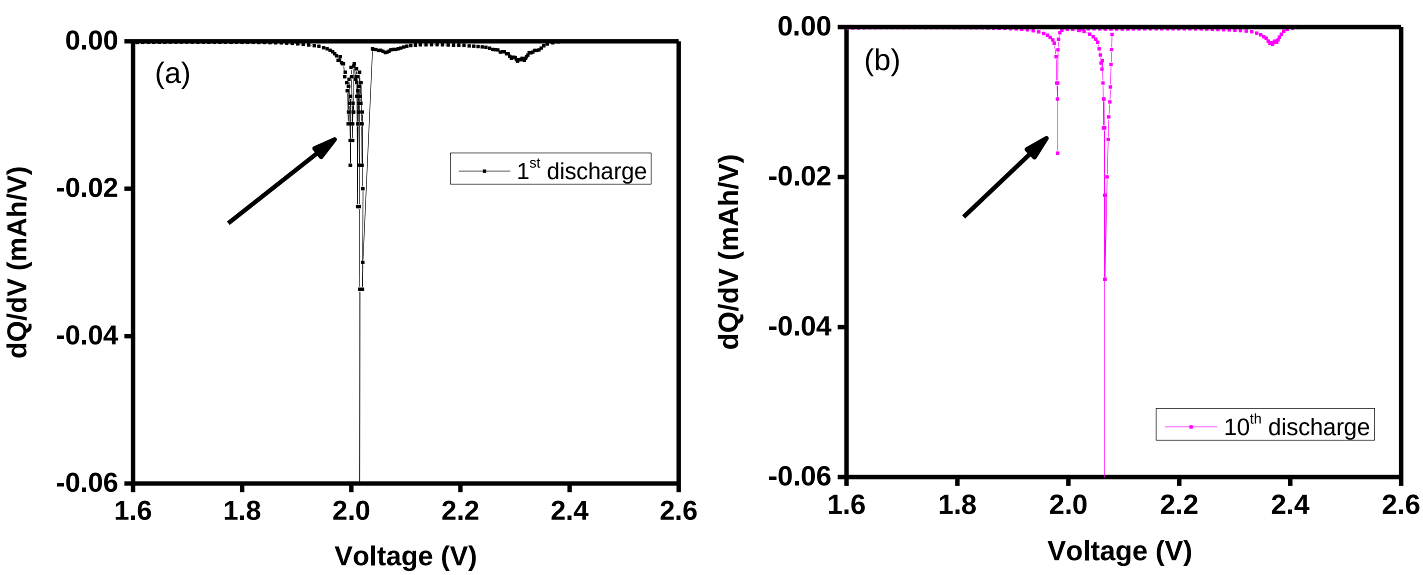

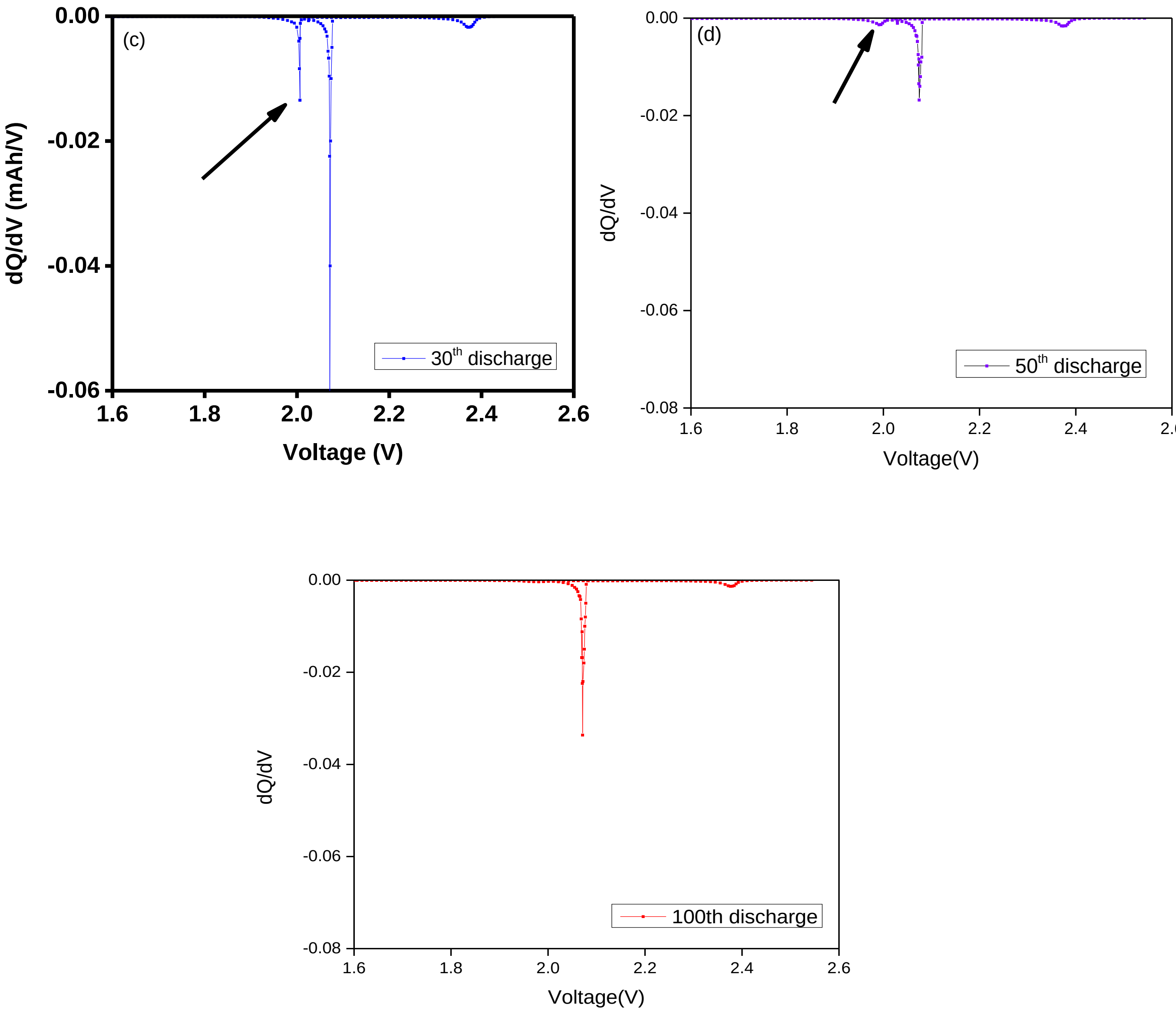

Figure 3. Differential capacity (dQ/dV) profiles of Li-S cell with 1.0 M LiPF6-1NM3 + 2% LiDFOB at (a) the 1st, (b) 10th, (c) 30th, (d) 50th and (e) 100th discharge.

LiTFSI is considered as the most suitable lithium salt for the Li-S battery due to its greater thermal and hydrolytic stability compared with $LiPF_6$. Figures 4a and 4b show the voltage profiles of the 1^{st} through the 20^{th} cycle for Li-S cells containing 1.0M LiTFSI-1NM3 with and without 2%

LiDFOB additive. The initial discharge capacity was 1300 mAh/g for both cells; however, the cell without the LiDFOB additive suffered from a severe redox shuttle reaction during the 1st charge, as evidenced by the flat and long plateau on the charge profile (Figure 4a), resulting in a low coulombic efficiency (45.5%). An even lower efficiency was observed for subsequent cycles. However, with 2% LiDFOB electrolyte additive, the coulombic efficiency significantly increased in the first cycle and stabilized in the following cycles, as clearly evidenced by the data shown in Figure 4b.

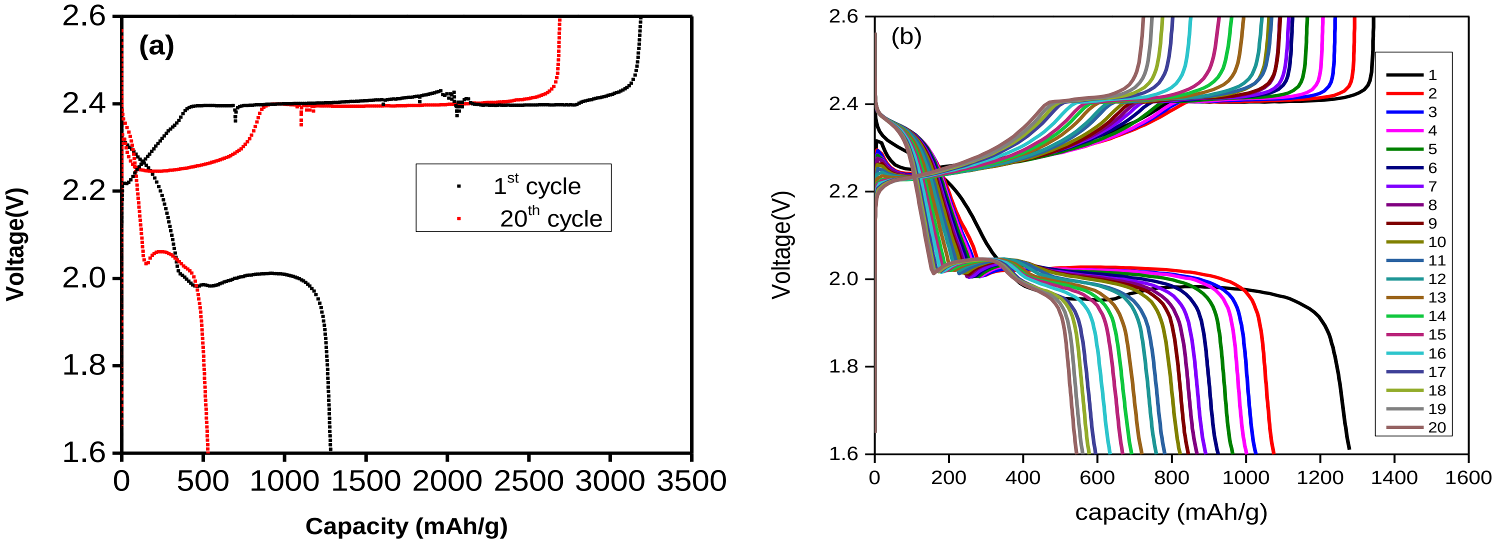

Figure 4**.** Galvanostatic potential profiles of Li-S cell for the 1st through 20th charge and discharge cycles at 0.1C rate with (a) 1.0M LiTFSI-1NM3 and (b) 1.0M LiTFSI-1NM3 + 2% LiDFOB electrolyte.

While LiDFOB additive proved to be effective, we also explored the effect of $LiNO_3$ additive when combined with 1NM3 electrolyte. Figure 5 shows the cell data for 2% $LiNO_3$ (or 0.2 M) added to the 1.0M $LiPF_6$-1NM3 electrolyte. As shown in Figure 5a, the coulombic efficiency was about 100% for all cycles with the $LiNO_3$-additive cell; however, the capacity decline of this cell is almost identical to the cell without $LiNO_3$ additive (Figure 5b).

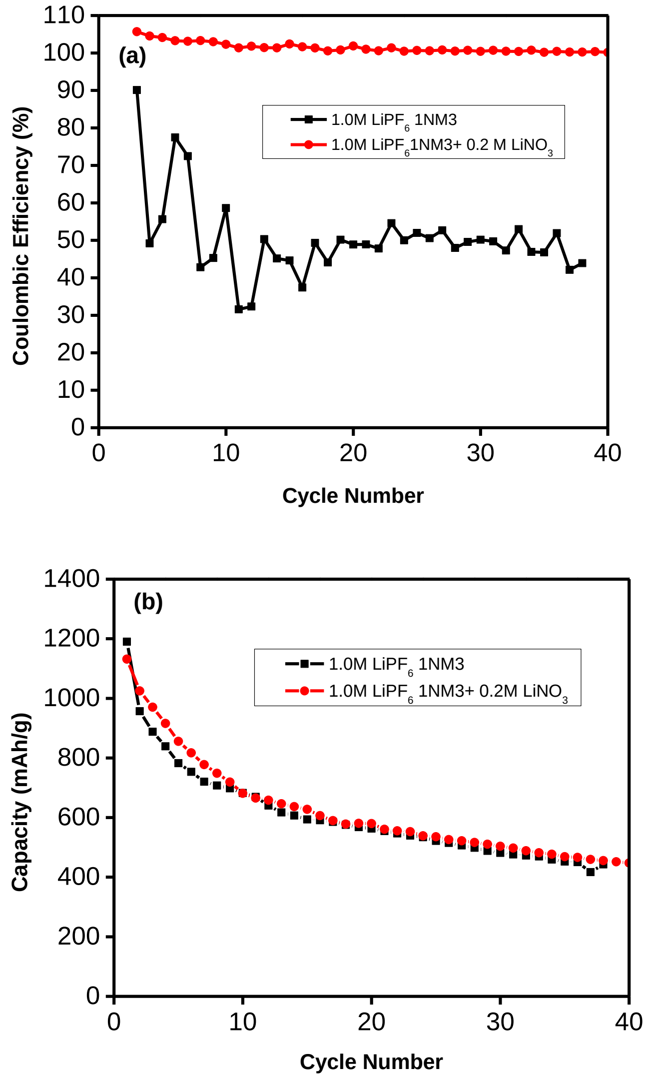

Figure 5. (a) Coulombic efficiency and (b) discharge capacity retention of Li-S cells with 1.0M LiPF6-1NM3 and 1.0 M LiPF6-1NM3 + 2% $LiNO_3$ electrolyte.

4.1.3 Electrochemical Impedance Spectroscopy

The effect of the LiDFOB additive was investigated by electrochemical impedance spectroscopy (EIS). Figure 6a shows the EIS spectra for cells at the 1st discharge stage using 0.8 M $LiPF_6$-1NM3 and 0.8 M $LiPF_6$-1NM3+2% LiDFOB electrolyte. The frequency-dependent impedance signifies the response of several parallel processes occurring in the cell. The Nyquist plots consist of two semicircles and a straight sloping line in the low-frequency region. The semicircle in the high-frequency region corresponds to the ionic conduction at the interphase of the sulfur/electrolyte (R_{int}), and the semicircle in the medium frequency region corresponds to the charge-transfer process (R_{ct}) occurring on the conductive agent of the sulfur electrode (19). As shown in Figure 6b, the charge transfer resistance for the cell containing 0.8 M $LiPF_6$-1NM3+2% LiDFOB (R_{ct} = 254.7 ohm) was significantly higher than that of the cell without LiDFOB (R_{ct} = 52.1 ohm) at the fully discharged state. The much higher R_{ct} for the additive cell is caused by the more discharged products (deep discharge) and the insulating property of the discharge products [20]. The interphasial resistance (R_{int}) was higher for the additive cell than that of the no additive cell, which was attributed to a resistive SEI layer formed on the cathode surface during the discharge process, verifying that the LiDFOB participated in the reductive decomposition reaction as observed in the short plateau and the dQ/dV profiles. In contrast, the cell with 2% LiDFOB showed lower cell resistance (R_e = 12.4 ohm), indicating that the SEI formed by the LiDFOB additive mitigates the dissolution of the lithium polysulfides, leading to lower viscosity and the higher conductivity of the electrolyte.

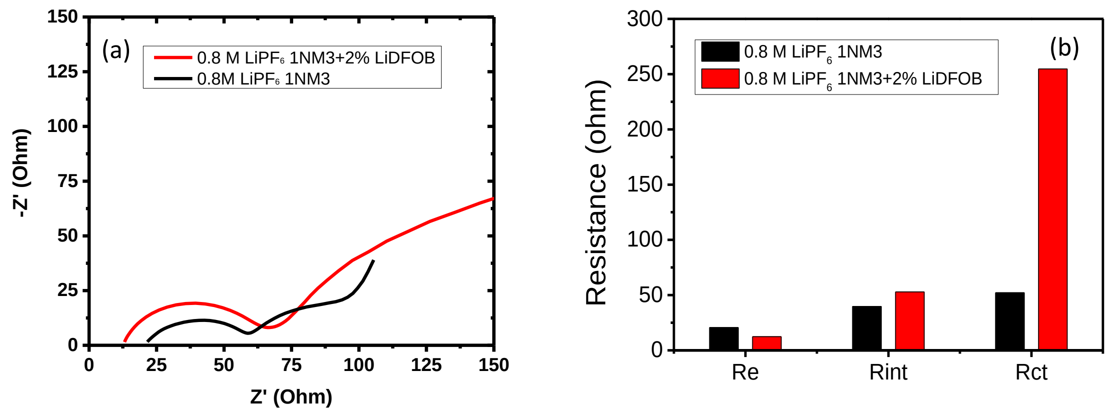

Figure 6. (a) Nyquist plots of the impedance response for Li-S cells after first discharge with 0.8M LiPF6-1NM3 and 0.8M LiPF6-1NM3+2% LiDFOB, and (b) cell resistance (Re), interphasial resistance (Rint), and the charge transfer resistance (Rct) fitted from the experimental data for the Li-S cell with and without LiDFOB additive.

4.1.4 Electrode Characterization

To understand the LiDFOB additive effect in the Li-S battery, we examined the morphology of the discharged sulfur cathode by SEM analysis. Figure 7a is an SEM image of the sulfur electrode after the first discharge in 1.0 M $LiPF_6$-1NM3 electrolyte. The surface of this electrode was covered by large quantities of crystal-like discharged products of insoluble lithium polysulfide (Li_2S_2 and Li_2S) species (12,21). The formation of these low-order polysulfides has a major effect in causing the capacity loss during long-term cycling. In contrast, the sulfur electrode showed a different morphology when cycled in 1.0 M $LiPF_6$-1NM3 electrolyte with 2% LiDFOB additive, as illustrated in Figure 7b. The particle size in the discharge products on the electrode surface was much smaller and uniformly distributed on the electrode surface. This morphology of the cathode maintained even at the 10th cycle, as shown in Fig.7c and d. This observation is consistent with the electrochemical cell data presented in Figs. 1, 2a, and 2b.

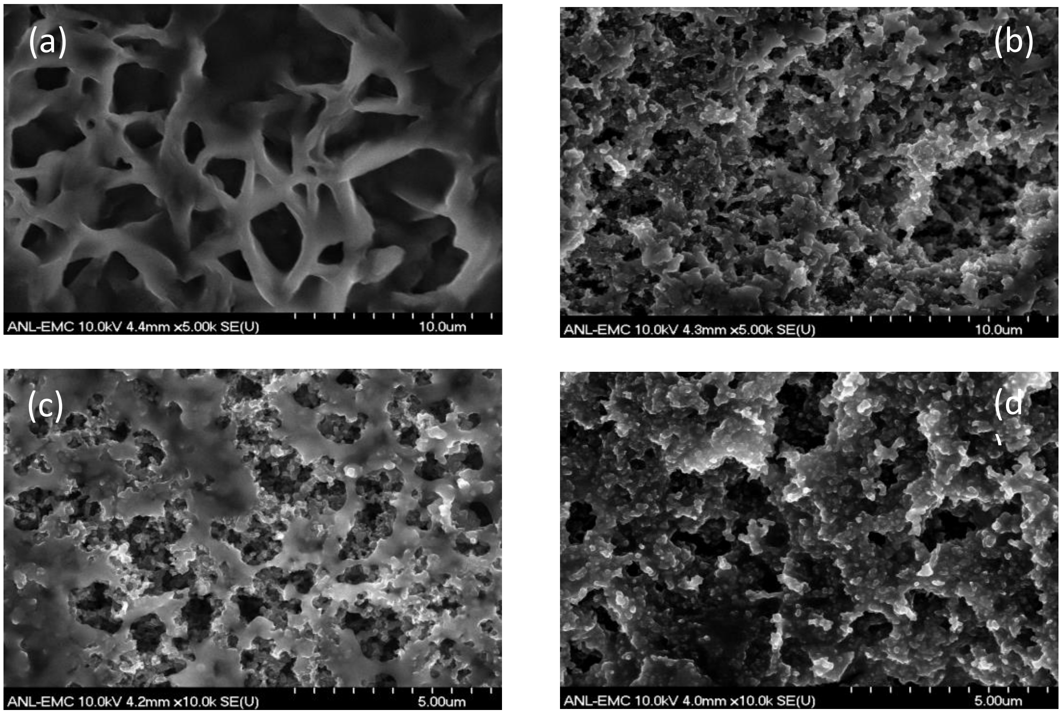

Figure 7. SEM image of sulfur cathode surface after 1st discharge with (a) 1.0 M LiPF6-1NM3, (b) 1.0 M LiPF6-1NM3 + 2% LiDFOB electrolyte, and after 10th discharge with (c) 1.0 M LiPF6-1NM3 and (d) 1.0 M LiPF6-1NM3 + 2% LiDFOB electrolyte.

4.2 Tris(Pentafluorophenyl)Borane (B(C6F5)3) Additive

In the next study of fluorinated electrolyte additives, the effect of Tris(pentafluorophenyl)borane ($B(C_6F_5)_3$) was investigated. ($B(C_6F_5)_3$) has been previously used as an anion receptor for lithium ion batteries (22). This additive has been shown to improve the performance of the Li-ion battery by capturing the intermediate oxygen anions. This prevents the oxygen from direct contact with the carbonate solvents, and therefore greatly suppresses the side reactions. For the first time in lithium sulfur batteries, B $(C_6F_5)_3$ was used as an electrolyte additive.

4.2.1 **Coulombic Efficiency Improvement**

Figure 8 shows the performance of the Li-S battery with a conventional electrolyte, and DOL/DME-1.0M LiTFSI, with and without the ($B(C_6F_5)_3$) additive. As shown in Figure 8a, using the baseline electrolyte will result in severe shuttling due to the high solubility of polysulfides in the electrolyte and their reaction with the lithium anode. This redox shuttle effect prevents the cell form charging to its cut-off voltage. However, by adding 5% $B(C_6F_5)_3$, shuttling is prevented significantly and the cell is charged to the 2.8V cut-off voltage (Figure 8b). By increasing the concentration of this additive to 10 and 20%, the initial efficiency has increased as shown in Figure 8c and d. Yet, as with the LiDFOB effect, using a higher concentration of this additive in the electrolyte will result in a significant drop in the capacity. This decrease was attributed to the formation of a thick and resistive decomposition layer on the electrode surface causing the low discharge capacity due to the high interfacial impedance.

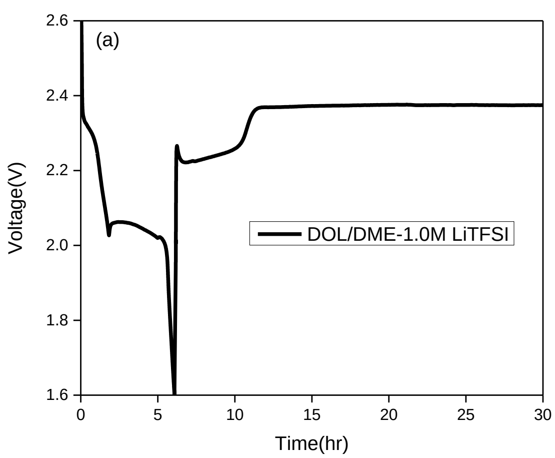

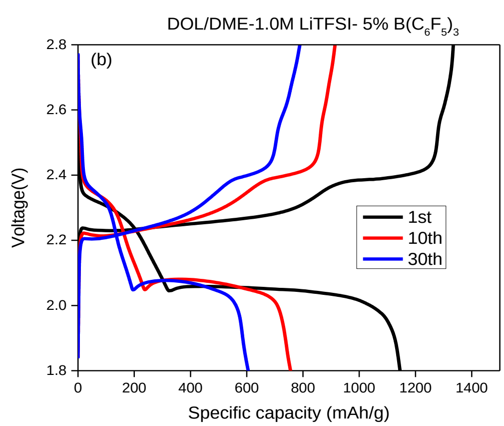

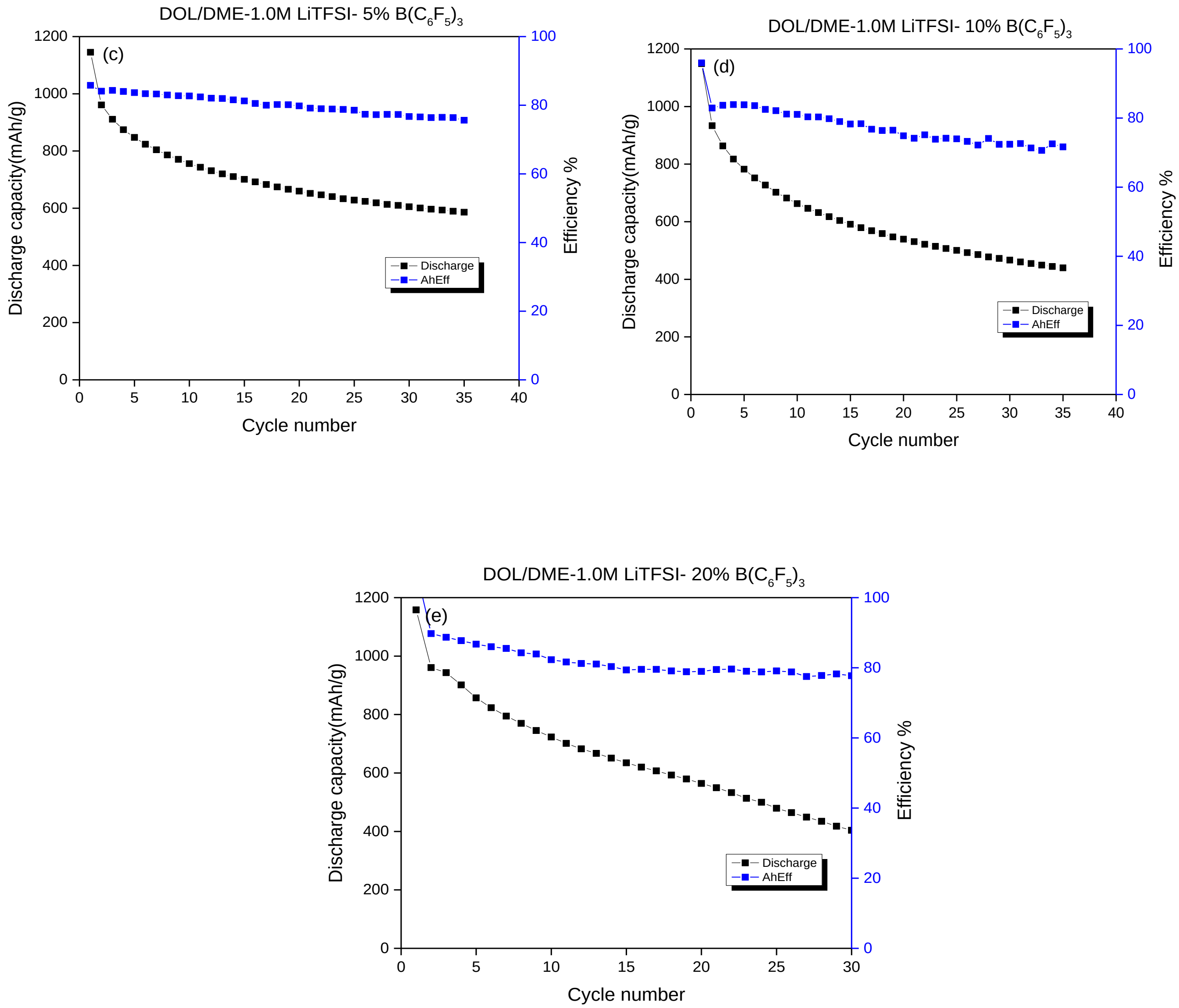

Figure 8. (a) Voltage profile for cell with DOL/DME-1.0M LiTFSI, and (b) DOL/DME-1.0M LiTFSI- 5% ($B(C_6F_5)_3$, and (c) discharge capacity retention and efficiency profile for Li-S cells with (c) DOL/DME-1.0M LiTFSI- 5% ($B(C_6F_5)_3$, (d) DOL/DME-1.0M LiTFSI- 10% ($B(C_6F_5)_3$ and (e) DOL/DME-1.0M LiTFSI- 20% ($B(C_6F_5)_3$.

4.2.2 <u>Cyclic Voltammetry</u>

To investigate the mechanism of the shuttle inhibition of the fluorinated additive, cyclic voltammetry measurements were conducted for the first 5 cycles on the baseline electrolyte and the electrolyte containing 5% ($B(C_6F_5)_3$). As shown in Figure 9a and b, two distinguished cathodic peaks are observed at 2.35 and 2.03 V in the first discharge corresponding to the reduction of elemental sulfur and the intermediate polysulfides (Figure 9a). For the cell containing the fluorinated additive, a noticeable difference is the significant decrease in redox current of the 2nd reduction peak. This is due to the lower formation of insoluble sulfur species after using this additive. Interestingly, there is also major decrease in the redox current for the anodic peak at 2.45 V for the cell containing this additive. This is due to the decomposition of this additive during the charging process.

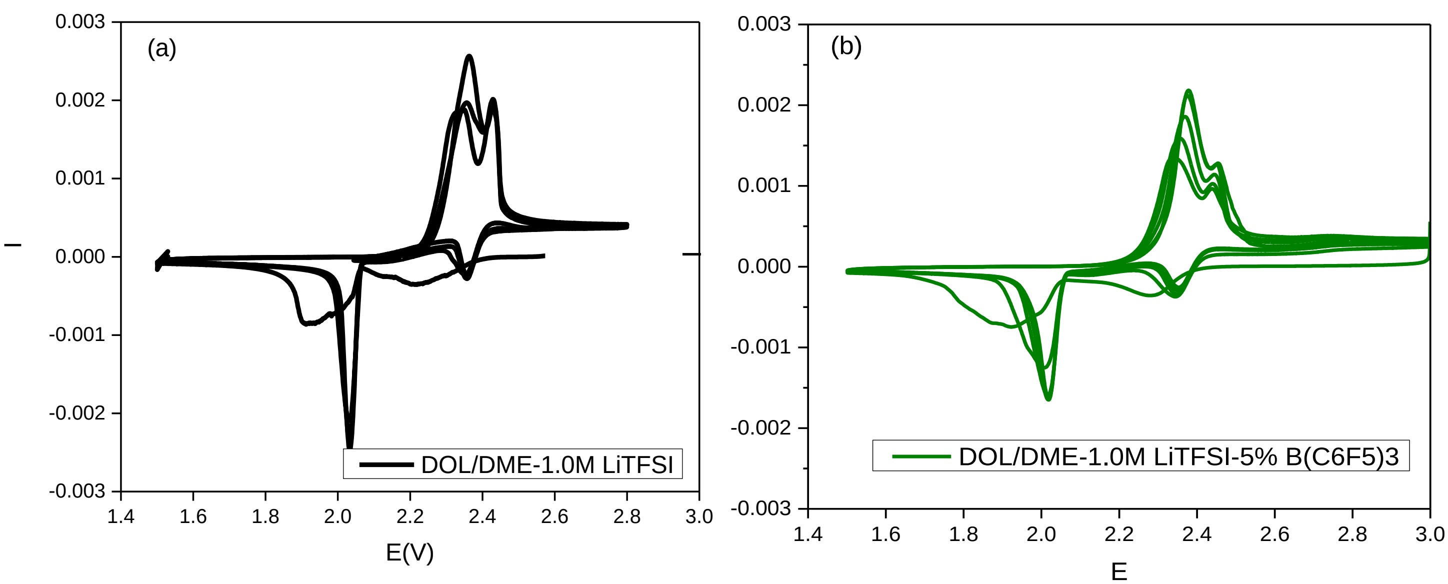

Figure 9. Cyclic voltammograms of the first 5 cycles for Li-S cell with (a) 1.0 M LiTFSI DOL/DME and (b) 1.0 M LiTFSI DOL/DME- 5% ($B(C_6F_5)_3$). (Scanning rate of 27 μV s-1).

4.2.3 Electrode Characterization

Next, x-ray photoelectron spectroscopy (XPS) was used to investigate the elemental composition on the cathode's surface after 1st charge and discharge and also the 20th charging and discharging cycles.

Figure 10 shows the S_{2P} spectra of the sulfur electrodes after cycling in DOL-DME-1.0M LiTFSI with and without 10% $B(C_6F_5)_3$ additive. Peaks at 164.4 eV and 165.7 eV are the characteristic peaks of S_8 in the pristine cathode as shown in Figure 10 a and b (23,24). After the first discharge, two other peaks at 162.6 and 163.8 eV appear in all samples which are assigned to Li_2S or Li_2S_2 (25, 26). By comparing the XPS S_{2p} spectra, it is clearly observed that the intensity of peaks assigned to Li_2S and Li_2S_2 at 162-164 eV, increase by multiple cycling in both electrolytes (fig 10 c and d); however when using the fluorinated additive, $B(C_6F_5)_3$, much less deposition of these insoluble sulfur species is observed on the surface of the cathode after the discharge process (Fig 10 b and d). This is due to the formation of a SEI on the cathode surface which also reduces the deposition of the polysulfides on the cathode surface. Also, a new peak at 164.4 eV appeared after the first charge which is assigned to the decomposition products of the additive during the charging process.

In addition, peaks at 169.4 eV and 170.4 eV are assigned to sulfone (SO_2) from LiTFSI salt. It is reported that the formation of Li_xSO_y species from the reaction of the salt with the active material increases with cycling and has been negatively effective in increasing the cell's capacity fading due to the active mass irreversible oxidation [24]. By comparing S_{2P} spectra from both electrolytes, it is noticed that at all charge and discharging states, the intensity of these peaks are much lower when this fluorinated additive is present in the electrolyte. This is due to the formation of a SEI layer on the surface of the cathode which is also confirmed by other electrochemical and characterization studies.

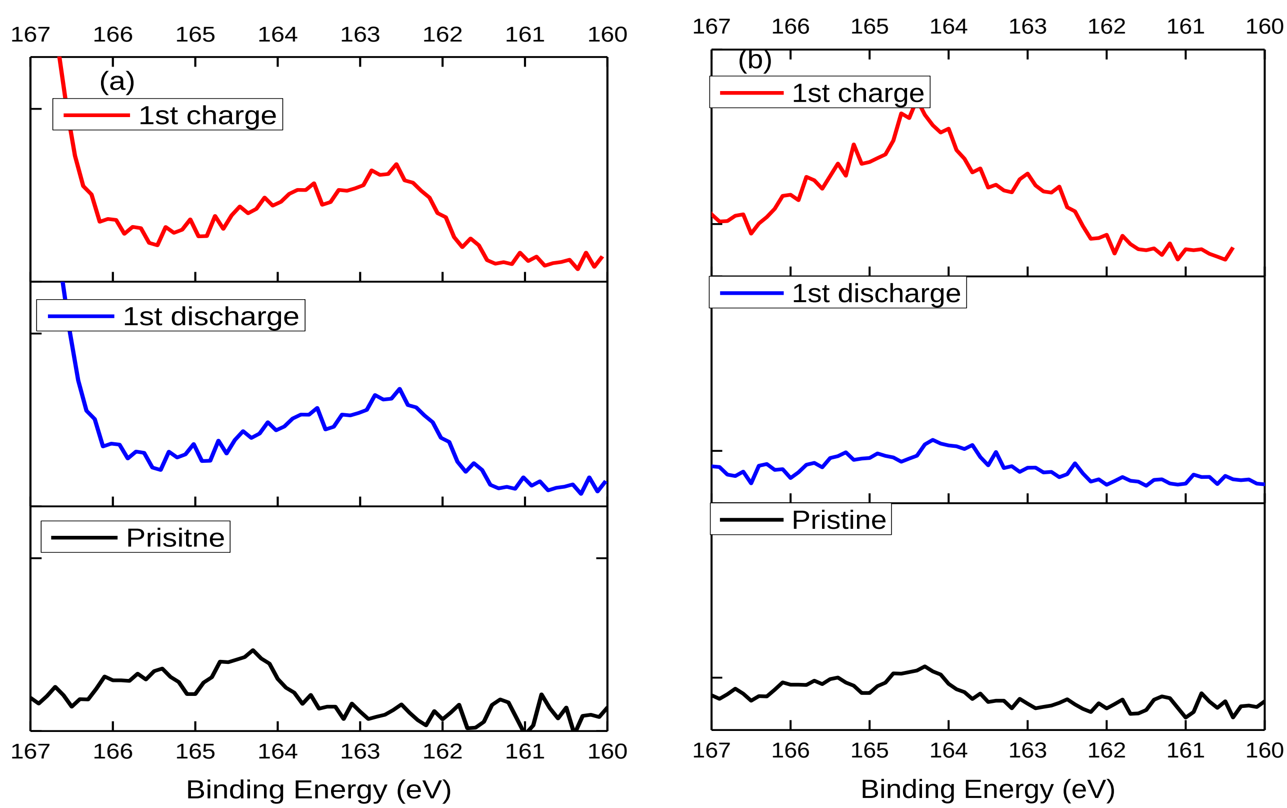

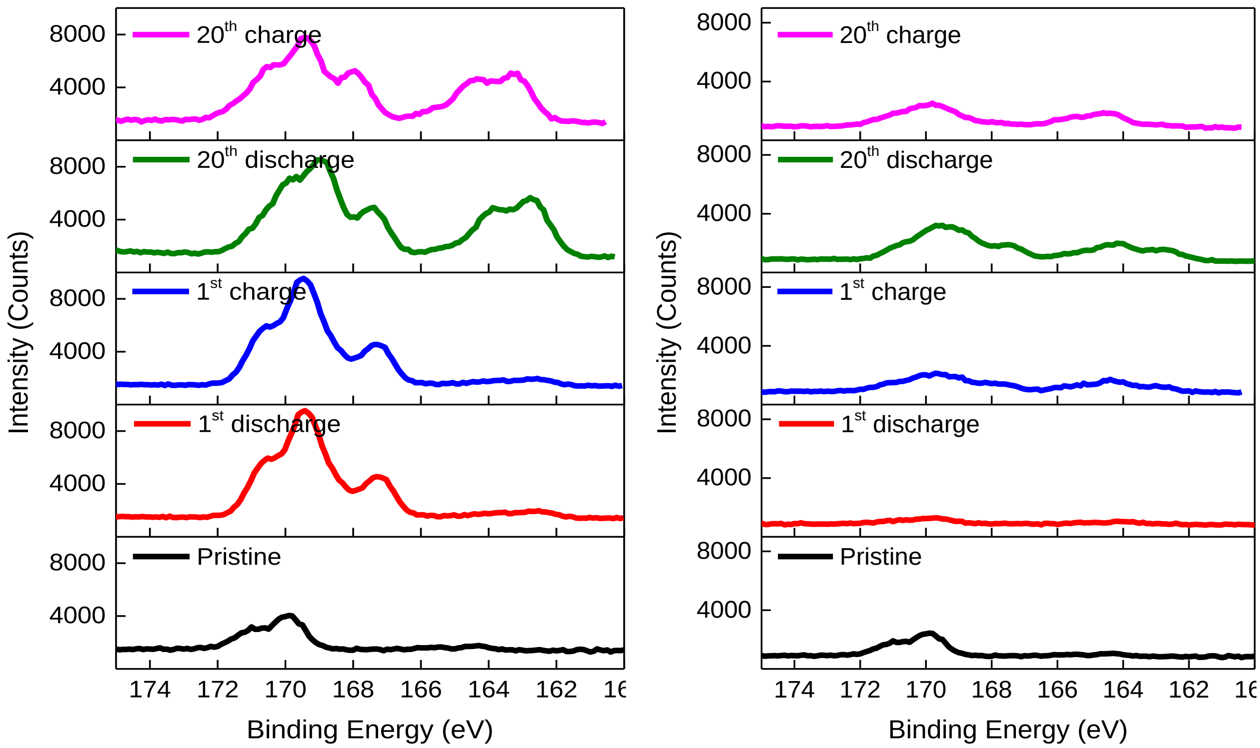

Figure 10. S_{2P} XPS spectra of sulfur cathodes after cycling for pristine cathode, cathode of the 1st discharge, and cathode of the 1st charge, in (a) DOL-DME-1.0M LiTFSI and (b) DOL-DME-1.0M LiTFSI- 10% $B(C_6F_5)_3$ additive and cathode of the pristine to 20th charge in (c) DOL-DME-1.0M LiTFSI and (d) DOL-DME-1.0M LiTFSI- 10% $B(C_6F_5)_3$ additive.

Figure 11 shows the F_{1S} and Li_{1S} spectra for cells cycled with and without the $B(C_6F_5)_3$ additive. By comparing the F_{1S} spectra in Figure 11a and 11b, it is observed that when using the baseline electrolyte, the position of the peak at 688 eV and its intensity are almost constant, since this peak is assigned to the C-F bond from the PVDF binder in the cathode composition. However, when 10% $B(C_6F_5)_3$ additive is added to the electrolyte, this peak gradually decreases and an additional peak at 685 eV appears after 1st charge. This is due to the decomposition of the additive and the formation of the Li-F bond on the surface of the cathode which is also confirmed by the cyclic voltammetry data in Figure 9. In addition, the Li_{1S} spectra shown in Figure 11c and d, also shows a significant difference when 10% $B(C_6F_5)_3$ additive is added to the electrolyte. Peaks at 55.5 eV assigned to Li_2S_n appear when using the baseline electrolyte while much lower intensity is observed for this peak when 10% $B(C_6F_5)_3$ additive is used. Almost no lithium is detected after first discharge due to low Li_2S deposition. This confirms the formation of a SEI on the surface of the cathode when fluorinated additive is used.

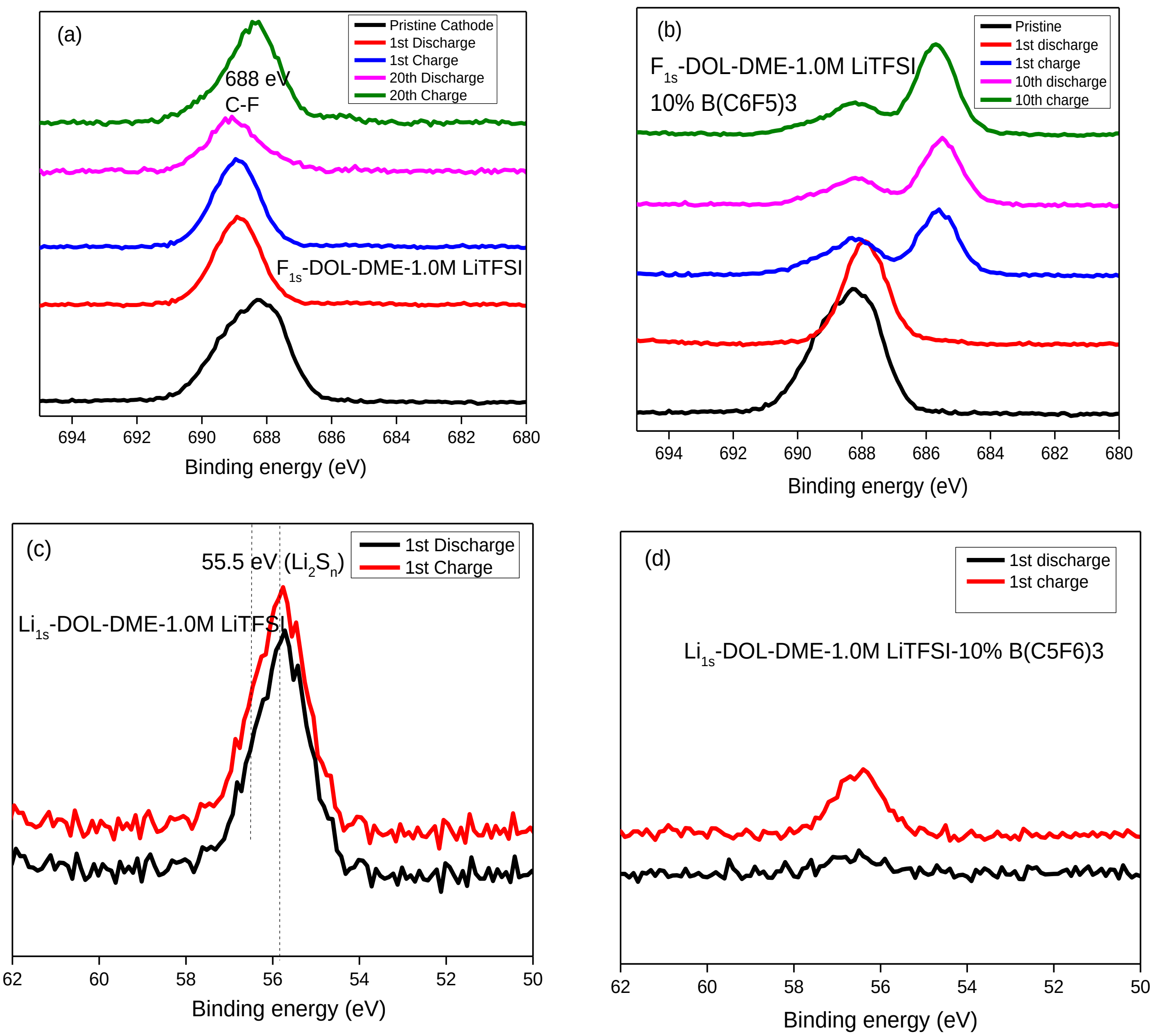

Figure 11. F_{1S} XPS spectra of sulfur cathodes after cycling for Pristine cathode, cathode of the 1st discharge, cathode of the 1st charge, cathode of the 20th discharge, and cathode of the 20th charge for in (a) DOL-DME-1.0M LiTFSI (b) in DOL-DME-1.0M LiTFSI- 10% $B(C_6F_5)_3$ additive and Li_{1S} XPS spectra of sulfur cathodes after cycling in (c) DOL-DME-1.0M LiTFSI and (d) in DOL-DME-1.0M LiTFSI- 10% $B(C_6F_5)_3$ additive.

4.3 <u>Conclusion</u>

We evaluated two fluorinated electrolyte additives for Li-S batteries in this study. In the first section, the new electrolyte solvent 1NM3 and the effects of the lithium salts and additives were investigated. In this work, coin cell data and EIS data showed LiDFOB to be an efficient additive in passivating the sulfur cathode surface and enabling reversible sulfur reduction and oxidation in the Li-S chemistry. By contrast, 1NM3 solvent with $LiNO_3$ additive in the electrolyte showed no improvement over the 1NM3 with no additive. The SEM analysis of a discharged sulfur cathode from a cell tested with the 1NM3 electrolyte confirmed that the LiDFOB additive is critical in improving the performance of the Li-S cell.

In the second part the effect of another fluorinated additive, Tris(pentafluorophenyl)borane ($B(C_6F_5)_3$), was also investigated with the conventional electrolyte. It was shown that using this additive assists in forming a stable SEI on the cathode surface which prevents the dissolution of the polysulfides and results in higher coulombic efficiency.

CITED LITERATURE

1. Elazari R, Salitra G, Garsuch A, Panchenko A, Aurbach D. Sulfur-Impregnated Activated Carbon Fiber Cloth as a Binder-Free Cathode for Rechargeable Li-S Batteries. Advanced Materials. 2011;23(47):5641-4.

2. Li N, Zheng M, Lu H, Hu Z, Shen C, Chang X, et al. High-rate lithium-sulfur batteries promoted by reduced graphene oxide coating. Chemical Communications. 2012;48(34):4106-8.

3. Wei W, Wang J, Zhou L, Yang J, Schumann B, NuLi Y. CNT enhanced sulfur composite cathode material for high rate lithium battery. Electrochemistry Communications. 2011;13(5):399-402.

4. Aurbach D, Pollak E, Elazari R, Salitra G, Kelley CS, Affinito J. On the Surface Chemical Aspects of Very High Energy Density, Rechargeable Li–Sulfur Batteries. Journal of The Electrochemical Society. 2009;156(8):A694-A702.

5. Mikhaylik YV, inventor2008.

6. Lin Z, Liu Z, Fu W, Dudney NJ, Liang C. Phosphorous Pentasulfide as a Novel Additive for High-Performance Lithium-Sulfur Batteries. Advanced Functional Materials. 2013;23(8):1064-9.

7. Kim S, Jung Y, Lim HS. The effect of solvent component on the discharge performance of Lithium–sulfur cell containing various organic electrolytes. Electrochimica Acta. 2004;50(2–3):889-92.

8. Gao J, Lowe MA, Kiya Y, Abruña HD. Effects of Liquid Electrolytes on the Charge–Discharge Performance of Rechargeable Lithium/Sulfur Batteries: Electrochemical and in-Situ X-ray Absorption Spectroscopic Studies. The Journal of Physical Chemistry C. 2011;115(50):25132-7.

9. Dokko K, Tachikawa N, Yamauchi K, Tsuchiya M, Yamazaki A, Takashima E, et al. Solvate Ionic Liquid Electrolyte for Li–S Batteries. Journal of The Electrochemical Society. 2013;160(8):A1304-A10.

10. Wang Y-X, Chou S-L, Liu H-K, Dou S-X. The electrochemical properties of high-capacity sulfur/reduced graphene oxide with different electrolyte systems. Journal of Power Sources. 2013;244(0):240-5.

11. Xiong S, Kai X, Hong X, Diao Y. Effect of LiBOB as additive on electrochemical properties of lithium–sulfur batteries. Ionics. 2012;18(3):249-54.

12. Azimi N, Weng W, Takoudis C, Zhang Z. Improved performance of lithium–sulfur battery with fluorinated electrolyte. Electrochemistry Communications. 2013;37(0):96-9.

13. Shui Zhang S. An unique lithium salt for the improved electrolyte of Li-ion battery. Electrochemistry Communications. 2006;8(9):1423-8.

14. Hu M, Wei J, Xing L, Zhou Z. Effect of lithium difluoro(oxalate)borate (LiDFOB) additive on the performance of high-voltage lithium-ion batteries. J Appl Electrochem. 2012;42(5):291-6.

15. Wu F, Qian J, Chen R, Lu J, Li L, Wu H, et al. An Effective Approach To Protect Lithium Anode and Improve Cycle Performance for Li–S Batteries. ACS Applied Materials & Interfaces. 2014;6(17):15542-9.

16. Scrosati B, Hassoun J, Sun Y-K. Lithium-ion batteries. A look into the future. Energy & Environmental Science. 2011;4(9):3287-95.

17. Rossi NAA, Zhang Z, Schneider Y, Morcom K, Lyons LJ, Wang Q, et al. Synthesis and Characterization of Tetra- and Trisiloxane-Containing Oligo(ethylene glycol)s Highly Conducting Electrolytes for Lithium Batteries. Chemistry of Materials. 2006;18(5):1289-95.

18. Dong J, Zhang Z, Kusachi Y, Amine K. A study of tri(ethylene glycol)-substituted trimethylsilane (1NM3)/LiBOB as lithium battery electrolyte. Journal of Power Sources. 2011;196(4):2255-9.

19. Deng Z, Zhang Z, Lai Y, Liu J, Li J, Liu Y. Electrochemical Impedance Spectroscopy Study of a Lithium/Sulfur Battery: Modeling and Analysis of Capacity Fading. Journal of The Electrochemical Society. 2013;160(4):A553-A8.

20. Zhang SS. Effect of Discharge Cutoff Voltage on Reversibility of Lithium/Sulfur Batteries with LiNO3-Contained Electrolyte. Journal of The Electrochemical Society. 2012;159(7):A920-A3.

21. Yeon J-T, Jang J-Y, Han J-G, Cho J, Lee KT, Choi N-S. Raman Spectroscopic and X-ray Diffraction Studies of Sulfur Composite Electrodes during Discharge and Charge. Journal of The Electrochemical Society. 2012;159(8):A1308-A14.

22. Zheng J, Xiao J, Gu M, Zuo P, Wang C, Zhang J-G. Interface modifications by anion receptors for high energy lithium ion batteries. Journal of Power Sources. 2014;250(0):313-8.

23. Fu Y, Su Y-S, Manthiram A. Highly Reversible Lithium/Dissolved Polysulfide Batteries with Carbon Nanotube Electrodes. Angewandte Chemie International Edition. 2013;52(27):6930-5.

24. Diao Y, Xie K, Xiong S, Hong X. Insights into Li-S Battery Cathode Capacity Fading Mechanisms: Irreversible Oxidation of Active Mass during Cycling. Journal of The Electrochemical Society. 2012;159(11):A1816-A21.

25. Zu C, Su Y-S, Fu Y, Manthiram A. Improved lithium-sulfur cells with a treated carbon paper interlayer. Physical Chemistry Chemical Physics. 2013;15(7):2291-7.

26. Kim HS, Arthur TS, Allred GD, Zajicek J, Newman JG, Rodnyansky AE, et al. Structure and compatibility of a magnesium electrolyte with a sulphur cathode. Nat Commun. 2011;2:427.

5. TEFLON-COATED CARBON PAPER ELECTRODES FOR LITHIUM-SULFUR BATTERIES

5.1 Introduction

Employing sulfur/carbon composites is currently the main approach attempted to conquer the limitations of Li-S batteries (1-5). Early work on this subject was performed by Shim et al. (1) who reported that more than 10% carbon black is necessary to meet the cathode conductivity. This method places emphasis on enhancing the electrical conductivity of the cathode and restraining the loss of soluble polysulfides during cycling. However, the main challenge of active material loss still remains. Some new concepts have recently been proposed to improve the performance of Li-S batteries by employing novel materials and innovative cell design. For instance, a bifunctional microporous carbon paper placed between the cathode and separator led to good capacity retention and coulombic efficiency of the cell (6,7). It is believed that the porous carbon interlayer plays a significant role in trapping the soluble lithium polysulfides and providing additional reaction sites to accommodate the formation of Li_2S_2 or Li_2S on discharge (7). In another example, using PTFE as the binder for a sulfur electrode was shown to improve cell performance, which was attributed to the high chemical stability and hydrophobicity of PTFE (8,9). Herein we report a simple modification to the traditional Li-S battery configuration by using Teflon®-coated carbon paper (TCCP) as a porous electrode matrix for the sulfur cathode. The TCCP is composed of interlaying carbon microfibers that act as an excellent substrate for mass transfer and electron conduction. The porous architecture and the hydrophobic Teflon (PTFE) coating facilitates the absorption and confinement of soluble polysulfides to the cathode, leading to high sulfur utilization and excellent capacity retention during cycling (9). This novel cathode design is a much simpler approach than synthesizing complex sulfur/carbon composites (10-12) to improve the capacity and cycle life of the Li-S battery.

5.2 Novel Cell Assembly

Due to the now known influence of fluorinated electrolytes on lithium ion (13-16) and Li-S batteries (17,18), additional investigation was sustained on engineering the electrode for the similar effect.

A sulfur/carbon composite (60% wt sulfur) with a sulfur loading of 3-4 mg/cm^2 was prepared by mixing Super P carbon and sulfur, followed by making a slurry of this material with a solution of poly(vinylidene fluoride) (PVDF) in *n*-methylpyrrolidone (NMP) (sulfur/ Super P/PVDF, 60/30/10 by weight). Microfiber carbon paper (MFCP) with 127 µm thickness and TCCP (TGP-060) with 190 µm thickness, 5wt % PTFE treatment, and 80% porosity were purchased from the Fuel Cell store. Three types of electrodes were made by casting the slurry onto aluminum foil (S/Al), microfiber carbon paper (S/MFCP), and the carbon side of TCCP (S/TCCP). The laminates were then placed in 70^{0}C oven overnight. The laminates were punched into circular disks of 14 mm in diameter and further dried at 60 °C under vacuum for 4 hours.

Single sided Teflon-coated carbon paper (TCCP) was used as the current collector for sulfur electrodes in this study, where TCCP carbon microfibers treated with 5wt% PTFE act as an excellent substrate (Figure 1). In addition, the PTFE coating facilitates the absorption of soluble lithium polysulfides to the cathode, therefore preventing them from diffusing into the electrolyte. While this has been shown to lead to high coulombic efficiency it will also result in high sulfur utilization and excellent capacity retention (9). Preliminary experimentation with a double-sided PTFE coating carbon paper was also investigated; in which sulfur slurry was coated on the Teflon coating. However, due to the hydrophobicity of PTFE and the hydrophilic property of the lithium polysulfides, very low solubility and low reduction of the sulfur species resulted in small discharge capacity for the Li-S cell. By coating sulfur on the carbon fibers and using the Teflon coating on other side in contact with the electrolyte, the polysulfides have the chance to fully reduce to the lower order polysulfides on the cathode surface without diffusing into the organic electrolyte.

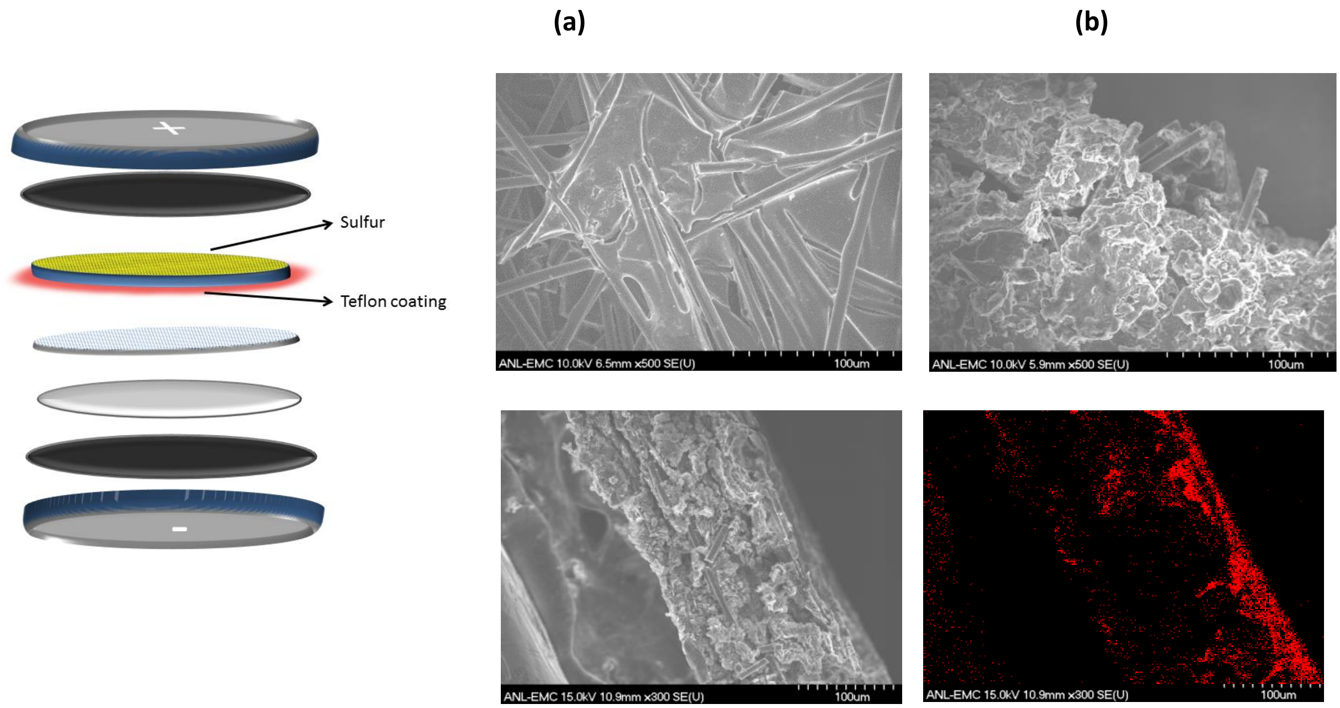

Figure 1. (a) From top to bottom: cathode cap, spacer, sulfur coated on TCCP (Teflon coating facing the separator), Celgard separator, lithium anode, spacer, anode cap and (b) SEM images and elemental mapping of Microfiber carbon paper (MFCP) (top left), Teflon coated carbon paper (TCCP) (top right), cross section for (TCCP) (bottom left), and EDS elemental mapping of fluorine (bottom right).

5.3 Effect Of Teflon Coated Carbon Paper

To investigate the effect of different current collectors on the electrochemical performance of the Li-S cell, we first experimented using the conventional DOL/DME-1.0M LiTFSI electrolyte with a sulfur cathode coated on an aluminum current collector (S/Al). The results presented in Figure 2a show an initial specific discharge capacity of only 660 mAh/g; which then decreased to 230 mAh/g within a few cycles. The low capacity was likely due to the limited capability of PVDF-bound Super P carbon to accommodate the formed discharge/charge products during cycling. Coulombic efficiency of the Li-S cells are also shown in figure 2b; where the cell using the S/Al cathode with conventional electrolyte has low coulombic efficiency due to severe shuttling. The procedure is modified such that the charge capacity was limited not to exceed 120% of the discharge capacity for the previous cycle.

The sulfur/Super P slurry was then coated on a microfiber carbon paper (S/MFCP) in the next study. As presented in Figure 2a, the cell with the S/MFCP electrode delivered a much higher initial specific capacity of over 1400 mAh/g compared to the S/Al cell. The capacity retention was still a major issue, because only 43% of the initial capacity remained after 50 cycles. In addition, a severe polysulfide shuttling effect was observed during the charging step, which resulted in very low coulombic efficiency (< 20%). Note that no additive, such as $LiNO_3$, was added in the electrolyte to protect the Li anode (19,20). Therefore, in order for the cell to cycle within a reasonable timeframe, the modification to the charge procedure was again applied. In sharp contrast to the sulfur/Al and sulfur/MFCP electrodes, significant improvement in cell performance was observed when the same sulfur slurry was coated on TCCP and used as the cathode with the conventional electrolyte. For direct comparison, the sulfur loading (3 mg/cm^2) was kept the same for all the cathodes regardless of the current collector type. Figure 2a shows that with the S/TCCP cathode, the discharge capacity was maintained at 800 mAh/g after 50 cycles. Although the coulombic efficiency was still about 80% due to polysulfide shuttling, this effect was much less pronounced compared to the S/MFCP electrode so that no charge capacity limit was programed into the testing procedures. These results suggest that the TCCP plays the same role as MFCP as a conductive carbon support for the sulfur species and, in addition, the Teflon coating may serve as a hydrophobic barrier that to some extent was able to resist the diffusion of the soluble polysulfides from TCCP to the bulk electrolyte. Nevertheless, some polysulfide shuttling effect was still evident from the low coulombic efficiency due to the use of DME as the solvent (21,22), which readily dissolves polysulfides and facilitates their diffusion.

We have recently reported a new electrolyte based on an organo-fluorine solvent (TTE) that prevents the shuttling effect and improves the performance of the Li-S battery (17). In that study, the SEM/EDS analysis confirmed the improved performance was due to the detainment of polysulfides inside the electrode (17). When this novel electrolyte was used with the sulfur/TCCP cathode, the cell delivered a discharge capacity of 1400 mAh/g with 96% coulombic efficiency in the first cycle (Figure 2a). Furthermore, a 980 mAh/g discharge capacity was retained after 50 cycles and the coulombic efficiency was above 90% for all cycles. This novel electrode/electrolyte combination is believed to be capable of “trapping” polysulfides that are formed on the cathode during cycling. The fibrous carbon permits effective mass transport of lithium ions while the Teflon coating on the surface of the TCCP blocks (hydrophilic) polysulfides from migrating out of the carbon paper. With the less solubility of the polysulfides in the fluorinated electrolyte, the diffusion of polysulfides into the bulk electrolyte was further hindered. These results have clearly demonstrated by using this cell configuration, sulfur loss from the cathode may be effectively minimized during continuous electrochemical cycling.

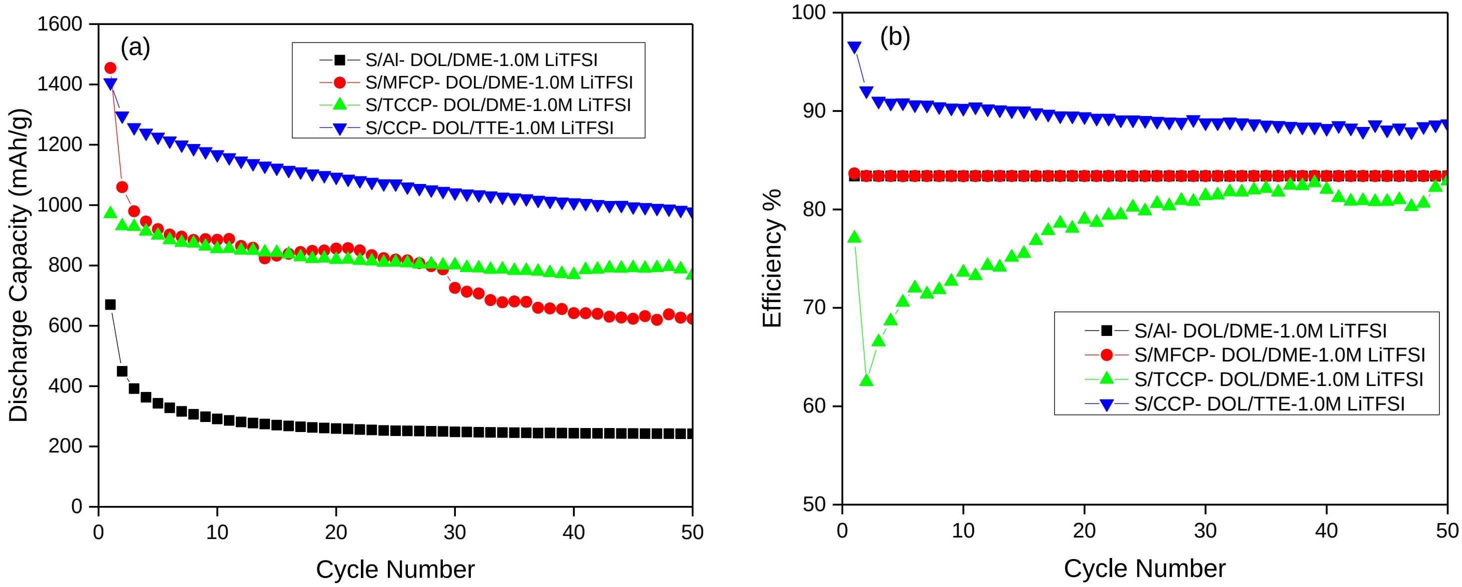

Figure 2**.** (a) Capacity retention and (b) coulombic efficiency of Li-S cell with: sulfur coated on Al current collector with DOL/DME-1.0 M LiTFSI, sulfur coated on MFCP with DOL/DME-1.0 M LiTFSI, sulfur coated on TCCP with DOL/DME-1.0 M LiTFSI, and sulfur coated on TCCP with DOL/TTE-1.0 M LiTFSI.

5.4 Cyclic Voltammetry

To study the electrochemical characteristics of S/Al and S/TCCP Li-S cells, cyclic voltammetry (CV) was performed at a scan rate of 0.03 mV/s. Cyclic voltammograms of the first

5 cycles for three cells with different electrolytes and current collectors are shown in Figure 3a. When the cell containing the conventional cathode, S/Al, and electrolyte is first discharged to 1.6V, two distinguishable reduction peaks are observed at 2.35 and 2.05 V during the first discharge, which are attributed to the reduction of elemental sulfur and the intermediate polysulfides, respectively. For the second cell containing the conventional electrolyte and the S/TCCP cathode there is an additional third reduction peak observed at 1.98 V, corresponding to the effect of the Teflon coated carbon paper interlayer. This layer forms a protection film over the cathode surface which prevents the diffusion of polysulfides into the organic electrolyte (17). When the voltage sweep was reversed, the CV plot exhibited two sharp anodic peaks at 2.3 and 2.4 V for both cells containing the conventional DOL/DME-1.0M LiTFSI electrolyte. By comparing both voltammograms it is clearly observed that the first peak at 2.3V which is assigned to the oxidation of low order PS (Li_2S and Li_2S_2) to higher order PS and the second peak at 2.4V which is due to the oxidation of those to sulfur almost have similar intensities when using the conventional cathode (due to the high concentration of low order PS) while the second peak has lower intensity when using the TCCP cathode. In the next case, the CV for the cell containing the combined effect of the TCCP cathode and the fluorinated electrolyte shows completely different results. The presence of only one broad reduction peak at 1.8-1.9 V with lower intensity is due to the: (1) relatively low reduction to lower order PS as a result of using the TTE electrolyte, (2) their negligible solubility in this electrolyte and (3) almost no diffusion of these species into the electrolyte as a result of using the Teflon coated carbon paper which results in high capacity and efficiency of the cell. This suggests that the higher order polysulfides are not fully reduced to insoluble low order polysulfides during the discharge, and thus can be converted to sulfur with fast

kinetics and therefore the oxidation reaction of high order polysulfides dominates the charging process when TCCP cathode is used as interlayer.

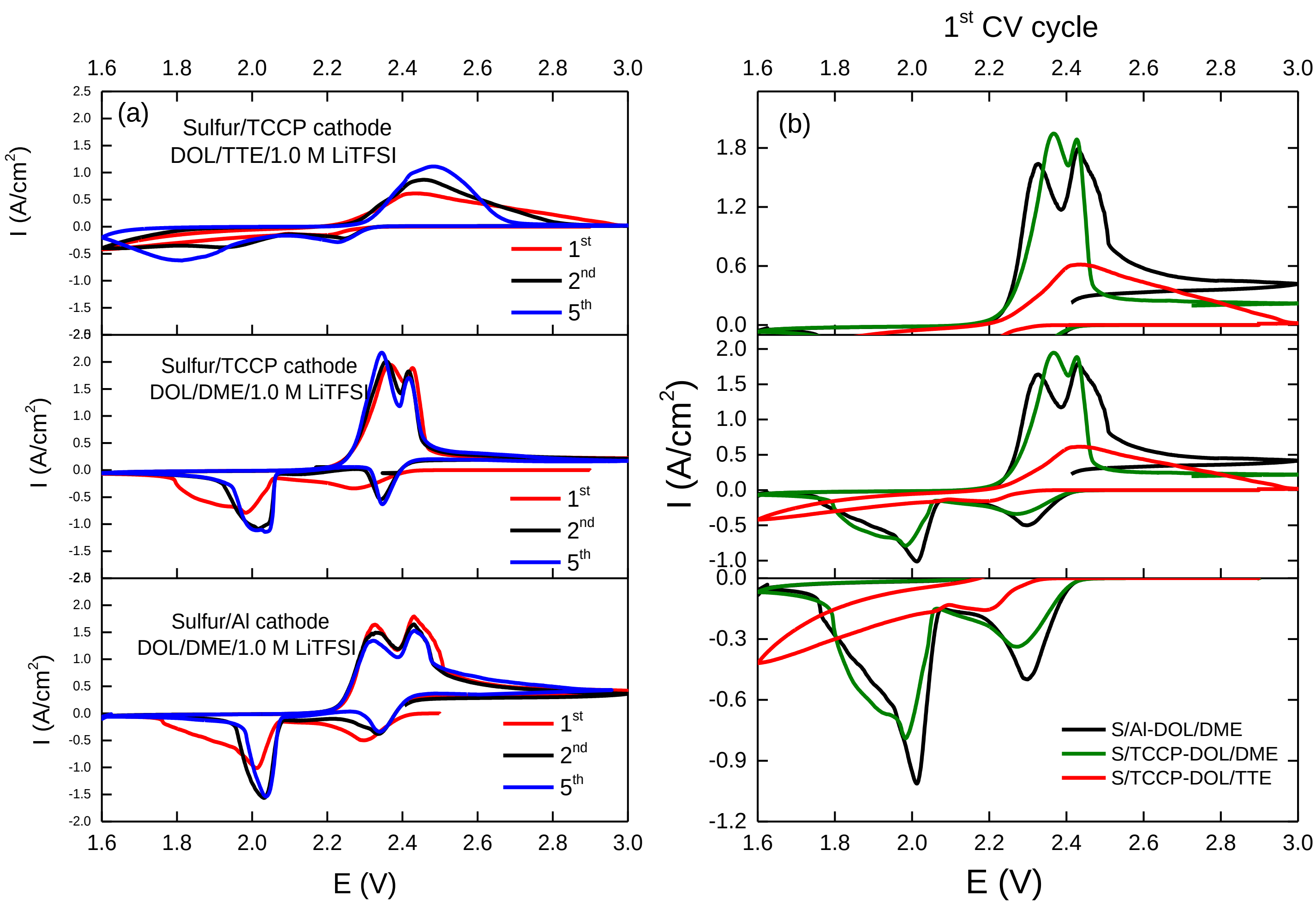

Figure 3. Cyclic voltammograms of (a) the first5 cycles and (b) first cycle for Li-S cell at scan rate of 0.03 mV/s with an aluminum current collector and 1.0M LiTFSI-DOL/DME, Teflon-coated carbon paper and 1.0M LiTFSI-DOL/DME, and Teflon-coated carbon paper and 1.0M LiTFSI-DOL/TTE electrolyte.

5.5 C-Rate Capability

To investigate and compare the effect of different current rates, a C-rate experiment was conducted on three cells with different current collectors and electrolytes. The cells were cycled at C/10, C/2 and 1C rates, as presented in Figure 4, and were then returned to the C/10 rate. As shown in Figure 4a, for the cell containing the sulfur slurry coated on aluminum and the conventional DOL-DME electrolyte an initial capacity of about 600mAh/g is observed at the C/10 current rate. After increasing the current to C/2, the capacity drops significantly as expected and a capacity of about 300mAh/g is observed. In addition, by returning the rate to C/10 the capacity does not completely recover. However, the capacity increases considerably when the same sulfur slurry is coated on TCCP regardless of using the conventional electrolyte, where an initial capacity of 1050mAh/g is observed at the C/10 current. At the higher current rates of 1C, the cell still delivers almost 400 mAh/g of capacity which is almost 3 times that of the cell containing the simple sulfur cathode on aluminum. In addition, the capacity has recovered about 80% by decreasing the current to C/10 which is much higher when compared to figure 4a. Finally, by using the combination of the fluorinated electrolyte and the TCCP cell configuration an initial capacity of 1200 mAh/g is achieved and the cell has recovered more than 90% of its initial capacity after increasing the cycling rates. These results clearly demonstrate the excellent rate capability of Li-S cells using the combination of the fluorinated electrolyte and Teflon-coated carbon paper where the initial capacity is practically recovered.

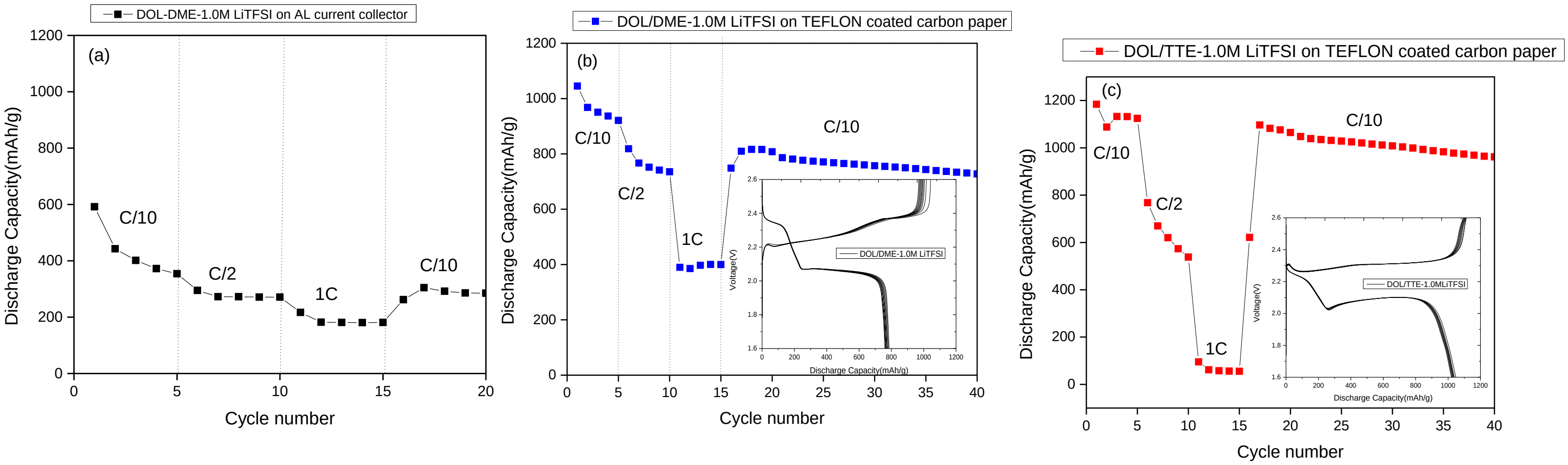

Figure 4. C-rate profiles of Li-S cell using (a) aluminum current collector with 1.0M LiTFSI-DOL/DME (b) Teflon coated carbon paper with 1.0M LiTFSI-DOL/DME, and (c) Teflon coated carbon paper with 1.0M LiTFSI-DOL/TTE electrolyte.

5.6 Electrode Characterization

To investigate and compare the morphological changes of the sulfur electrode coated on MFCP and TCCP at different charge and discharge stages, SEM imaging was employed and the results are shown in Figure 5a. As observed, there is homogenous distribution of carbon and sulfur on the surface of the pristine electrode (S/TCCP) which ensures an appropriate re-utilization of the active material. It is also noticed that after 1st discharge and charge, there is a very uniform distribution of sulfur and carbon on the sulfur side of the electrode without any sign of deposited polysulfides on the surface of the electrode. This is due to using the Teflon-coated carbon paper as a current collector where the residue of the PTFE coating on the carbon side of the electrode can also cause lower deposition of the insoluble low order polysulfides. Although this Teflon coating in contact with the electrolyte can act as a shield to block the migration of polysulfides out of the cathode and improve the efficiency of the cell, it also results in higher capacity retention due to the uniform deposition of the insoluble species and less agglomeration. To distinguish the effect of Teflon coated carbon paper and plain carbon paper, SEM images from cycling with S/MFCP were also investigated as shown in Figure 5b. Even though carbon paper interlayer has been reported to improve the performance (6,7), the surface of the electrode is deposited with crystal structure species on the sulfur side after discharge and also layers of insoluble PS products on the carbon side as well. This confirms the significant role of Teflon coating on the carbon paper which effectively improves the capacity retention and cycling efficiency. In addition Figure 5b shows SEM images of the cross-sections of the sulfur cathode coated on the Teflon coated carbon, paper which clearly indicate the more diffusion of sulfur into the carbon paper as cycling increases.

(a)

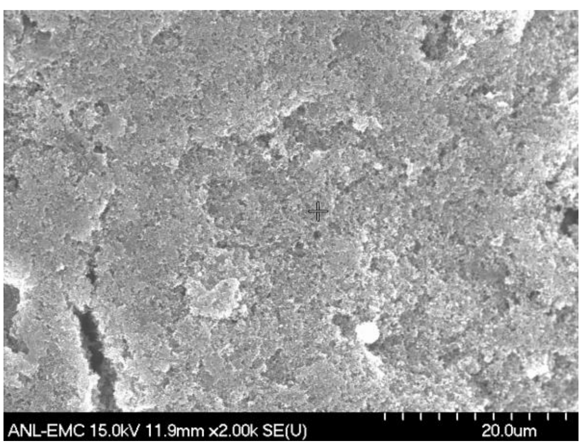

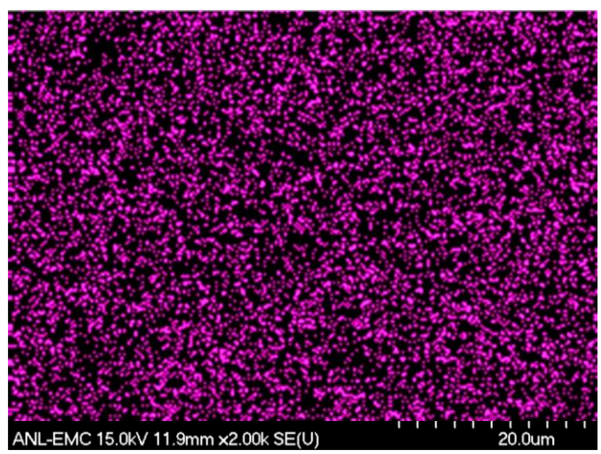

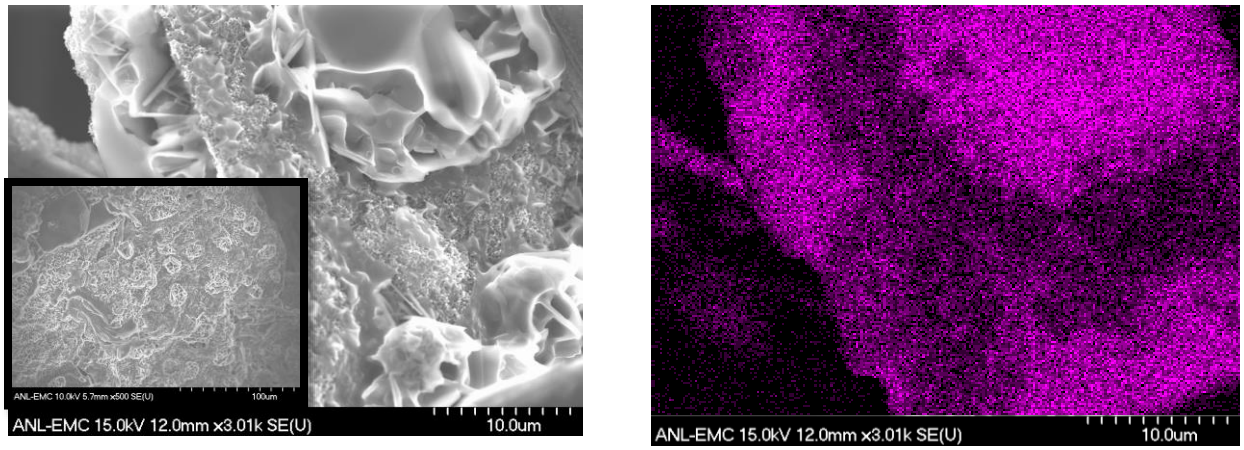
ANL-EMC 10.0kV 5.7mm x500 SE(U)
100um
ANL-EMC 15.0kV 12.0mm x3.01k SE(U)
10.0um
ANL-EMC 15.0kV 12.0mm x3.01k SE(U)
10.0um

(b)

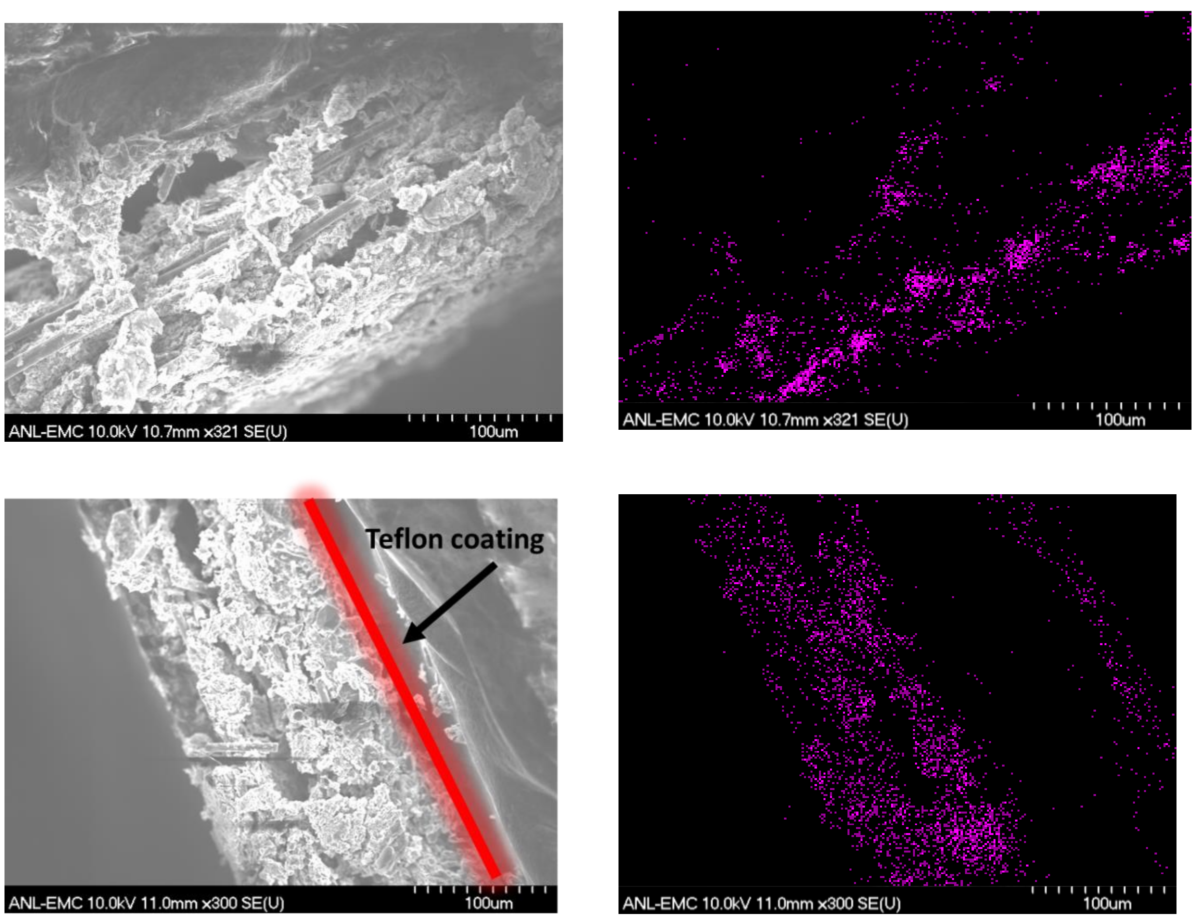
ANL-EMC 10.0kV 10.7mm x321 SE(U)
100um
ANL-EMC 10.0kV 10.7mm x321 SE(U)
100um
Teflon coating
ANL-EMC 10.0kV 11.0mm x300 SE(U)
100um
ANL-EMC 10.0kV 11.0mm x300 SE(U)
100um

Figure 5. SEM images of (a) sulfur coated on TCCP (top left) and MFCP (bottom left) after 1st discharge with EDS elemental mappings of sulfur and (b) cross section of sulfur electrode coated on TCCP for pristine (top left) and after 1st discharge (bottom left) with EDS elemental mappings of sulfur; all cycled with DOL/DME-1.0M LiTFSI electrolyte.

5.7 Conclusions

In summary for this section, the effect of sulfur coated on Teflon-coated carbon paper was investigated. The cycling data, C-rate procedure, and CV and SEM data all confirm the improvement of cell performance in comparison to the control cells using either aluminum or plain carbon paper as current collector. Using sulfur coated on Teflon coated carbon paper acts as a shield blocking the migration of polysulfides out of the cathode due to the hydrophobic property of this material. In this study the effects of plain carbon paper and Teflon coated carbon paper have been studied and compared. Although using a carbon paper interlayer has shown improvements in the performance of the Li-S battery, deposition of an insoluble sulfur species is detected with SEM which results in lower efficiency. Using Teflon as a protective layer on one side of the electrode shows improved performance of the cell due to the less loss of the active material and the reduced shuttling effect

CITED LITERATURE

1. Shim J, Striebel KA, Cairns EJ. The Lithium/Sulfur Rechargeable Cell: Effects of Electrode Composition and Solvent on Cell Performance. Journal of The Electrochemical Society. 2002;149(10):A1321-A5.

2. Ji X, Lee KT, Nazar LF. A highly ordered nanostructured carbon-sulphur cathode for lithium-sulphur batteries. Nat Mater. 2009;8(6):500-6.

3. Ji L, Rao M, Aloni S, Wang L, Cairns EJ, Zhang Y. Porous carbon nanofiber-sulfur composite electrodes for lithium/sulfur cells. Energy & Environmental Science. 2011;4(12):5053-9.

4. Zheng W, Liu YW, Hu XG, Zhang CF. Novel nanosized adsorbing sulfur composite cathode materials for the advanced secondary lithium batteries. Electrochimica Acta. 2006;51(7):1330-5.

5. Ahn W, Kim K-B, Jung K-N, Shin K-H, Jin C-S. Synthesis and electrochemical properties of a sulfur-multi walled carbon nanotubes composite as a cathode material for lithium sulfur batteries. Journal of Power Sources. 2012;202(0):394-9.

6. Su Y-S, Manthiram A. Lithium–sulphur batteries with a microporous carbon paper as a bifunctional interlayer. Nat Commun. 2012;3:1166.

7. Zu C, Su Y-S, Fu Y, Manthiram A. Improved lithium-sulfur cells with a treated carbon paper interlayer. Physical Chemistry Chemical Physics. 2013;15(7):2291-7.

8. Kim N-I, Lee C-B, Seo J-M, Lee W-J, Roh Y-B. Correlation between positive-electrode morphology and sulfur utilization in lithium–sulfur battery. Journal of Power Sources. 2004;132(1–2):209-12.

9. Schneider H, Garsuch A, Panchenko A, Gronwald O, Janssen N, Novák P. Influence of different electrode compositions and binder materials on the performance of lithium–sulfur batteries. Journal of Power Sources. 2012;205(0):420-5.

10. Wang J-Z, Lu L, Choucair M, Stride JA, Xu X, Liu H-K. Sulfur-graphene composite for rechargeable lithium batteries. Journal of Power Sources. 2011;196(16):7030-4.

11. Li G-C, Li G-R, Ye S-H, Gao X-P. A Polyaniline-Coated Sulfur/Carbon Composite with an Enhanced High-Rate Capability as a Cathode Material for Lithium/Sulfur Batteries. Advanced Energy Materials. 2012;2(10):1238-45.

12. Cao Y, Li X, Aksay IA, Lemmon J, Nie Z, Yang Z, et al. Sandwich-type functionalized graphene sheet-sulfur nanocomposite for rechargeable lithium batteries. Physical Chemistry Chemical Physics. 2011;13(17):7660-5.

13. Ohmi N, Nakajima T, Ohzawa Y, Koh M, Yamauchi A, Kagawa M, et al. Effect of organo-fluorine compounds on the thermal stability and electrochemical properties of electrolyte solutions for lithium ion batteries. Journal of Power Sources. 2013;221(0):6-13.

14. Ishikawa M, Yamagata M, Sugimoto T, Atsumi Y, Kitagawa T, Azuma K. Li-Ion Battery Performance with FSI-Based Ionic Liquid Electrolyte and Fluorinated Solvent-Based Electrolyte. ECS Transactions. 2011;33(28):29-36.

15. Kitagawa T, Azuma K, Koh M, Yamauchi A, Kagawa M, Sakata H, et al. Application of Fluorine-containing Solvents to LiCoO₂ Cathode in High Voltage Operation. Electrochemistry. 2010;78(5):345-8.

16. Achiha T, Nakajima T, Ohzawa Y, Koh M, Yamauchi A, Kagawa M, et al. Thermal Stability and Electrochemical Properties of Fluorine Compounds as Nonflammable Solvents for Lithium-Ion Batteries. Journal of The Electrochemical Society. 2010;157(6):A707-A12.

17. Azimi N, Weng W, Takoudis C, Zhang Z. Improved performance of lithium–sulfur battery with fluorinated electrolyte. Electrochemistry Communications. 2013;37(0):96-9.

18. Cuisinier M, Cabelguen PE, Adams BD, Garsuch A, Balasubramanian M, Nazar LF. Unique behaviour of nonsolvents for polysulphides in lithium-sulphur batteries. Energy & Environmental Science. 2014;7(8):2697-705.

19. Liang X, Wen Z, Liu Y, Wu M, Jin J, Zhang H, et al. Improved cycling performances of lithium sulfur batteries with LiNO3-modified electrolyte. Journal of Power Sources. 2011;196(22):9839-43.

20. Zhang SS. Role of LiNO3 in rechargeable lithium/sulfur battery. Electrochimica Acta. 2012;70(0):344-8.

21. Kim S, Jung Y, Lim HS. The effect of solvent component on the discharge performance of Lithium–sulfur cell containing various organic electrolytes. Electrochimica Acta. 2004;50(2–3):889-92.

22. Chang D-R, Lee S-H, Kim S-W, Kim H-T. Binary electrolyte based on tetra(ethylene glycol) dimethyl ether and 1,3-dioxolane for lithium–sulfur battery. Journal of Power Sources. 2002;112(2):452-60.

6. CONCLUDING REMARKS AND FUTURE PROSPECTIVES

6.1 Conclusions

Lithium sulfur batteries are a promising candidate for the next generation of electric vehicles due to their many advantages over lithium ion batteries. Sulfur is abundant, inexpensive, and reveals a high theoretical specific capacity and energy of 1672 mAh/g and 2600 W h/kg . Even though these batteries provide us with much hope, there are various problems such as poor cyclic ability, low efficiency and severe self-discharge which arise from a complex multi-step discharge process. In recent years, great improvement in the cycling performances of the Li-S batteries has been made; however, all of these achievements are obtained at the expense of the energy density and process cost.

Nano-structured sulfur composites based on various types of carbon materials and conducting polymers have driven the specific capacity of sulfur to approach the theoretical value with acceptable cycling efficiency and cycle number. However, syntheses of these composites are very costly; furthermore the cathodes using these composites contain low sulfur content (< 60 %) and low sulfur-loading (< 2 mg/cm^2), which dramatically reduces the energy density of Li-S batteries. On the other hand, Li-S batteries are fundamentally a liquid electrochemical system, in which elemental sulfur must dissolve into the liquid electrolyte in the form of long-chain PS and serve as the liquid catholyte. Dissolution of PS in the liquid electrolyte on one hand facilitates the electrochemical reactions of insulating sulfur species, and on the other hand causes severe redox shuttle and parasitic reactions with the Li anode.

In this study, a detailed investigation was conducted on the electrolyte and electrode part of this battery. First, the effect of different fluorinated solvents was investigated on the performance of the Li-S cell. It was noticed that solvents having one or two non-fluorinated alkyl chains show low or no capacity. A more detailed investigation was conducted on the solvent 1,1,2,2-Tetrafluoroethyl-2,2,3,3-tetrafluoropropyl ether (TTE) which when used as co-solvent exhibited a significant improvement to cell performance. It was realized that cells containing this electrolyte show no sign of a redox shuttling effect and much higher capacity. After conducting a solvent ratio study, it was noticed that the cell with a DOL/TTE ratio of 1/2 shows the best capacity retention but when the ratio is increased to (1/3) the capacity has dropped due to the very low solubility of the lithium salt and sulfur in this electrolyte. However, the efficiency of the cell containing the (1/3) ratio has the highest value among the other solvent ratios due to the higher concentration of the fluorinated electrolyte and the concentrated effect of SEI formation and low polysulfide solubility.

For a better understanding of the complex discharge mechanism in the baseline electrolyte, DOL-DME-1.0M LiTFSI, and the fluorinated electrolyte characterization techniques such as HPLC, and UV-VIS were used for the harvested electrolyte. The lithium polysulfide species generated in a Li-S cell were quantitatively compared in this study. The results suggested that the improved performance of a Li-S cell with DOL-TTE-1.0M LiTFSI is due to less solubility of long chain polysulfides in the fluorinated electrolyte, which was confirmed with HPLC and UV-VIS data. . XPS and SEM studies were also used to study the sulfur electrodes after different charging and discharging state. Much lower Li_2S and Li_2S_2 deposition was observed on the surface of the cathode cycled with TTE as confirmed with XPS results.

In the next part, the effect of a fluorinated electrolyte on the self-discharge behavior of Li-S cells was studied. Self-discharge is one of the major issues preventing the commercialization of this battery due to the severe corrosion of the lithium metal anode in the presence of the lithium polysulfides in the electrolyte. However, this issue has not received much attention in the literature, even though these cells suffer from severe self-discharge. Self-discharge was tested by charging and discharging the cells with a C/10 rate for five cycles and then resting them for 10 hours between the fifth charge and sixth discharge step and was then calculated by comparing the discharge capacity of the 6^{th} cycle to the 5th cycle. In this study our test results suggested that utilizing the fluorinated electrolyte, 1,1,2,2-Tetrafluoroethyl-2,2,3,3-tetrafluoropropyl ether (TTE), in combination with the $LiNO_3$ additive can effectively suppress this effect even for high loading sulfur cathodes at room temperature and at elevated-temperature storage. This is due to the combined effect of lithium anode protection by the $LiNO_3$ operation and also the protection of the sulfur cathode due to using the fluorinated electrolyte. In addition, the low solubility of the lithium polysulfides in this electrolyte will lead to lower redox shuttle effect and therefore a major improvement in the capacity of the cell even after long resting times. Using high concentrations of $LiNO_3$ clearly shows that even though using this additive results in lower rate of self-discharge for the lithium sulfur cell, it does not completely prevent this behavior. This is due to the fact that the irreversible reduction of $LiNO_3$ reduces reversibility of Li_2S and this will result in permanent loss in the reversibility of the Li-S cell. This could indicate that the major part of self-discharge is due to irreversible loss of active material rather than polysulfide shuttling. Lower solubility of lithium polysulfides , higher reversibility of sulfur species in the fluorinated electrolyte and also the formation of the protective layer as a result of $LiNO_3$ reduction is the reason that DOL/TTE-1.0M LiTFSI- 0.2M $LiNO_3$ is the most effective in preventing the self-discharge behavior of the cell.

Based on the idea that using fluorinated electrolyte solvents can improve cell performance due to SEI formation on the cathode surface, other fluorinated additives were also investigated. In this part, $(CH_3)_3Si(OCH_2CH_2)_3OCH_3$ (1NM3) was evaluated as a new solvent for Li-S batteries. The effects of lithium salts and electrolyte additives were studied in order to optimize the electrolyte for the Li-S chemistry. Our results showed that the cell performance was much improved when 1NM3 electrolyte was combined with Lithium difluoro(oxalato) borate (LiDFOB) as additive. Impedance spectroscopy studies indicated that LiDFOB is an effective additive due to its capability of forming a passivation layer on the surface of the sulfur electrode. Also SEM studies confirm the lower deposition of insoluble products on the cathode surface when LiDFOB is used as electrolyte additive. In the second section of this part of the study, the effect of another fluorinated additive, Tris(pentafluorophenyl)borane ($B(C_6F_5)_3$), was also investigated with the conventional electrolyte. XPS studies show that using this additive assists in forming a stable SEI on the cathode surface which prevents dissolution of the polysulfides and results in higher coulombic efficiency.

In the last part of this study, we report on a modification to the traditional Li-S battery configuration that has shown to result in high capacity and efficiency of the Li-S cell. Teflon-coated carbon paper (TCCP) was used as an electrode matrix and the sulfur active material are embedded inside the pore structures of the paper. The TCCP was composed of carbon microfibers that act as an excellent substrate for mass transfer and electron conduction while the hydrophobic Teflon (PTFE) coating facilitates the absorption and confinement of soluble polysulfides to the cathode. The cell containing cathode coated on TCCP showed an initial discharge capacity of 1400 mAh/g while maintaining a capacity of 1000 mAh/g after 50 cycles. The efficiency was also stable at 90% for the first 50 cycles. In the next part of this study excellent capacity recovery is reported for cells using the combination of the fluorinated electrolyte and TCCP cell configuration where the cell has recovered more than 90% of its initial capacity after increasing the cycling rates. SEM studies also confirm the outstanding effect of using TCCP by where no sulfur deposition is observed on the surface of the electrode after discharge. However the surface of the electrode using MFCP without the Teflon coating is deposited with crystal structure species on the sulfur side after discharge and also layers of insoluble PS products on the carbon side as well. This novel cathode design is not only simpler than methods used in synthesizing sulfur carbon composites, but also it improves the capacity and cycle life of the lithium sulfur battery considerably.

6.2 Future Prospective

Even though significant advancements in Li/S cells have been made in recent years, challenges still remain. In order to enhance the performance of the Li-S batteries more detailed research is needed in the area of the electrolyte and the electrodes of this battery. A deep understanding of the complex discharge mechanism of the Li-S cell can indeed assist in a better understanding of this battery system and lead to improvements in the battery life and performance. Future improvements should be made by balancing the various positive and negative effects of the polysulfide dissolution, as discussed in the recommendations that follows:

1. Sulfur cathode: To meet the requirements of low cost and high energy density, elemental sulfur should be preferentially considered as the cathode active material, and the cathode should contain at least 70% sulfur and have a sulfur-loading of not less than 2 mg/cm^2. Furthermore, the cathode structure should be tolerant enough to stand the large volume expansion and contraction incurred by the discharging and charging of the sulfur active material.
2. Anode material: When metallic Li is used as the anode material, it is essential to develop an effective and cost-acceptable approach for protecting the Li anode from reactions with the dissolved PS and from the growth of Li dendrites. To completely solve the problem of Li dendrites, it is essential to develop an alternative anode material free of Li metal for the safety of Li-S batteries. In this case, a facile and cost-acceptable lithiation technique should be explored either for the anode or for the sulfur cathode.
3. Electrolyte: The electrolyte is key to determining the operational temperature range of Li-S batteries, and to the dissolution and chemical stability of PS. The PS in the electrolyte will spontaneously disproportionate into low-soluble or insoluble short-chain PS and elemental sulfur, which could precipitate out of the liquid electrolyte and clog the pores of the separator. Therefore, in view of sulfur utilization and reaction kinetics, a liquid electrolyte that can well dissolve and stabilize the PS is in great demand; however, this promotes the redox shuttle effect of the polysulfides. The electrolyte also affects the coulombic efficiency of the Li anode and the formation of a passivation layer on the Li surface.
4. Battery design: The electrochemical process in Li-S batteries is much more complicated than that in all other rechargeable batteries. Battery design plays a crucial role in affecting the cycling performance of Li-S batteries. As suggested by the fundamental chemistry of

the Li-S battery, the dissolution of PS in the liquid electrolyte is essential to enable the electrochemical reactions of insulating sulfur species, however, it meanwhile causes a severe redox shuttle effect and Li corrosion. All sulfur composites, such as S-C composites and S-polymer composites, are designed to confine the dissolved PS within the composites. In this case, the electrolyte absorbed in the pores between the composite (and the conducting carbon) particles cannot be utilized to dissolve PS, a design that can confine the dissolved PS within the cathode, other than within the composite particles, must increase the loading and utilization of sulfur in the Li-S batteries.

Although the current status of the Li-S batteries is still far wary from the requirements for practical applications, it is possible that in near future, major advances in the materials and battery designs drive the Li-S batteries to the practical applications.

CITED LITURATURES

Achiha, T., et al.: Thermal Stability and Electrochemical Properties of Fluorine Compounds as Nonflammable Solvents for Lithium-Ion Batteries. Journal of The Electrochemical Society 157(6):A707-A712, 2010.

Achiha, T., Nakajima, T., Ohzawa, Y., Koh, M., Yamauchi, A., Kagawa, M., and Aoyama, H.: Journal of The Electrochemical Society 157:A707, 2010.

Agilent Technologies, I. Fundamentals of Liquid Chromatography (HPLC) Available at http://polymer.ustc.edu.cn/xwxx_20/xw/201109/P020110906263097048536.pdf.

Ahn, W., Kim, K.-B., Jung, K.-N., Shin, K.-H., and Jin, C.-S.: Journal of Power Sources 202:394, 2012.

Aihara, Y., et al.: Ion Transport Properties of Six Lithium Salts Dissolved in γ-Butyrolactone Studied by Self-Diffusion and Ionic Conductivity Measurements. Journal of the Electrochemical Society 151(1):A119-A122, 2004.

Akridge, J.R.: Lithium Sulfur Rechargeable Battery Safety, Moltech Corporation dba Sion Power Corporation, 2001.

Armand, M., and Tarascon, J.M.: Building better batteries. Nature 451(7179):652-657, 2008.

Aurbach, D., Pollak, E., Elazari, R., Salitra, G., Kelley, C S., and Affinito, J.: Journal of The Electrochemical Society 156:A694, 2009.

Azimi, N., et al.: Improved performance of lithium–sulfur battery with fluorinated electrolyte. Electrochemistry Communications 37(0):96-99, 2013.

Azimi, N., Weng, W., Takoudis, C., and Zhang, Z.: Electrochemistry Communications 37:96, 2013.

Azimi, N., Xue, Z., Bloom, I., Wang, D., Daniel, T., Takoudis, C., and Zhang, Z.: Fluoroether-Based Electrolytes for Lithium-Sulfur Batteries. Advanced Energy Materials 2014. (submitted)

Azimi, N., Xue, Z., Dietz Rago, N., Takoudis, C., Gordin, M.L., Song, J., Wang, D., and Zhang, Z.: Fluorinated Electrolytes for Li-S Battery: Suppressing the Self-discharge with an Electrolyte Containing Fluoroether Solvent. Journal of the Electrochemistry Society 2014. (submitted)

Bao, W., Zhang, Z., Gan, Y., Wang, X., and Lia, J.: Journal of Energy Chemistry 22:790, 2013.

Barchasz, C., Molton, F., Duboc, C., Leprêtre, J.-C., Patoux, S., Alloin, F.: Lithium/Sulfur Cell Discharge Mechanism: An Original Approach for Intermediate Species Identification. Analytical Chemistry 84(9):3973-3980, 2012.

Barchasz, C., Leprêtre, J.-C., Patoux, S., and Alloin, F.: Electrochimica Acta 89:737, 2013.

Barchasz, C., Leprêtre, J.-C., Patoux, S., and Alloin, F.: Journal of The Electrochemical Society 160:A430, 2013.

Barron, A.R., and Oliva-Chatelain, B.L.: Basics of UV-Visible Spectroscopy. 2014. Available at http://cnx.org/contents/02e7b3d6-cf47-4c92-a380-d011ce5658b1@1/Basics_of_UV-Visible_Spectrosc.

Barsoukov, E., and Macdonald, J.R.: Impedance Spectroscopy: Theory, Experiment, and Applications. Hoboken, NJ: Wiley-Interscience, 2005:

Bruce, P.G., Freunberger, S.A., Hardwick, L.J., Tarascon, J.-M.: Li-O_2 and Li-S batteries with high energy storage. Nat Mater 11(1):19-29, 2012.

Bruce, P.G., Hardwick, L.J., and Abraham, K.M., Lithium-air and lithium-sulfur batteries. MRS Bulletin 36:506, 2011.

California State University, Northridge: Experiment 4: Conductivity of electrolyte solutions, 2009. Available at https://www.csun.edu/~jeloranta/CHEM355L/experiment4.pdf.

Cañas, N.A., Wolf, S., Wagner, N., and Friedrich, K.A.: In-situ X-ray diffraction studies of lithium–sulfur batteries. Journal of Power Sources 226(0):313-319, 2013.

Cao, Y., Li, X., Aksay, I.A., Lemmon, J., Nie, Z., Yang, Z., and Liu, J.: Sandwich-type functionalized graphene sheet-sulfur nanocomposite for rechargeable lithium batteries. Physical Chemistry Chemical Physics 13(17):7660-7665, 2011.

Chang, D.-R., Lee, S.-H., Kim, S.-W., and Kim, H.-T.: Journal of Power Sources 112:452, 2002.

Chen, H., Dong, W., Ge, J., Wang, C., Wu, X., Lu, W., and Chen, L.: Sci. Rep. 3, 2013.

Chen, L., and Shaw, L.L.: Recent advances in lithium–sulfur batteries. Journal of Power Sources 267(0):770-783, 2014.

Chen, S., Dai, F., Gordin, M.L., and Wang, D.: RSC Advances 3:3540, 2013.

Cheon, S.-E., Cho, J.-H., Ko, K.-S., Kwon, C.-W., Chang, D.-R., Kim, H.-T., and Kim, S.-W.: Journal of The Electrochemical Society 149:A1437, 2002.

Choi, J.-W., Kim, J.-K., Cheruvally, G., Ahn, J.-H., Ahn, H.-J., and Kim, K.-W.: Rechargeable lithium/sulfur battery with suitable mixed liquid electrolytes. Electrochimica Acta 52(5):2075-2082, 2007.

Chu, M.Y., et al.: Liquid electrolyte lithium-sulfur batteries. Google Patents, 2000.

Chung, K.-I., Kim, W.-S., and Choi, Y.-K.: Lithium phosphorous oxynitride as a passive layer for anodes in lithium secondary batteries. Journal of Electroanalytical Chemistry 566(2):263-267, 2004.

Clark, J.: High Performance Liquid Chromatography – HPLC. 2007. Available at http://www.chemguide.co.uk/analysis/chromatography/hplc.html.

Croce, F., Appetecchi, G.B., Persi, L., and Scrosati, B.: Nature 394:456, 1998.

Cuisinier, M., Cabelguen, P.E., Adams, B.D., Garsuch, A., Balasubramanian, M., and Nazar, L.F.: Unique behaviour of nonsolvents for polysulphides in lithium-sulphur batteries. Energy & Environmental Science 7(8):2697-2705, 2014.

Deng, Z., Zhang, Z., Lai, Y., Liu, J., Li, J., and Liu, Y.: Journal of The Electrochemical Society 160:A553, 2013.

Diao, Y., Xie, K., Xiong, S., and Hong, X.: Insights into Li-S Battery Cathode Capacity Fading Mechanisms: Irreversible Oxidation of Active Mass during Cycling. Journal of The Electrochemical Society 159(11):A1816-A1821, 2012.

Dokko, K., Tachikawa, N., Yamauchi, K., Tsuchiya, M., Yamazaki, A., Takashima, E., Park, J.-W., Ueno, K., Seki, S., Serizawa, N., and Watanabe, M.: Journal of The Electrochemical Society 160:A1304, 2013.

Dong, J., Zhang, Z., Kusachi, Y., and Amine, K.: Journal of Power Sources 196:2255, 2011.

Elazari, R., Salitra, G., Garsuch, A., Panchenko, A., and Aurbach, D.: Advanced Materials 23:5641, 2011.

Evers, S., and Nazar, L.F.: New Approaches for High Energy Density Lithium–Sulfur Battery Cathodes. Accounts of Chemical Research 46(5):1135-1143, 2012.

Fu, Y., and Manthiram, A.: Chemistry of Materials 24:3081, 2012.

Fu, Y., and Manthiram, A.: RSC Advances 2:5927, 2012.

Fu, Y., and Manthiram, A.: The Journal of Physical Chemistry C 116:8910, 2012.

Fu, Y., Su, Y.-S., and Manthiram, A.: Advanced Energy Materials 4:n/a., 2014.

Fu, Y., Su, Y.-S., and Manthiram, A.: Highly Reversible Lithium/Dissolved Polysulfide Batteries with Carbon Nanotube Electrodes. Angewandte Chemie International Edition 52(27):6930-6935, 2013.

Fu, Y., Su, Y.-S., and Manthiram, A.: Journal of The Electrochemical Society 159: A1420, 2012.

Gamry Instruments: Basics of Electrochemical Impedance Spectroscopy. 2014. Available at http://www.gamry.com/application-notes/basics-of-electrochemical-impedance-spectroscopy/.

Gao, J., Lowe, M.A., Kiya, Y., and Abruña, H.D.: Effects of Liquid Electrolytes on the Charge–Discharge Performance of Rechargeable Lithium/Sulfur Batteries: Electrochemical and in-Situ X-ray Absorption Spectroscopic Studies. The Journal of Physical Chemistry C 115(50):25132-25137, 2011.

Gordin, M.L., et al.: Bis(2,2,2-trifluoroethyl) Ether as an Electrolyte Co-solvent for Mitigating Self-Discharge in Lithium–Sulfur Batteries. ACS Applied Materials & Interfaces 6(11):8006-8010, 2014.

Harrop, P., Das, R.: Hybrid and Pure Electric Cars 2009-2019. 2009.

Hassoun, J., and Scrosati, B.: Advanced Materials 22:5198, 2010.

Hassoun, J., Kim, J., Lee, D.-J., Jung, H.-G., Lee, S.-M., Sun, Y.-K., and Scrosati, B.: Journal of Power Sources 202:308, 2012.

Hassoun, J., Sun, Y.-K., and Scrosati, B.: Journal of Power Sources 196:343, 2011.

Hayashi, A., Ohtomo, T., Mizuno, F., Tadanaga, K., and Tatsumisago, M.: Electrochimica Acta 50:893, 2004.

Hayashi, A., Ohtomo, T., Mizuno, F., Tadanaga, K., and Tatsumisago, M.: Electrochemistry Communications 5:701, 2003.

He, M., Yuan, L.-X., Zhang, W.-X., Hu, X.-L., and Huang, Y.-H.: The Journal of Physical Chemistry C 115:15703, 2011.

Hickman, J.: Clean Vehicles. Energy Focus (March/April):33-34, 2009.

Hofmann, A.F., Fronczek, D.N., and Bessler, W.G.: Mechanistic modeling of polysulfide shuttle and capacity loss in lithium–sulfur batteries. Journal of Power Sources 259(0):300-310, 2014.

Hollander, J.M., and Jolly, W.L.: X-ray photoelectron spectroscopy. Accounts of Chemical Research 3(6):193-200, 1970.

Hu, M., Wei, J., Xing, L.,and Zhou, Z.: J Appl Electrochem 42:291, 2012.

Huang, Y., Sun, J., Wang, W., Wang, Y., Yu, Z., Zhang, H., Wang, A., and Yuan, K.: Journal of The Electrochemical Society 155:A764, 2008.

Indiana University: Cyclic Voltammetry. Undated. Available at http://courses.chem.indiana.edu/a315/documents/CVhandout_000.pdf.

Ishikawa, M., Yamagata, M., Sugimoto, T., Atsumi, Y., Kitagawa, T., and Azuma, K.: Li-Ion Battery Performance with FSI-Based Ionic Liquid Electrolyte and Fluorinated Solvent-Based Electrolyte. ECS Transactions 33(28):29-36, 2011.

Ishikawa, M., ECS Transactions 33:29, 2011.

Jeddi, K., et al.: Fabrication and Characterization of an Effective Polymer Nanocomposite Electrolyte Membrane for High Performance Lithium/Sulfur Batteries. Journal of The Electrochemical Society 160(8):A1052-A1060, 2013.

Jeddi, K., Ghaznavi, M., and Chen, P.: A novel polymer electrolyte to improve the cycle life of high performance lithium-sulfur batteries. Journal of Materials Chemistry A 1(8):2769-2772, 2013.

Jeddi, K., Sarikhani, K., Qazvini, N.T., and Chen, P.: Journal of Power Sources 245:656, 2014.

Jeddi, K., Zhao, Y., Zhang, Y., Konarov, A., and Chen, P.: Journal of The Electrochemical Society 160:A1052, 2013.

Jeon, B.H., Yeon, J.H., Kim, K.M., and Chung, I.J.: Journal of Power Sources 109:89, 2002.

Jeong, S., et al.: Carbon coated lithium sulfide particles for lithium battery cathodes. Journal of Power Sources 235(0):220-225, 2013.

Jeong, S.S., Lim, Y.T., Choi, Y.J., Cho, G.B., Kim, K.W., Ahn, H.J., and Cho, K.K.: Journal of Power Sources 174:745, 2007.

Ji, L., Rao, M., Aloni, S., Wang, L., Cairns, E.J., and Zhang, Y.: Energy & Environmental Science 4:5053, 2011.

Ji, X., and Nazar, L.F.: Advances in Li-S batteries. Journal of Materials Chemistry 20(44):9821-9826, 2010.

Ji, X., Lee, K.T., and Nazar, L.F.: A highly ordered nanostructured carbon-sulphur cathode for lithium-sulphur batteries. Nat Mater 8(6):500-506, 2009.

Jin, J., Wen, Z., Liang, X., Cui, Y., and Wu, X.: Solid State Ionics 225:604, 2012.

Jung, Y., and Kim, S.: Electrochemistry Communications 9:249, 2007.

Kanno, R., and Murayama, M.: Journal of The Electrochemical Society 148:A742, 2001.

Kawase, A., et al.: Electrochemical reactions of lithium-sulfur batteries: an analytical study using the organic conversion technique. Physical Chemistry Chemical Physics 16(20):9344-9350, 2014.

Kazazi, M., Vaezi, M.R., and Kazemzadeh, A.: Improving the self-discharge behavior of sulfur-polypyrrole cathode material by $LiNO_3$ electrolyte additive. Ionics 20(9):1291-1300, 2014.

Kim, H.S., Arthur, T.S., Allred, G.D., Zajicek, J., Newman, J.G., Rodnyansky, A.E., Oliver, A.G., Boggess, W.C., and Muldoon, J.; Structure and compatibility of a magnesium electrolyte with a sulphur cathode. Nat Commun 2:427, 2011.

Kim, N.-I., Lee, C.-B., Seo, J.-M., Lee, W.-J., and Roh, Y.-B.: Journal of Power Sources 132:209, 2004.

Kim, S., Jung, Y., and Lim, H.S.: Electrochimica Acta 50:889, 2004.

Kissinger, P.T., and Heineman, W.R.: Cyclic voltammetry. Journal of Chemical Education 60(9):702, 1983.

Kitagawa, T., Azuma, K., Koh, M., Yamauchi, A., Kagawa, M., Sakata, H., Miyawaki, H., Nakazono, A., Arima, H., Yamagata, M., and Ishikawa, M.: Application of Fluorine-containing Solvents to $LiCoO_2$ Cathode in High Voltage Operation. Electrochemistry 78:345, 2010.

Kitagawa, T., et al.: Application of Fluorine-containing Solvents to $LiCoO_2$ Cathode in High Voltage Operation. Electrochemistry 78(5):345-348, 2010.

Knowles, M.: Through-life Management of Electric Vehicles. Procedia CIRP **11**(0):260-265, 2013.

Kobayashi, T., Imade, Y., Shishihara, D., Homma, K., Nagao, M., Watanabe, R., Yokoi, T., Yamada, A., Kanno, R., and Tatsumi, T.: Journal of Power Sources 182:621, 2008.

Kolosnitsyn, V.S., et al.: Cycling a Sulfur Electrode in Mixed Electrolytes Based on Sulfolane: Effect of Ethers. Russian Journal of Electrochemistry 38(12):1314-1318, 2002.

Lacey, M.J., Jeschull, F., Edstrom, K., and Brandell, D.: Chemical Communications 49:8531, 2013.

Lai, C., Gao, X.P., Zhang, B., Yan, T.Y., and Zhou, Z.: The Journal of Physical Chemistry C 113:4712, 2009.

Lee, Y.M., et al.: Electrochemical performance of lithium/sulfur batteries with protected Li anodes. Journal of Power Sources 119–121(0):964-972, 2003.

Li, G.-C., Li, G.-R., Ye, S.-H., and Gao, X.-P.: Advanced Energy Materials 2:1238, 2012.

Li, N., Zheng, M., Lu, H., Hu, Z., Shen, C., Chang, X., Ji, G., Cao, J., and Shi, Y.: Chemical Communications 48:4106, 2012.

Liang, X., Wen, Z., Liu, Y., Wu, M., Jin, J., Zhang, H., and Wu, X.: Improved cycling performances of lithium sulfur batteries with $LiNO_3$-modified electrolyte. Journal of Power Sources 196(22):9839-9843, 2011.

Liang, X., Liu, Y., Wen, Z., Huang, L., Wang, X., and Zhang, H.: Journal of Power Sources 196:6951, 2011.

Liang, X., Wen, Z., Liu, Y., Zhang, H., Huang, L., and Jin, J.: Journal of Power Sources 196:3655, 2011.

Liebhafsky, H.A., and Pfeiffer H.G.: Beer's law in analytical chemistry. Journal of Chemical Education 30(9):450, 1953.

Lin, Z., Liu, Z., Fu, W., Dudney, N J., and Liang, C.: Advanced Functional Materials 23:1064, 2013.

Lin, Z., Liu, Z., Fu, W., Dudney, N.J., and Liang, C.: Angewandte Chemie International Edition 52:7460, 2013.

Liu, N., Hu, L., McDowell, M.T., Jackson, A., and Cui, Y.: ACS Nano 5:6487, 2011.

Ltd, W. C. 2005.

Marmorstein, D., Yu, T.H., Striebel, K.A., McLarnon, F.R., Hou, J., and Cairns, E.J.: Journal of Power Sources 89:219, 2000.

Mikhaylik, Y.V., and Akridge, J.R.: Polysulfide Shuttle Study in the Li/S Battery System. Journal of The Electrochemical Society 151(11):A1969-A1976, 2004.

Mikhaylik, Y.V., et al.: High Energy Rechargeable Li-S Cells for EV Application: Status, Remaining Problems and Solutions. ECS Transactions 25(35):23-34, 2010.

Mikhaylik, Y.V.: U.S. Patent 7,354,680, 2008.

Mikhaylik, Y.V.: U.S. Patent 7,352,680, 2008.

Nagao, M., Hayashi, A., and Tatsumisago, M.: Electrochimica Acta 56:6055, 2011.

Nagao, M., Hayashi, A., and Tatsumisago, M.: Journal of Materials Chemistry 22:10015, 2012.

Natalia A. Cañasa, Batteries 2nd Workshop on Lithium sulfur batteries, 2013.

Nelson, J., Misra, S., Yang, Y., Jackson, A., Liu, Y., Wang, H., Dai, H., Andrews, J.C., Cui, Y., Toney, M.F.: In Operando X-ray Diffraction and Transmission X-ray Microscopy of

Lithium Sulfur Batteries. Journal of the American Chemical Society 134(14):6337-6343, 2012.

Nicholson, R.S.: Theory and Application of Cyclic Voltammetry for Measurement of Electrode Reaction Kinetics. Analytical Chemistry 37(11):1351-1355, 1965.

Nishi, Y.: Past, Present and Future of Lithium-Ion Batteries: Can New Technologies Open up New Horizons? In: Lithium-Ion Batteries, ed. Pistoia, pp. 21-39. Amsterdam, Elsevier, 2014.

Ohmi, N., Nakajima, T., Ohzawa, Y., Koh, M., Yamauchi, A., Kagawa, M., and Aoyama, H.: Effect of organo-fluorine compounds on the thermal stability and electrochemical properties of electrolyte solutions for lithium ion batteries. Journal of Power Sources 221(0):6-13, 2013.

Park, J.-W., Yamauchi, K., Takashima, E., Tachikawa, N., Ueno, K., Dokko, K., and Watanabe, M.: The Journal of Physical Chemistry C 117:4431, 2013.

Paterson, E., and Swaffield, R.: X-ray photoelectron spectroscopy. In Clay Mineralogy: Spectroscopic and Chemical Determinative Methods, ed., M.J. Wilson, Netherlands: Springer. p. 226-259, 1994.

Peled, E., et al.: Lithium-Sulfur Battery: Evaluation of Dioxolane-Based Electrolytes. Journal of The Electrochemical Society 136(6):1621-1625, 1989.

Petrucci, R.H., Herring, F.G., and Madura, J.D.: General Chemistry: Principles and Modern Applications. New Jersey, Prentice Hall, 9 edition, 2007.

Purdue University: Scanning Electron Microscope, 2014. Available at http://www.purdue.edu/ehps/rem/rs/sem.htm.

Rao, M., Song, X., Liao, H., and Cairns, E J.: Electrochimica Acta 65:228, 2012.

Rauh, R.D., et al.: Formation of lithium polysulfides in aprotic media. Journal of Inorganic and Nuclear Chemistry 39(10):1761-1766, 1977.

Reusch, W.: Visible and Ultraviolet Spectroscopy. 2013. Available at https://www2.chemistry.msu.edu/faculty/reusch/virttxtjml/Spectrpy/UV-Vis/spectrum.htm.

Rossi, N.A.A., Zhang, Z., Schneider, Y., Morcom, K., Lyons, L.J., Wang, Q., Amine, K., and West, R.: Chemistry of Materials 18:1289, 2006.

Ryu, H.-S., Ahn, H.-J., Kim, K.-W., Ahn, J.-H., and Lee, J.-Y.: Journal of Power Sources 153:360, 2006.

Ryu, H.-S., Ahn, H.-J., Kim, K.-W., Ahn, J.-H., Cho, K.-K., Nam, T.-H., Kim, J.-U., and Cho, G.-B.: Discharge behavior of lithium/sulfur cell with TEGDME based electrolyte at low temperature. Journal of Power Sources 163:201, 2006.

Ryu, H.S., et al.: Self-discharge characteristics of lithium/sulfur batteries using TEGDME liquid electrolyte. Electrochimica Acta 52(4):1563-1566, 2006.

Ryu, H.S., et al.: Self-discharge of lithium–sulfur cells using stainless-steel current-collectors. Journal of Power Sources 140(2):365-369, 2005.

Schneider, H., Garsuch, A., Panchenko, A., Gronwald, O., Janssen, N., and Novák, P.: Journal of Power Sources 205:420, 2012.

Scrosati, B., and Garche, J.: Lithium batteries: Status, prospects and future. Journal of Power Sources 195(9):2419-2430, 2010.

Scrosati, B., Hassoun, J., and Sun, Y.-K.: Lithium-ion batteries. A look into the future. Energy & Environmental Science 4(9):3287-3295, 2011.

Shim, J., Striebel, K.A., and Cairns, E.J.: Journal of The Electrochemical Society 149:A1321, 2002.

Shim, J., Striebel, K.A., and Cairns, E.J.: The Lithium/Sulfur Rechargeable Cell: Effects of Electrode Composition and Solvent on Cell Performance. Journal of The Electrochemical Society 149(10):A1321-A1325, 2002.

Shin, J.H., Jung, S.S., Kim, K.W., Ahn, H.J., and Ahn, J.H.: Journal of Materials Science: Materials in Electronics 13:727, 2002.

Shin, J.H., Lim, Y.T., Kim, K.W., Ahn, H.J., and Ahn, J.H.: Journal of Power Sources 107:103, 2002.

Shizhao, X., Xie, K., Xiaobin, H., and Yan, D.: Ionics, 18:249, 2012.

Shui Zhang, S.: Electrochemistry Communications 8:1423, 2006.

Skoog, D.A., Holler, F.J., and Crouch, S.R.: Principles of Instrumental Analysis, 6th Ed. Thomson Brooks/Cole, 2007.

Sohn, H., et al.: Porous Spherical Carbon/Sulfur Nanocomposites by Aerosol-Assisted Synthesis: The Effect of Pore Structure and Morphology on Their Electrochemical Performance as Lithium/Sulfur Battery Cathodes. ACS Applied Materials & Interfaces 6(10):7596-7606, 2014.

Su, Y.-S., and Manthiram, A.: Nat Commun 3:1166, 2012.

Su, Y.-S., et al.: A strategic approach to recharging lithium-sulphur batteries for long cycle life. Nat Commun 4, 2013.

Sun, J., Huang, Y., Wang, W., Yu, Z., Wang, A., and Yuan, K.: Electrochimica Acta 53:7084, 2008.

Sun, J., Huang, Y., Wang, W., Yu, Z., Wang, A., and Yuan, K.: Electrochemistry Communications 10:930, 2008.

Sun, M., Zhang, S., Jiang, T., Zhang, L., and Yu, J.: Electrochemistry Communications 10:1819, 2008.

Suo, L., Hu, Y.-S., Li, H., Armand, M., and Chen, L.: Nat Commun 4:1481, 2013.

Swapp, S.: Scanning Electron Microscopy (SEM). University of Wyoming, undated. Available at http://serc.carleton.edu/research_education/geochemsheets/techniques/SEM.html.

Tarascon, J.M., and Armand, M.: Issues and challenges facing rechargeable lithium batteries. Nature 414(6861):359-367, 2001.

Thackeray, M.M., Wolverton, C., and Isaacs, E.D.: Electrical energy storage for transportation-approaching the limits of, and going beyond, lithium-ion batteries. Energy & Environmental Science 5(7):7854-7863, 2012.

Trofimov, B.A., Morozova, L.V., Markova, M.V., Mikhaleva, A.I., Myachina, G.F., Tatarinova, I.V., and Skotheim, T.A.: Journal of Applied Polymer Science 101:4051, 2006.

Vielstich, W.: Cyclic voltammetry. In Handbook of Fuel Cells. Hoboken, NJ: John Wiley & Sons, Ltd., 2010.

Wang, H., Yang, Y., Liang, Y., Robinson, J.T., Li, Y., Jackson, A., Cui, Y., and Dai, H.: Graphene-Wrapped Sulfur Particles as a Rechargeable Lithium–Sulfur Battery Cathode Material with High Capacity and Cycling Stability. Nano Letters 11(7):2644-2647, 2011.

Wang, J., Chen, J., Konstantinov, K., Zhao, L., Ng, S.H., Wang, G.X., Guo, Z.P., and Liu, H.K.: Electrochimica Acta 51:4634, 2006.

Wang, J., Yang, J., Wan, C., Du, K., Xie, J., and Xu, N.: Advanced Functional Materials 13:487, 2003.

Wang, J., Yang, J., Xie, J., and Xu, N.: Advanced Materials 14:963, 2002.

Wang, J., Yao, Z., Monroe, C.W., Yang, J., and Nuli, Y.: Advanced Functional Materials 23:1194, 2013.

Wang, J.-Z., Lu, L., Choucair, M., Stride, J.A., Xu, X., and Liu, H.-K.: Journal of Power Sources 196:7030, 2011.

Wang, Q., Wang, W., Huang, Y., Wang, F., Zhang, H., Yu, Z., Wang, A., and Yuan, K.: Journal of The Electrochemical Society 158:A775, 2011.

Wang, W., et al.: The electrochemical performance of lithium–sulfur batteries with LiClO4 DOL/DME electrolyte. Journal of Applied Electrochemistry 40(2):321-325, 2010.

Wang, Y., Huang, Y., Wang, W., Huang, C., Yu, Z., Zhang, H., Sun, J., Wang, A., and Yuan, K.: Electrochimica Acta 54:4062, 2009.

Wang, Y.-X., Chou, S.-L., Liu, H.-K., and Dou, S.-X.: Journal of Power Sources 244:240, 2013.

Waters: How Does High Performance Liquid Chromatography Work? 2014. Available at http://www.waters.com/waters/en_US/How-Does-High-Performance-Liquid-Chromatography-Work%3F/nav.htm?cid=10049055&locale=en_US.

Wei Seh, Z., et al.: Sulphur–TiO2 yolk–shell nanoarchitecture with internal void space for long-cycle lithium–sulphur batteries. Nature Communications 4:1331, 2013.

Wei, W., Wang, J., Zhou, L., Yang, J., Schumann, B., and NuLi, Y.: Electrochemistry Communications 13:399, 2011.

Weng, W., Pol, V.G., and Amine, K.: Ultrasound Assisted Design of Sulfur/Carbon Cathodes with Partially Fluorinated Ether Electrolytes for Highly Efficient Li/S Batteries. Advanced Materials 25(11):1608-1615, 2013.

Whittingham, M.S.: Electrical Energy Storage and Intercalation Chemistry. Science 192(4244):1126-1127, 1976.

Wu, F., Chen, J., Chen, R., Wu, S., Li, L., Chen, S., and Zhao, T.: The Journal of Physical Chemistry C 115:6057, 2011.

Wu, F., Chen, J., Li, L., Zhao, T., and Chen, R.: The Journal of Physical Chemistry C 115:24411, 2011.

Wu, F., et al.: Electrochemical performance of sulfur composite cathode materials for rechargeable lithium batteries. Chinese Chemical Letters 20(10):1255-1258, 2009.

Wu, F., Qian, J., Chen, R., Lu, J., Li, L., Wu, H., Chen, J., Zhao, T., Ye, Y., and Amine, K.: ACS Applied Materials & Interfaces 6:15542, 2014.

Wu, F., Wu, S., Chen, R., Chen, J., and Chen, S.: Electrochemical and Solid-State Letters 13:A29, 2010.

Xiao, L., Cao, Y., Xiao, J., Schwenzer, B., Engelhard, M.H., Saraf, L.V., Nie, Z., Exarhos, G.J., and Liu, J.: Advanced Materials 24:1176, 2012.

Xiong, S., et al.: Oxidation process of polysulfides in charge process for lithium–sulfur batteries. Ionics 18(9):867-872, 2012.

Xiong, S., Kai, X., Hong, X., and Diao, Y.: Ionics 18:249, 2012.

Yang, Y., et al.: High-Capacity Micrometer-Sized Li2S Particles as Cathode Materials for Advanced Rechargeable Lithium-Ion Batteries. Journal of the American Chemical Society 134(37):15387-15394, 2012.

Yang, Y., McDowell, M.T., Jackson, A., Cha, J.J., Hong, S.S., and Cui, Y.: Nano Letters 10:1486, 2010.

Yang, Y., Yu, G., Cha, J.J., Wu, H., Vosgueritchian, M., Yao, Y., Bao, Z., and Cui, Y.: ACS Nano 5:9187, 2011.

Yang, Y., Zheng, G., and Cui, Y.: Energy & Environmental Science 6:1552, 2013.

Yang, Y., Zheng, G., Misra, S., Nelson, J., Toney, M.F., and Cui, Y.: Journal of the American Chemical Society 134:15387, 2012.

Yazami, R., and Reynier, Y.F.: Mechanism of self-discharge in graphite–lithium anode. Electrochimica Acta 47(8):1217-1223, 2002.

Yeon, J.-T., Jang, J.-Y., Han, J.-G., Cho, J., Lee, K. T., and Choi, N.-S.: Journal of The Electrochemical Society 159:A1308, 2012.

Yin, L., Wang, J., Lin, F., Yang, J., and Nuli, Y.: Energy & Environmental Science 5:6966, 2012.

Yin, L., Wang, J., Yang, J., and Nuli, Y.: Journal of Materials Chemistry 21:6807, 2011.

Yu, M., et al.: Performance enhancement of a graphene-sulfur composite as a lithium-sulfur battery electrode by coating with an ultrathin Al_2O_3 film via atomic layer deposition. Journal of Materials Chemistry A 2(20):7360-7366, 2014.

Yuan, L. X., Feng, J.K., Ai, X.P., Cao, Y.L., Chen, S.L., and Yang, H.X.: Electrochemistry Communications 8:610, 2006.

Yuan, L., et al.: Improvement of cycle property of sulfur-coated multi-walled carbon nanotubes composite cathode for lithium/sulfur batteries. Journal of Power Sources 189(2):1141-1146, 2009.

Zhang, B., Qin, X., Li, G. R., and Gao, X. P.: Energy & Environmental Science 3:1531, 2010.

Zhang, S. S.: Journal of The Electrochemical Society 159:A920, 2012.

Zhang, S.: Energies 5:5190, 2012.

Zhang, S.-C., Zhang, L., Wang, W.-K., and Xue, W.-J.: Synthetic Metals 160:2041, 2010.

Zhang, S.S., and Read, J.A.: Journal of Power Sources 200:77, 2012.

Zhang, S.S., and Tran, D.T.: A proof-of-concept lithium/sulfur liquid battery with exceptionally high capacity density. Journal of Power Sources 211(0):169-172, 2012.

Zhang, S.S.: Electrochimica Acta 97:226, 2013.

Zhang, S.S.: Journal of The Electrochemical Society 159:A1226, 2012.

Zhang, S.S.: Journal of The Electrochemical Society 160:A1421, 2013.

Zhang, S.S.: Liquid electrolyte lithium/sulfur battery: Fundamental chemistry, problems, and solutions. Journal of Power Sources 231(0):153-162, 2013.

Zhang, S.S.: Role of $LiNO_3$ in rechargeable lithium/sulfur battery. Electrochimica Acta 70(0):344-348, 2012.

Zhang, W., Huang, Y., Wang, W., Huang, C.; Wang, Y., Yu, Z., and Zhang, H.: Journal of The Electrochemical Society 157:A443, 2010.

Zhang, Z., Bao, W., Lu, H., Jia, M., Xie, K., Lai, Y., and Li, J.: ECS Electrochemistry Letters 1:A34, 2012.

Zhao, X., et al.: Recovery from self-assembly: a composite material for lithium-sulfur batteries. Journal of Materials Chemistry A 2(20):7265-7271, 2014.

Zhao, X., Kim, J.-K., Ahn, H.-J., Cho, K.-K., and Ahn, J.-H.: Electrochimica Acta 109:145, 2013.

Zheng, J., Xiao, J., Gu, M., Zuo, P., Wang, C., and Zhang, J.-G.: Journal of Power Sources 250;313, 2014.

Zheng, S., et al.: High Performance C/S Composite Cathodes with Conventional Carbonate-Based Electrolytes in Li-S Battery. Sci. Rep. 4, 2014.

Zheng, W., Liu, Y.W., Hu, X.G., and Zhang, C.F.: Electrochimica Acta 51:1330, 2006.

Zhou, W., Apkarian, R., Wang, Z.L., and Joy, D.: Fundamentals of Scanning Electron Microscopy (SEM). New York, Springer, 2007

Zhu, X., Wen, Z., Gu, Z., and Lin, Z.: Journal of Power Sources 139:269, 2005.

Zu, C., et al.: Improved lithium-sulfur cells with a treated carbon paper interlayer. Physical Chemistry Chemical Physics 15(7):2291-2297, 2013.

Zu, C., Fu, Y., and Manthiram, A.: Journal of Materials Chemistry A 1:10362, 2013.

Zu, C., Su, Y.-S., Fu, Y., and Manthiram, A.: Physical Chemistry Chemical Physics 15:2291, 2013.

VITA

NAME: Nasim Azimi

EDUCATION: Ph.D., Chemical Engineering, University of Illinois at Chicago, Chicago, Illinois, 2014

M.S., Chemical Engineering, University of Illinois at Chicago, Chicago, Illinois, 2011

B.S., Polymer Science and Engineering, Amirkabir University of Technology, Tehran, Iran, 2008

HONORS: Research Assistant, Argonne National Laboratory, Lemont, Illinois, (2011-2014).

PROFESSIONAL MEMBERSHIP: American Institute of Chemical Engineers
The Electrochemical Society

AWARDS: Chancellor's graduate research fellowship, 2013 and 2014.

Travel grant for the symposium in the ECS Prime meeting, 2012.

PUBLICATIONS AND PRESENTATIONS:

Nasim Azimi, Wei Weng, Christos Takoudis, and Zhengcheng Zhang, "*Improved Performance of Lithium-Sulfur Battery with Fluorinated Electrolyte"***,** Electrochemistry Communications (2013), DOI: 10.1016/j.elecom.2013.10.020

Nasim Azimi **,** Zheng Xue **,** Libo Hu **,** Christos Takoudis, Shengshui Zhang **,** and Zhengcheng Zhang, *"Additive Effect on the Electrochemical Performance of Lithium-Sulfur Battery" (submitted to Electrochimica Acta, 2014)*

Nasim Azimi, Zheng Xue, Ira bloom, Donghai Wang, Tad Daniel, Christos Takoudis , Zhengcheng Zhang. **"***Fluorinated Electrolytes for Lithium-Sulfur Batteries" (submitted to Advanced Energy Material, 2014.)*

Nasim Azimi, Zheng Xue, Nancy Dietz Rago, Christos Takoudis , Mikhail L. Gordin, Jiangxuan Song, Donghai Wang, Zhengcheng Zhang, "*Fluorinated Electrolytes for Li-S Battery: Suppressing the Self-discharge with an Electrolyte Containing Fluoroether Solvent" (submitted to Journal of The Electrochemical Society, 2014)*

Nasim Azimi, Zheng Xue , Libo Hu , Christos Takoudis and Zhengcheng Zhang, *"Teflon-Coated Carbon Paper Electrodes for Rechargeable Lithium-Sulfur Batteries". Submitted*

Jinhua Huang **, Nasim Azimi**, Lei Cheng, Junjie Zhang, Zhengcheng Zhang, Larry A. Curtiss, Lu Zhang "*Novel Organophosphine Oxide Based Redox Shuttle Additives for 4V Lithium Ion Batteries"(submitted to EES, 2014)*

Wei Weng, Shengwen Yuan, **Nasim Azimi**, Zhang Jiang, Yuzi Liu, Yang Ren, Ali Abouimrane, Zhengcheng Zhang, "*Improved Cyclability of Lithium-Sulfur Battery with POP-Sulfur Composite Materials" RSC Advances - Manuscript ID RA-COM-03-2014-002589*

Mikhail L. Gordin, Fang Dai, Shuru Chen, Terrence Xu, Jiangxuan Song, Duihai Tang, **Nasim Azimi**, Zhengcheng Zhang, and Donghai Wang, " *Bis(2,2,2-trifluoroethyl) Ether As an Electrolyte* Co-solvent for Mitigating *Self-Discharge in Lithium−Sulfur Batteries "* dx.doi.org/10.1021/am501665s| ACS Appl. Mater. Interfaces

Runshen Xu, Sathees K. Selvaraj, **Nasim Azimi**, and Christos G. Takoudis, "*Growth Characteristics and Properties of Yttrium Oxide Thin Films by*

Atomic Layer Deposition from Novel $Y(iPrCp)_3$ Precursor and O_3 ", PRIME, ECS meeting, October 2012, ECS Transactions, 50 (13) 107-116 (2012)

Lu Zhang, Zhengcheng Zhang, **Nasim Azimi**, Khalil Amine, "*Development of ANL- 2 redox shuttle for overcharge protection of lithium-ion batteries*", 5th International Conference On Polymer Batteries And Fuel Cells (Pbfc-5),PBFC 2011, August, 2011

L. Zhang , Z. Zhang, **N. Azimi**, and K. Amine, **"***Redox Shuttles for Overcharge Protection of Lithium-Ion Battery***",** 221st ECS Meeting, Seatle, Washington, May 6-10, 2012

Libo Hu., Zheng Xue., **Nasim Azimi**, and Zhengcheng Zhang, "*Fluorinated Electrolytes for 5 V Li-Ion Chemistry"***,** ECEE - March 13-16, 2014 (Energy and the Environment) and ECS Abstract (June 10-14, 2014)

Zhengcheng Zhang, Libo Hu, Zheng Xue and **Nasim Azimi**, "*Fluorinated Electrolytes for 5 V Li-Ion Chemistry*", 225th ECS Meeting, Orlando, Florida, May 11-15, 2014

Nasim Azimi, Christos G Takoudis and Zhengcheng Zhang, "*Improved Performance of Lithium Sulfur Battery with Fluorinated Electrolyte",* 225th ECS Meeting, Orlando, Florida, May 11-15, 2014

Book Chapters

Nasim Azimi, Zheng Xue, Shengshui Zhang, Zhengcheng Zhang, Chapter 18. Recent Advances of Lithium Sulfur Battery in "*Rechargeable lithium batteries: from fundamentals to applications*", book edited by Alejandro A. Franco. (Publisher: Woodhead, UK), in preparation (2013).

ELSEVIER LICENSE
TERMS AND CONDITIONS

Dec 16, 2014

This is a License Agreement between Nasim Azimi ("You") and Elsevier ("Elsevier") provided by Copyright Clearance Center ("CCC"). The license consists of your order details, the terms and conditions provided by Elsevier, and the payment terms and conditions.

All payments must be made in full to CCC. For payment instructions, please see information listed at the bottom of this form.

Supplier	Elsevier Limited The Boulevard,Langford Lane Kidlington,Oxford,OX5 1GB,UK
Registered Company Number	1982084
Customer name	Nasim Azimi
Customer address	14698 BriarForest Drive HOUSTON, TX 77077
License number	3531110145736
License date	Dec 16, 2014
Licensed content publisher	Elsevier
Licensed content publication	Electrochemistry Communications
Licensed content title	Improved performance of lithium–sulfur battery with fluorinate electrolyte
Licensed content author	None
Licensed content date	December 2013
Licensed content volume number	37
Licensed content issue number	n/a
Number of pages	4

Start Page	96
End Page	99
Type of Use	reuse in a thesis/dissertation
Portion	full article
Format	electronic
Are you the author of this Elsevier article?	Yes
Will you be translating?	No
Title of your thesis/dissertation	High Performance Lithium-Sulfur Battery with Fluorinated Electrolytes
Expected completion date	Jan 2015
Estimated size (number of pages)	200
Elsevier VAT number	GB 494 6272 12
Permissions price	0.00 USD
VAT/Local Sales Tax	0.00 USD / 0.00 GBP
Total	0.00 USD

Terms and Conditions

INTRODUCTION

1. The publisher for this copyrighted material is Elsevier. By clicking "accept" in connection with completing this licensing transaction, you agree that the following terms and conditions apply to this transaction (along with the Billing and Payment terms and conditions established by Copyright Clearance Center, Inc. ("CCC"), at the time that you opened your Rightslink account and that are available at any time at http://myaccount.copyright.com).

GENERAL TERMS

2. Elsevier hereby grants you permission to reproduce the aforementioned material subject tothe terms and conditions indicated.

3. Acknowledgement: If any part of the material to be used (for example, figures) hasappeared in our publication with credit or acknowledgement to another source, permission must also be sought from that source. If such permission is not obtained then that material may not be included in your publication/copies. Suitable acknowledgement to the source must be made, either as a footnote or in a reference list at the end of your publication, as follows:

“Reprinted from Publication title, Vol /edition number, Author(s), Title of article / title of chapter, Pages No., Copyright (Year), with permission from Elsevier [OR APPLICABLE SOCIETY COPYRIGHT OWNER].” Also Lancet special credit - “Reprinted from The Lancet, Vol. number, Author(s), Title of article, Pages No., Copyright (Year), with permission from Elsevier.”

4. Reproduction of this material is confined to the purpose and/or media for whichpermission is hereby given.

5. Altering/Modifying Material: Not Permitted. However figures and illustrations may bealtered/adapted minimally to serve your work. Any other abbreviations, additions, deletions and/or any other alterations shall be made only with prior written authorization of Elsevier Ltd. (Please contact Elsevier at permissions@elsevier.com)

6. If the permission fee for the requested use of our material is waived in this instance,please be advised that your future requests for Elsevier materials may attract a fee.

7. Reservation of Rights: Publisher reserves all rights not specifically granted in thecombination of (i) the license details provided by you and accepted in the course of this licensing transaction, (ii) these terms and conditions and (iii) CCC's Billing and Payment terms and conditions.

8. License Contingent Upon Payment: While you may exercise the rights licensedimmediately upon issuance of the license at the end of the licensing process for the transaction, provided that you have disclosed complete and accurate details of your proposed use, no license is finally effective unless and until full payment is received from you (either by publisher or by CCC) as provided in CCC's Billing and Payment terms and conditions. If full payment is not received on a timely basis, then any license preliminarily granted shall be deemed automatically revoked and shall be void as if never granted. Further, in the event that you breach any of these terms and conditions or any of CCC's Billing and Payment terms and conditions, the license is automatically revoked

and shall be void as if never granted. Use of materials as described in a revoked license, as well as any use of the materials beyond the scope of an unrevoked license, may constitute copyright infringement and publisher reserves the right to take any and all action to protect its copyright in the materials.

9. Warranties: Publisher makes no representations or warranties with respect to the licensedmaterial.

10. Indemnity: You hereby indemnify and agree to hold harmless publisher and CCC, andtheir respective officers, directors, employees and agents, from and against any and all claims arising out of your use of the licensed material other than as specifically authorized pursuant to this license.

11. No Transfer of License: This license is personal to you and may not be sublicensed,assigned, or transferred by you to any other person without publisher's written permission.

12. No Amendment Except in Writing: This license may not be amended except in a writingsigned by both parties (or, in the case of publisher, by CCC on publisher's behalf).

13. Objection to Contrary Terms: Publisher hereby objects to any terms contained in anypurchase order, acknowledgment, check endorsement or other writing prepared by you, which terms are inconsistent with these terms and conditions or CCC's Billing and Payment terms and conditions. These terms and conditions, together with CCC's Billing and Payment terms and conditions (which are incorporated herein), comprise the entire agreement between you and publisher (and CCC) concerning this licensing transaction. In the event of any conflict between your obligations established by these terms and conditions and those established by CCC's Billing and Payment terms and conditions, these terms and conditions shall control.

14. Revocation: Elsevier or Copyright Clearance Center may deny the permissions describedin this License at their sole discretion, for any reason or no reason, with a full refund payable to you. Notice of such denial will be made using the contact information provided by you. Failure to receive such notice will not alter or invalidate the denial. In no event will Elsevier or Copyright Clearance Center be responsible or liable for any costs, expenses or damage incurred by you as a result of a denial of your permission request, other than a refund of the amount(s) paid by you to Elsevier and/or Copyright Clearance Center for denied permissions.

LIMITED LICENSE

The following terms and conditions apply only to specific license types:

15. Translation: This permission is granted for non-exclusive world English rights only unless your license was granted for translation rights. If you licensed translation rights you may only translate this content into the languages you requested. A professional translator must perform all translations and reproduce the content word for word preserving the integrity of the article. If this license is to re-use 1 or 2 figures then permission is granted for non-exclusive world rights in all languages.

16. Posting licensed content on any Website: The following terms and conditions apply as follows: Licensing material from an Elsevier journal: All content posted to the web site must maintain the copyright information line on the bottom of each image; A hyper-text must be included to the Homepage of the journal from which you are licensing at http://www.sciencedirect.com/science/journal/xxxxx or the Elsevier homepage for books at http://www.elsevier.com; Central Storage: This license does not include permission for a scanned version of the material to be stored in a central repository such as that provided by Heron/XanEdu.

Licensing material from an Elsevier book: A hyper-text link must be included to the Elsevier homepage at http://www.elsevier.com . All content posted to the web site must maintain the copyright information line on the bottom of each image.

Posting licensed content on Electronic reserve: In addition to the above the following clauses are applicable: The web site must be password-protected and made available only to bona fide students registered on a relevant course. This permission is granted for 1 year only. You may obtain a new license for future website posting.

For journal authors: the following clauses are applicable in addition to the above:

Permission granted is limited to the author accepted manuscript version* of your paper.

*Accepted Author Manuscript (AAM) Definition: An accepted author manuscript (AAM) is the author's version of the manuscript of an article that has been accepted for publication and which may include any author-incorporated changes suggested through the processes of submission processing, peer review, and editor-author communications. AAMs do not include other publisher value-added contributions such as copy-editing, formatting, technical enhancements and (if relevant) pagination.

You are not allowed to download and post the published journal article (whether PDF or HTML, proof or final version), nor may you scan the printed edition to create an electronic version. A hyper-text must be included to the Homepage of the journal from which you are licensing at http://www.sciencedirect.com/science/journal/xxxxx. As part of our normal production process, you will receive an e-mail notice when your article appears on Elsevier's online service ScienceDirect (www.sciencedirect.com). That e-mail will include the article's Digital Object Identifier (DOI). This number provides the electronic link to the published article and should be included in the posting of your personal version. We ask that you wait until you receive this e-mail and have the DOI to do any posting.

Posting to a repository: Authors may post their AAM immediately to their employer's institutional repository for internal use only and may make their manuscript publically available after the journal-specific embargo period has ended.

Please also refer to Elsevier's Article Posting Policy for further information.

18. For book authors the following clauses are applicable in addition to the above: Authors are permitted to place a brief summary of their work online only.. You are not allowed to download and post the published electronic version of your chapter, nor may you scan the printed edition to create an electronic version. Posting to a repository: Authors are permitted to post a summary of their chapter only in their institution's repository.

20. Thesis/Dissertation: If your license is for use in a thesis/dissertation your thesis may be submitted to your institution in either print or electronic form. Should your thesis be published commercially, please reapply for permission. These requirements include permission for the Library and Archives of Canada to supply single copies, on demand, of the complete thesis and include permission for Proquest/UMI to supply single copies, on demand, of the complete thesis. Should your thesis be published commercially, please reapply for permission.

Elsevier Open Access Terms and Conditions

Elsevier publishes Open Access articles in both its Open Access journals and via its Open Access articles option in subscription journals.

Authors publishing in an Open Access journal or who choose to make their article Open Access in an Elsevier subscription journal select one of the following Creative Commons user licenses, which define how a reader may reuse their work: Creative Commons

Attribution License (CC BY), Creative Commons Attribution – Non Commercial ShareAlike (CC BY NC SA) and Creative Commons Attribution – Non Commercial – No Derivatives (CC BY NC ND)

Terms & Conditions applicable to all Elsevier Open Access articles:

Any reuse of the article must not represent the author as endorsing the adaptation of the article nor should the article be modified in such a way as to damage the author's honour or reputation.

The author(s) must be appropriately credited.

If any part of the material to be used (for example, figures) has appeared in our publication with credit or acknowledgement to another source it is the responsibility of the user to ensure their reuse complies with the terms and conditions determined by the rights holder.

Additional Terms & Conditions applicable to each Creative Commons user license:

CC BY: You may distribute and copy the article, create extracts, abstracts, and other revised versions, adaptations or derivative works of or from an article (such as a translation), to include in a collective work (such as an anthology), to text or data mine the article, including for commercial purposes without permission from Elsevier

CC BY NC SA: For non-commercial purposes you may distribute and copy the article, create extracts, abstracts and other revised versions, adaptations or derivative works of or from an article (such as a translation), to include in a collective work (such as an anthology), to text and data mine the article and

ELSEVIER LICENSE
TERMS AND CONDITIONS

Jun 13, 2015

This is a License Agreement between Nasim Azimi ("You") and Elsevier ("Elsevier") provided by Copyright Clearance Center ("CCC"). The license consists of your order details, the terms and conditions provided by Elsevier, and the payment terms and conditions.

All payments must be made in full to CCC. For payment instructions, please see information listed at the bottom of this form.

Supplier Elsevier Limited
The Boulevard,Langford Lane
Kidlington,Oxford,OX5 1GB,UK
Registered Company Number 1982084
Customer name Nasim Azimi
Customer address 14698 BriarForest Drive
HOUSTON, TX 77077
License number 3647280299295
License date Jun 13, 2015
Licensed content publisher Elsevier
Licensed content publication Electrochimica Acta
Licensed content title Additive Effect on the Electrochemical Performance of Lithium–Sulfur Battery
Licensed content author Nasim Azimi,Zheng Xue,Libo Hu,Christos Takoudis,Shengshui Zhang,Zhengcheng Zhang
Licensed content date 1 February 2015
Licensed content volume number 154
Licensed content issue number n/a
Number of pages 6
Start Page 205
End Page 210
Type of Use reuse in a thesis/dissertation
Portion full article
Format both print and electronic
Are you the author of this Elsevier article? Yes
Will you be translating? No
Title of your thesis/dissertation High Performance LithiumSulfur Battery with Fluorinated

Electrolytes

Expected completion date Jul 2015
Estimated size (number of
pages)
200
Elsevier VAT number GB 494 6272 12
Permissions price 0.00 USD
VAT/Local Sales Tax 0.00 USD / 0.00 GBP
Total 0.00 USD
Terms and Conditions
INTRODUCTION
1. The publisher for this copyrighted material is Elsevier. By clicking "accept" in
connection with completing this licensing transaction, you agree that the following terms
and conditions apply to this transaction (along with the Billing and Payment terms and
conditions established by Copyright Clearance Center, Inc. ("CCC"), at the time that you
opened your Rightslink account and that are available at any time at http://myaccount.copyright.com).
GENERAL TERMS
2. Elsevier hereby grants you permission to reproduce the aforementioned material subject to
the terms and conditions indicated.
3. Acknowledgement: If any part of the material to be used (for example, figures) has
appeared in our publication with credit or acknowledgement to another source, permission
must also be sought from that source. If such permission is not obtained then that material
may not be included in your publication/copies. Suitable acknowledgement to the source
must be made, either as a footnote or in a reference list at the end of your publication, as
follows:
"Reprinted from Publication title, Vol /edition number, Author(s), Title of article / title of
chapter, Pages No., Copyright (Year), with permission from Elsevier [OR APPLICABLE
SOCIETY COPYRIGHT OWNER]." Also Lancet special credit "

Reprinted from The
Lancet, Vol. number, Author(s), Title of article, Pages No., Copyright (Year), with
permission from Elsevier."
4. Reproduction of this material is confined to the purpose and/or media for which
permission is hereby given.
5. Altering/Modifying Material: Not Permitted. However figures and illustrations may be
altered/adapted minimally to serve your work. Any other abbreviations, additions, deletions
and/or any other alterations shall be made only with prior written authorization of Elsevier
Ltd. (Please contact Elsevier at permissions@elsevier.com)
6. If the permission fee for the requested use of our material is waived in this instance,
please be advised that your future requests for Elsevier materials may attract a fee.
7. Reservation of Rights: Publisher reserves all rights not specifically granted in the
combination of (i) the license details provided by you and accepted in the course of this
licensing transaction, (ii) these terms and conditions and (iii) CCC's Billing and Payment

terms and conditions.
8. License Contingent Upon Payment: While you may exercise the rights licensed
immediately upon issuance of the license at the end of the licensing process for the
transaction, provided that you have disclosed complete and accurate details of your proposed
use, no license is finally effective unless and until full payment is received from you (either
by publisher or by CCC) as provided in CCC's Billing and Payment terms and conditions. If
full payment is not received on a timely basis, then any license preliminarily granted shall be
deemed automatically revoked and shall be void as if never granted. Further, in the event

that you breach any of these terms and conditions or any of CCC's Billing and Payment
terms and conditions, the license is automatically revoked and shall be void as if never
granted. Use of materials as described in a revoked license, as well as any use of the
materials beyond the scope of an unrevoked license, may constitute copyright infringement
and publisher reserves the right to take any and all action to protect its copyright in the
materials.
9. Warranties: Publisher makes no representations or warranties with respect to the licensed
material.
10. Indemnity: You hereby indemnify and agree to hold harmless publisher and CCC, and
their respective officers, directors, employees and agents, from and against any and all
claims arising out of your use of the licensed material other than as specifically authorized
pursuant to this license.
11. No Transfer of License: This license is personal to you and may not be sublicensed,
assigned, or transferred by you to any other person without publisher's written permission.
12. No Amendment Except in Writing: This license may not be amended except in a writing
signed by both parties (or, in the case of publisher, by CCC on publisher's behalf).
13. Objection to Contrary Terms: Publisher hereby objects to any terms contained in any
purchase order, acknowledgment, check endorsement or other writing prepared by you,
which terms are inconsistent with these terms and conditions or CCC's Billing and Payment
terms and conditions. These terms and conditions, together with CCC's Billing and Payment
terms and conditions (which are incorporated herein), comprise the entire agreement
between you and publisher (and CCC) concerning this licensing transaction. In the event of

any conflict between your obligations established by these terms and conditions and those
established by CCC's Billing and Payment terms and conditions, these terms and conditions
shall control.
14. Revocation: Elsevier or Copyright Clearance Center may deny the permissions described
in this License at their sole discretion, for any reason or no reason, with a full refund payable
to you. Notice of such denial will be made using the contact information provided by you.
Failure to receive such notice will not alter or invalidate the denial. In no event will Elsevier
or Copyright Clearance Center be responsible or liable for any costs, expenses or damage
incurred by you as a result of a denial of your permission request, other than a refund of the
amount(s) paid by you to Elsevier and/or Copyright Clearance Center for denied
permissions.
LIMITED LICENSE

The following terms and conditions apply only to specific license types:
15. Translation: This permission is granted for nonexclusive world English rights only
unless your license was granted for translation rights. If you licensed translation rights you
may only translate this content into the languages you requested. A professional translator
must perform all translations and reproduce the content word for word preserving the
integrity of the article. If this license is to reuse
1 or 2 figures then permission is granted for
nonexclusive
world rights in all languages.
16. Posting licensed content on any Website: The following terms and conditions apply as
follows: Licensing material from an Elsevier journal: All content posted to the web site must

maintain the copyright information line on the bottom of each image; A hypertext must be included to the Homepage of the journal from which you are licensing at http://www.sciencedirect.com/science/journal/xxxxx or the Elsevier homepage for books at http://www.elsevier.com; Central Storage: This license does not include permission for a scanned version of the material to be stored in a central repository such as that provided by Heron/XanEdu.

Licensing material from an Elsevier book: A hypertext link must be included to the Elsevier homepage at http://www.elsevier.com . All content posted to the web site must maintain the copyright information line on the bottom of each image.

Posting licensed content on Electronic reserve: In addition to the above the following clauses are applicable: The web site must be passwordprotected and made available only to bona fide students registered on a relevant course. This permission is granted for 1 year only.

You may obtain a new license for future website posting.

17. For journal authors: the following clauses are applicable in addition to the above:

Preprints:

A preprint is an author's own writeup of research results and analysis, it has not been peerreviewed, nor has it had any other value added to it by a publisher (such as formatting, copyright, technical enhancement etc.).

Authors can share their preprints anywhere at any time. Preprints should not be added to or enhanced in any way in order to appear more like, or to substitute for, the final versions of articles however authors can update their preprints on arXiv or RePEc with their Accepted Author Manuscript (see below).

If accepted for publication, we encourage authors to link from the preprint to their formal

publication via its DOI. Millions of researchers have access to the formal publications on
ScienceDirect, and so links will help users to find, access, cite and use the best available
version. Please note that Cell Press, The Lancet and some societyowned
have different
preprint policies. Information on these policies is available on the journal homepage.
Accepted Author Manuscripts: An accepted author manuscript is the manuscript of an
article that has been accepted for publication and which typically includes authorincorporated
changes suggested during submission, peer review and editorauthor communications.

Authors can share their accepted author manuscript:
– immediately
via their noncommercial
person homepage or blog
by updating a preprint in arXiv or RePEc with the accepted manuscript
via their research institute or institutional repository for internal institutional
uses or as part of an invitationonly
research collaboration workgroup
directly by providing copies to their students or to research collaborators for
their personal use
for private scholarly sharing as part of an invitationonly
work group on
commercial sites with which Elsevier has an agreement
– after the embargo period
via noncommercial
hosting platforms such as their institutional repository
via commercial sites with which Elsevier has an agreement
In all cases accepted manuscripts should:
– link to the formal publication via its DOI
– bear a CCBYNCND
license this

is easy to do
– if aggregated with other manuscripts, for example in a repository or other site, be
shared in alignment with our hosting policy not be added to or enhanced in any way to
appear more like, or to substitute for, the published journal article.
Published journal article (JPA): A published journal article (PJA) is the definitive final
record of published research that appears or will appear in the journal and embodies all
valueadding
publishing activities including peer review coordination, copyediting,
formatting, (if relevant) pagination and online enrichment.
Policies for sharing publishing journal articles differ for subscription and gold open access
articles:
Subscription Articles: If you are an author, please share a link to your article rather than the
fulltext.
Millions of researchers have access to the formal publications on ScienceDirect,
and so links will help your users to find, access, cite, and use the best available version.
Theses and dissertations which contain embedded PJAs as part of the formal submission can
be posted publicly by the awarding institution with DOI links back to the formal
publications on ScienceDirect.
If you are affiliated with a library that subscribes to ScienceDirect you have additional
private sharing rights for others' research accessed under that agreement. This includes use
for classroom teaching and internal training at the institution (including use in course packs

and courseware programs), and inclusion of the article for grant funding purposes.
Gold Open Access Articles: May be shared according to the authorselected

enduser
license and should contain a CrossMark logo, the end user license, and a DOI link to the
formal publication on ScienceDirect.
Please refer to Elsevier's posting policy for further information.
18. For book authors the following clauses are applicable in addition to the above:
Authors are permitted to place a brief summary of their work online only. You are not
allowed to download and post the published electronic version of your chapter, nor may you
scan the printed edition to create an electronic version. Posting to a repository: Authors are
permitted to post a summary of their chapter only in their institution's repository.
19. Thesis/Dissertation: If your license is for use in a thesis/dissertation your thesis may be
submitted to your institution in either print or electronic form. Should your thesis be
published commercially, please reapply for permission. These requirements include
permission for the Library and Archives of Canada to supply single copies, on demand, of
the complete thesis and include permission for Proquest/UMI to supply single copies, on
demand, of the complete thesis. Should your thesis be published commercially, please
reapply for permission. Theses and dissertations which contain embedded PJAs as part of
the formal submission can be posted publicly by the awarding institution with DOI links
back to the formal publications on ScienceDirect.
Elsevier Open Access Terms and Conditions
You can publish open access with Elsevier in hundreds of open access journals or in nearly
2000 established subscription journals that support open access publishing. Permitted third
party reuse
of these open access articles is defined by the author's choice of Creative
Commons user license. See our open access license policy for more information.

Terms & Conditions applicable to all Open Access articles published with Elsevier:
Any reuse of the article must not represent the author as endorsing the adaptation of the
article nor should the article be modified in such a way as to damage the author's honour or
reputation. If any changes have been made, such changes must be clearly indicated.
The author(s) must be appropriately credited and we ask that you include the end user
license and a DOI link to the formal publication on ScienceDirect.
If any part of the material to be used (for example, figures) has appeared in our publication
with credit or acknowledgement to another source it is the responsibility of the user to
ensure their reuse complies with the terms and conditions determined by the rights holder.
Additional Terms & Conditions applicable to each Creative Commons user license:
CC BY: The CCBY
license allows users to copy, to create extracts, abstracts and new works from the Article, to alter and revise the Article and to make commercial use of the
Article (including reuse and/or resale of the Article by commercial entities), provided the
user gives appropriate credit (with a link to the formal publication through the relevant

DOI), provides a link to the license, indicates if changes were made and the licensor is not
represented as endorsing the use made of the work. The full details of the license are
available at http://creativecommons.org/licenses/by/4.0.
CC BY NC SA: The CC BYNCSA
license allows users to copy, to create extracts,
abstracts and new works from the Article, to alter and revise the Article, provided this is not
done for commercial purposes, and that the user gives appropriate credit (with a link to the